DISSERTATION

THE ROLE OF ECDYSTEROIDS ON MYOSTATIN AND MTOR SIGNALING GENE

EXPRESSION IN MOLT-DEPENDENT GROWTH AND ATROPHY OF SKELETAL MUSCLE IN

GECARCINUS LATERALIS AND *CARCINUS MAENAS*

Submitted by

Kathy S. Cosenza

Graduate Degree Program in Cell and Molecular Biology

In partial fulfillment of the requirements

For the Degree of Doctor of Philosophy

Colorado State University

Fort Collins, Colorado

Spring 2016

Doctoral Committee :

      Advisor: Donald L. Mykles

      Sandra L. Quackenbush
      Shane Kanatous
      Jennifer G. DeLuca

ABSTRACT

THE ROLE OF ECDYSTEROIDS ON MYOSTATIN AND MTOR SIGNALING GENE
EXPRESSION IN MOLT-DEPENDENT GROWTH AND ATROPHY OF SKELETAL MUSCLE IN
GECARCINUS LATERALIS AND *CARCINUS MAENAS*

During premolt, increasing ecdysteroid levels are correlated with increased protein
synthesis in the claw of decapod crustaceans. Increased protein synthesis is necessary to
remodel the claw muscle in preparation for rapid hypertrophy immediately after ecdysis.
Ecdysteroids are negatively correlated with *G. lateralis*-Myostatin (*Gl-Mstn*) mRNA levels,
allowing upregulation of protein synthesis. Conversely, steroids upregulate Mstn expression in
mammals. Glucocorticoids inhibit protein synthesis in mammals through downregulation of the
mechanistic Target of Rapamycin (mTOR)-dependent protein synthesis pathway, and
upregulation of Mstn. Here, we look at the relationship between ecdysteroids and the mRNA
levels of Mstn and mTOR pathway components in different skeletal muscles of *G. lateralis* and
C. maenas. The claw muscle and limb bud muscles respond to increasing premolt ecdysteroid
levels with increased protein synthesis, while thoracic muscle does not change in protein
synthesis.

Our first hypothesis is that ecdysteroid levels will be negatively correlated with Mstn
mRNA levels in the claw muscle and the limb bud muscles (muscles with increased protein
synthesis), but not in thoracic muscle (no change in protein synthesis). Our second hypothesis
is that *Gl-Rheb* mRNA levels of will be positively correlated with ecdysteroid levels, and
negatively correlated with Mstn levels in the claw and limb bud muscles, but not in thoracic
muscle. Our third hypothesis is that ecdysteroids directly regulate *Gl-Mstn* promoter expression
through an ecdysone response element (EcRE) in the *Gl-Mstn* promoter. Through molt
manipulations, or allowing natural molts, we showed that ecdysteroid levels were negatively
correlated with *Gl-Mstn* mRNA levels, but not correlated with *C. maenas-Mstn* (*Cm-Mstn*)

mRNA levels, in claw muscle. In limb bud muscle, there was no correlation between ecdysteroid levels and *Gl-Mstn* levels. *Gl-Mstn* levels remained very low, whether limb buds were growing or growth had been suspended. There were no correlations between ecdysteroids and Mstn mRNA levels in the thoracic muscle of either species. These data indicate that ecdysteroid regulation of Mstn is not consistent between species, and that ecdysteroid regulation is muscle specific. Contrary to our second hypothesis, Mstn was positively correlated with mTOR signaling components in the claw muscle of both *G. lateralis* and *C. maenas*, not negatively correlated. There was no correlation between *Gl-Mstn* and mTOR component mRNA levels in the limb buds. This indicates that in specific situations with dramatically changing protein synthesis, Mstn as a chalone that has a modulating effect, to prevent excessive protein synthesis. Using DNA walking, a putative EcRE was located in the promoter region of the *Gl-Mstn* gene. A heterologous ecdysteroid cell system was developed in mammalian cells to determine *Gl-Mstn* promoter activity in response to precisely controlled ecdysteroid levels. The heterologous system showed that the *Gl-Mstn* promoter was functional in this system, but we were unable to demonstrate direct regulation of the *Gl-Mstn* promoter by ecdysteroids. Further work with the heterologous cell system may determine whether the putative EcRE in the *Gl-Mstn* is functional.

TABLE OF CONTENTS

Chapter 1

Introduction and literature review

Introduction

Muscle tissue adapts and changes in mass or structure according to internal and external environmental stimuli (Egerman and Glass, 2014; Rodriguez et al., 2014; Sartori et al., 2014). In mammals, mechanistic Target of Rapamycin complex 1 (mTORC1) is the main transducer of environmental stimuli which enhances protein synthesis in skeletal muscle (Amirouche et al., 2009), while myostatin (Mstn) signaling through Smad transcription factors is an inhibitor of mTOR-dependent protein synthesis (Goodman et al., 2013; Hitachi et al., 2014; Hulmi et al., 2013; Sakuma et al., 2014; Sartori et al., 2014; Schiaffino et al., 2013; Welle et al., 2009).

mTOR properties and function

mTORC1 subunits

mTOR forms two complexes, mTORC1 and mTORC2, each with a specific set of subunits which are involved in distinct cell signaling pathways (Loewith et al., 2002). Here, I will focus on mTORC1, as it is the main transducer of signaling which activates protein synthesis, although mTORC2 is involved in amplification of growth factor signaling. mTORC1 consists of two subunits each of mTOR, Regulatory-associated protein of mTOR (Raptor) (Hara et al., 2002; Kim et al., 2002), lethal with SEC13 protein 8 (LST8), DEP domain-containing protein 6 (Deptor) (Peterson et al., 2009), and proline-rich Akt-substrate of 40-kDa (PRAS40) (Fig. 1.1) (Baretic and Williams, 2014; Kovacina et al., 2003; Wang et al., 2007). LST8 and Raptor are positive regulators of mTORC1, but LST8 appears to be dispensable for mTORC1 signaling (Duan et al., 2015; Guertin et al., 2006). Raptor is essential for mTORC1 formation (Kim et al., 2002), inducing mTOR dimerization by binding to the N-terminal HEAT repeats of one mTOR molecule, and the C-terminal end of the other mTOR molecule, with a second Raptor molecule binding the reciprocal N- and C-terminal ends (Baretic and Williams, 2014). Raptor is further

1

essential for mTORC1 localization (Alayev and Holz, 2013; Dodd and Tee, 2012; Duan et al., 2015; Jewell et al., 2013; Malik et al., 2013; Sengupta et al., 2010; Yoon et al., 2011) and for binding mTOR substrates for signaling (Alayev and Holz, 2013; Populo et al., 2012; Proud, 2009), including negative feedback signaling (Baretic and Williams, 2014; Sengupta et al., 2010). Raptor can also inhibit mTORC1 signaling when there is a deficiency of amino acids (Kim et al., 2002). The Deptor and PRAS40 subunits of mTORC1 are negative regulators of mTORC1 signaling (Kovacina et al., 2003; Peterson et al., 2009; Wang et al., 2007). Deptor, the most recently discovered subunit of mTORC1 (Peterson et al., 2009), has only been observed in vertebrates (Baretic and Williams, 2014). Deptor directly binds the FRB domain of mTOR to suppress mTORC1 signaling (Yoon et al., 2015). PRAS40 binds Raptor, inhibiting the substrate-binding capabilities of Raptor (Duan et al., 2015; Sengupta et al., 2010; Wiza et al., 2012).

mTOR domains

mTOR is categorized as a phosphatidylinositol 3-kinase-related kinase (PIKK) due to the high conservation of its catalytic domain to the phosphatidylinositol kinases (PIKs) (Abraham, 1996). Like other PIKKS, it is an atypical protein kinase that phosphorylates serines and threonines (Brunn et al., 1997a; Hara et al., 1998; Laplante and Sabatini, 2012). Like most other protein kinases, the kinase domain is a two-lobed structure (N-lobe and C-lobe) with the catalytic cleft located between the lobes (Baretic and Williams, 2014). However, the kinase domain is more complicated than a typical protein kinase, containing the FKBP12-Rapamycin binding (FRB) domain, the LST8 binding element (LBE) and the FATC domain, named for the three proteins know to contain this domain near the C-terminal end—FRAP (a prior name for mTOR), ATM (ataxia telangiectasia mutated) and TRRAP (transformation/transcription domain-associated protein) (Fig. 1.2). The complex kinase domain allows increased control of kinase activity (Baretic and Williams, 2014).

The FRB domain was named upon the discovery that rapamycin-FKBP12 binds mTOR at this site and inhibits mTORC1 signaling (Chen et al., 1995; Chiu et al., 1994). It is located on

the opposite side of the cleft from the LBE, which binds to LST8 (Baretic and Williams, 2014).

The rigid FRB domain generally restricts access to the kinase domain while promoting access to

specific mTORC1 substrates such as S6k (Baretic and Williams, 2014), and is now considered

to be a part of the kinase domain (Baretic and Williams, 2014). Deptor binds the FRB domain of

mTOR, thereby repressing mTORC1 activity (Peterson et al., 2009; Yoon et al., 2015).

The smaller N-lobe of the kinase domain contains Lys 2187 and the five-residue P-loop

with Ser 2165 (*Homo sapiens*) that interact with the beta phosphate of ATP (Baretic and

Williams, 2014). The C-lobe contains the activation loop of 26 residues, the catalytic loop of 9

residues, and the 32 amino acid C-terminal FATC domain (Bosotti et al., 2000; Keith and

Schreiber, 1995). The FATC domain is an integral part of the kinase domain, and forms part of

the substrate loading site involved in substrate recognition (Baretic and Williams, 2014). The

activation and catalytic loops contact bound ATP on the P-loop (Baretic and Williams, 2014).

The activation loop has an HIDFG motif highly conserved in all protein kinases and a

(P/Y)E(K/R)(VI)PFRL motif conserved only with Class I PI3Ks (Baretic and Williams, 2014). The

catalytic loop consists of the sequence GLGDRHPSN, which is highly conserved in all mTOR

proteins (Baretic and Williams, 2014). All three of these conserved motifs are 100% conserved

in the mTOR protein in *Gecarcinus* lateralis, the blackback land crab (Abuhagr et al., 2014b). In

both the ATP-bound state and the ADP-bound state, the activation and catalytic loops of mTOR

are directed toward the catalytic center, indicating that mTOR is an intrinsically active kinase

(Baretic and Williams, 2014). By contrast, typical protein kinases regulate kinase activation by

switching between the active and inactive states (activation and catalytic domains directed away

from the catalytic center) (Baretic and Williams, 2014). If the mTORC1 kinase is intrinsically

active, it would explain the need for multiple domains and subunits such as the FRB domain and

the Raptor subunit to regulate substrate access to the kinase domain.

The FAT domain (also named for FRAP, ATM, and TRRAP) (Bosotti et al., 2000; Keith

and Schreiber, 1995; Laplante and Sabatini, 2012) consists of approximately 100 residues, and

subdues mTORC1 hyperactivity by interacting with the kinase domain through several hydrogen bonds (Baretic and Williams, 2014).

mTOR is a very large protein of about 250 kDa, and the largest domain is the HEAT repeats, named for the first four proteins discovered to contain these domains—Huntingtin, elongation factor 3, protein phosphatase 2A and TOR) (Andrade and Bork, 1995). The HEAT repeats are found in proteins that form complexes and enable protein interactions (Andrade and Bork, 1995).

mTORC1 activation of protein synthesis

mTORC1 is involved in protein and lipid synthesis, nutrient import, metabolism, growth, cell cycle progression and autophagy (Laplante and Sabatini, 2012). Here, I will limit my discussion to the involvement of mTORC1 in protein synthesis.

When cellular conditions are energetically favorable, mTORC1 upregulates protein translation (Barbet et al., 1996), ribosomal RNA (rRNA) transcription and ribosomal protein transcription (Thomas and Hall, 1997) (Fig. 1.3). mTORC1 increases protein synthesis through upregulation of key eukaryotic translation initiation factors (eIFs) and eukaryotic elongation factors (eEFs). eIFs are necessary to form the initiation complex in order for translation to occur. A pre-initiation complex consists of the 40S ribosomal subunit, eIF1 (Valášek et al., 2004), eIF1A (Passmore et al., 2007), eIF5 (Valášek et al., 2004), eIF3, and GTP-bound eIF2A, bound to the loaded methionine transfer RNA (Met-tRNA^{Met}) (Chaudhuri et al., 1999). eIF4, consisting of eIF4A (an RNA helicase), eIF4B, eIF4G and eIF4E bind the mRNA and are also necessary for translation initiation (Gingras et al., 1999). eIF4E binds eIF4G and then binds the 5' 7-methylguanylate mRNA cap (Rhoads, 1988). eIF4G binds the eIF poly(A)-binding protein (PABP) (Imataka et al., 1998), thereby circularizing the mRNA for more efficient translation (Kahvejian et al., 2005; Wells et al., 1998). eIF4A and eIF4B unwind the 5'UTR of the mRNA, and eIF3 of the preinitiation complex binds eIF4G (Gingras et al., 1999) and eIF4B (Méthot et al., 1996). The 5'UTR is scanned by the preinitiation complex until the anticodon of the Met-

tRNA^{Met} binds the start codon of the mRNA (Cigan et al., 1988). When this is accomplished, some initiation factors are released and the 60S ribosomal subunit joins the 40S ribosomal subunit with the mRNA and the Met-tRNA^{Met} bound to the start codon in the peptidyl (P) site of the ribosome (Unbehaun et al., 2004). The remainder of the initiation factors are released (Unbehaun et al., 2004), and the complex is now ready for translation elongation.

Translation elongation begins when the GTP-loaded eEF1α brings each amino acid-loaded tRNA to the ribosome (Moon et al., 1972), where the appropriate tRNA binds the next codon on the mRNA in the aminoacyl-tRNA (A) site (Agrawal et al., 1996; Watson, 1964). With GTP hydrolysis, eEF1α is released (Moon et al., 1972; Weissbach et al., 1973), and the rRNA of the large subunit catalyzes the transfer of the amino acid bound to its tRNA in the P site to the incoming amino acid bound to its tRNA in the A site, thus forming a peptide bond. GTP-bound eEF2 then binds ribosomal proteins of the large subunit (Bargis-Surgey et al., 1999) and mediates the translocation of the ribosome along the mRNA (Spahn et al., 2004), with hydrolysis of the GTP bound to eEF2 allowing translocation of one codon—from the A and P sites to the P and exit (E) sites, respectively (Taylor et al., 2007). These elongation steps are repeated to add each additional amino acid to form the complete peptide chain (Taylor 1997).

Two main downstream effectors of mTORC1-dependent protein synthesis are translation initiation factor 4E-binding protein 1 (4E-BP)(Brunn et al., 1997b) and p70 S6 kinase (S6K) (Brown et al., 1995; Thomas and Hall, 1997), both of which contain TOR signaling (TOS) motifs, which bind Raptor and are necessary for mTORC1-catalyzed phosphorylation (Nojima et al., 2003; Schalm et al., 2003). Translation initiation is regulated by mTORC1 through phosphorylation of 4E-BP. When not phosphorylated, 4E-BP binds eIF4E on a site that prevents the binding of eIF4E to eIF4G, thereby preventing translation initiation (Gingras et al., 1999; Haghighat et al., 1995). A cascade of mTORC1-dependent phosphorylations of 4E-BP begins with amino acid stimulation of threonine 37 and threonine 46, respectively, while insulin can then stimulate mTORC1 phosphorylation of threonine 70 and serine 65, respectively (Fadden et

al., 1997; Miron et al., 2003; Proud, 2009; Wang et al., 2005). As increased sites are phosphorylated (Wang et al., 2005), 4E-BP dissociates from eIF4E thereby allowing eIF4G access to eIF4E with the resulting formation of the preinitiation complex and an increase in translation initiation (Gingras et al., 1999; Haghighat et al., 1995).

Activated mTORC1 phosphorylates S6k on threonine 389 (Burnett et al., 1998; Dennis et al., 1996), causing dissociation of S6k from eIF3 and allowing mTOR binding to eIF3 (Holz et al., 2005). eIF3 acts as a scaffold, positioning S6k and mTORC1 near the translation initiation factors where further phosphorylations of translation-associated proteins takes place (Holz et al., 2005). Once S6k dissociates from eIF3, PDK1 fully activates S6k by phosphorylating it on threonine 229 of the activation loop (Alessi et al., 1998; Holz et al., 2005). Activated S6k phosphorylates programmed cell death protein 4 (PDCD4), eIF4B, and ribosomal protein S6 (rpS6). Phosphorylation of PDCD4, an inhibitor of eIF4A, leads to PDCD4 ubiquitination and degradation (Dorrello et al., 2006). S6k phosphorylates eIF4B on serine 422, which was thought to increase the ability of eIF4B to assist eIF4A in its helicase activity and to promote the association of eIF4B with eIF3 to form the pre-initiation complex (Raught et al., 2004). S6k phosphorylation of rpS6 on serines 235, 236, 240, 244 and 247 (Krieg et al., 1988) was correlated with increased protein synthesis (Duncan and McConkey, 1982; Thomas et al., 1982; Trevillyan et al., 1985), specifically increased translation of 5' terminal oligopyrimidine tract (5' TOP) mRNA (Jefferies et al., 1997). mTORC1 does increase 5' TOP mRNA translation, including all ribosomal proteins (Amaldi and Pierandrei-Amaldi, 1997; Iadevaia et al., 2014; Powers and Walter, 1999). However, involvement of S6k (Pende et al., 2004) or rpS6 (Ruvinsky and Meyuhas, 2006) has been refuted. Recent studies indicate that in cells without S6k, global translation initiation is not altered, even though phosphorylation of rpS6 and eIF4B is decreased (Chauvin et al., 2014; Mieulet et al., 2007). Transcription of mRNA is necessary for ribosome assembly and processing of ribosomal components (mainly 5'TOR mRNA), and both processes require S6k and S6, thus affecting protein translation indirectly (Chauvin et al., 2014).

mTORC1 regulates ribosome biogenesis in an S6k-dependent manner through regulation of RNA polymerase I (Pol I), which transcribes 5.8S, 18S and 28S ribosomal RNA (Iadevaia et al., 2014). Pol I activity requires the transcription factors upstream binding transcription factor (UBF), Pol I, transcription initiation factor 1A (TIF-1A) and TIF-1B (Beckmann et al., 1995). mTORC1 signaling increases the expression and phosphorylation of UBF which binds the rDNA promoter (Hannan et al., 2003). UBF then binds TIF-1B (Hempel et al., 1996), which recruits the TIF-1A/Pol I complex to the rDNA promoter (Iadevaia et al., 2014; Sanij and Hannan, 2009). mTORC1 further upregulates this process by regulating the localization and phosphorylation of TIF-1A (Mayer et al., 2004). Upon mTORC1 signaling, TIF-1A is translocated to the nucleus, phosphorylated on serine 44, and de-phosphorylated on serine 199 (Mayer et al., 2004). mTORC1 represses protein phosphatase 2A (PP2A), which then cannot dephosphorylate serine 44, allowing TIF-1A to interact with Pol I, thus initiating transcription of the ribosomal RNA (Mayer et al., 2004).

mTORC1 signaling indirectly upregulates translation by increasing RNA polymerase III (Pol III) transcription (Mahajan, 1994) of 5S rRNA and transfer RNA (tRNA) (Kantidakis et al., 2010; Moir and Willis, 2013; Shor et al., 2010; Tsang et al., 2010; Weinmann and Roeder, 1974) which appears to have both S6k-dependent and S6k-independent components (Shor et al., 2010). Pol III transcription requires the transcription factor IIIC (TFIIIC) and TFIIIB (Kassavetis et al., 1990; Moir and Willis, 2013). mTORC1 associates with TFIIIC via Raptor through a TOS motif on TFIIIC (Kantidakis et al., 2010), which positions mTORC1 at the 5S rRNA and tRNA promoters (Kantidakis et al., 2010; Moir and Willis, 2013; Tsang et al., 2010), where mTORC1 can phosphorylate Maf1. When unphosphorylated, Maf1 is a repressor of Pol III, but phosphorylation by mTORC1 on serines 60, 68 and 75 (Michels et al., 2010; Moir and Willis, 2013) relieves Maf1 inhibition, allowing Pol III to transcribe the 5S rRNA and tRNA genes (Moir and Willis, 2013), thus increasing protein synthesis indirectly by increasing translational capacity (Kantidakis et al., 2010).

Phosphorylation of eEF2 on threonine 56 by eEF2 kinase inhibits the translation elongation function of eEF2 (Wang and Proud, 2006). Although phosphorylation of eEF2 kinase on serine 366 by S6k was originally thought to inactivate eEF2 kinase, thereby allowing eEF2 to proceed with translation elongation (Wang et al., 2001), a more recent study found that eEF2 kinase is not affected by S6k signaling (Mieulet et al., 2007). However, eEF2 kinase is phosphorylated and inhibited in an mTORC1-dependent but S6k-independent manner on serines 78 and 359, thereby allowing increased eEF2 translation elongation activity (Proud, 2009).

In conclusion, mTORC1 upregulates translation initiation through 4E-BP, translation elongation in an S6k- and 4E-BP-independent manner, and translational capacity in both S6k-dependent and S6k-independent ways. Although S6k phosphorylates various translation factors, it does not appear to directly regulate translation initiation or elongation. Instead, mTORC1 phosphorylation of S6k upregulates transcription of proteins necessary for ribosome biogenesis through phosphorylation of rpS6 (Chauvin et al., 2014).

mTORC1 up-regulation of protein degradation

A recent paper shows that mTORC also increases protein degradation through upregulation of the expression of proteasome components (Zhang et al., 2014). This upregulation of protein degradation is dependent on signaling through nuclear factor erythroid-derived 2-related factor 1 (NRF1) (Zhang et al., 2014). They suggest that this upregulation of protein degradation allows increased availability of amino acids for protein synthesis (Zhang et al., 2014). But mTORC1 upregulation of both protein degradation and protein synthesis may contribute to the type of muscle atrophy which requires protein synthesis for remodeling at the same time as protein degradation for atrophy, such as occurs in the *G. lateralis* claw closer muscle during premolt. (See the "Effects of ecdysteroids on claw muscle and limb regeneration" subsection).

Regulation of the insulin/mTOR-dependent protein synthesis pathway

mTORC1 regulation by amino acids

Nutrients, especially amino acids, are the fundamental regulators of mTORC1 in all animals (Takahara and Maeda, 2013; Zoncu et al., 2011b). Amino acid availability, particularly leucine and glutamine, controls mTORC1 activity by localizing mTORC1 to the lysosomal membrane where it can interact with Rheb (Dodd and Tee, 2012; Duan et al., 2015; Efeyan and Sabatini, 2013; Huang and Fingar, 2014; Jewell et al., 2013; Kim et al., 2013; Laplante and Sabatini, 2012; Laplante and Sabatini, 2013; Malik et al., 2013; Sengupta et al., 2010; Takahara and Maeda, 2013), and by activating mTORC1 (Adegoke et al., 2012; Byfield et al., 2005; Dodd and Tee, 2012; Duan et al., 2015; Huang and Fingar, 2014; Malik et al., 2013; Takahara and Maeda, 2013; Yoon et al., 2011). Cellular energy deficiency, hypoxia and other environmental stressors can limit the mTORC1 response to amino acids (Aramburu et al., 2014; Laplante and Sabatini, 2012). In multicellular animals, growth factors and hormones regulate mTORC1, coordinating overall body homeostasis and growth (Takahara and Maeda, 2013). In addition, muscle activity regulates mTORC1 signaling in muscle cells (Adegoke et al., 2012; Drummond et al., 2009a; Schiaffino et al., 2013; Takahara and Maeda, 2013). Altogether, hundreds of proteins may contribute to mTOR regulation (Aramburu et al., 2014; Caron et al., 2010).

Amino acids (Hara et al., 1998; Oldham et al., 2000; Zhang et al., 2000), especially leucine and glutamine, (Han et al., 2012; Jewell et al., 2015; Sancak et al., 2008) are crucial regulators of mTORC1 signaling. Most amino acids are pumped into the cell in an ion- and ATP-dependent manner (Dodd and Tee, 2012). System A and system L amino acid transporters work together to increase intracellular leucine levels (Dodd and Tee, 2012). In muscle cells, which require an abundant supply of amino acids (especially leucine), SNAT2 is a Na^+-linked System A transporter that uses ATP to pump glutamine and other small neutral amino acids into the cytoplasm from the extracellular space (Dodd and Tee, 2012; Evans et al., 2007). Then

Lat1, a system L transporter, pumps glutamine out in exchange for leucine (Baird et al., 2009; Dodd and Tee, 2012).

The general amino acid control non-derepressible 2 (GCN2) pathway in yeast (ATF4 in mammals) is one of several pathways that sense amino acid levels, leading to control of mTORC1 activity (Chantranupong et al., 2015). Upon binding uncharged tRNAs, GCN2 dimerizes and autophosphorylates, allowing it to phosphorylate eukaryotic initiation factor 2a (eIF2a) (Chantranupong et al., 2015; Diallinas et al., 1994; Narasimhan et al., 2004). Phosphorylation of eIF2a generally represses mRNA translation initiation, but GCN2 translation is increased, allowing it to upregulate transcription of genes required for amino acid biosynthesis (Chantranupong et al., 2015; Hinnebusch, 2005). The upregulation of GCN2 is complicated. GCN2 has 4 upstream open reading frames (uORFs) in addition to the main ORF (Hinnebusch, 2005). When ribosomes start scanning the GCN2 mRNA, the AUG of the first uORF is encountered, GTP is hydrolyzed and eIF2 is released. The ribosome continues moving down the mRNA, another AUG is encountered, and in conditions of sufficient amino acids with abundant transcription complexes (TCs), another TC forms at uORFs 2-4, inhibiting the main ORF. Under conditions of amino acid insufficiency, there are fewer TCs due to lack of GCN2 phosphorylation, and the ribosome travels further after the first uORF, half of the time reaching the main ORF before the TC is reloaded. This allows GCN2 translation expression which results in GCN2-controlled transcription of about 30 amino acid synthesis genes (Hinnebusch, 2005). The GCN2 pathway feeds into the mTORC1 protein synthesis pathway by providing amino acid information (Chantranupong et al., 2015).

The main method of amino acid activation of mTORC1 is through the Ras-related small GTP-binding proteins (Rags), which are tethered at the lysosome by the pentameric Ragulator complex (Bar-Peled et al., 2012; Sancak et al., 2010) (fig. 1.4). Rags are heterodimers of RagA or RagB (RagA/B) with RagC or RagD (RagC/D), which activate the amino acid-mTORC1 protein synthesis pathway when RagA/B is GTP-loaded and RagC/D is GDP-loaded (Han et al.,

2012; Kim et al., 2008; Sancak et al., 2008). Leucyl-tRNA synthetase (LRS), when activated by

leucine, acts as a GTPase-activating protein (GAP) for RagC/D, setting the stage for formation

of the active RagA/B-GTP complex (Han et al., 2012). Ragulator tethers the Rag heterodimer to

the lysosome, and amino acid concentrations within the lysosome control the activity of

Ragulator as a guanine nucleotide exchange factor (GEF) for RagA/B (Zoncu et al., 2011a).

When amino acid concentrations inside the lysosomal lumen are low, vATP-ase binds Ragulator

tightly, preventing its GEF activity; but when amino acid concentrations are high, vATP-ase

dissociates from Ragulator, allowing GEF activity (Zoncu et al., 2011a). Also, when amino acid

levels are low, the GTPase-activating protein activity towards Rags protein, (GATOR),

inactivates RagA/B (Bar-Peled et al., 2013). When RagA/B is GTP-loaded by Ragulator, then

RagA/B-GTP interacts with Raptor, initiating the localization of mTORC1 to the lysosomal

membrane (Sancak et al., 2008), where activated Rheb is localized (Groenewoud and

Zwartkruis, 2013). Rheb then activates mTORC1 via two methods. First, Rheb physically

interacts with mTORC1, displacing the mTORC1 inhibitor FKBP38 (Bai et al., 2007). Second,

Rheb activates phospholipase D1 (PLD1),

which produces unsaturated phosphatidic acid (PA) (Yoon et al., 2015) from the hydrolysis of

phosphatidylcholine (Fang et al., 2001; Fang et al., 2003; Sun et al., 2008; Yoon et al., 2011;

Yoon et al., 2015). PA binds the FRB domain of mTOR and activates mTORC1 by displacing

Deptor (Fang et al., 2001; Sun et al., 2008). Interestingly, only unsaturated PA, the type

produced by PLD1, is able to activate mTORC1, allowing the specificity of this pathway (Yoon et

al., 2015).

　　　The presence of leucine and glutamine enhances RagA/B-GTP-loading by stimulating

glutamate dehydrogenase (GDH) activity, a key enzyme in the conversion of glutamine to α-keto

glutarate (α-KG). α-KG then enhances RagA/B-GTP loading and mTORC1 localization to the

lysosomal membrane through an unknown mechanism (Duran et al., 2012). Glutamine can

activate mTORC1 in an alternate pathway that still requires v-ATPase, but does not require the

Rag proteins (Jewell et al., 2015). This alternate pathway requires the GEF activity of ADP

ribosylation factor 1 (Arf1) to localize mTORC1 to the lysosomal membrane and to activate

mTORC1 signaling (Jewell et al., 2015).

An additional pathway through which amino acids activate mTORC1 is by causing

calcium ion influx into the cytoplasm, with subsequent binding to calmodulin. The Ca^{++}-

calmodulin complex binds and activates vacuolar protein sorting 34 (Vps34). Activated Vps34, a

class III phosphoinositide 3-kinase (PI3K), phosphorylates phosphatidylinositol to form

phosphatidylinositol (3) phosphate (PI3K) (Gulati et al., 2008). PI3K recruits phospholipase D

(PLD) to the lysosome, where PLD catalyzes production of PA, as described above (Yoon et al.,

2015) Phosphatidic acid then activates mTORC1 by displacing the inhibitor Deptor (Fang et al.,

2001; Yoon et al., 2011), as described above.

Amino acids contribute to mTORC1 activation through several additional mechanisms.

Mitogen-activating protein kinase kinase kinase kinase-3 (MAP4K3) activates mTORC1 when

amino acids are sufficient (Duan et al., 2015; Yan et al., 2010) in a Rag-dependent manner (Kim

and Guan, 2011). Activation requires MAP4K3 phosphorylation on Ser170, while a protein

phosphatase 2A (PP2A) removes the phosphate when amino acids are insufficient (Yan et al.,

2010). Amino acid sufficiency also stimulates Ras-like protein A (RalA) GTP-loading, which

appears to be necessary to activate mTORC1 (Duan et al., 2015; Maehama et al., 2008). And

finally, leucine associates with unbranched chain amino acid receptors 1 and 2 (UBR1 and 2),

which are ubiquitin E3 ligases, and may thereby prevent the breakdown of some components of

the mTOR pathway (Duan et al., 2015; Kume et al., 2010).

In muscle cells, neuronal nitric acid synthetase (nNOS) responds to mechanical overload

by producing NO which reacts with superoxide to form peroxynitrite (Ito et al., 2013).

Peroxynitrite then activates the transient receptor potential cation channel, subfamily V, member

1 (Trpv1) calcium channel, allowing calcium ions to enter the cytoplasm from the endoplasmic

reticulum (Ito et al., 2013). Calcium ions then activate mTORC1 through an unknown

mechanism (Ito et al., 2013). As amino acids and mechanical overload both increase cytoplasmic calcium ion concentration which trigger mTORC1 activity, it is interesting to speculate whether both pathways work through PA activation.

mTORC1 activation by growth factors

Muscle protein synthesis is increased by insulin stimulation (Stetten, 1953) through the mTORC1 pathway (Cantley, 2002; Jefferies et al., 1997; Mendez et al., 1996; Saltiel, 1994). IGF-1 (Daughaday et al., 1959) was found to have insulin-like effects on cell metabolism (Rinderknecht and Humbel, 1978), including promotion of protein synthesis in muscle cells (Coleman et al., 1995), through activation of the mTORC1 signaling pathway (Rommel et al., 2001). Although insulin and IGF-1 have differential effects on cells, they both regulate the mTORC1 pathway in a similar fashion to coordinate the rate of growth with nutrient availability (Mirth and Shingleton, 2012). Insulin and IGF-1 are the main growth factors that regulate mTORC1-dependent protein synthesis, but epidermal growth factor (EGF) also contributes to mTORC1 regulation (Foster et al., 2010)

Insulin is produced and stored by the beta cells in the pancreas, and secreted as needed. By contrast, high quantities of IGF-1 can be produced by numerous different tissues, which are then sequestered in the circulation by IGF-1 binding proteins (IGF-1BPs) until needed (Holly, 2004). Insulin and IGF-1 are both growth factors that bind their cognate receptor to initiate cell signaling. The insulin receptor (IR) and the IGF-1 receptor (IGF-1R) are both receptor tyrosine kinase dimers that autophosphorylate upon ligand binding (Ullrich et al., 1986; White et al., 1988). Both insulin and IGF-1 can bind with reduced affinity to the other's receptor, and both can bind an insulin/IGF-1 heterodimer receptor (De Meyts et al., 2004). Downstream signaling from the receptor through mTORC1-dependent protein synthesis is similar for both insulin and IGF-1, although pathway regulation can be slightly different (Foti et al., 2004)

Once the IR/IGF-1R autophosphorylate, IRS-1 binds through a phosphotyrosine binding (PTB) domain and becomes phosphorylated by the receptor (Valdes et al., 2013; White et al.,

13

1985; White et al., 1988) on several tyrosine residues (Gual et al., 2005) (Fig. 1.5). The p85 regulatory subunit of phosphoinositide 3 kinase (PI3K) binds IRS-1 at phosphorylated tyrosines 612 and 632 via an SH domain (all numbering is presented as *Homo sapiens* equivalent numbering), which activates the p110 catalytic subunit of PI3K (Cantley, 2002; Zick, 2004). Activated PI3K phosphorylates phosphatidylinositol 4,5-bisphosphate (PIP2) on the 3-carbon of inositol, producing PIP3 (Cantley, 2002; Zick, 2004). Phosphoinositide-dependent kinase 1 (PDK1) and Akt bind PIP3 through PH domains, bringing them into close proximity where PDK1 can phosphorylate Akt (Cantley, 2002; Haissaguerre et al., 2014; Zick, 2004) in the activation loop on threonine 308 (Alessi et al., 1996; Chan et al., 1999). Additional phosphorylation on Serine 473 by mTORC2 (PI3K-dependent) increases Akt activity by about 10-fold (Huang and Fingar, 2014). Akt then phosphorylates tuberous sclerosis factor 2 (TSC2) on several sites, including serine 939 and threonine 1462 (Huang and Fingar, 2014), which allows 14-3-3 binding (Cai et al., 2006; Sengupta et al., 2010). The binding of 14-3-3 proteins sequesters TSC2 away from the lysosomal membrane into the cytoplasm (Heard et al., 2014; Menon et al., 2014), thus preventing the GTPase activating protein (GAP) activity of the TSC1/2 complex towards Ras homolog enriched in brain (Rheb) (Potter et al., 2002). This allows the active form of GTP-Rheb to accumulate, which can then activate mTORC1 through the mechanisms described above, as long as sufficient amino acids are available for mTORC1 signaling (Sun et al., 2008). Akt can also phosphorylate PRAS40, an mTORC1 inhibitor, on threonine 246 (Kovacina et al., 2003; Vander Haar et al., 2007), allowing 14-3-3 protein binding to sequester PRAS40 away from mTORC1 (Sengupta et al., 2010). Activated mTORC1 enhances its own activity by phosphorylating and inactivating Raptor on Serine 863 (Foster et al., 2010; Wang et al., 2009), and phosphorylating Deptor on serines 293 and 299, resulting in Deptor degradation (Duan et al., 2011)

Both EGF and IGF-1/insulin signaling contributes to mTORC1 activation through a MAPK signaling pathway (Amali et al., 2004; Festuccia et al., 2009; Foster et al., 2010; Grey et

14

al., 2003; Hatakeyama et al., 2008). EGF binding to its tyrosine receptor results in dimerization (Greenfield et al., 1989) and autophosphorylation (Carpenter et al., 1979; Cohen et al., 1982; Downward et al., 1984). As the IR/IGF-1 receptor is already dimerized, ligand binding results in autophosphorylation. In both cases, the activated receptor binds Grb2 through an SH domain (Gale et al., 1993) and Grb2 binds son of sevenless (SOS) through an SH3 domain (Buday and Downward, 1993). SOS then acts as a GEF for Ras (Buday and Downward, 1993), allowing Ras to activate a kinase cascade with ultimate phosphorylation of p90 ribosomal S6 kinase 1 (RSK1) (Roux et al., 2004). Activated RSK1 phosphorylates TSC2 on Serine 1798, resulting in dissociation of the TSC2 subunits (Ma et al., 2005), and thereby activating Rheb, as previously described. MAPK also phosphorylates Raptor on several sites, with Serine 863 (*Homo sapiens*) being the most important for mTORC1 activation (Carriere et al., 2011).

Regulation of the insulin/mTORC1 pathway

Within the growth factor-stimulated mTORC1 protein synthesis pathway, there are several junctures where regulation occurs. Following ligand stimulation, the IR and IGF1R are internalized within clathrin-coated pits in endocytic vesicles (Fan et al., 1983; Foti et al., 2004). Insulin is rapidly degraded within the vesicle, effectively terminating its signal and the IR is recycled back to the cell surface (Carpentier, 1993; Carpentier, 1994; Foti et al., 2004). The entire IGF-1/IGF-1R complex may be degraded, or only the ligand degraded with the receptor recycled, to regulate cell signaling as necessary (Carpentier, 1993; Foti et al., 2004).

IRS-1, specific to the insulin/IGF-1 signaling pathway (Youngren, 2007) and directly activated by the receptor, is a prime target for mTOR-dependent protein synthesis regulation. IRS-1 contains 21 potential tyrosine phosphorylation sites and more than 50 serine phosphorylation sites that are phosphorylated by many different kinases to fine-tune insulin signaling (Sun et al., 1993; Sun and Liu, 2009). Tyrosine phosphorylation of the IR/IGF-1R is maximal 1 minute after insulin stimulation, gradually declining over the next 60 minutes with a concomitant rise in serine/threonine phosphorylation (Paz et al., 1999). The numerous

phosphorylation sites allows an intricate control of the insulin signaling pathways by various kinases.

Inhibitory phosphorylations of IRS-1 include S6k-dependent phosphorylation of IRS-1 serine 1101 (Smadja-Lamere et al., 2013; Tremblay et al., 2007) serine 312, serine 636 and serine 639 (Malik et al., 2013; Um et al., 2004), MAPK-dependent phosphorylation of IRS-1 serine 636 and serine 616 (Bouzakri et al., 2003; Gual et al., 2003), mTOR-dependent phosphorylation of IRS-1 serine 312 (Aguirre et al., 2000; Carlson et al., 2004; Gual et al., 2003) and serines 636 and 639 via Raptor (Tzatsos and Kandror, 2006), mTOR- and nutrient-dependent phosphorylation of IRS-1 serine 307 (Giraud et al., 2004), and PKC zeta-dependent phosphorylation of IRS-1 serine 318 (Beck et al., 2003; Liu et al., 2001; Ravichandran et al., 2001). Inhibition occurs by preventing IRS-1 from binding the IR or PI3K (Paz et al., 1997; Sengupta et al., 2010), translocating IRS-1 to the cytoplasm (Carlson et al., 2004), stabilizing an inhibitor (Yu et al., 2011), or proteasome degradation of IRS-1 via several different E3 ligases (Greene et al., 2003; Lee et al., 2000; Shi et al., 2011; Takano et al., 2001; Xu et al., 2008; Zhande et al., 2002). Proteasomal degradation results in rapid inhibition of insulin signaling, unless the IRS-1 proteins are being synthesized (Egerman and Glass, 2014).

Positive regulation may occur with Akt-dependent phosphorylation of IRS-1 serines 270, 307, 330 and 362, which protects IRS-1 from tyrosine phosphatases (Paz et al., 1999). In addition, IRS-1 serine 323 phosphorylation is necessary for Akt activation (Weigert et al., 2005). Note, IRS-1 serine 307 phosphorylation can positively or negatively regulate insulin signaling, dependent on other signaling parameters.

Phosphatases are also involved in regulating insulin/IGF-1 signaling. Phosphatase and tensin homologue (PTEN) is a phosphatase for PIP3, thereby negatively regulating Akt activation (Maehama and Dixon, 1999; Ozes et al., 2001). Without insulin signaling, mTORC1-dependent protein translation is controlled by a balance between the activities of Rheb and PTEN (Lequieu et al., 2011). Insulin signaling production of PIP3 shifts the balance, increasing

Rheb stimulation of protein synthesis (Lequieu et al., 2011). Other known phosphatases involved in regulating insulin signaling include protein phosphatase 2A (PP2A) and protein phosphatase-1 (PP-1). PP2A can increase insulin signaling by an mTOR-dependent dephosphorylation and protection of IRS-1 (Hartley and Cooper, 2002), and by dephosphorylating Akt which reduces negative feedback of insulin signaling (Ni et al., 2007). Conversely, PP2A can inhibit mTOR-dependent protein synthesis by dephosphorylating Akt (Li et al., 2013b; Tsuchiya et al., 2014), S6k (Hahn et al., 2010), and 4EBP (Nho and Peterson, 2011), depending on the signaling context (Gao et al., 2015).

MicroRNA (miR) contribute substantially to the regulation of insulin/IGF-1-mTORC1 signaling. MiRs are short (~22 nucleotides) noncoding RNA that complementary base pair to the 3' untranslated region (UTR) of their target mRNA, causing transcription suppression or cleavage and degradation of the target mRNA (Lau et al., 2001). MiR that target and downregulate mTOR directly include the miR-99a/99b/100 cluster (Grundmann et al., 2011; Jin et al., 2013; Li et al., 2013a; Nagaraja et al., 2010; Sun et al., 2013; Wang et al., 2014a), miR-144 (Iwaya et al., 2012), miR-199a-3p (Fornari et al., 2010), miR-520c (Liu and Wilson, 2012), miR-373 (Liu and Wilson, 2012),and miR-193a-5p (Yu et al., 2015). The miR-99a/99b/100 cluster also targets Akt (Jin et al., 2013) and IGF-1R (Jin et al., 2013; Li et al., 2013a). Other miR that target the IGF1R, includes miR-148a/152 (Xu et al., 2013), miR-223 (Jia et al., 2011) and miR-122 (Wang et al., 2012). miR-148/152 also targets IRS-1 (Xu et al., 2013). PI3k is targeted by miR-125b (Li et al., 2014) and miR-7 (Fang et al., 2012) and the EGFR is targeted by miR-27a (Wu et al., 2013) and miR-7 (Kalinowski et al., 2012). mTOR itself, through an unknown mechanism, can downregulate miR-125b. Each of these miR that target insulin/IGF-1/EGF-mTORC1 signaling components was found to be down-regulated in at least one type of cancer, thus allowing excessive mTORC1 activity (Fornari et al., 2010; Iwaya et al., 2012; Jia et al., 2011; Kalinowski et al., 2012; Li et al., 2014; Liu et al., 2012; Sun et al., 2013; Wang et al., 2012; Xu et al., 2013; Yu et al., 2015; Zhu et al., 2008).

The negative regulator of the insulin/mTORC1 pathway, PTEN, is also targeted by miRs, including miR-221 (Xue et al., 2013), miR-19 (Liang et al., 2011; Olive et al., 2009), miR-205 (Cai et al., 2013), miR-17-92 (Danielson et al., 2013; Wu et al., 2012), miR-29 (Tumaneng et al., 2012), miR-519d (Fornari et al., 2012), miR-21 (Dey et al., 2012; Meng et al., 2006; Small et al., 2010; Zhou et al., 2013), miR-718 (Xue et al., 2014), and miR-93 (Fu et al., 2012). Each of these miR are up-regulated in various cancerous cells, effectively removing PTEN from its function as an insulin/IGF-1-mTORC1 negative regulator (Cai et al., 2013; Fornari et al., 2012; Fu et al., 2012; Hayashita et al., 2005; Meng et al., 2006; Mott et al., 2007; Oh et al., 2011; Olive et al., 2009; Tumaneng et al., 2012; Xue et al., 2014; Xue et al., 2013).

mTORC1 regulation by low cellular energy levels

Energy levels regulate the growth factor-stimulated mTORC1 protein synthesis pathways through 5' adenosine monophosphate-activated protein kinase (AMPK) (Bolster et al., 2002; Steinberg and Kemp, 2009). The optimal ATP/AMP ratio in cells is 100:1 (Hardie et al., 1998). Cellular stresses, such as pathogens (Shaw et al., 2004), reactive oxygen species (Emerling et al., 2009; Shaw et al., 2004), hypoxia (Corton et al., 1994; Horman et al., 2002; Shaw et al., 2004), and glucose deprivation (Shaw et al., 2004), result in decreased ATP production (Horman et al., 2002; Lau et al., 2004; O'Malley et al., 2003; Sofer et al., 2005) and thus increased AMP levels (Corton et al., 1994). In muscle cells, ischemia (Fogarty and Hardie, 2010) and endurance exercise (Atherton et al., 2005; Dreyer et al., 2006; Rivas et al., 2009) also reduce the ATP/AMP ratio (Fogarty and Hardie, 2010). Reduced ATP/AMP ratios activate AMPK which then inhibits anabolic pathways (Oakhill et al., 2010), including m-TOR-dependent protein synthesis, to conserve cellular energy (Aguilar et al., 2007; Bolster et al., 2002; Cheng et al., 2004; Corton et al., 1994; Dreyer et al., 2006; Gwinn et al., 2008; Kimura et al., 2003; Steinberg and Kemp, 2009). In muscle cells, endurance training exercise initiates AMPK signaling and depresses mTORC1 signaling (Atherton et al., 2005), while intense resistance

exercise depresses AMPK activity and initiates mTORC1 signaling, resulting in muscle hypertrophy (Goodman et al., 2011).

AMPK consists of three subunits, the catalytic alpha subunit (Carling et al., 1989) and the regulatory beta and gamma subunits (Cheung et al., 2000; Davies et al., 1994). The presence of glycogen (an energy source) allosterically inhibits AMPK by binding to the regulatory beta subunit (McBride et al., 2009), whereas the ATP/AMP ratio regulates AMPK through the regulatory gamma subunit. When ATP levels are high, AMPK is distributed in the cytosol (Oakhill et al., 2010), the gamma subunit is bound to two molecules of ATP, and AMPK is only active at a basal level (Scott et al., 2004). When cellular stresses decrease the ATP/AMP ratio, myristoylated AMPK binds cellular membranes where the AMPK substrates are located, AMP displaces ATP from the gamma subunit of AMPK (Cheung et al., 2000; Scott et al., 2004), and AMPK is activated by three methods (Hardie, 2004). First, AMP binding to AMPK results in increased phosphorylation of the alpha subunit of AMPK on threonine 172 by liver kinase B1 (LKB1) associated with the Ste20-related adaptor protein (STRAD) and the scaffolding protein mouse protein 25 (MO25) (Boudeau et al., 2003; Hawley et al., 2003). LKB1 activates AMPK at least 50-fold (Hardie, 2004; Hawley et al., 1996; Hawley et al., 1995; Oakhill et al., 2010; Shaw et al., 2004). After threonine 172 phosphorylation (Oakhill et al., 2010), AMP allosterically increases AMPK activation (Ferrer et al., 1985; Oakhill et al., 2010) up to 5-fold more (Carling et al., 1989; Hawley et al., 1995). Finally, AMP binding to AMPK prevents protein phosphatases from dephosphorylating threonine 172 (Davies et al., 1995; Hardie, 2004).

In response to energy depletion, AMPK switches off energy consuming processes such as protein synthesis to conserve ATP (Choo et al., 2010; Steinberg and Kemp, 2009). AMPK regulates mTORC1-dependent protein synthesis through phosphorylation of several different proteins that affect this pathway. AMPK phosphorylates protein phosphatase 2A (PP2A), which then dephosphorylates serine 473 of Akt, thereby inactivating mTORC1 signaling (Kim et al., 2009b). AMPK phosphorylates TSC2 threonine 1227 and serine 1345, which activate TSC2, an

inhibitor of mTORC1 signaling (Inoki et al., 2003). AMPK directly inactivates mTORC1 signaling by phosphorylating mTOR threonine 2446 (Cheng et al., 2004). AMPK also phosphorylates the positive regulator of mTORC1, Raptor, on serines 722 and 792, which inactivate Raptor via 14-3-3 binding (Gwinn et al., 2008). Phosphorylation of each of these substrates decreases mTORC1-dependent protein synthesis through decreased phosphorylation of 4E-BP at threonines 37 and 46 (Dreyer et al., 2006; Shaw et al., 2004) and S6k threonine 412 (Kimura et al., 2003; Shaw et al., 2004).Decreased 4E-BP phosphorylation results in decreased translation initiation, while decreased S6k phosphorylation results in decreased translational capacity. In addition, AMPK phosphorylates eEF2 kinase, which phosphorylates and inhibits eEF2 (Horman et al., 2002), resulting in decreased translation elongation.

Non-glucocorticoid regulation of mTORC1 in response to stress

Stressors such as hypoxia, oxidants, inflammation, and an excess of fatty acids decrease mTORC1 signaling by contributing to endoplasmic reticulum (ER) stress and the unfolded protein response (UPR) (Khan and Wang, 2014). The UPR is a consequence of insufficient functioning of the ER, and can result in activation of JNK (Khan and Wang, 2014; Urano et al., 2000), which negatively regulates mTORC1 signaling through phosphorylation of IRS-1 at serine 307 (Hirosumi et al., 2002; Khan and Wang, 2014). ER stress also results in activation of NFκB, which can negatively regulate mTORC1 signaling through down-regulation of mTOR transcription (Park et al., 2009).

Mstn properties, signaling, and regulation

Mstn

In adult muscle cells, Mstn regulates fiber size (Zimmers et al., 2002) by limiting protein synthesis (Amthor et al., 2009; Lee et al., 2012; Sartori et al., 2014; Sartori et al., 2009) and increasing protein degradation (Sartori 2014, Han 2013). Mstn is a member of the TGFβ superfamily, containing all of the identifying characteristics of this family, including a signal sequence, an RXXR proteolytic processing site, and a conserved pattern of cysteine residues

(McPherron et al., 1997). Mstn is translated into the Mstn prepropeptide, which has an N-terminal signal sequence that targets Mstn for secretion (Lee, 2004). In addition, the Mstn prepropeptide contains an RXXR sequence, which is cleaved by furin, creating an N-terminal Mstn propeptide and a C-terminal fragment that dimerizes (McPherron et al., 1997) to form the mature peptide (Lee, 2004). Mstn is found in all metazoans (Herpin et al., 2004), and the mature peptide is highly conserved, with 100% amino acid identity between human, rat, mouse, pig, turkey and chicken protein sequences (McPherron et al., 1997). The Mstn propeptide is essential for proper folding, dimerization and secretion of the mature peptide (McFarlane et al., 2005). In addition, the Mstn propeptide non-covalently associates with the mature peptide, creating a latent complex (Lee and McPherron, 2001).

Mstn promoter

The Mstn promoter was first analyzed in humans (Ma 2001). To date, several Mstn gene promoters have been analyzed and compared, including at least nine mammals (Allen and Du, 2008; Deng et al., 2012; Du et al., 2011; Du et al., 2005; Grade et al., 2009; Li et al., 2012b; Ma et al., 2001; Singh et al., 2014; Spiller et al., 2002), one marsupial (Grade et al., 2009), one reptile (Grade et al., 2009), five birds (Grade et al., 2009; Gu et al., 2004), one amphibian (Grade et al., 2009), nine fish (Funkenstein et al., 2009; Galt et al., 2014; Grade et al., 2009; Kerr et al., 2005; Li et al., 2012a; Nadjar-Boger et al., 2012; Nadjar-Boger et al., 2013), two mollusks (Guo et al., 2012; Hu et al., 2010) and one crustacean (Kim et al., 2009a). All of these Mstn promoters contained at least one TATA box and one CAAT box in their core promoter sequence, except no TATA box was found in the bay scallop, *Argopecten irradians* (Guo et al., 2012). All Mstn promoters contained one to sixteen E boxes, which are binding sites for muscle-specific transcription factors (Du et al., 2011; Du et al., 2005; Funkenstein et al., 2009; Gu et al., 2004; Guo et al., 2012; Hu et al., 2010; Kerr et al., 2005; Kim et al., 2009a; Li et al., 2012a; Li et al., 2012b; Ma et al., 2001; Nadjar-Boger et al., 2012; Nadjar-Boger et al., 2013; Singh et al., 2014; Spiller et al., 2002). Glucocorticoid response elements (GREs)nwere identified in the Mstn

promoters of humans (Ma et al., 2001), sheep (Du et al., 2005), goats (Singh et al., 2014), and three fish species (Kerr et al., 2005; Nadjar-Boger et al., 2012; Nadjar-Boger et al., 2013), but pig (Deng et al., 2012) and rainbow trout (Galt et al., 2014) Mstn promoters did not contain GREs. Androgen response elements were identified in the Mstn promoters of humans (Ma et al., 2001) and three fish species (Kerr et al., 2005; Nadjar-Boger et al., 2012; Nadjar-Boger et al., 2013). In addition, cAMP response element (CRE), which is bound by cAMP response element binding (CREB) protein, was identified in several Mstn promoters (Deng et al., 2012; Grade et al., 2009; Ma et al., 2001; Nadjar-Boger et al., 2012; Nadjar-Boger et al., 2013).

History of Chalones/Mstn as a Chalone

In 1916, Schafer coined the term chalone (from the Greek word "to slacken") to describe "an endocrine product which inhibits or diminishes activity (Shafer, 1916). Simms published experiments that a substance produced by the liver inhibits cell division in the liver (Simms and Stillman, 1937), but did not call it a chalone (Elgjo and Reichelt, 2004; Saetren, 1956). Bullough appears to be the first researcher to use the term chalone, since Shafer in 1916 (Bullough et al., 1964; Bullough and Laurence, 1964). Bullough defined a chalone as a tissue-specific inhibitor of cell division that acts on the tissue from which it originates in a negative feedback system (Bullough, 1965). In the late 1960s and early 1970s, several chalones were described (Bichel, 1973; Brugal and Pelmont, 1975; Chopra and Simnett, 1969; Clermont and Mauger, 1974; Dewey, 1973; Florenti et al., 1973; Froese, 1971; Hinderer et al., 1970; Houck et al., 1971; Kivilaak.E and Rytomaa, 1971; Moorhead et al., 1969; Philpott, 1971; Rytomaa and Kiviniem.K, 1968; Simnett et al., 1969; Verly, 1973; Voaden, 1968), but conflicting results and an inability to purify a single chalone substance (Barfod and Bichel, 1976; Boldingh and Laurence, 1968; Brandt and Grosse, 1992; Lehmann et al., 1989; Rytomaa and Kiviniem.K, 1968), resulted in skepticism of the existence of chalones (Elgjo 2004). However, in 1982, a pentapeptide chalone was finally purified that inhibits myeloid cells (Paukovits and Laerum, 1982). Several other tissue-specific chalones, consisting of three to ten peptides each, were purified soon after (Elgjo

and Reichelt, 1984; Gembitsky et al., 1998; Gianfranceschi et al., 1994; Lenfant et al., 1989; Lindenskov et al., 2002; Liu et al., 2000; Paulsen et al., 1987; Skraastad et al., 1987). However, "chalone" was not applied to these peptides, probably due to the skepticism associated with the word (Elgjo and Reichelt, 2004). At least some, and maybe all, of these peptide chalones bind G-protein coupled receptors to initiate signaling (Elgjo and Reichelt, 1994; Elgjo and Reichelt, 2004; Laerum et al., 1990; Liu et al., 2003).

Mstn was discovered in 1997 (McPherron et al., 1997), and found to inhibit muscle growth (McPherron et al., 1997; McPherron and Lee, 1997). McKnight proposed that Mstn is a muscle chalone (McKnight, 1997), and several authors have used this term for Mstn, indicating that Mstn limits muscle growth (Braulke et al., 2010; Ciarmela et al., 2010; Druet et al., 2014; Finsterer, 2014; Georges, 2010; Gokoffski et al., 2011; Han et al., 2010; Lander, 2011; Long et al., 2009; Mak and Cheung, 2009; Szent-Györgyi, 2010; Wang et al., 2014b; Zhang, 2008). However, in Shafer's definition, a chalone can "diminish activity" or modulate excessive growth of a tissue, in addition to inhibiting growth (Shafer, 1916). Several authors have described Mstn as a chalone that modulates the effects of growth-promoting factors such as androgens (Dubois et al., 2012; Dubois et al., 2014) and IGF-1 (Chien et al., 2013; Garikipati and Rodgers, 2012; Kawada and Ishii, 2009; Marcotte et al., 2014; Matsakas et al., 2006; Paoli et al., 2015; Price et al., 2011; Yang et al., 2007; Zhou et al., 2015). Androgens directly upregulate Mstn transcription via the androgen receptor (Dubois et al., 2014). In cultured skeletal myoblasts, IGF-1 upregulates Mstn transcription through cAMP response element binding (CREB) to the CREB response element (CRE) in the Mstn promoter (Valdes et al., 2013; Zuloaga et al., 2013). These data indicate that Mstn is both an inhibitor of growth and a moderator of excessive growth. As an inhibitor of growth, we would expect increased levels of Mstn to prevent growth. As a moderator of excessive growth, we would expect increased levels of Mstn in growth-promoting situations to moderate the effects of the growth-promoting factor.

Mstn signaling

Some cell studies have reported that cleavage of the Mstn prepropeptide by furin occurs in the Golgi apparatus and that the latent complex is secreted (Harrison et al., 2011; Lee, 2004; McFarlane et al., 2005; Sharma et al., 2015), but Anderson reported that in muscle tissue, the Mstn prepropeptide is secreted, with cleavage by furin in the extracellular matrix (EM) at the time of signal activation (Anderson et al., 2008) (Fig. 1.6). Whether secreted in the form of the prepropeptide (with signaling sequence removed) or secreted as the latent complex, Mstn is covalently bound to the EM via latent TGFβ-binding proteins (LTBPs). Thus, the majority of Mstn is retained in the muscle tissue where it is secreted, allowing localized activation of Mstn (Anderson et al., 2008; Harrison et al., 2011). After furin cleavage, the latent Mstn complex is activated by Bone Morphogenetic protein-1/Tolloid (BMP/TLD) metalloproteases that cleave the propeptide and release the mature peptide dimer (Wolfman et al., 2003). Some Mstn circulates in the blood, where more than 70% is bound to the propeptide in a latent complex (Hill et al., 2002).

Activated Mstn binds the Activin receptor type IIB (ACTRIIB), which then forms a dimer with Activin receptor type I (ACTRI) (Lee and McPherron, 2001; MacDonald et al., 2014; Morrison et al., 2009; Tsuchida et al., 2006) (Fig. 1.7). This allows the constitutively active ACTRIIB to phosphorylate serines in the glycine serine (GS) domain of ACTRI (Herpin et al., 2004). Phosphorylated ACTRI can no longer be inhibited by FK506-binding protein 12 (FKBP12) (Herpin et al., 2004), and phosphorylates Smad 2 or Smad 3 on the second and third serines (Abdollah et al., 1997) of the C-terminal SSXS motif (Ikushima and Miyazono, 2011; Mehra and Wrana, 2002). Smad is a meshing of the names of two proteins—SMA (*Caenorhabditis elegans* Small body size) and MAD (*Drosophila* Mothers Against Decapentaplegic). Smads contain N-terminal MAD-homology 1 (MH1) and C-terminal MAD-homology 2 (MH2) globular domains, separated by a linker domain (Massague et al., 2005). The MH2 domain functions in protein-protein interactions, and the MH1 domain functions in

nuclear localization, DNA binding and interactions with other transcription factors (Macias et al., 2015; Mehra and Wrana, 2002). Receptor-regulated Smads (R-Smads), which include Smad2 and Smad 3, are localized to the membrane for ACTRI phosphorylation by the proteins Smad anchor for receptor activation (SARA) (Macias et al., 2015; Tsukazaki et al., 1998) and hepatic growth factor-regulated tyrosine kinase substrate (Hgs) (Macias et al., 2015; Miura et al., 2000). Both SARA and Hgs bind the MH2 domain of Smad2/3 and contain FYVE zinc-finger domains, which bind PI3P in the membrane (Macias et al., 2015; Miura et al., 2000), thus localizing Smad to the vicinity of the ACTRI (Macias et al., 2015; Mehra and Wrana, 2002). Once phosphorylated by the ACTRI, Smad forms a hetero-trimer of two Smad2 or two Smad3 with a Smad4 (Macias et al., 2015; Massague, 2012). Smad4 is a common mediator Smad (Co-Smad) that lacks the SSXS motif, but contains the MH1 and MH2 domains (Macias et al., 2015; Massague, 2012). R-Smads and Co-Smads continuously shuttle between the cytoplasm and the nucleus, whether stimulated by Mstn or not (Hill, 2009). However, with Mstn signaling, the Smad complexes remain in the nucleus longer, through increased nuclear tethering and decreased nuclear export (Hill, 2009). In the nucleus, the Smad heterotrimer complex is phosphorylated in the linker region by cyclin-dependent kinases 8 and 9 (CDK 8/9), which increase Smad transcriptional activity by increasing the interaction of Smad with coactivators (Macias et al., 2015). The Smad complex binds the Smad binding element (SBE), sequence (C)AGAC, and AP-1 sites TGA(G/C)TCA (Koinuma et al., 2009) with low affinity, but require additional DNA-binding factors for high-affinity DNA binding (Ross and Hill, 2008) to regulate the transcriptional activity of hundreds of genes (Koinuma et al., 2009; Massague et al., 2005). Transcription factor AP-2 (TFAP2A) and v-ets erythroblastosis virus E26 oncogene homolog (ETS) are two transcription factors that assist Smads in implementing the TGFβ signal (Koinuma et al., 2009).

Regulation of Mstn signaling

Growth and differentiation factor-associated serum protein-1 (GASP-1) can regulate Mstn activity by reversibly binding to the Mstn mature dimer (Hill et al., 2003). Follistatin or the follistatin related gene (FLRG) permanently inactivate Mstn by binding the mature dimer and preventing Mstn from binding to the ACTRII (Hill et al., 2002; Lee and McPherron, 2001). Follistatin and FLRG may be responsible for terminating Mstn signaling after Mstn has bound the ACTRII (Hill et al., 2002; Lee, 2004).

The continuous shuttling of Smads between the cytoplasm and the nucleus has been proposed as a mechanism that allows continuous monitoring of the ACTRI signaling activity (Hill, 2009; Inman et al., 2002). When ACTRI is no longer stimulated by ligand, the majority of Smad is re-distributed to the cytoplasm (Hill, 2009). Protein phosphatase, Mg^{2+}/Mn^{2+}-dependent, 1A (PPM1A) has been reported to dephosphorylate the SSXS motif of R-Smads, thus terminating signaling (Lin et al., 2006; Macias et al., 2015). Further reports by the same group of scientists indicate that PPM1A dephosphorylates Ran-binding protein 3 (RanBP3), resulting in increased nuclear export of Smads (Dai et al., 2011). However, in this report, there was no further mention of Smad dephosphorylation by PPM1A (Bruce and Sapkota, 2012; Dai et al., 2011). Mstn signaling is also terminated when Glycogen Synthase Kinase 3 beta (GSK3β) phosphorylates the R-Smad linker region, resulting in ubiquitination and proteasome degradation of the R-Smads (Macias et al., 2015).

Mstn signaling through R-Smads increases expression of Smad7, an inhibitory Smad (I-Smad), which results in negative feedback of Mstn signaling (Mehra and Wrana, 2002; Sharma et al., 2015). Smad7 inhibits Mstn signaling by recruiting protein phosphatase 1 to dephosphorylate the ACTRI (Hill, 2009; Mehra and Wrana, 2002; Shi et al., 2004), and by recruiting the Smad-specific E3 ubiquitin protein ligase (Smurf) to promote degradation of the ACTRI by the proteasome (Ebisawa et al., 2001; Kavsak et al., 2000; Massague, 2012; Shi and

Massague, 2003). Mstn signaling is also terminated by R-Smad-dependent expression of miR-27a/b in a negative feedback loop that targets Mstn for degradation (McFarlane et al., 2014).

Mstn signaling and the mTORC1-dependent protein synthesis pathway

There is crosstalk between the Mstn signaling pathway and the IGF/mTORC1-dependent protein synthesis pathways. The IGF/mTORC1-dependent protein synthesis pathway inhibits Mstn signaling. Activated Akt directly interacts with Smad3, forming a complex that sequesters Smad 3 in the cytoplasm, and inhibits Smad3 phosphorylation (Conery et al., 2004; Remy et al., 2004; Sartori et al., 2014). Akt also inhibits Smad3 through mTORC1 signaling (Song et al., 2006; Welle et al., 2009), and Akt results in decreased expression of the ACTRIIB (Sartori et al., 2009). The presence of amino acids, required for the mTORC1 pathway, increase the expression of several microRNA that target Mstn, including miR-27a (Chen et al., 2013; Sharma et al., 2015), miR-499, and miR-208b (Chen et al., 2013; Drummond et al., 2009b; Sharma et al., 2015). Likewise, activated R-Smads inhibit the IGF/mTORC1 pathway (Sartori et al., 2014). Phosphorylated R-Smads decrease Akt phosphorylation through an unknown mechanism (Allen et al., 2009; McFarlane et al., 2006; Sartori et al., 2014; Trendelenburg et al., 2009). Decreased Akt phosphorylation results in decreased forkhead boxO 1 (FOXO1) phosphorylation, which allows FOXO1 to enter the nucleus and increase the transcription of MAFbx, an atrogene, that targeting some mTOR signaling components for proteasomal degradation (McFarlane et al., 2006; Sartori et al., 2009). Smad3 negatively regulates miRNA-29 (Goodman et al., 2013; Sartori et al., 2014) and miRNA-486 (Hitachi et al., 2014; Sartori et al., 2014), both of which target PTEN. Thus Smad3 allows PTEN to negatively regulate the mTORC1-dependent protein synthesis pathway (Goodman et al., 2013; Hitachi et al., 2014; Sartori et al., 2014), resulting in decreased phosphorylation of both 4E-BP and S6 in mammals (Amirouche et al., 2009) and fish (Seiliez et al., 2013).

Muscle atrophy

Vertebrate muscle atrophy

Internal and external environmental stimuli maintain or alter muscle mass through regulation of protein synthesis and protein degradation (Phillips et al., 2012; Phillips et al., 2009; Schiaffino et al., 2013). Nutrition, energy levels, muscle activity, aging, many diseases, and growth-promoting factors affect muscle mass (Egerman and Glass, 2014; Rodriguez et al., 2014; Sartori et al., 2014; Schiaffino et al., 2013) through altered production or degradation of myofibrils (Sandri, 2008). Stimuli that produce muscle hypertrophy can result from both decreased protein degradation and increased protein synthesis, increased protein synthesis (Schiaffino et al., 2013), or decreased protein degradation (Piccirillo and Goldberg, 2012). Likewise, stimuli that produce muscle atrophy can decrease protein synthesis and increase protein degradation (Li and Goldberg, 1976; Schiaffino et al., 2013), decrease protein synthesis and degradation (Phillips et al., 2009), decrease protein synthesis only (Argadine et al., 2009; Emery et al., 1984; Lundholm et al., 1982; Quy et al., 2013; Schiaffino et al., 2013) or increase protein synthesis and protein degradation (Argadine et al., 2009; Argadine et al., 2011; Goldspink, 1976). Increased protein synthesis during atrophy allows remodeling of muscle fibers to accommodate altered muscle use (Bassel-Duby and Olson, 2006; Mykles and Medler, 2015). The specific muscle response depends on the species, the stimulus, the specific muscle, and the muscle fiber type.

Activation of the mTORC1 pathway is primarily responsible for increased protein synthesis in muscle tissue (Amirouche et al., 2009), while activated Mstn is the primary inhibitor of mTORC1-dependent protein synthesis (Goodman et al., 2013; Hitachi et al., 2014; Hulmi et al., 2013; Sakuma et al., 2014; Sartori et al., 2014; Schiaffino et al., 2013; Welle et al., 2009). Inhibition of Akt phosphorylation results in decreased mTORC1-dependent protein synthesis and can result in increased protein degradation due to activation of Forkhead Box O (FOXO) transcription factors (Lokireddy et al., 2011). FOXO transcription factors induce expression of

28

MuRF1, an E3 ligase that tags myosin light chain and myosin heavy chain myofibrils for proteasome degradation (Cohen et al., 2009; Cohen et al., 2015).

Glucocorticoid effect on vertebrate muscle mass in response to stress

Glucocorticoid signaling results in rapid muscle loss and decreased myofibrillar size (Piccirillo et al., 2014; Qin et al., 2013). Glucocorticoids contribute to muscle atrophy by decreasing synthesis of muscle proteins, primarily by inhibiting mTORC1 signaling (Bodine and Furlow, 2015), thus redirecting the cell's energy into glucose production (Braun and Marks, 2015). Decreased mTORC1 signaling is achieved by decreasing the availability of amino acids in muscle cells, decreasing insulin and IGF1 levels, and decreasing PI3K activity (Bodine and Furlow, 2015). In addition, glucocorticoids increase the transcription of genes that inhibit mTORC1 signaling, such as REDD1, Mstn and specific miR (Bodine and Furlow, 2015).

In response to inflammation or stress, hypothalamic and anterior pituitary signaling result in the release of glucocorticoids (GCs) from the adrenal cortex. In the traditional pathway of glucocorticoid activation, glucocorticoids bind the glucocorticoid receptor (GR) in the cytoplasm of the target cell, then the activated GR translocates to the nucleus (Kuo et al., 2012; Yamamoto, 1985). In the nucleus, the GR becomes a transcription factor by binding glucocorticoid response elements (GREs) of the DNA of target genes, and either increasing or decreasing transcription of these genes (Kuo et al., 2012; Yamamoto, 1985). In addition to the traditional pathway, the ligand-bound GR can physically interact with some proteins, thereby altering their activity. Glucocorticoid activity results in the breakdown of carbohydrates, fats and proteins (including muscle myofibrillar proteins), which increases blood glucose levels to combat the stressful situation (Braun and Marks, 2015; Goldberg et al., 1980; Kuo et al., 2012; Lofberg et al., 2002; Sapolsky et al., 2000; Schakman et al., 2008; Tomas et al., 1979). Glucocorticoids also inhibit anabolic processes such as muscle protein synthesis to conserve energy (Braun and Marks, 2015; Goldberg et al., 1980; Kuo et al., 2012; Lofberg et al., 2002; Sapolsky et al., 2000; Tomas et al., 1979). In situations of chronic stress or inflammation, prolonged glucocorticoid

signaling results in muscle atrophy due to decreased protein synthesis and increased protein degradation (Braun and Marks, 2015). Glucocorticoid regulation of protein synthesis will be the focus in this section, but the mechanisms of glucocorticoid-induced protein degradation will be briefly addressed next.

Glucocorticoids increase protein degradation in vertebrate muscle through up-regulation of the lysosomal, calpain and ubiquitin proteosomal catabolic pathways (Schakman et al., 2013), which is dependent on Mstn (Allen and Loh, 2011; Braun and Marks, 2015; Gilson et al., 2007; Ma et al., 2003). The first change noted after glucocorticoid administration is increased expression of cathepsin L (Komamura et al., 2003), a lysosomal hydrolytic enzyme whose upregulation is associated with muscle atrophy (Hasselgren and Fischer, 2001). Glucocorticoids also increase the expression of calpains, which are proteases that release myofilaments from the sarcomere (Hasselgren and Fischer, 2001; Schakman et al., 2008). The released myofilaments are then degraded by the ubiquitin proteasomal system (UPS) (Hasselgren and Fischer, 2001; Schakman et al., 2008). Glucocorticoids stimulate the expression of UPS components, including muscle-specific RING-finger protein 1 (MuRF1), which is an E3 ligase (Bodine et al., 2001; Braun and Marks, 2015; Mitch and Goldberg, 1996; Schakman et al., 2013). The glucocorticoid/GR complex increases MuRF1 transcription by directly binding the GRE of MuRF1, and by stimulating expression of Kruppel-like factor 15 (KLF15), a transcription factor that increases MuRF1 expression. MuRF1 ubiquinates myofibrils, preferentially myosin light chain and myosin heavy chain type II (MHCII) fibers, marking them for degradation by the proteasome (Cohen et al., 2009; Cohen et al., 2015). Thus, chronic stress or inflammation results in muscle atrophy as glucocorticoids break down muscle proteins to continuously supply the blood with elevated glucose levels via gluconeogenesis. Glucocorticoids preferentially cause atrophy of fast-twitch, type II, glycolytic muscle fibers (Bodine and Furlow, 2015; Schakman et al., 2013) containing MHCII. The preference of MuRF1 for ubiquitinating MHCII may help explain why type II muscle fibers are more susceptible to atrophy by glucocorticoids.

Glucocorticoids regulate the growth factor-stimulated mTORC1 protein synthesis pathway at several junctures. Muscles require an abundant supply of leucine (See mTORC1 regulation by amino acids section), which is one of the three branched chain amino acids (BCAAs). KLF15, transcriptionally upregulated by glucocorticoids, activates transcription of branched chain amino transferase 2 (BCAT2) (Braun and Marks, 2015). BCAT2 degrades BCAAs (Braun and Marks, 2015), thus reducing the substrates required for mTORC1-dependent protein synthesis. Inhibition of IGF transcription (Delany et al., 2001) eliminates the main activator of mTORC1-dependent protein synthesis. Glucocorticoids can inhibit the expression of IRS-1 (Morgan et al., 2009), increase the degradation of IRS-1 (Bodine and Furlow, 2015; Braun and Marks, 2015; Morgan et al., 2009; Schakman et al., 2013) or tag IRS-1 for degradation (Koh et al., 2013; Schakman et al., 2013) by stimulating dephosphorylation of IRS-1 on tyrosine 612 (Schakman et al., 2013) or causing phosphorylation of IRS-1 on serine 307 (Morgan et al., 2009). Glucocorticoid-induced transcriptional activation of p85α, the regulatory subunit of PI3K, prevents the interaction of PI3K with IRS-1, thus inhibiting insulin/IGF activation of mTORC1 signaling (Kuo et al., 2013; Schakman et al., 2013). The ligand-bound GR also physically interacts with p85α, increasing the ability of p85α to inhibit PI3K signaling (Hu et al., 2009; Schakman et al., 2013).

Glucocorticoids decrease protein synthesis by increasing the expression of Mstn (Zhang et al., 2007) through direct binding of the glucocorticoid receptor to a GRE on the Mstn promoter (Ma et al., 2001; Qin et al., 2013). Glucocorticoids also upregulate transcription of the gene *regulated in development and DNA damage response* (*REDD1*) (Schakman et al., 2013; Wang et al., 2006), whose protein product interferes with the binding of the inhibitory protein 14-3-3 to TSC2 (DeYoung et al., 2008). This allows the TSC1/TSC2 complex to form and deactivate Rheb, thereby inhibiting mTORC1 signaling (Laplante and Sabatini, 2012; Schakman et al., 2013).

mTORC1 independent inhibition of protein synthesis occurs through the increased expression of KLF15, which increases the transcription of the muscle atrophy F-box (MAFbx) protein (Braun and Marks, 2015). MAFbx is an E3 ligase that ubiquinates and degrades eIF3-f, contributing to decreased initiation of protein translation (Braun and Marks, 2015).

Crustaceans and molting

Molting

Crustaceans grow in a step-wise fashion during the process of molting, when the hardened old exoskeleton is shed, and a soft new exoskeleton is expanded with water or air before rapidly hardening (Chang and Mykles, 2011; Hopkins, 2009). The molting process is initiated by increased production of ecdysteroids (molting hormones) by the Y organ (molting gland) (Covi et al., 2009; Skinner, 1985b). In *Gecarcinus lateralis*, the blackback land crab, ecdysteroid levels increase during premolt (McCarthy and Skinner, 1979) from approximately 10-20 pg/μl during intermolt to over 400 pg/μl (Covi et al., 2010). The major ecdysteroids in the blackback land crab are 20-hydroxyecdysone (20E) and Ponasterone A (Pon A), occurring in an approximately 3:1 ratio, respectively, during intermolt and most of premolt (McCarthy, 1982; McCarthy and Skinner, 1977b; McCarthy and Skinner, 1979). Five major stages of premolt, D_0-D_4, have been described (Drach, 1939), and Skinner applied these stages to *Gecarcinus lateralis* (Skinner, 1985b). During the D_0 stage, ecdysteroid levels begin to rise and changes in multiple tissues have been described (Mykles, 2001; Skinner, 1985b). However, it is not until the D_1 stage that these changes become irreversible and the crab becomes committed to molting (Chang and Mykles, 2011). Here, I will focus on the effects of ecdysteroids on claw muscle atrophy and limb regeneration (Covi et al., 2010). As thoracic muscle does not significantly change in mass or protein synthesis during premolt, it served as an internal control (Covi et al., 2010; Mykles, 1999).

Claw muscle during the molt cycle

The claw muscle in the decapod crustacean is a unique model to study a natural cycle of premolt atrophy followed by extensive growth immediately after ecdysis. The claw muscle atrophies during premolt to enable withdrawal of the claw muscle from the old exoskeleton at ecdysis (Mykles and Skinner, 1982a; Skinner, 1966). Concomitantly, there is increased synthesis of muscle proteins during the premolt atrophy to remodel the claw muscle (Covi et al., 2010; Skinner, 1965). In addition, there is no degeneration or fiber type switching during this atrophy (Mykles, 1997), as can occur in vertebrate muscle atrophy (Ciciliot et al., 2013; Sandri, 2008).

Dramatic atrophy of the claw closer muscles, 40% (Skinner, 1966) to 78% (Ismail and Mykles, 1992), occurs in response to increasing ecdysteroids, which enables withdrawal of the claw muscle from the old exoskeleton at ecdysis (Mykles and Skinner, 1982a; Skinner, 1966). The claw muscle is composed of slow (S1) fibers primarily, with some slow tonic (S2) fibers located centrally (Mykles, 1988; Mykles and Medler, 2015). Most of the claw muscle atrophy in response to increasing ecdysteroids occurs in the S1 fibers (Ismail and Mykles, 1992; Mykles and Medler, 2015; Mykles and Skinner, 1981). Ten-fold more actin filaments are degraded than myosin filaments (Mykles and Skinner, 1981; Mykles and Skinner, 1982a), resulting in a decrease in the actin:myosin ratio from 9:1 in intermolt crabs to 6:1 in premolt crabs (Mykles and Skinner, 1981; Mykles and Skinner, 1982a).

Protein synthesis of both myofibrillar (11-fold) and soluble (13-fold) proteins increase during premolt claw atrophy (Covi et al., 2010; Skinner, 1965). Increased protein synthesis is necessary to remodel the muscle structure, both for atrophy and for claw remodeling. Although premolt atrophy is necessary for successful ecdysis, the muscle must be prepared for rapid growth immediately following ecdysis to maximize muscle size in the newly enlarged exoskeleton of the chelae (Covi et al., 2010; Skinner, 1965).

IGF injection in *Cherax quadricarinatus*, the redclaw crayfish, resulted in increased protein synthesis in muscles (Richardson et al., 1997). In addition, insulin-like peptides, insulin-like growth factor binding proteins, and insulin binding proteins have been identified (Chandler et al., 2015), with several additional studies indicating that insulin-like peptides and IGFs are present in crustaceans (Chaulet et al., 2012; Chung, 2014; Davidson et al., 1971; Gutierrez et al., 2007; Kucharski et al., 1999; Kucharski et al., 2002; Richardson et al., 1997; Sanders, 1983a; Sanders, 1983b). Increased protein synthesis in the claw muscle is associated with decreased *Gl-Mstn* (Covi et al., 2010) and increased *Gl-Rheb* mRNA expression (MacLea et al., 2012). Taken together, these data indicate that the insulin-mTORC1 pathway functions similarly in crustaceans and vertebrates. Further, Mstn inhibits the insulin-mTORC1 protein synthesis pathway similarly in vertebrates and crustaceans. However, unlike vertebrates (Allen and Loh, 2011; Braun and Marks, 2015; Gilson et al., 2007; Ma et al., 2003; Schakman et al., 2013), atrophy occurs with decreasing Mstn levels, indicating that Mstn is not involved in stimulating protein degradation in the claw closer muscle (Covi et al., 2010). In crustaceans, calpains and the ubiquitin proteasome systems are responsible for muscle atrophy, in a Mstn-independent manner (Covi et al., 2010; Mykles and Medler, 2015).

Limb regeneration and growth during the molt cycle

In the process of autotomy, crustaceans release a limb at a preformed fracture plane, usually in response to an injured or trapped limb (Hopkins, 1993; Mykles, 2001; Skinner, 1985a). Basal growth occurs following autotomy, during which differentiation of a new limb occurs, including limb segmentation and muscle formation with functional synapses (Das and Durica, 2013; Govind et al., 1973; Hopkins, 1993). This growing limb, enclosed within a cuticular sac for protection, is called a limb bud (Hopkins, 1993). When basal growth is complete, limb bud growth is arrested until rising ecdysteroid levels during premolt stimulate proecdysial growth of the limb bud (Bliss, 1956; Emmel, 1910; Hopkins, 1993; Mykles, 2001; Skinner, 1985a; Skinner, 1985b; Skinner and Graham, 1970; Skinner and Graham, 1972). Proecdysial limb bud

growth can only occur during premolt, and consists mainly of protein synthesis in muscle cells,

leading to hypertrophic growth (Bliss, 1956; Hopkins, 1993; Mykles, 2001). At ecdysis, the limb

is withdrawn from the cuticular sac and becomes a fully functional limb (Mykles, 2001; Skinner,

1985a; Skinner, 1985b; Skinner and Graham, 1970).

Differential muscle response to ecdysteroids

The differential responses of these three muscle types—claw closer, limb bud, and

thoracic—are likely due to the expression of various combinations of ecdysteroid receptor

isoforms in the different muscles (Kim et al., 2005b; Wang et al., 2000). Three isoforms of Gl-

EcR (Das, 2014; Kim et al., 2005a; Kim et al., 2005b) and nine isoforms of Gl-RXR have been

identified in *G. lateralis* (Kim et al., 2005b). In summary, both claw closer muscle and limb bud

muscle respond to increasing ecdysteroids with increased protein synthesis. However, Limb bud

muscles rapidly increase in mass, while claw closer muscle atrophies, indicating that protein

degradation is much greater than protein synthesis in the claw closer muscle (Covi et al., 2010).

As Mstn mRNA levels decrease during claw muscle atrophy, it follows that Mstn does not signal

for increased protein degradation, as Mstn does in vertebrates. However, Mstn inhibits protein

synthesis in crustaceans, similar to its function in vertebrates (Covi et al., 2010).

The ecdysteroid receptor

The ecdysteroid receptor consists of a heterodimer of retinoid X receptor (RXR) and

ecdysone receptor (EcR) (Koelle et al., 1991; Yao et al., 1993). Both EcR and RXR are

members of the nuclear receptor (NR) superfamily (King-Jones and Thummel, 2005), containing

the six domains, A-F, consistent with this superfamily (Henrich, 2009; Moras and Gronemeyer,

1998). The A and B domains interact with other transcription factors, and thus are highly

variable between nuclear receptors (Henrich, 2009). The C domain is the DNA-binding domain

(DBD), and codes for a 66 to 68 amino acid sequence in all nuclear receptors that contains two

conserved cysteine-cysteine zinc fingers for DNA binding (Henrich, 2009; Robinson-Rechavi et

al., 2003). The D domain is the hinge domain, with some conserved areas that function in

dimerization. The E domain is a highly conserved ligand binding domain containing 12 alpha helices that form a ligand-binding pocket (Henrich, 2009; King-Jones and Thummel, 2005; Moras and Gronemeyer, 1998; Wurtz et al., 1996). Only some nuclear receptors have an F domain, which is a highly variable sequence with no known function (Henrich, 2009).

Ecdysteroids, including 20-hydroxyecdysone (20E) and ponasterone A, bind the ligand-binding pocket of EcR to initiate transcriptional signaling (Henrich, 2009; Hill et al., 2012). Ecdysteroids are unable to bind the ligand-binding pocket of RXR (Clayton et al., 2001; Hu et al., 2003). However, EcR must be heterodimerized with RXR for efficient ecdysteroid binding, as RXR stabilizes EcR in a conformation that allows ecdysteroid binding (Grebe et al., 2004; Henrich et al., 2009; Hu et al., 2003).

The ecdysteroid receptor shuttles between the cytoplasm and the nucleus, but is predominately located in the nucleus (Nieva et al., 2005; Spindler et al., 2009). Ecdysteroid receptors bind ecdysteroid response elements (EcREs) on DNA and repress transcriptional activity until transcription is activated by ecdysteroid binding (Henrich et al., 2009; Hu et al., 2003; Nakagawa and Henrich, 2009; Riddiford et al., 2001). Increased EcR/RXR binding to EcREs upon ecdysteroid signaling has also been noted (Cronauer et al., 2007; Spindler et al., 2009). In general, activated nuclear receptors can increase or decrease gene transcription (Moras and Gronemeyer, 1998).

In vertebrates, steroid response elements are usually palindromes, but can also be direct repeats (Aumais et al., 1996). Similarly, most EcREs that have been identified are imperfect or perfect palindromes separated by a spacer of one (Cherbas et al., 1991; Lehmann and Korge, 1995; Nishita, 2014; Riddihough and Pelham, 1987; Vögtli et al., 1998). A consensus sequence of (A/G)G(G/T)TCANTGA(C/A)C(C/T) (Cherbas et al., 1991; Nishita, 2014) consisting of a perfect or imperfect palindrome separated by one spacer nucleotide is currently used. However, additional functional sequences have been identified (Antoniewski et al., 1996; Gauhar et al., 2009; Lehmann and Korge, 1995; Nishita, 2014), including direct

repeats with no spacer (Antoniewski et al., 1996; D'Avino et al., 1995). Various ecdysteroid receptor isoform combinations (Mouillet et al., 2001) bind alternate EcREs with varying affinity, allowing a modulated response to ecdysteroid signaling (Beatty et al., 2006; Ozyhar and Pongs, 1993; Schauer et al., 2011; Wang et al., 1998).

Ecdysteroid heterologous cell cultures

Heterologous cell cultures in mammalian cells have been developed for ecdysteroid functional assays (Christopherson et al., 1992; Henrich et al., 2009). As mammalian cells have no endogenous ecdysteroids, exogenous ecdysteroids can be added for precise control of ecdysteroid levels (Christopherson et al., 1992; Henrich et al., 2009). Likewise, EcR DNA must be added to this system in order to form a functional ecdysteroid receptor, but RXR may or may not be added, as mammalian cells do express RXR (Henrich et al., 2009). In each of these systems, the EcR and/or RXR receptor proteins were modified to enhance DNA binding (Christopherson et al., 1992; No et al., 1996; Wyborski et al., 2001), enhance dimer interaction (Hoppe et al., 2000), or to substitute the A and B domains of EcR (Christopherson et al., 1992; Hoppe et al., 2000; Mouillet et al., 2001; No et al., 1996; Palli et al., 2003; Panguluri et al., 2006; Vaillancourt and Felts, 2003; Wyborski et al., 2001). As the RXR A/B domains are often inhibitory in mammalian cells (Beatty et al., 2006; Betanska et al., 2009; Henrich et al., 2009; Henrich et al., 2003; Hu et al., 2003; Palli et al., 2003; Palli et al., 2005; Tran et al., 2001), the RXR A/B domains were removed and replaced with the virion protein 16 (Vp16) activating domain (Betanska et al., 2009; Palli et al., 2003; Panguluri et al., 2006). Several mammalian cell lines have been used, including HeLa (Mouillet et al., 2001), 3T3 (Panguluri et al., 2006; Wu et al., 2004), Chinese hamster ovary (CHO) (Betanska et al., 2009; Palli et al., 2003; Vaillancourt and Felts, 2003; Wyborski et al., 2001), CV-1 (Hoppe et al., 2000; No et al., 1996), and Human embryonic kidney 293 (HEK293) (Christopherson et al., 1992; Vaillancourt and Felts, 2003). The first study of an ecdysteroid heterologous culture in mammalian cells found that 1 µM muristerone A (Mur A) was very effective at stimulating ecdysteroid receptor-dependent

transcription, and 1 µM ponasterone A (Pon A) was ~ 15% as effective as Mur A

(Christopherson et al., 1992). However, neither 1 µM 20E nor 1 µM α-ecdysone was able to

stimulate transcription (Christopherson et al., 1992). Subsequently, researchers mainly used 1-

10 µM Mur A (Betanska et al., 2009; Mouillet et al., 2001; No et al., 1996; Wyborski et al., 2001)

or 10 µM Pon A (Hoppe et al., 2000; Palli et al., 2003; Vaillancourt and Felts, 2003) to stimulate

EcR/RXR transcriptional activity.

Uca pugilator RXR and EcR

The first crustacean ecdysteroid receptors cloned were from *Uca pugilator*, the fiddler

crab (Chung et al., 1998; Durica and Hopkins, 1996; Durica et al., 2002). The DBD of EcR and

RXR was 76% and 82% conserved, respectively, with *Drosophila* (Durica and Hopkins, 1996).

Both the EcR and RXR DBD contain the two zinc fingers, identifying them as members of the

nuclear hormone superfamily (Durica and Hopkins, 1996). Four isoforms of RXR were

identified—all combinations of + or – 5 base pairs in the D domain, and + or – 33 amino acids in

the LBD (Durica et al., 2002; Wu et al., 2004). The DEF domains were cloned into a plasmid

containing the Vp16 activator and transfected into 3T3 cells (Wu et al., 2004). Each of the RXR

isoforms bound various EcREs with varying affinities however, only the +33 isoforms were able

to heterodimerize with EcR (Wu et al., 2004). When 3T3 cells were stimulated with Ponasterone

A, the -33 RXR isoforms were not transcriptionally activated, but the +33 isoforms were

activated 18-fold (Wu et al., 2004).

Measurement of molting

Molt stage can be determined by observation of maxilliped endopodite setal

development under 100X microscopy (Moriyasu and Mallet, 1986), but this can only be done

after the animal is dead. The R-index ((length of LB /carapace width) times 100) was developed

as a reliable external measure of molt stage for crabs which are still alive (Bliss, 1956; Bliss and

Boyer, 1964). The R-index is correlated to Drach's molt stages (Chang and Mykles, 2011; Covi

et al., 2010; Drach, 1939; Skinner, 1962; Skinner, 1985b) and allows determination of each

crab's progress through premolt. During basal growth, the R-value of a LB increases from 0 to approximately 10 (Mykles, 2011). During the D_0 stage of premolt, the R-value increases to about 16 (Mykles, 2011). At an R-value of about 17, the crab has reached the D_1 stage of premolt, which is irreversible, and the crab is committed to molting (Bliss, 1956; Mykles, 2011).

Manipulation of molting

Multiple leg autotomy (MLA) of 5 or more walking legs stimulates a precocious molt in many crustaceans (Skinner, 1985b), including *Gecarcinus lateralis* (Mykles, 2001). As limbs are fully regenerated only during premolt, a shortened intermolt allows the regeneration of a full set of walking legs sooner (Holland and Skinner, 1976; Skinner, 1985b; Skinner and Graham, 1972). By contrast, Limb bud autotomy (LBA) of one or more regenerating limbs inhibits premolt progress if done during the D_0 stage (at R-values of ~ 10 - 16 (Chang and Mykles, 2011; Holland and Skinner, 1976; McCarthy and Skinner, 1977a). Ecdysteroid levels fall back toward intermolt levels, and premolt progress is delayed for about three weeks, giving the crab time to regenerate the newly autotomized limb bud, thus allowing it to molt with a full set of walking legs (Chang and Mykles, 2011; Holland and Skinner, 1976; McCarthy and Skinner, 1977a). Limb buds will not regenerate before ecdysis if autotomized after reaching stage D_1 (an R-value of ~ 17 or higher), as the crab is already committed to molting, and it molts without a full set of legs (Chang and Mykles, 2011). Another way to initiate premolt is through removal of molt inhibiting hormone (MIH) (Mykles, 2011). MIH is produced and released in the eyestalks, travels in the hemolymph, and binds receptors on the Y organ to inhibit synthesis of ecdysteroids (Mykles, 2011). Therefore, eyestalk ablation (ESA) removes the major source of MIH, and allows the Y organs to synthesize ecdysteroids thus initiating premolt (Abramowitz and Abramowitz, 1940; McCarthy and Skinner, 1977b; Mykles, 2001).
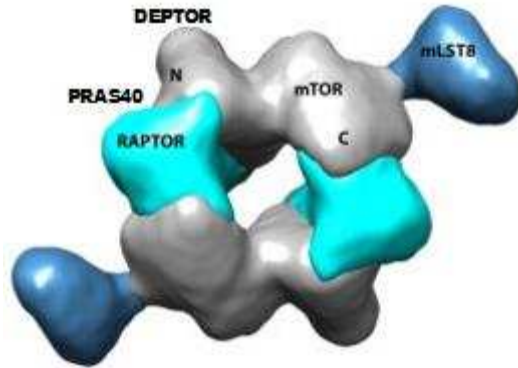
Fig. 1.1. A model of the mTORC1 dimer. The mTORC1 complex consists of two subunits each of mTOR, Raptor, mLST8, Deptor and PRAS40. The core activating subunits, mTOR, Raptor and mLST8 are shown in the model. Approximate binding sites of the inhibitory subunits, Deptor and PRAS40 are indicated. Deptor binds the FRB domain, located in the N-lobe of the mTOR kinase domain. PRAS40 binds Raptor through a TOS motif. Diagram modified from Baretic and Williams, 2014.
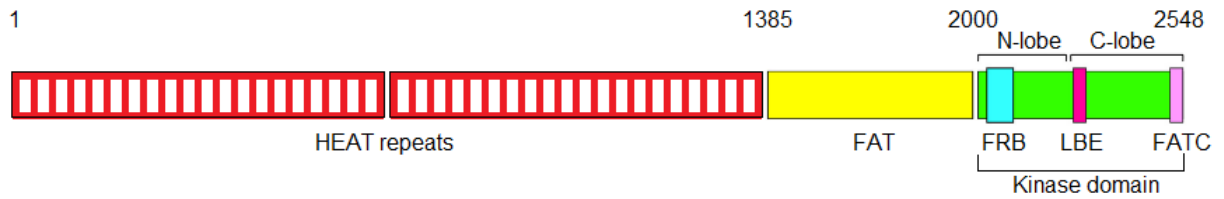
Fig. 1.2. mTOR domains. The major portion of the mTOR protein consists of HEAT repeats (red bars). The FAT domain (yellow) follows the HEAT repeats. The kinase domain (green) is divided into the FRB domain (turquoise) , the LBE domain (hot pink) and the FATC domain (light pink). Numbers at the top indicate amino acid residue number at the beginning and end of the major domains. Domains are not drawn to scale. Modified from Baretic and Williams, 2014 and Laplante and Sabatini, 2012.
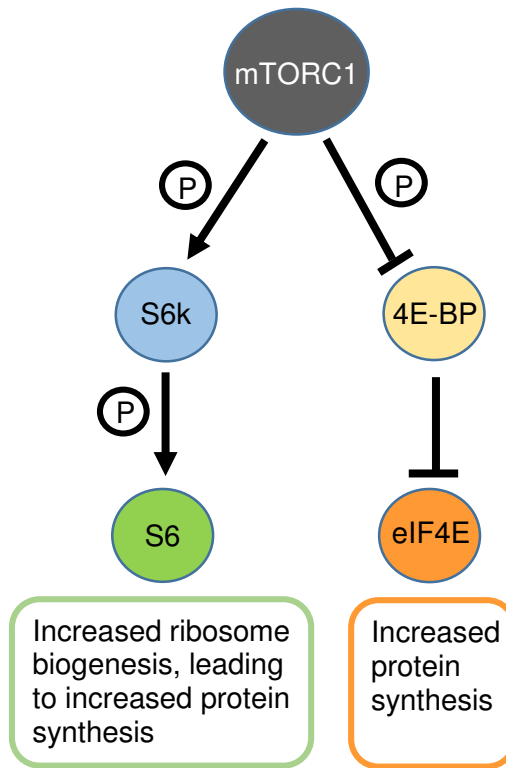
Fig. 1.3. Activated mTORC1 increases protein synthesis by phosphorylating S6k and 4E-BP. When S6k (blue) is phosphorylated (P inside circle) by mTORC1 (gray), S6k phosphorylates S6 (green). Phosphorylated S6 results in ribosome biogenesis, which allows increased translational capacity. mTORC1 phosphorylation of 4E-BP inhibits binding of 4E-BP to eIF4E. Released eIF4E can then participate in translation initiation, resulting in increased protein synthesis.
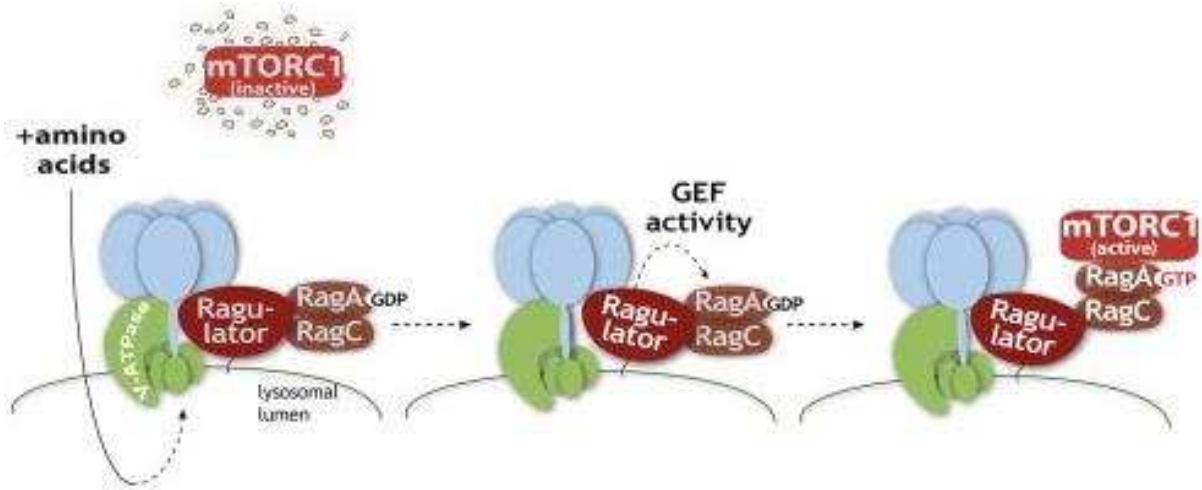
Fig. 1.4. Amino acid activation of mTORC1 through Ragulator. When lysosomal amino acid concentrations are low, V-ATPase is tightly bound to Ragulator, preventing the GEF activity of Ragulator. When lysosomal amino acid concentrations are high, V-ATPase dissociates from Ragulator, and the GEF activity of Ragulator activates RagA/B (RagA/B-GTP). Activated RagA/B localizes mTORC1 to the membrane where it can interact with Rheb. Diagram from Bar-Peled et al., 2012.
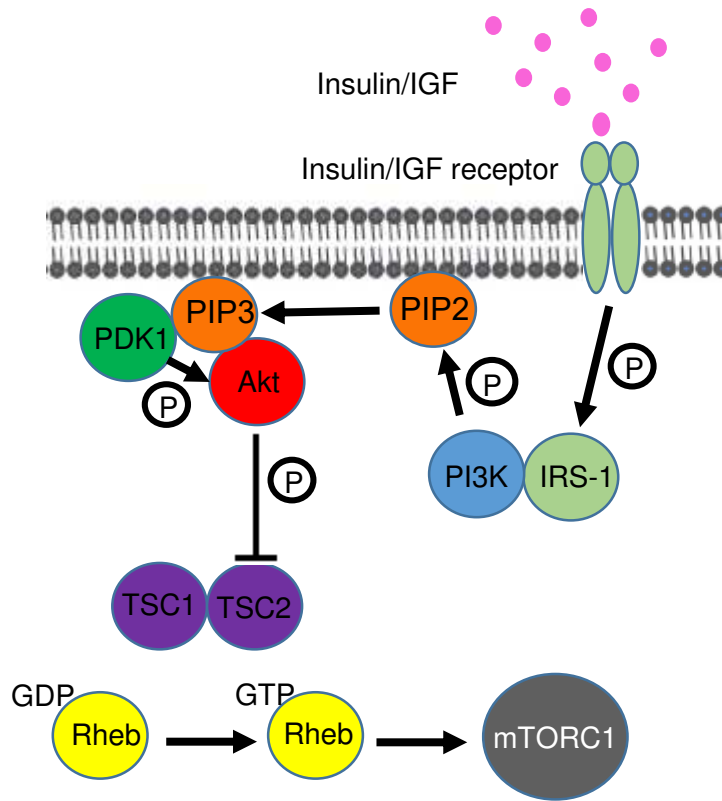
Fig. 1.5. Pathway for insulin/IGF1 activation of mTORC1. Insulin (pink) binding to the insulin receptor (light green) results in phosphorylation of IRS-1 (dark blue). Phosphorylated IRS-1 binds and activates PI3K (light blue). Activated PI3K phosphorylates PIP2 to PIP3 (orange). PIP3 binds PDK1 (green) and Akt (red), allowing PDK1 to phosphorylate and activate Akt. Phosphorylated Akt phosphorylates TSC2 (purple), causing inactivation of the TSC1/TSC2 complex. TSC1/TSC2 can no longer function as a Rheb GAP, so GTP-Rheb (yellow) levels are increased. GTP-Rheb activates mTORC1. Modified from Huang and Fingar, 2014.
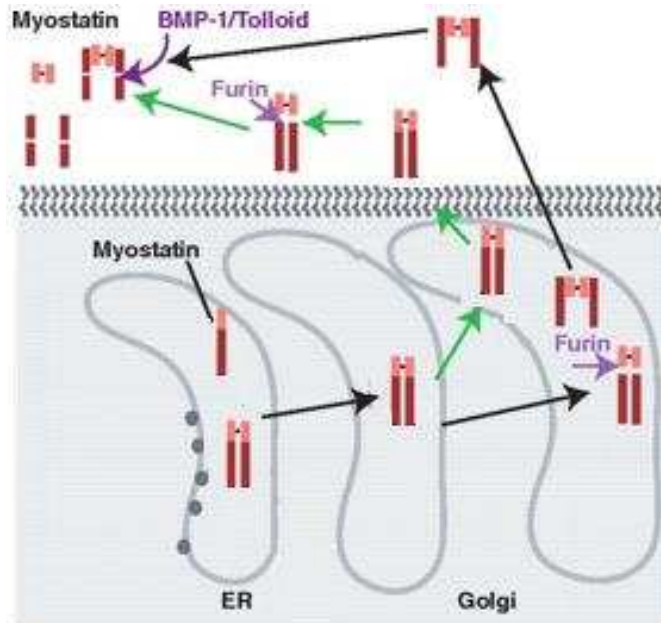
Fig. 1.6. Two models of Mstn processing. The traditional Mstn processing pathway (black arrows) is based on research on cultured cells. The newer model (green arrows) is based on muscle tissue research. The Mstn mature peptide (pink) and the propeptide (red) dimerizes in the endoplasmic reticulum (ER). In the traditional pathway, furin cleaves at the RXXR site (purple arrow) while Mstn is still in the Golgi body. The Mstn propeptide then noncovalently binds the mature peptide, forming an inactive complex.This complex is secreted and remains inactive until BMP-1/Tolloid cleaves the Mstn propeptide. Cleavage of the Mstn propeptide releases the Mstn active mature peptide, which initiates Mstn signaling. In the muscle model (green arrows), the intact Mstn peptide is secreted into the extracellular matrix and remains bound to matrix proteins until activated by furin and BMP-1/Tolloid proteases. Modified from Anderson et al., 2008.
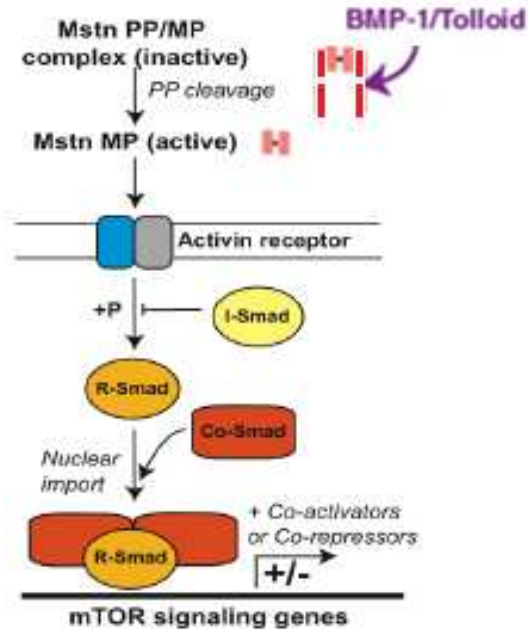
Fig. 1.7. Activated Mstn mature peptide signaling through Smad transcription factors. After cleavage of the Mstn propeptide (red bars) by BMP-1/Tolloid metalloproteases, the activated Mstn mature peptide (pink) binds the activing receptor type IIB (blue). Mstn binding causes heterodimerization of the activing receptor type IIB and type I (gray), which results in phosphorylation of R-Smad (gold). Phosphorylated R-Smad binds Co-Smad (rust) and translocates to the nucleus, where it becomes a transcription factor either up-regulating or down-regulating the transcription of hundreds of genes. We propose that the transcription of some mTOR signaling genes is regulated, thus decreasing protein synthesis. Modified from Mykles, personal communication, and Anderson et al., 2008.
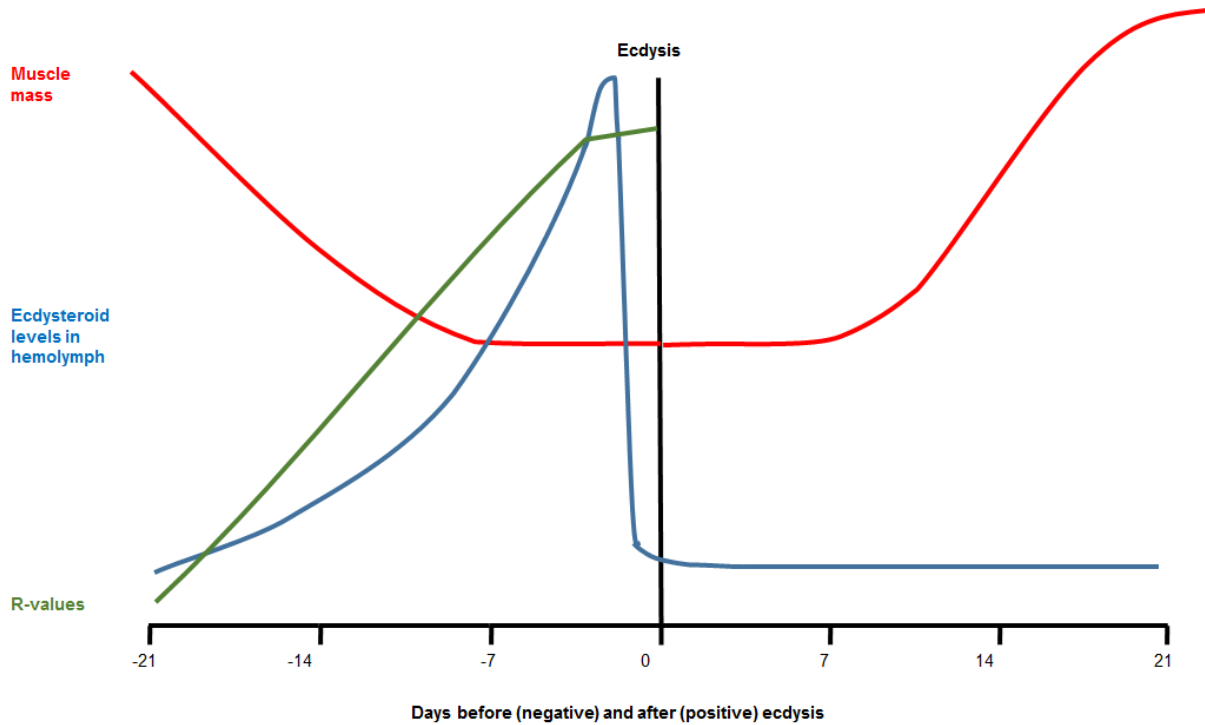
Fig. 1.8. Changes in closer claw muscle mass (red), hemolymph levels (blue and R-values (green) 3 weeks before and after ecdysis. R-values increase steadily all through the premolt period. Hemolymph ecdysteroid levels increase during premolt, with the greatest increase during the last week before ecdysis. However, two to three days before ecdysis, hemolymph levels fall dramatically, which is necessary for successful ecdysis. Claw muscle mass decreases by approximately fifty percent during the first two weeks of premolt, then does not change much the last week of premolt and the first week of postmolt. During the second and third weeks of postmolt, claw closer muscle mass increases rapidly, resulting in approximately 10% greater mass than before ecdysis, as the muscle tissue fills the new enlarged chelae.

47
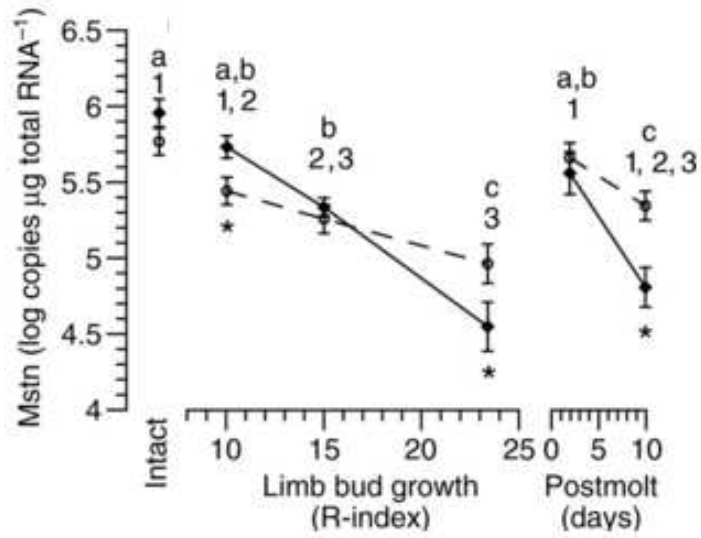
Fig. 1.9. Mstn mRNA levels decrease ten-fold in thoracic (broken line) and 17-fold in claw closer muscle (solid line) during premolt. We hypothesize that decreased Mstn allows increased protein synthesis. Early in postmolt, Mstn levels are high when muscle mass is not yet changing. By 10 days postmolt, Mstn levels have decreased, which is the same time that muscle mass begins increasing rapidly in the claw closer muscle. From Covi et al., 2010.

Chapter 2

The effect of ecdysteroid manipulation on Mstn and mTOR pathway gene expression in

***Gecarcinus lateralis* skeletal muscles.**

Summary

Ecdysteroid levels increase during premolt. The effects of increasing ecdysteroids in the claw muscle is increased atrophy to allow claw withdrawal at ecdysis, and increased protein synthesis to initiate atrophy and prepare for rapid muscle hypertrophy immediately after ecdysis. The effects of increasing ecdysteroids on limb bud muscle is increased hypertrophy and increased protein synthesis. Ecdysteroids have little effect on thoracic muscle mass or protein synthesis rates, so thoracic muscle can be used as an internal control.

In mammals, mTORC1 increases protein synthesis, while Mstn inhibits protein synthesis. After MLA to induce molting in *G. lateralis*, then LBA to suspend molting progress, ecdysteroid levels, and mRNA levels of *Gl-Mstn*, some components of the mTORC1 protein synthesis pathway (*Gl-Akt, Gl-Rheb*, *Gl-mTOR* and *Gl-S6k*) and *Gl-EF2* were measured in claw muscle, limb bud muscle and thoracic muscle. *Gl-EF2* is used as a sample positive control, as it is a constitutively expressed gene with high expression levels in all tissues. In the claw muscle, *Gl-Mstn* mRNA levels were negatively correlated with ecdysteroid levels, and were significantly higher in molting suspended animals, compared to molting continued animals, as expected. mTORC1 pathway component mRNA levels were not directly correlated with ecdysteroid levels, but unexpectedly, all were positively correlated with *Gl-Mstn* mRNA levels in the claw muscle, and *Gl-EF2*, *Gl-Akt* and *Gl-mTOR* were positively correlated with *Gl-Mstn* in the thoracic muscle, although the correlations were weaker. Multiple linear regression showed that *Gl-Rheb* and *Gl-S6k* mRNA levels were both predicted by ecdysteroid levels and *Gl-Mstn* mRNA levels, together. Taken together, these results indicate that ecdysteroids, *Gl-Mstn*, *Gl-Rheb*, and *Gl-S6k* are all involved in regulating the increased protein synthesis in premolt claw muscle. Further, *Gl-Mstn* is a chalone that modulates the mTORC1 protein synthesis pathway by

matching increased mTORC1 component levels with increased *Gl-Mstn* mRNA levels. By contrast, *Gl-Mstn* does not appear to regulate protein synthesis in the limb buds. The growth suspended limb buds had decreased mRNA levels of *Gl-Rheb*, *Gl-mTOR*, and *Gl-S6k*, compared to growing limb buds, but *Gl-Mstn* mRNA was present at very low levels, which did not change in response to ecdysteroid levels.

Introduction

In mammals, mechanistic Target of Rapamycin complex 1 (mTORC1) is the main transducer of stimuli which increases protein synthesis in skeletal muscle (Amirouche et al., 2009), while myostatin (Mstn) signaling inhibits mTORC1-dependent protein synthesis (Goodman et al., 2013; Hitachi et al., 2014; Hulmi et al., 2013; Sakuma et al., 2014; Sartori et al., 2014; Schiaffino et al., 2013; Welle et al., 2009). mTORC1 upregulates protein translation (Barbet et al., 1996), ribosomal RNA (rRNA) transcription and ribosomal protein transcription (Thomas and Hall, 1997) in mammals, through upregulation of key eukaryotic translation initiation factors (eIFs) and eukaryotic elongation factors (eEFs). Translation initiation is regulated by mTORC1 through phosphorylation of 4E-BP. As increased sites are phosphorylated (Wang et al., 2005), 4E-BP dissociates from eIF4E, allowing eIF4E to participate in translation initiation (Gingras et al., 1999; Haghighat et al., 1995). Activated mTORC1 phosphorylates S6k, which results in upregulation of RNA polymerase I (Pol I) (Iadevaia et al., 2014). Activated Pol I transcribes 5.8S, 18S and 28S ribosomal RNA, resulting in increased translational capacity due to increased ribosomes in the cell (Iadevaia et al., 2014).

mTORC1 also increases protein degradation through upregulating expression of proteasome subunits (Zhang et al., 2014). Increased protein synthesis, along with increased protein degradation occurs in some types of muscle atrophy, including denervation atrophy (Argadine et al., 2009; Argadine et al., 2011; Goldspink, 1976) and premolt claw closer muscle atrophy (Covi et al., 2010). Increased protein synthesis at the same time as muscle atrophy may

seem counterproductive, but it allows muscle remodeling during atrophy to accommodate altered muscle use (Bassel-Duby and Olson, 2006; Mykles and Medler, 2015).

Mstn is a chalone (Lee, 2004), a product secreted by a tissue that inhibits that tissue's growth (Bullough, 1962; Lee and McPherron, 1999). Mstn regulates muscle cell size (Zimmers et al., 2002) by limiting protein synthesis (Amthor et al., 2009; Lee et al., 2012; Sartori et al., 2014; Sartori et al., 2009) and increasing protein degradation (Sartori 2014, Han 2013). Mstn is secreted by muscle cells, and then covalently bound to the extracellular matrix by latent TGFβ-binding proteins (LTBPs) (Anderson et al., 2008; Harrison et al., 2011; Lee, 2004; McFarlane et al., 2005; Sharma et al., 2015). Thus, the majority of Mstn is retained in the muscle tissue where it is secreted, allowing localized activation of Mstn (Anderson et al., 2008; Harrison et al., 2011). After cleavage by furin, the latent Mstn complex is activated by Bone Morphogenetic protein-1/Ttolloid (BMP/TLD) metalloproteases that cleave the propeptide and release the mature peptide dimer (Wolfman et al., 2003). Activated Mstn signals through the Activin receptor, resulting in phosphorylation of R-Smads (Smad 2 or Smad 3) (Lee and McPherron, 2001; MacDonald et al., 2014; Morrison et al., 2009; Tsuchida et al., 2006). Phosphorylated R-Smad translocates to the nucleus (Macias et al., 2015), regulating the transcriptional activity of hundreds of genes (Koinuma et al., 2009; Massague et al., 2005), including transcription inhibition of miRNA-29 (Goodman et al., 2013; Sartori et al., 2014) and miRNA-486 (Hitachi et al., 2014; Sartori et al., 2014). Both of these miRNA target PTEN, which is an inhibitor of the insulin/mTORC1-dependent protein synthesis pathway. Thus Mstn/Smad signaling allows PTEN to negatively regulate the mTORC1-dependent protein synthesis pathway (Goodman et al., 2013; Hitachi et al., 2014; Sartori et al., 2014), resulting in decreased phosphorylation of both 4E-BP and S6k in mammals (Amirouche et al., 2009) and fish (Seiliez et al., 2013).

Mstn and mTOR regulate skeletal muscle protein synthesis in response to ecdysteroid levels in decapods (Abuhagr et al., 2014b; Chaulet et al., 2012; Covi et al., 2010; MacLea et al., 2012). Ecdysteroids increase during premolt from approximately 10-20 pg/µl during intermolt to

over 400 pg/µl (Covi et al., 2010) three to six days before ecdysis (McCarthy and Skinner, 1977b). The major ecdysteroid in the land crab is 20-hydroxyecdysone (20E) with Ponasterone A (Pon A) secondary, occurring in an approximately 3:1 ratio, respectively, during intermolt and most of premolt (McCarthy and Skinner, 1977b; McCarthy and Skinner, 1979). Insulin or IGF-1 may stimulate the mTORC1 protein synthesis pathway in crustaceans, as it does in mammals. Insulin-like peptides, insulin-like growth factor binding proteins, and insulin binding proteins have been identified in crustaceans, (Chandler et al., 2015; Chaulet et al., 2012; Chung, 2014; Davidson et al., 1971; Gutierrez et al., 2007; Kucharski et al., 1999; Kucharski et al., 2002; Richardson et al., 1997; Sanders, 1983a; Sanders, 1983b). IGF injections have resulted in increased muscle protein synthesis in muscles in crustaceans, similar to vertebrates (Richardson et al., 1997).

Three different muscles—the claw closer muscle, the limb bud muscles, and the thoracic muscles—in *Gecarcinus lateralis*, the blackback land crab, show a differential response to increasing ecdysteroid levels in the hemolymph during premolt. The different responses are likely due to the expression of varying combinations of ecdysteroid receptor isoforms expressed in the different muscles. The ecdysteroid receptor consists of a heterodimer of retinoid X receptor (RXR) and ecdysone receptor (EcR). When ecdysteroids enter the cell, they bind with an EcR/RXR heterodimer, and then the ecdysteroid/heterodimer complex binds ecdysteroid response elements (EcRE) to affect the transcription of many genes. Nine isoforms of *Gl-RXR* have been identified in *G. lateralis*, with varying expression patterns in different tissues observed (Kim et al., 2005b). Three isoforms of *Gl-EcR* have been identified in *G. lateralis* (Das, 2014).

The claw closer muscles respond to increasing ecdysteroids during premolt with increased protein synthesis to remodel the claw muscle in preparation for rapid growth immediately after molting (Covi et al., 2010; Skinner, 1965). The increased protein synthesis in the claw muscle is associated with decreased *Gl-Mstn* (Covi et al., 2010) and increased *Gl-Ras*

homolog enriched in the brain (*Gl-Rheb*) (an activator of mTOR signaling) mRNA levels (MacLea et al., 2012). During this premolt time of increased protein synthesis, dramatic atrophy of the claw muscle occurs to enable withdrawal of the claw muscle at ecdysis (Mykles and Skinner, 1982a; Skinner, 1966). By contrast, limb bud muscles respond to increasing ecdysteroids with increased protein synthesis and rapid growth, as any missing limbs are regenerated only during the three weeks of premolt (Mykles, 2001; Skinner, 1985a; Skinner, 1985b; Skinner and Graham, 1970). Thoracic muscle serves as an internal control, as thoracic muscle does not significantly change in mass or protein synthesis during the increasing ecdysteroid levels of premolt (Covi et al., 2010; Mykles, 1999).

Natural molt induction techniques included multiple leg autotomy (MLA) to initiate molting, and limb bud autotomy (LBA) to suspend premolt progress. Autotomy is the self-initiated release of a limb at a pre-formed fracture plane in response to a mechanical stimulation (gripping) of the limb. The R-index ((length of LB /carapace width) times 100) was developed to allow a reliable external measure of molt stage for all crabs, regardless of size (Bliss, 1956; Bliss and Boyer, 1964). As duration of premolt after MLA is variable (Skinner and Graham, 1972), the R-index was correlated to Drach's molt stages (Chang and Mykles, 2011; Covi et al., 2010; Drach, 1939; Skinner, 1962; Skinner, 1985b). This allowed determination of each crab's progress through premolt. MLA shortens the intermolt period by initiating premolt to allow the crab to regenerate limbs, which can only be regenerated during premolt (Holland and Skinner, 1976; Skinner, 1985b; Skinner and Graham, 1972). After MLA, R-values were calculated on the right third primary regenerate (limb bud (LB)) every few days until harvest, to determine premolt progress.

By contrast, limb bud autotomy (LBA) of one or more primary regenerates can inhibit progress through premolt for about three weeks, to give the crab time to regenerate the newly autotomized limb bud (secondary regenerate), thus allowing it to molt with a full set of walking legs (Chang and Mykles, 2011; Holland and Skinner, 1976; McCarthy and Skinner, 1977a).

Limb buds will normally regenerate before ecdysis if autotomized before reaching a critical R-value of approximately 15 or 16 (stage D_0 of premolt corresponds to R-values between 11 and 16), but will not regenerate before the next ecdysis at higher R-values (corresponding to premolt stages D_1 to D_4) (Chang and Mykles, 2011). The beginning of stage D_1 is when the crab becomes committed to molting due to changes in gene expression and ecdysteroid secretion levels from the Y-organ (Chang and Mykles, 2011). During stage D_1, the crab begins irreversible physical processes such as separation of the epidermal cells from the old exoskeleton, and resorption of the old exoskeleton (Skinner, 1985b), thus physically committing the crab to molting.

We were specifically interested in the interaction between *Gl-Mstn* mRNA levels and the levels of mTOR dependent protein synthesis pathway genes in response to changing ecdysteroid levels. Previous work in our lab showed that after MLA to induce premolt, the claw closer muscle atrophies. During atrophy, protein synthesis increases, *Gl-Mstn* mRNA levels decrease (Covi et al., 2010) and *Gl-Rheb* mRNA levels increase (MacLea et al., 2012). In this study, ecdysteroid levels were manipulated, both naturally and artificially, and mRNA levels of *Gl-Mstn* and the mTOR signaling genes were quantified in the claw closer muscle, limb bud muscle, and thoracic muscle. Our hypothesis was that ecdysteroids down-regulate *Gl-Mstn* mRNA levels in atrophic claw closer muscle and in growing limb buds during premolt to allow increased mTOR-dependent protein synthesis. Specifically: 1) after LBA, *Gl-Mstn* mRNA levels will be higher in the claw muscle of molting suspended (MS) animals, compared to molting continued (MC) animals; 2) *Gl-Mstn* mRNA levels will be higher in the growth suspended (GS) LBs, compared to the growing (G) LBs; 3) *Gl-Rheb* mRNA levels in both the claw closer muscle and the LBs will be positively correlated with ecdysteroid levels, and negatively correlated with *Gl-Mstn* mRNA levels; 4) *Gl-Mstn* mRNA levels will be negatively correlated with ecdysteroid levels after 20E injections and negatively correlated with *Gl-Rheb* mRNA levels; and 5) *Gl-Mstn* and *Gl-Rheb* mRNA levels in thoracic muscle will not change as much as in claw muscle.

Materials and Methods

Animals

Male *Gecarcinus lateralis* (Fréminville 1835), blackback land crabs, were collected from the southern coast of the Dominican Republic and flown to Colorado, USA. Crabs were kept in plastic containers at 27^0C and 75-90% relative humidity on a 12 h light: 12 h dark schedule. Containers held eight to twelve crabs in aspen bedding dampened with 5 parts per thousand (p.p.t.) Instant Ocean (Aquarium Systems, Mentor, OH). After multiple leg autotomy (MLA) (discussed in next paragraph), crabs were kept in a reduced light environment in individual containers in sand dampened with 10 p.p.t. Instant Ocean. This provided an environment conducive to molting—darkness, moisture, privacy and favorable temperature (Bliss, 1956; Bliss and Boyer, 1964), normally provided by a burrow in the crabs' native habitat (Bliss, 1979; Hartnoll, 1988). All crabs were fed lettuce, carrots and raisins twice per week. Within two weeks of arrival in Colorado, the right third walking leg was autotomized, and the resulting basal limb bud (LB) was observed before MLA to confirm that the crab was in intermolt (no premolt LB growth observed).

LBA experiments

Two LBA experiments were conducted. In the first, LBs were autotomized at about the critical R-value, with some crabs continuing toward molting, and some crabs suspending molting. If molting continued (MC), then R-values and ecdysteroid levels continued to increase (with or without an initial delay), and if molting suspended (MS), R-values and ecdysteroid levels did not increase after LBA. MC and MS groups were determined by R-index values and later confirmed by ecdysteroid levels. MC animals had R-values greater than 15 at harvest, and MS animals had R-values less than 15 at harvest. Three crabs suspended progress toward molting after LBA, but resumed molting progress two to four weeks later. These crabs had delayed, then continued, molting and were placed in the molting continued (MC) category, as they were

harvested when R-values were increasing (Fig. 1A). For each crab, one LB was autotomized at LBA, and claw and thoracic muscle was harvested 2, 7, 14, 21 and 28 days later.

The second LBA experiment measured differences in mRNA levels between actively growing LBs and growth suspended LBs. Initially, actively growing LBs were autotomized when ecdysteroid levels were high. One week later, after suspension of growth, the remaining LBs were harvested when ecdysteroid levels had decreased due to suspension of molting. LBA suspended growth in all but one animal. For both experiments, LBs with an R-value between 11 and 19 were induced to autotomize by gripping the limb bud (LB) with forceps.

20E injection experiments

Two 20-hydroxyecdysone (20E) injection experiments artificially increased ecdysteroid levels in intermolt animals. The 24-hour experiment was one injection of 0.41 µg 20E/g of crab weight to approximate ecdysteroid levels in the second week of premolt (Lee et al., 2007a). Initially, 10 mg 20E was dissolved in 1 ml 95% ethanol, then distilled water was added to dilute to 10% ethanol. The resulting 1.052 µg 20E/µl 10% ethanol was used for all injections. A 50 µl Hamilton syringe (Hamilton Co., Reno, NV) was used to inject each animal through the arthrodial membrane at the base of a leg. Experimental crabs were injected with 20E, while control crabs were injected with an equivalent volume of 10% ethanol. For the 24-h experiment, random groups were harvested 4, 8, 12, and 24 h after injection with 20E or 10% ethanol. (N=6 for each group.)

A two-week experiment consisted of daily injections for one or two weeks with harvest at the end of the injection periods, with daily injections as described above. For the two-week experiment, animals were randomly placed into groups—no injection controls, one week or two weeks of 10% ethanol injection controls, and one week or two weeks of 20E in 10% ethanol. (N=8 for each group.)

Animal harvest

For all experiments, hemolymph was withdrawn before LBA or before injection, and then again at harvest, using a 1 ml slip-tip tuberculin syringe (Becton, Dickinson & Co (BD), Franklin Lakes, NJ, USA) and a 22G sterile needle. 100 ul of hemolymph was added to 300 ul of 100% methanol, and stored at -20^0C until shipped to the Chang lab at the University of California Bodega Marine lab for analysis of ecdysteroid levels in each sample. This competitive ELISA preferentially binds ecdysone and 20-hydroxy ecdysone (20E) (Abuhagr et al., 2014a; Kingan, 1989).

After removing the hemolymph sample, animals were placed in ice for 5 min to anesthetize them. The entire cheliped and the anterior thorax with attached muscles were removed and placed in ice 4 h to allow apolysis (the separation of the claw muscle from the membranous layer of the exoskeleton) to occur (Obrien et al., 1986). Claw closer muscle and thoracic muscles were dissected from the exoskeleton, rinsed in crab saline (430 mmol NaCl, 5 mmol K_2SO4, 12.5 mmol MgCl, 4.5 mmol $CaCl_2$, and 9 mmol HEPES), wrapped in foil, frozen immediately in liquid nitrogen, and stored at -80^0C. LBs from one crab were flash frozen directly in liquid nitrogen, placed in a 1.5 ml tube with two 5 mm stainless steel balls (Abbott Ball Co., West Hartford, CT, USA), and then placed in a TissueLyzer II adaptor (Qiagen Inc., Frederick, MD, USA) before storage at -80^0C.

RNA isolation

RNA was isolated from tissue samples with TRIzol (Invitrogen, Carlsbad, CA, USA) as described previously ((Covi et al., 2010). Approximately 100-150 mg muscle (claw closer or thoracic) was homogenized for 5 min in 1 ml of Trizol in glass homogenizers. LBs were homogenized in a TissueLyzer II (Qiagen, Inc.) for two minutes at a frequency of 30 revolutions per second. TRIzol (1 ml) was added and samples were vortexed. Homogenized tissues were centrifuged 15 min at 12,000g. Chloroform was added to the supernatant, and samples were centrifuged for 15 min at 16,000g. Approximately 400 µl of the aqueous layer containing RNA

was transferred into a clean microcentrifuge. The extraction process was repeated to obtain more RNA. One volume isopropanol (approximately 800 µl) was added to the aqueous layer and samples were placed at 4^0C for overnight precipitation of RNA. Samples were centrifuged the next day at 16,000g to pellet the RNA, supernatant was removed, and the pellet was washed twice in cold 75% ethanol in diethylpyrocarbonate-treated water, centrifuging after each wash to re-pellet the RNA. The supernatant was removed and the pellet was dried on ice. Each sample was suspended in 22 µl nuclease-free water, then treated with which 1 µl DNase I (Life Technologies) and 0.25 µl Ribolock RNase Inhibitor (Thermo Fisher Scientific, Waltham, MA, USA) and incubated at 37^0C for 30 min according to the manufacturer's directions. After the DNase treatment, 170 µl nuclease-free water, 100 µl acidic phenol (pH 4.3) and 100 µl 24:1 isoamyl alcohol were added to extract the RNA, then centrifuged at 21,000g for 15 min to separate the layers. The aqueous phase containing the RNA was transferred to a clean tube, and the extraction process was repeated to obtain more RNA. RNA was precipitated by adding 1.5 volumes isopropanol and 0.5 volumes sodium acetate (pH 5.2) to the aqueous phase, and leaving overnight at 4^0C. The precipitate was centrifuged at 16,000g for 15 min, then washed two times with 70% ethanol, similar to the first RNA precipitation. After removing the supernatant, pellets were dried on ice, resuspended in 22 µl nuclease-free water, and the RNA was quantified with a NanoDrop 1000 V3.8.1 (Fisher Scientific, Waltham, MA, USA).

cDNA synthesis

For the claw and thoracic muscle LBA experiment and the 20E injection experiments, single-strand cDNA was synthesized from 4 µg total RNA per sample, using Transcriptor Reverse Transcriptase (Roche, Indianapolis, IN, USA). Ribolock RNase inhibitor (Thermo Fisher Scientific), dNTP mix (Thermo Fisher Scientific) and 50 µM oligo dT(22) primers (Integrated DNA Technologies, Inc., (IDT) Coralville, IA) were added to each RNA sample, following the manufacturer's protocol. For the LB experiment, single-strand cDNA was

synthesized fromμμg total RNA per sample using qScript cDNA SuperMix kit (Quanta

Biosciences, Gaithersburg, MD, USA).

For the 2-week 20E injection experiment, 10 µg RNA was used for each claw sample,

except 4.5 µg of RNA was used for five samples with lower concentrations. For thoracic muscle.

9 µg RNA was used, except 4 µg RNA was used for nine low concentration samples. For the

24-hour experiment, single-strand cDNA was synthesized from 9 µg total RNA per sample,

except 5 µg RNA was used for 11 samples, and 2.5 µg RNA was used for seven samples which

did not yield enough RNA for 9 µg of RNA each. For all experiments, 20 µl of cDNA was made

per sample.

qPCR

Quantitative polymerase chain reaction (qPCR) was used to quantify mRNA levels of the

following genes: elongation factor 2 *(Gl-EF2)* [GenBank AY552550 (Kim et al., 2004a)],

myostatin (*Gl-Mstn*) [GenBank EU432218 (Covi et al., 2008)], *Gl-Akt* [GenBank HM989974.3]

(also known as protein kinase B (PKB)), Ras homolog enriched in brain (*Gl-Rheb*) [GenBank

HM989971 (MacLea et al., 2012)], mechanistic Target of Rapamycin (*Gl-mTOR*) [GenBank

HM989973], and p70 ribosomal protein S6 kinase (*Gl-S6k*) [GenBank 989975.3] (Abuhagr et al.,

2014b). One µl of sample was used in a 10 µl reaction with nuclease-free water, and 1 µM gene

specific primers (IDT) (Table 1). LightCycler 480 SYBR Green I Master mix (Roche) was

included in the reaction for all genes except for *Gl-EF2* and *Gl-Akt* in the LB experiment, which

included Fast Start DNA Master plus SYBR Green 1 Reaction Mix (Roche), instead. LightCycler

480, 384 Multiwell Plates (Roche) were used to run the reactions in a LightCycler 480 Real-

Time PCR instrument (Roche). PCR settings were: activation for 5 min at 95^0C, followed by 40

to 50 cycles of 95^0C for 10 s (denature), 62^0C for 20 s (anneal) and 72^0C for 20 s (elongation)

for all genes except the annealing temperature for Mstn was 60^0C (Table 1). These cycles were

followed by a melt curve cycle to analyze product homogeneity. Absolute quantification was

done by the LightCycler 480 software, version 1.5 (Roche), comparing each sample to external

standards for each gene. Concentrations from the LightCycler software were converted to copy number per µg RNA in Microsoft Excel. As EF2 is constitutively expressed at high levels in all tissues, EF2 was used as a positive control to determine quality of RNA isolation and cDNA synthesis. Any sample with EF2 values 1000-fold or less compared to similar samples was not used, as this indicated a problem with RNA isolation or cDNA synthesis.

External standards for each gene were made by amplifying cDNA in a thermocycler with the same primers used in the qPCR reactions. The amplified product was separated on a gel, extracted from the gel, and then measured with a nanodrop. The sample was diluted to make concentrations from 10^{-9} to 10^{-18} g/µl in 10-fold increments. Three replicas of each concentration were quantified with qPCR, using the same primers as when first amplifying the gene. The qPCR crossing point for the log concentrations that are in the linear range are selected as the external standards, and all unknown samples are compared to the external standards for quantification.

Statistics

Sigma Plot 12.5 software (Systat Software, Inc., Chicago, IL, USA) was used for all graphs and statistical analyses, except 3-D bubble charts showing multiple linear regressions were made in Microsoft Excel. Box plots of non-transformed and transformed data (data not shown) indicated that, in general, $\log_{10}$ transformed data had a more normal distribution with equal variances. Subsequently, all data was $\log_{10}$ transformed for further statistical analyses. The Pearson correlation was used to assess the linear relationship between ecdysteroid levels and the R-index, and between mRNA and ecdysteroid levels in the LBA MC/MS experiment. The Pearson correlation was also used to assess the linear relationship between *Gl-Mstn* mRNA levels and *Gl-EF2*, *Gl-Akt*, *Gl-Rheb*, *Gl-mTOR* and *Gl-S6k* mRNA levels in the LBs and each muscle type. Since there appeared to be a MC/MS effect in addition to a *Gl-Mstn* effect on the levels of some genes, multiple linear regressions with *Gl-Mstn* and ecdysteroids were included in the models. In the MC/MS LBA experiment, the student's t-test was used to compare

ecdysteroid levels and mRNA levels between MC and MS animals. The paired t-test was used in the limb bud LBA experiment to compare ecdysteroid levels and LB mRNA levels between M and MS animals. For both types of t-tests, if the Shapiro-Wilk Normality test or the Equal Variance Test failed, then the Mann-Whitney Rank Sum Test was initiated. An alpha level of 0.01 was chosen for all mRNA level tests to control for the Type I error rate due to multiple testing. All t-test results are shown as the mean plus one standard error of the mean (+1 SEM).

For the two-week 20E injection experiment, one-way ANOVAs between the three types of negative controls—no injection, one week of ethanol (vehicle) injections, and two weeks of ethanol injections indicated no significant differences in ecdysteroid levels or any mRNA levels in either muscle. Therefore, the negative controls were combined into one group of negative controls for ecdysteroids and each gene for each muscle. One-way ANOVAs were then used to compare the grouped negative controls, the animals injected with 20E daily for one week, and the animals injected with 20E daily for two weeks. The one-way ANOVAs were done for ecdysteroid levels, and mRNA levels in each muscle for *Gl-EF2*, *Gl-Mstn, Gl-Akt*, *Gl-Rheb*, *Gl-mTOR* and *Gl-S6k*. If a significant difference was found in a one-way ANOVA, then the Holm-Sidak All Pairwise Multiple Comparison Procedure was initiated. If the Shapiro-Wilk Normality Test or the Equal Variance Test failed, then the Kruskal-Wallis one-way ANOVA on ranks was initiated. If a significant difference was found in a one-way ANOVA on ranks, then Dunn's All Pairwise Multiple Comparison Procedure was initiated.

<div align="center">

Results

</div>

Claw/thoracic muscle LBA experiment: R-values and ecdysteroids

In general, R-values and ecdysteroid levels increased in the MC animals, while both remained nearly constant in MS animals (Fig. 2.1). The only MC animal with a substantial decrease in ecdysteroid levels in the hemolymph, from 226.4 pg/µl at LBA to 158.2 pg/µl at harvest (Fig 2.1C), had a 25.0 R-value at harvest, indicating that molting was imminent. During the last 2-3 days of premolt, ecdysteroid levels fall precipitously in crabs (McCarthy and Skinner,

1977a) and this animal's lower ecdysteroid level was likely due to this drastic decrease in ecdysteroid levels just before molting. Comparatively, ecdysteroid levels in MS animals were stable (Fig. 2.1D).

Ecdysteroid levels were correlated (R^2=0.687) with R-index values (Fig. 2.2A), confirming that the R-index was a reliable indicator of molting progress for this experiment. Direct comparison of the means of ecdysteroid levels between MC and MS animals at harvest, 2-28 days after LBA, showed 6-fold higher ecdysteroid levels in the MC animals versus the MS animals (Fig 2.2B), consistent with previously published work (McCarthy and Skinner, 1977a).

Claw/thoracic muscle LBA experiment: mRNA levels and correlations

In thoracic muscle, there were no significant differences in mRNA levels of any of the genes quantified (*Gl-EF2*, *Gl*-Mstn, Gl-*Akt*, *Gl-Rheb*, *Gl-mTOR*, and *Gl-S6k*) between MS and MC animals (Fig. 2.3A). In claw muscle, the only mRNA levels that were significantly different between MS and MC animals was *Gl-Mstn* (Fig 2.3B), which was eight-fold higher in MS animals compared to MC animals (Fig. 2.3B). In addition, *Gl-Mstn* mRNA levels in claw muscle were negatively correlated (P=0.0055, R^2=0.217) with ecdysteroid levels in the hemolymph (Fig. 2.4D). No other mRNA levels were significantly correlated with ecdysteroid levels in either muscle type (Fig. 2.4). Linear regression showed that in thoracic muscle, *Gl-Mstn* levels were positively correlated with *Gl-EF2*, *Gl-Akt* and *Gl-mTOR* (Fig 2.5A, C and G). In claw muscle, *Gl-Mstn* mRNA levels were positively correlated with *Gl-EF2* (R^2= 0.604), *Gl-Akt* (R^2= 0.488), *Gl-Rheb* (R^2= 0.506), *Gl-mTOR* (R^2= 0.627), and *Gl-S6k* (R^2=0.463; P<0.001)—much stronger correlations than in thoracic muscle (Fig. 2.5B,D,F,H and J). Even though ecdysteroid levels had no direct significant correlation with mRNA levels of any of the mTOR components, the correlations between *Gl-Mstn* and two of the mTOR components, *Gl-Rheb* (Fig. 2.5F) and *Gl-S6k* (Fig. 2.5J), indicated an ecdysteroid effect. The mRNA levels of these two genes were higher in MC animals than in MS animals. Multiple linear regressions showed that *Gl-Mstn* and ecdysteroids, together, strongly predicted *Gl-Rheb* (P<0.001, R^2=0.770) (Fig. 2.6A) and *Gl-S6k*

(P<0.001, R^2=0.631) (Fig. 2.6B) mRNA levels in claw muscle. Ecdysteroids and *Gl-Mstn* together, correlated with either *Gl-Rheb* or *Gl-S6k*, are much stronger than *Gl-Mstn* alone correlated with either gene. There were no multiple correlations of ecdysteroids and *Gl-Mstn* together with the mRNA levels of any genes in thoracic muscle.

Limb bud muscle LBA experiment

In the LBA experiment examining mRNA levels in LBs, R-values indicated that the autotomy of 3-4 growing LBs resulted in suspended growth in the remaining LBs. R-values did not increase, indicating that LBA was performed before the critical point, and molting was suspended. Ecdysteroid levels at the time of the initial LBA were 2.5-fold higher than one week later, confirming that premolt had been suspended (Fig. 2.7). In the LBs, *Gl-Mstn* mRNA levels were very low (approximately 300 copies Mstn/µg RNA compared to ~16,000 copies Mstn/µg RNA in claw muscle) whether G or GS (Fig. 2.8). The growth suspended LBs had decreased mRNA levels of several mTOR genes, including *Gl-Rheb*, *Gl-mTOR*, and *Gl-S6k. Gl-EF2* is constitutively expressed, and was not expected to alter mRNA levels, however, *Gl-EF2* mRNA levels were significantly decreased in the growth suspended LBs. *Gl-Rheb* and *Gl-S6k* mRNA levels were both positively correlated with ecdysteroid levels in the LBs (Fig. 2.9A and B). There were no significant correlations between *Gl-Mstn* mRNA levels and the mRNA levels of the mTOR genes in the LBs (data not shown).

24-h 20E injection experiment

In the 24-h 20E experiment, ecdysteroid levels were significantly increased at 4, 8 and 12 h, compared to controls, with the highest levels at 4 h (Fig. 2.10). By 24 h after the 20E injection, ecdysteroid levels were no longer significantly higher than in controls (Fig. 2.10). This contrasts to the relatively stable hourly ecdysteroid levels found in intermolt animals, which did not change more than 3.5 pg/µl in any control crab.

mRNA levels of *Gl-EF2*, *Gl-Mstn, Gl-Rheb*, *Gl-mTOR* and *Gl-S6k* in claw muscle were unchanged throughout the 24-h period (Fig. 2.11). *Gl-Akt* mRNA in claw muscle was expressed

significantly higher 4 h after injection than at 12 or 24 h after injection, but Akt levels were not

significantly different than controls at any time point after injection (Fig. 2.11).

2-week 20E injection experiment

Ecdysteroid levels were significantly increased in animals with daily 20E injections after

one and two weeks (Fig. 2.12), with the highest ecdysteroid levels found one week after

beginning daily injections.There were no significant changes in mRNA levels of *Gl-EF2*, *Gl-*

Mstn, Gl-Akt, *Gl-mTOR* and *Gl-S6k* in claw or thoracic muscle tissue throughout the 2-week 20E

experiment (Fig. 2.13A and B). *Gl-Rheb* mRNA was expressed at higher levels in thoracic

muscle after one week of daily injections, compared to two weeks of 20E injections, but there

was no significant difference from controls (Fig. 13A). *Gl-Rheb* mRNA was expressed at higher

levels in claw muscle after one week of daily 20E injections, compared to controls and to two

weeks of 20E injections (Fig. 2.13B). However, multiple linear regression indicated that

ecdysteroids and Mstn together, were able to predict Rheb mRNA levels (P<0.001, R^2= 0.448,

N=36) (Fig 2.14). Significant differences are indicated with an α=0.01 throughout this chapter.

Discussion

Previous research showed that MLA initiates a precocious premolt (increasing

ecdysteroid levels) (Skinner, 1985b), while LBA halts premolt (falling ecdysteroid levels)

(Holland and Skinner, 1976; Skinner, 1985b; Skinner and Graham, 1972). LBA in this research

resulted in decreased ecdysteroid levels in molting suspended animals, supporting previous

research (Holland and Skinner, 1976; Skinner, 1985b; Skinner and Graham, 1972). In previous

research, *Gl-Mstn* mRNA levels decreased after MLA to initiate premolt, and *Gl-Mstn* mRNA

levels in the claw muscle were negatively correlated with ecdysteroid levels (Covi et al., 2010).

In this study, after LBA to suspend premolt progress, *Gl-Mstn* levels increased in the claw

muscle of the molting suspended animals, and were negatively correlated with ecdysteroid

levels. Both results supported our hypotheses. In mTORC1 pathway components, there were no

significant changes in the mRNA levels in the claw muscle, and mRNA levels were not directly

correlated with ecdysteroid levels, both of which did not support our hypotheses. Further, there was a moderate positive correlation between the mRNA levels of *Gl-Mstn* and both *Gl-Rheb* and *Gl-S6k*, while our hypothesis predicted a negative correlation. When the molting continued group and the molting suspended group were separated in *Gl-Mstn* and *Gl-Rheb* or *Gl-S6k* correlations, there was a differential response in mRNA levels of *Gl-Rheb* and *Gl-S6k*, dependant on ecdysteroid levels. Multiple linear regression with both ecdysteroids and *Gl-Mstn*, demonstrate that these two factors, together, strongly predicted both *Gl-Rheb* (R^2=0.77) and *Gl-S6k* (R^2=0.63) mRNA levels.

We knew that Mstn is a chalone that represses growth, which is why we hypothesized that *Gl-Mstn* and *Gl-Rheb* mRNA levels would be negatively correlated. However, in mouse myocyte hypertrophy in response to stretch (Shyu et al., 2005), and in sparrow flight muscles preparing for migration (Price et al., 2011), increased protein synthesis corresponded to increased Mstn synthesis. A chalone not only suppresses growth, but a chalone can be a moderator of excessive growth (Shafer, 1916). In both of the above situations, there was a dramatic increase in protein synthesis, similar to what occurs in the crab claw muscle during premolt. As a modulator of excessive growth, we would expect increased *Gl-Mstn* during periods of dramatically increased protein synthesis, with a positive correlation between *Gl-Mstn* and mTOR pathway components. Previous work in our lab has shown that multiple leg autotomy (MLA) to stimulate premolt, with concomitant increasing ecdysteroid levels, results in decreased *Gl-Mstn* (Covi et al., 2010) and increased *Gl-Rheb* (MacLea et al., 2012) mRNA levels in the claw muscle. However, they found that *Gl-Mstn* and *Gl-Rheb* mRNA levels were not correlated in the claw muscle after MLA (MacLea et al., 2012). *Gl-Mstn* mRNA levels decreased 94%, while *Gl-Rheb* mRNA levels increased 3.4–fold during premolt. *Gl-Mstn* mRNA levels were negatively correlated with ecdysteroid levels (Covi et al., 2010), and *Gl-Rheb* mRNA levels were positively correlated with ecdysteroid levels (MacLea et al., 2012). However, there was no significant correlation between *Gl-Rheb* and *Gl-Mstn* mRNA levels in that study (MacLea

et al., 2012). In this study, *Gl-Mstn* mRNA levels were strongly positively correlated with *Gl-Rheb* and *Gl-S6k* mRNA levels. Perhaps the difference in results from MacLea (MacLea et al., 2012) is that changing Mstn mRNA levels to modulate protein synthesis would be expected to occur when protein synthetic rates are actively changing. MacLea used intermolt animals (steady state for protein synthesis) in addition to premolt animals (MacLea et al., 2012), while all of the *G. lateralis* animals studied in chapter 3 of this dissertation were either increasing protein synthesis during premolt or rapidly halting protein synthesis in the molting suspended animals.

In the 20E injection experiments, there was no overall difference in mRNA levels, compared to controls, in either the claw muscle or thoracic muscle. This contrasts with the 8-fold decrease in *Gl-Mstn* with increasing ecdysteroid levels after LBA in the MC animals. The claw muscle's response to ecdysteroids in the intermolt state is different than in the premolt state. Possible explanations include different ecdysteroid receptor isoforms expressed in a molt stage-specific manner as has been demonstrated in *Drosophila melanogaster* (Schauer et al., 2011). In addition, a different set of cofactors expressed during intermolt could alter the transcription effect on *Gl-Mstn* by the ecdysteroid/ecdysteroid receptor complex. However, multiple linear regression indicated that ecdysteroids and *Gl-Mstn*, together, moderately predicted *Gl-Rheb* levels in the claw muscle of 20E-injected animals. This further indicates that ecdysteroids, *Gl-Mstn*, and *Gl-Rheb* all have an effect on protein synthesis levels in the claw closer muscle. *Gl-Mstn* acts as a restraint on the activity of *Gl-Rheb* and *Gl-S6k*, with increasing *Gl-Mstn* mRNA levels providing *a* braking action on increasing *Gl-Rheb* and *Gl-S6k* mRNA levels.

The mRNA levels of several mTOR pathway components decreased in the growth suspended limb buds after LBA. However, there were no significant changes in *Gl-Mstn* mRNA levels. Further, *Gl-Mstn* mRNA levels were very low in the limb buds. Taken together, this indicates that *Gl-Mstn* is not involved in the suppression of growth in the LBs after LBA. The difference in response to suspension of growth in the limb buds may be due to a different set of ecdysteroid receptor isoforms expressed in the limb bud muscles compared to the claw

muscles. Previous work showed a different set of RXR isoforms expressed in the claw muscle

compared to thoracic muscle (Kim et al., 2005b), but limb muscle RXR isoform expression was

not studied.

Table 2.1. Oligonucleotide primers used in mRNA analysis of *Gecarcinus lateralis* Mstn and mTOR signaling. Gene abbreviations: EF2, elongation factor 2; Mstn, myostatin; Akt, also called protein kinase B (PKB); Rheb, Ras homolog enriched in brain; mTOR, mechanistic Target of Rapamycin; S6k, p70 ribosomal protein S6 kinase. Additional abbreviations: forward primer (F), reverse primer (R), bp, base pairs.

Primer pairs	Sequence (5'- 3')	Product Size (bp)	Annealing Temperature
Gl-EF2 F	TTCTATGCCTTTGGCCGTGTC	227	62
Gl-EF2 R	ATGGTGCCCGTCTTAACCA		
Gl-Mstn F	GCTGTCGCCGATGAAGATGT	118	60
Gl-Mstn R	ACGGGATTGAGGTCCCCAGCCT		
Gl-Akt F	AACTCAAGTACTCCAGCGATG	156	62
Gl-Akt R	GGTTGCTACTCTTTTCACGAC		
Gl-Rheb F	TTTGTGGACAGCTATGATCCC	119	62
Gl-Rheb R	AAGATGCTATACTCATCCTGA		
Gl-mTOR F	AGAAGATCCTGCTGAACATCG	159	62
Gl-mTOR R	AGGAGGGACTCTTGAACCACA		
Gl-S6k F	GGACATGTGAAGCTCACAGAC	239	62
Gl-S6k R	TTCCCCTTCAGGATCTTCTCTA		
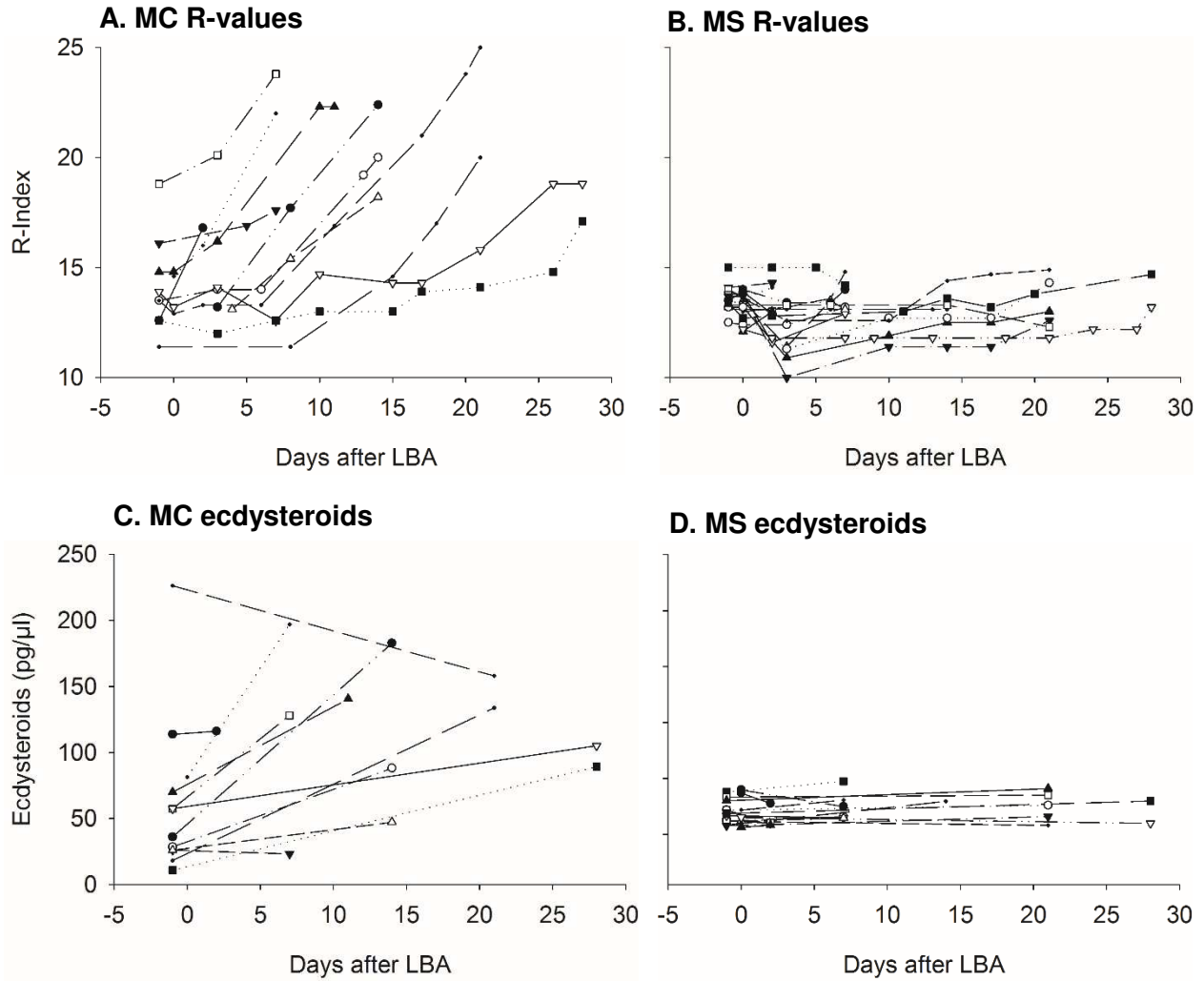
Fig. 2.1. R-values before and after LBA in molting continued (MC) (A) and molting suspended (MS) crabs (B), and ecdysteroid levels in MC (C) and MS (D) crabs. Crabs were separated into MC and MS categories based on R-values at harvest, greater than 15 for MC (A), less than 15 for MS (B). Ecdysteroid levels for MC crabs were increasing (C), in general, whereas in MS crabs, ecdysteroid levels remained low (D).
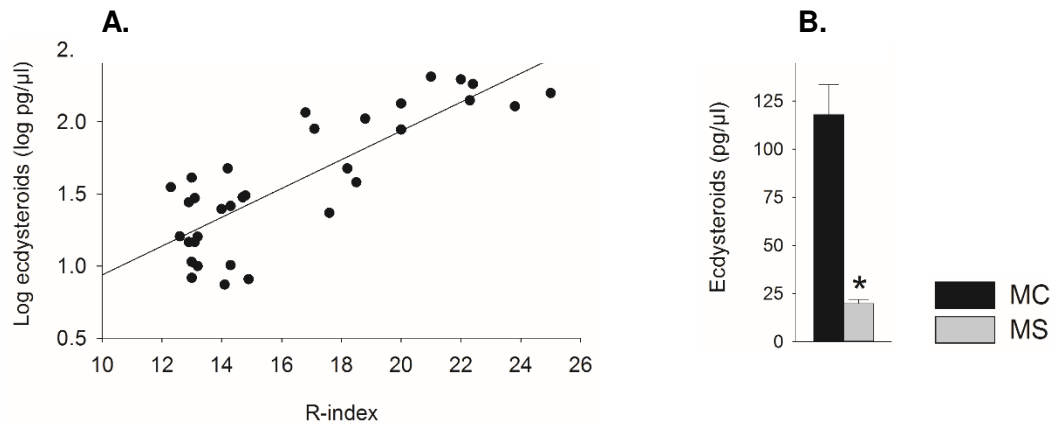
Fig. 2.2. Ecdysteroid levels in hemolymph correlated to R-index values (A) and compared between molt continued (MC) crabs and molt suspended (MS) crabs after LBA (B). Ecdysteroid levels in hemolymph, measured using a competitive ELISA, are strongly correlated with R-index values (R^2=0.687) (A). R-index indicates progress through premolt from a value of 7 (initiation of premolt) to a value of 22-25 (ecdysis). R-index values are calculated by measuring ((LB length/ carapace width) * 100). (N=33). Ecdysteroid levels in hemolymph after LBA, comparing MS to MC (B). Asterisk indicates significant difference at α=0.01 level. Data are presented as means + SEM. (MC, N=14; MS, N=20)

A. Thoracic muscle

B. Claw muscle

Fig. 2.3. Molt continued (MC) and molt suspended (MS) mRNA levels in thoracic and claw muscle after LBA. Claw muscle *Gl-Mstn* mRNA levels were significantly increased in the MS compared to the MC animals. No other genes in either muscle showed a significant difference in mRNA levels between MS and MC. Asterisk indicates significant difference at $\alpha = 0.01$ level. Data are presented as means + SEM. MC, N=14; MS, N=20 for all genes in both muscles except in claw muscle *Gl-Rheb* (MC, N=13) and *Gl-mTOR* (MC, N=12 and MS, N=19).

Thoracic muscle   **Claw muscle**

A. *Gl-EF2*   B. *Gl-EF2*

C. *Gl-Mstn*   D. *Gl-Mstn*

E. *Gl-Akt*   F. *Gl-Akt*

G. *Gl-Rheb*   H. *Gl-Rheb*

Log copy number/µg RNA

Log ecdysteroids (log pg/µl)   Log ecdysteroids (log pg/µl)

Thoracic muscle   **Claw muscle**

I. *Gl-mTOR*   **J. *Gl-mTOR***

K. *Gl-S6k*   **L. *Gl-S6k***
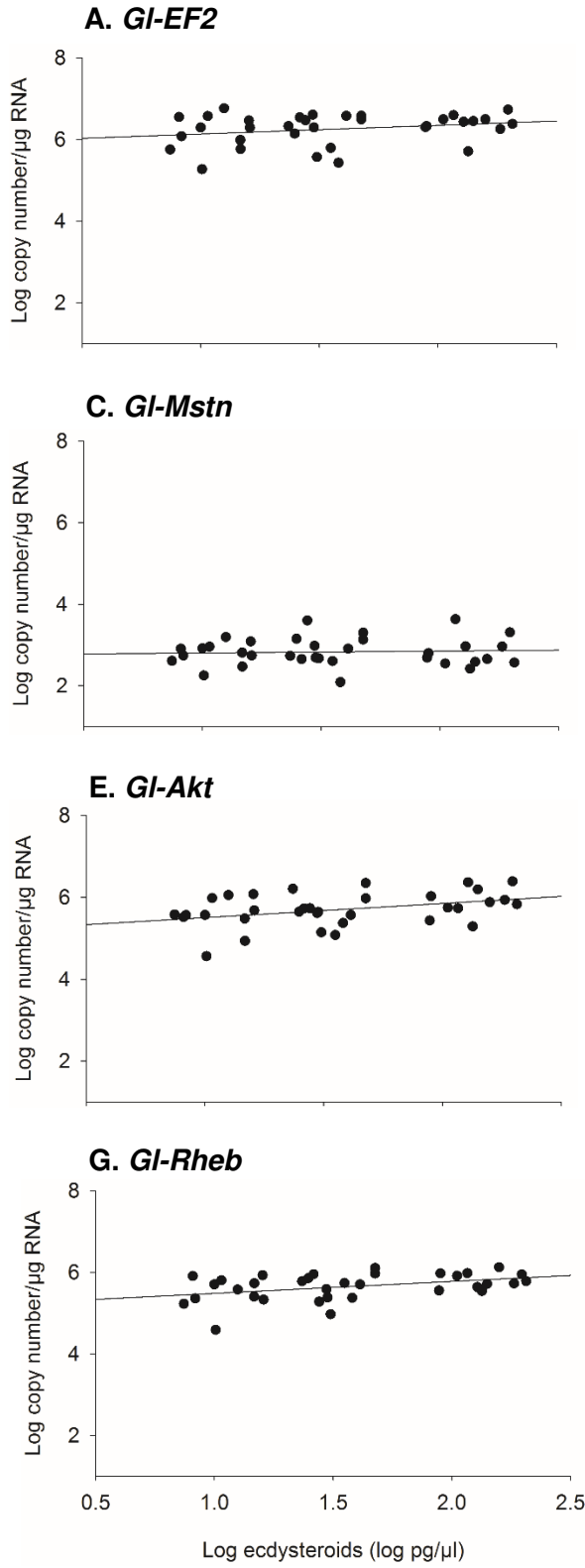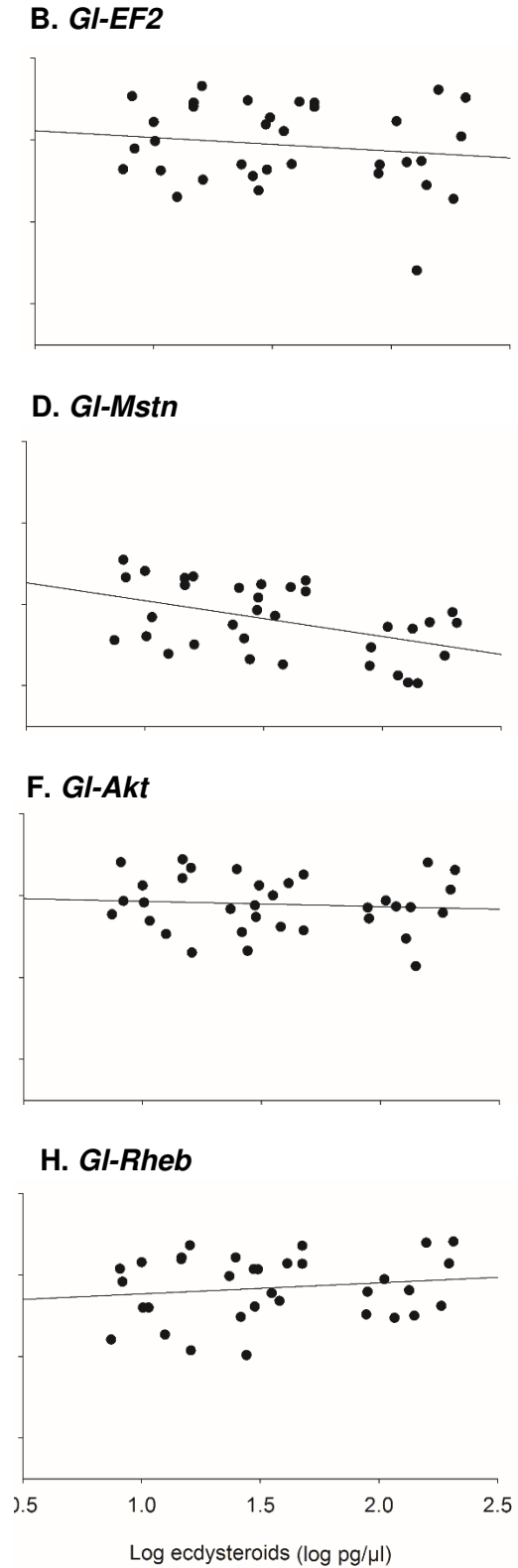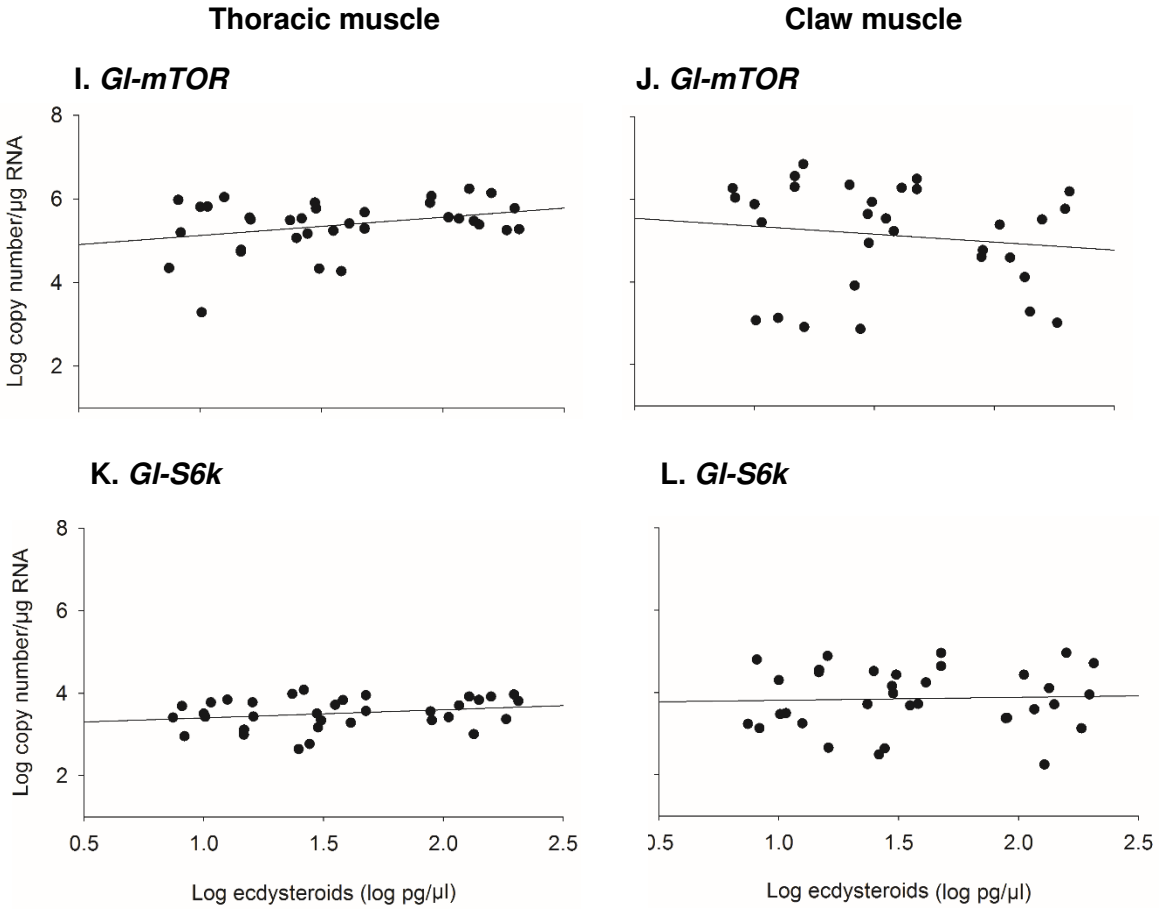
Fig. 2.4. Thoracic (left column) and claw (right column) log muscle mRNA levels correlated to log ecdysteroid levels in hemolymph. Ecdysteroid levels in hemolymph were measured with a competitive ELISA. Gene expression was measured with quantitative reverse transcriptase-polymerase chain reaction (qRT-PCR). All samples (MC and MS) presented for each gene in both muscles. Pearson correlation demonstrated that log *Gl-Mstn* mRNA levels in claw muscle was negatively correlated to log ecdysteroid levels at α=0.01 (R^2=0.217 and P=0.0055). No other genes were significantly correlated with ecdysteroid levels. N=34 for all genes in both muscles, except for claw muscle *Gl-Rheb* (N=33) and *Gl-mTOR* (N=31).

73

Thoracic muscle **Claw muscle**

A. *Gl-EF2* B. *Gl-EF2*

C. *Gl-Akt* D. *Gl-Akt*

E. *Gl-Rheb* F. *Gl-Rheb*

G. *Gl-mTOR* H. *Gl-mTOR*

Log copy number Mstn/µg RNA

MC
MS

Thoracic muscle

Claw muscle

I. *Gl-S6k*

J. *Gl-S6k*
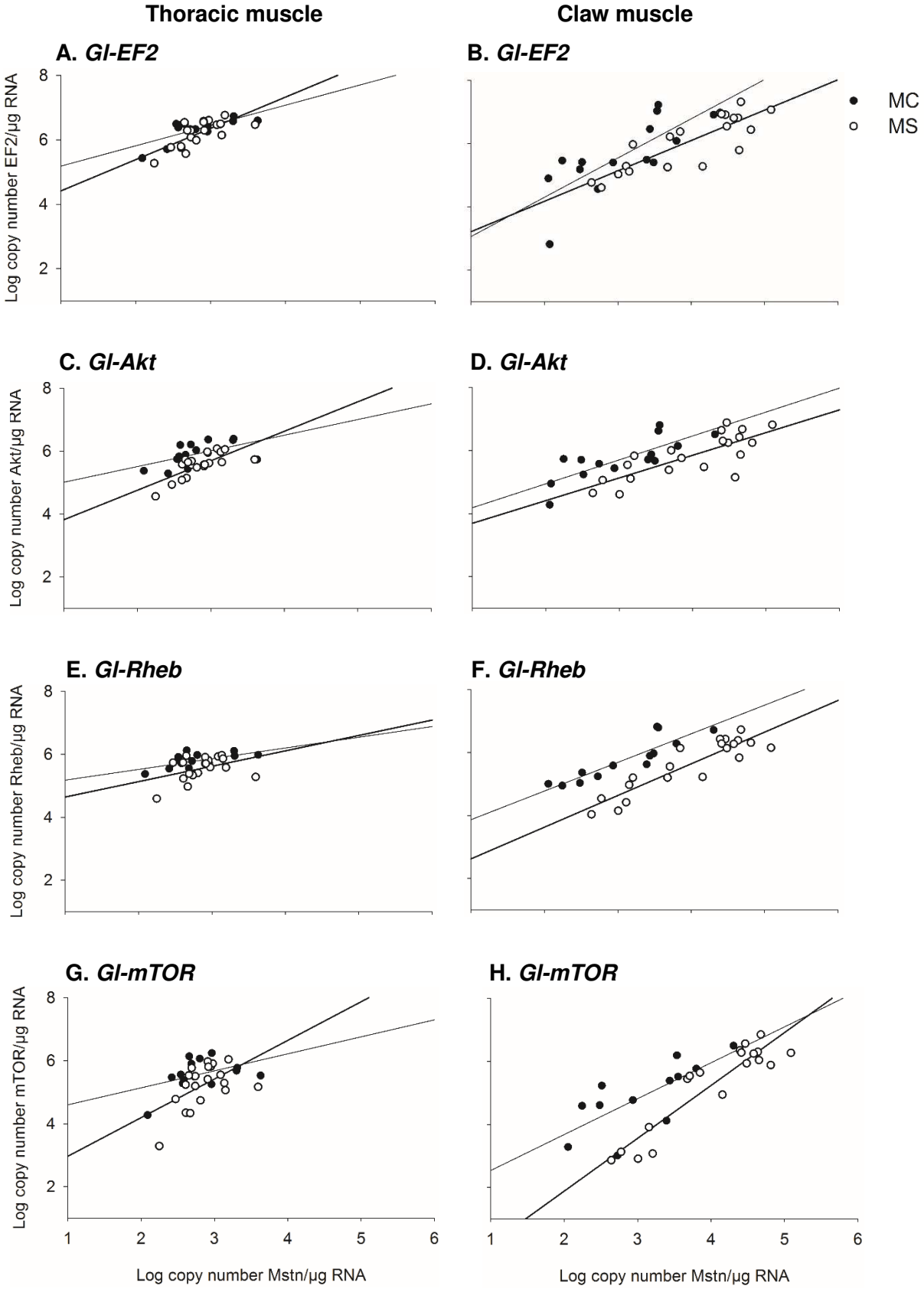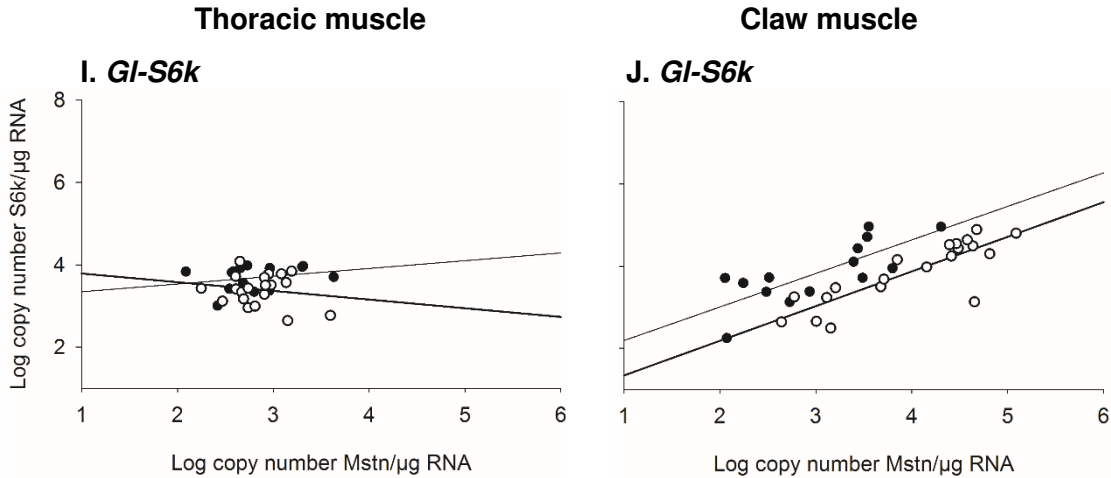
Fig. 2.5. Claw and thoracic muscle log mRNA *Gl-EF2*, *Gl-Akt*, *Gl-Rheb*, *Gl-mTOR* and *Gl-S6k* mRNA levels correlated with log *Gl-Mstn* mRNA levels for molting continued (MC) and molting suspended (MS) animals. Thoracic muscle *Gl-EF2*, *Gl-Akt* and *Gl-mTOR* mRNA levels were positively correlated with thoracic muscle *Gl-Mstn* mRNA levels (*Gl-EF2*, R^2=0.465, $P<0.00001$; *Gl-Akt* R^2=0.291, $P<0.001$ and *Gl-mTOR* R^2=0.192, $P<0.01$). Thoracic muscle *Gl-Rheb* and *Gl-S6k* mRNA levels were not correlated to thoracic muscle *Gl-Mstn* mRNA levels. All claw muscle gene expression was significantly (positively) correlated with *Gl-Mstn* mRNA levels (*Gl-EF2*, R^2=0.604; *Gl-Akt*, R^2=0.489; *Gl-Rheb* R^2=0.506; *Gl-mTOR* R^2=0.627 and *Gl-S6k* R^2=0.464; $P<0.00001$ for each gene). Pearson correlations used for each gene. N=34 for all genes in both muscles, except for claw muscle *Gl-Rheb* (N=33) and *Gl-mTOR* (N=31).

Fig. 2.6. *Gl-Rheb* and *Gl-S6k* mRNA levels correlated to both ecdysteroid levels and *Gl-Mstn* mRNA levels. Multiple linear regression indicated that *Gl-Mstn* mRNA levels and ecdysteroid levels, together, strongly predicted the expression of *Gl-Rheb* (P<0.001, R^2=0.770, MC N=13, MS N=20) and *Gl-S6k* (P<0.001, R^2=0.631, MC N=14, MS N=20) mRNA levels. Bubble size is relative to *Gl-Rheb* mRNA levels. MC=light-colored bubbles, MS=dark-colored bubbles.
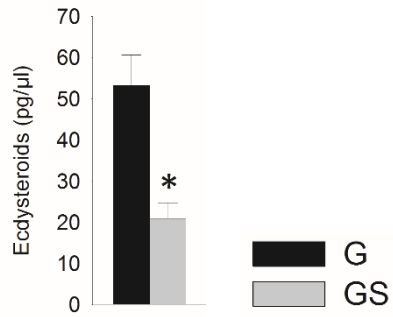
Fig. 2.7. Ecdysteroid levels in hemolymph compared between animals in premolt (G) and 7 days after limb bud autotomy (LBA) when molting growth had been suspended (GS). Significant difference measured with paired t-test. Asterisk indicates significant difference at α=0.01 level. Data are presented as means + SEM. N=13, P=0.0001.
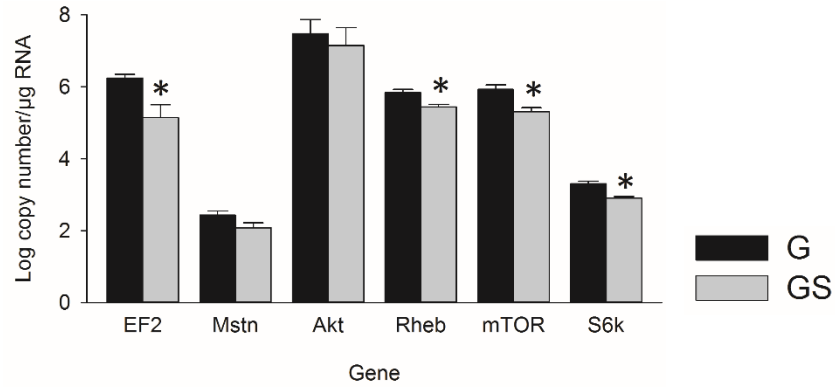
Fig. 2.8. mRNA levels in growing (G) and growth suspended (GS) limb buds. Paired t-tests showed that *Gl-EF2*, *Gl-Rheb*, *Gl-mTOR* and *Gl-S6k* mRNA levels were significantly reduced 7 days after molt suspension by LBA (GS) compared to LBs actively growing during premolt (G). Asterisk indicates significance at α=0.01 level. Data are presented as means + SEM. (N=12 or 13 for all genes.)
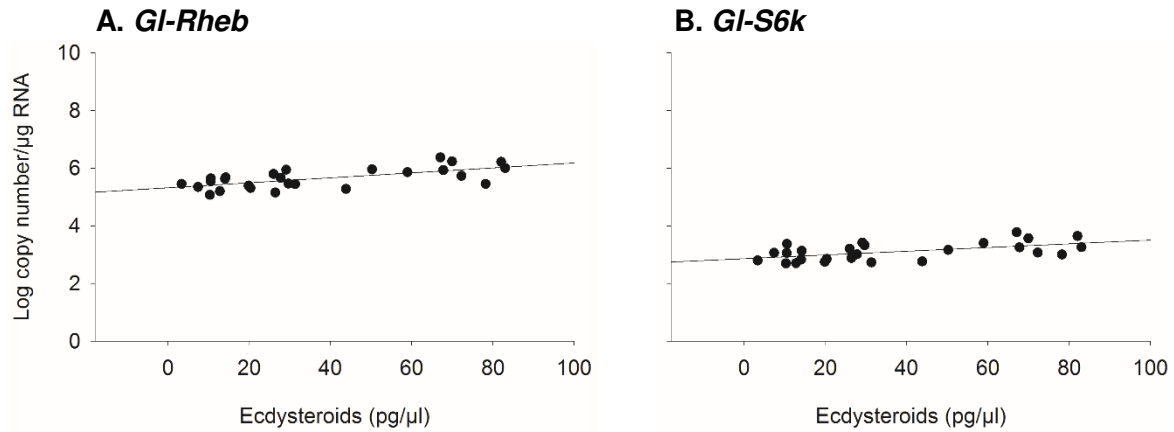
A. *Gl-Rheb*

B. *Gl-S6k*

Fig. 2.9. Limb bud mRNA levels correlated to ecdysteroid levels in hemolymph. *Gl-Rheb* (R^2=0.359, P=0.00123, n=26) and *Gl-S6k* (R^2=0.267, P=0.0069, n=26) Limb bud mRNA levels were correlated with hemolymph ecdysteroid levels. All other genes calculated (*Gl-EF2, Gl-Mstn, Gl-Akt, Gl-mTOR*) had no significant correlation between mRNA levels and ecdysteroid levels in hemolymph (data not shown).
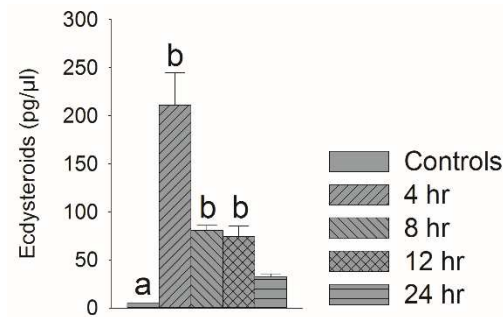
Fig. 2.10. Ecdysteroid levels for controls and after a single injection of 20-hydroxyecdysone (20E). Ecdysteroid levels were significantly increased in animals by 4 h after the injection, and remained elevated through 12 h, compared to controls. Different letters (a, b) indicate significant differences at α=0.01 level. Data are presented as means + SEM. (Controls, N=31; all time points for all genes, N=6).
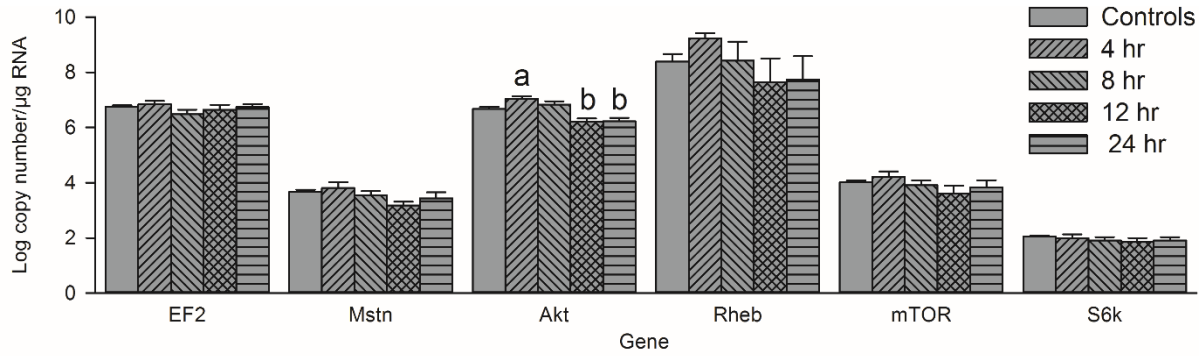
Fig. 2.11. mRNA levels in claw muscle after a single injection of 20-hydroxyecdysone (20E), compared to controls. *Gl-Akt* mRNA levels were down-regulated at 12 h and 24 h, compared to 4 h after injection. There were no significant differences from controls. Significant differences at α=0.01 level are shown with different letters. Data are presented as means + SEM. (Controls, N=30; all time points after injection N=6; except *Gl-Rheb* controls N=27 and *Gl-Rheb* 4 hr after injection N=5).
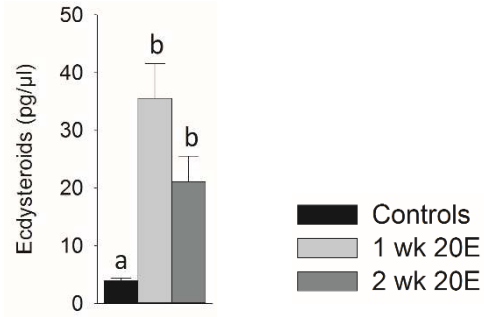
Fig. 2.12. Ecdysteroid levels from controls and animals injected daily with 20-hydroxyecdysone (20E). Ecdysteroid levels were significantly increased in animals both one week and two weeks after beginning injections, compared to controls. Different letters (a, b) indicate significant differences at α=0.01 level. Data are presented as means + SEM. (Controls, N=24; 1 wk 20E, N=8; and 2 wk 20E, N=8.)

A. Thoracic muscle

B. Claw muscle
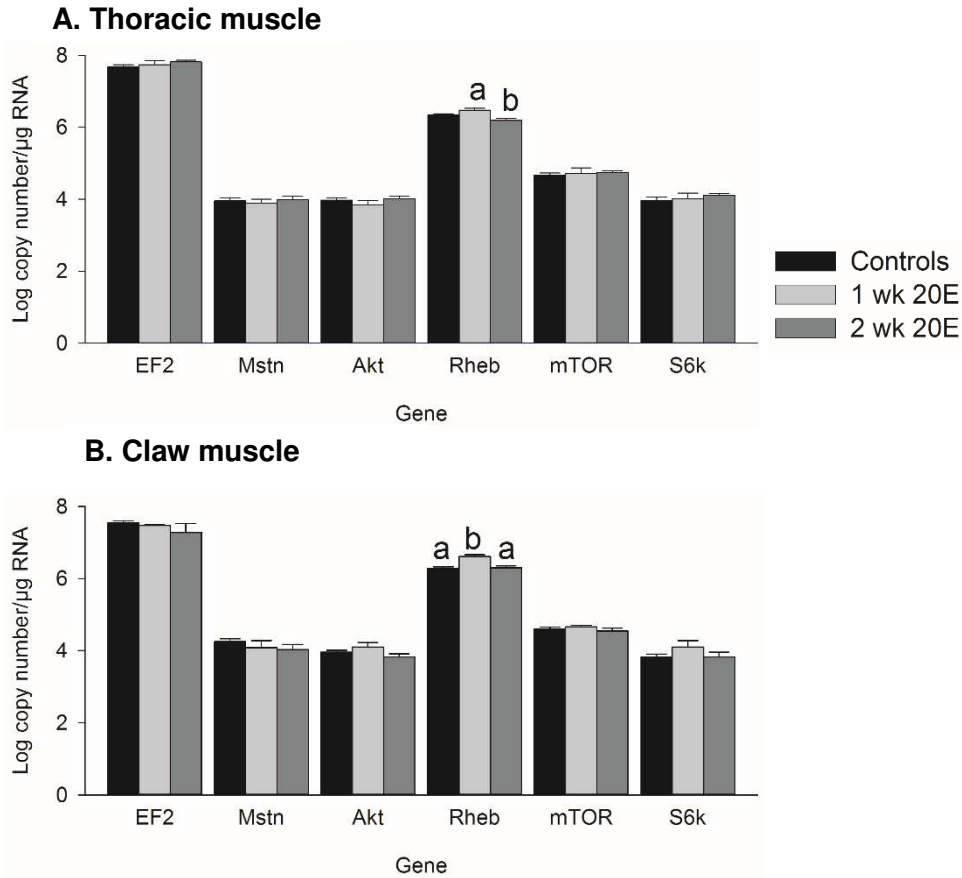
Fig. 2.13. mRNA levels in thoracic (A) and claw (B) muscle in controls, and animals injected daily with 20-hydroxyecdysone (20E) for one week (1 wk 20E) and for two weeks (2 wk 20E). Significant differences are shown with different letters. Data are presented as means + SEM. (Controls, N=23 (claw muscle) or 24 (thoracic muscle); 1 wk 20E, N=6 (claw muscle) or 8 (thoracic muscle); and 2 wk 20E, N=8 for all genes.)
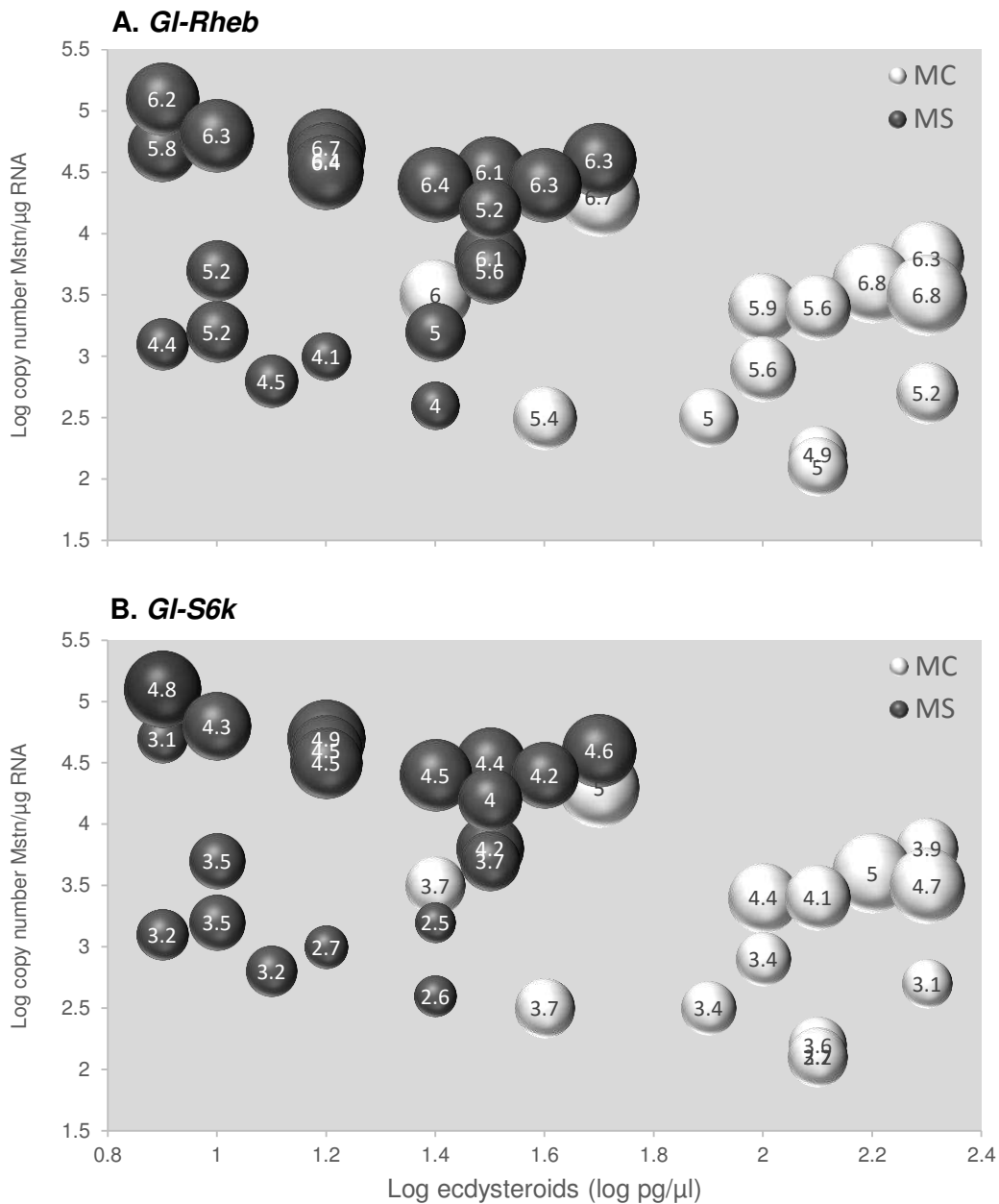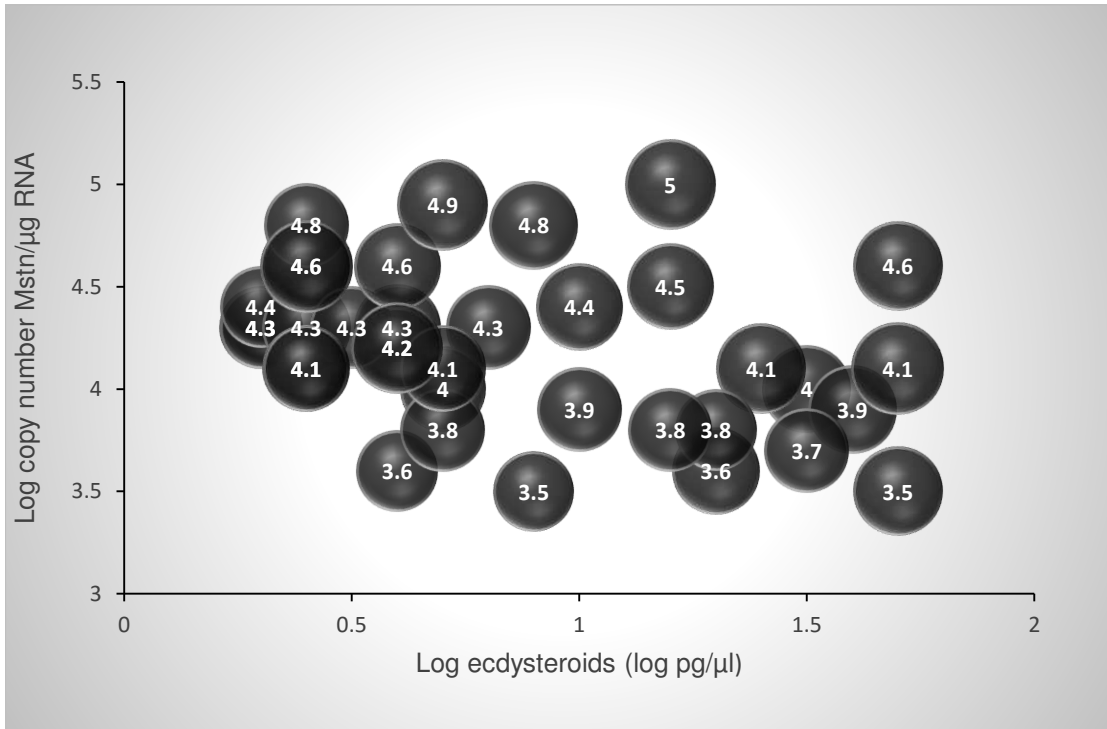
Fig. 2.14. *Gl-Rheb* mRNA levels correlated to both ecdysteroid levels and *Gl-Mstn* mRNA levels. Multiple linear regression indicated that *Gl-Mstn* and ecdysteroids, together, predicted *Gl-Rheb* mRNA levels (P<0.001, R^2=0.448, N=36). Bubble size is relative to *Gl-Rheb* mRNA levels.

Chapter 3

The effects of ecdysteroids on the activity of the *Gecarcinus lateralis myostatin* (*Gl-mstn*) promoter in a heterologous mammalian expression system.

Summary

Mstn is a muscle chalone that represses muscle growth and prevents an excessive hypertrophic response to growth promoting factors. Decreased protein synthesis is a major effect of Mstn signaling. In mammals, steroid signaling results in increased Mstn expression, but in a decapod, *Gl-Mstn* mRNA levels in the claw closer muscle are negatively correlated with ecdysteroid levels. As ecdysteroid levels increase during premolt, decreasing *Gl-Mstn* levels allow increased protein synthesis. Protein synthesis is necessary for remodeling the claw muscle in preparation for rapid growth immediately after ecdysis. In this study, we sequenced the *Gl-Mstn* promoter and identified a putative EcRE. As endogenous ecdysteroid signaling is absent in mammalian cells, we created a heterologous ecdysteroid system in HeLa cells, which allowed precise control of ecdysteroid levels. We found that the *Gl-Mstn* promoter was functional in the heterologous cell system, but further work will be necessary to determine the functionality of the putative EcRE in the *Gl-Mstn* promoter.

Introduction

Muscle mass is in a constant state of flux, even in adults. Muscle tissue fibers hypertrophy or atrophy in response to various stimuli such as mechanical loading (Ellman et al., 2013; Fitts et al., 2000; Miyazaki and Esser, 2009; Phillips et al., 2009), diet (Carbone et al., 2012; Martin et al., 2015; Matsakas and Patel, 2009), disease (Ciciliot et al., 2013; Sakuma et al., 2014; Sakuma and Yamaguchi, 2012), and aging (Goldspink, 2012; Nilwik et al., 2013). In mammals, growth promoting factors such as IGF-1 (Egerman and Glass, 2014; Sandri et al., 2013) and androgens (Dubois et al., 2012; Dubois et al., 2014; Sheffield-Moore, 2000) initiate signaling that result in muscle hypertrophy, while glucocorticoid signaling results in muscle atrophy (Braun and Marks, 2015; Egerman and Glass, 2014). Glucocorticoid (Ma et al., 2001;

Qin et al., 2013; Zhang et al., 2007), androgen (Dubois et al., 2012; Dubois et al., 2014) and IGF-1 (Valdes et al., 2013; Zuloaga et al., 2013) signaling all increase myostatin (Mstn) expression. Myostatin is a muscle chalone—a growth factor secreted by muscle that represses muscle growth in general (Braulke et al., 2010; Ciarmela et al., 2010; Druet et al., 2014; Finsterer, 2014; Georges, 2010; Gokoffski et al., 2011; Han et al., 2010; Lander, 2011; Long et al., 2009; Mak and Cheung, 2009; McKnight, 1997; Szent-Gyérgyi, 2010; Wang et al., 2014b; Zhang, 2008), or modulates excessive hypertrophy in response to growth promoting factors (Chien et al., 2013; Dubois et al., 2012; Dubois et al., 2014; Garikipati and Rodgers, 2012; Kawada and Ishii, 2009; Marcotte et al., 2014; Matsakas et al., 2006; Paoli et al., 2015; Price et al., 2011; Yang et al., 2007; Zhou et al., 2015). Glucocorticoid signaling results in muscle atrophy by increasing expression of Mstn (Zhang et al., 2007), through direct binding of the glucocorticoid receptor to a glucocorticoid response element (GRE) on the Mstn promoter (Ma et al., 2001; Qin et al., 2013). Androgens cause muscle hypertrophy, but modulate excessive muscle growth by binding androgen response elements (AREs) in the Mstn promoter, causing increased Mstn expression. Likewise, IGF-1 stimulates Mstn modulation of muscle growth by initiating cAMP response element binding (CREB) to the CREB response element (CRE) in the Mstn promoter (Valdes et al., 2013; Zuloaga et al., 2013). In mammals, Mstn signaling contributes to muscle atrophy by inhibiting protein synthesis (Goodman et al., 2013; Hitachi et al., 2014; Hulmi et al., 2013; Sakuma et al., 2014; Sartori et al., 2014; Schiaffino et al., 2013; Welle et al., 2009), and increasing protein degradation (Allen and Loh, 2011; Braun and Marks, 2015; Gilson et al., 2007; Ma et al., 2003).

In crustaceans, ecdysteroid signaling results in muscle atrophy of the claw closer muscle. The molting process is initiated by increased production of ecdysteroids (molting hormones) by the Y organ (molting gland) (Covi et al., 2009; Skinner, 1985b). In *Gecarcinus lateralis*, the blackback land crab, ecdysteroid levels increase from approximately 10-20 pg/µl during intermolt to over 400 pg/µl during premolt (Covi et al., 2010; McCarthy and Skinner,

1979). The major ecdysteroids in the blackback land crab are 20-hydroxyecdysone (20E) and Ponasterone A (Pon A), occurring in an approximately 3:1 ratio, respectively (McCarthy, 1982; McCarthy and Skinner, 1977b; McCarthy and Skinner, 1979). As ecdysteroids increase during premolt, the claw closer muscles atrophy between 40% (Skinner, 1966) and 78% (Ismail and Mykles, 1992), enabling withdrawal of the claw muscle from the old exoskeleton at ecdysis (Mykles and Skinner, 1982a; Skinner, 1966). During atrophy of the claw closer muscle, there is increased protein degradation, and increased protein synthesis (Covi et al., 2010). This is similar to denervation atrophy in mammals (Argadine et al., 2009; Quy et al., 2013), when increased protein synthesis allows remodeling of muscle fibers to accommodate altered muscle use (Bassel-Duby and Olson, 2006; Mykles and Medler, 2015). In mammals, steroids increase Mstn expression, but in *G. lateralis, Gl-Mstn* levels are negatively correlated with ecdysteroid levels during premolt (Covi et al., 2010). *Gl-Mstn* is also negatively correlated with protein synthesis, indicating that *Gl-Mstn* negatively regulates protein synthesis, the same role as Mstn has in mammals (Covi et al., 2010). However, unlike mammals, *Gl-Mstn* does not appear to increase protein degradation in crustaceans, as decreasing *Gl-Mstn* is correlated with increasing protein degradation (Covi et al., 2010). Ecdysteroids signal through the ecdysteroid receptor, a heterodimer consisting of RXR and EcR (Koelle et al., 1991; Yao et al., 1993). Ecdysteroid receptors bind ecdysteroid response elements (EcREs) on DNA and normally repress transcriptional activity until transcription is activated by ligand (ecdysteroid) binding (Henrich et al., 2009; Hu et al., 2003; Nakagawa and Henrich, 2009; Riddiford et al., 2001). Only a limited number of EcREs have been used in assays, and to my knowledge, ecdysteroid stimulation always results in increased transcription of the target genes. However, activated nuclear receptors, in general, can increase or decrease gene transcription (Moras and Gronemeyer, 1998).

The purpose of this research was to sequence the *Gl-Mstn* promoter, analyze the promoter for transcription binding sites, and perform functional studies on the activity of the *Gl-*

Mstn promoter. Specifically, we wanted to determine if ecdysteroids directly inhibit transcriptional activity of the *Gl-Mstn* gene through binding of ligand-activated ecdysteroid receptors to the ecdysone response element (EcRE) in the *Gl-Mstn* promoter. We developed a heterologous mammalian cell culture system in HeLa cells, to be able to precisely control ecdysteroid levels, as mammalian cells contain no endogenous ecdysteroids. Our hypothesis is that increased ecdysteroid levels will inhibit *Gl-Mstn* promoter activity.

Materials and methods

Animals

Male *Gecarcinus lateralis* (Fréminville 1835), blackback land crabs, were collected from the southern coast of the Dominican Republic and flown to Colorado, USA. Crabs were kept in plastic containers at 27^0C and 75-90% relative humidity on a 12 h light: 12 h dark schedule. Containers held eight to twelve crabs in aspen bedding dampened with 5 parts per thousand (p.p.t.) Instant Ocean (Aquarium Systems, Mentor, OH). All crabs were fed lettuce, carrots and raisins two times per week.

Genomic DNA isolation

Genomic DNA was isolated from thoracic ganglia or claw muscle freshly dissected from *G.lateralis* following the manufacturer's protocol for animal tissues, with 1 h for thoracic ganglia tissue lysis, and three h for claw muscle tissue lysis (Qiagen Inc., Frederick, MD, USA). Genomic DNA was quantified (79.22 ng/µl) with a NanoDrop 1000 V3.8.1 (Thermo Fisher Scientific, Inc., Waltham, MA, USA), then stored in a -20°C freezer.

DNA Walking

The DNA Walking SpeedUp™ Premix Kit (Seegene, Gaithersburg, MD, USA) was used to obtain the *G. lateralis* promoter sequence. Genomic DNA (1 µl), purified from the thoracic ganglion, was used as the template in a 20 µl PCR reaction, along with 2 µl DW2-ACP11, the non-specific forward primer (Table 3.1), 1 µl R4, the *Gl-Mstn*-specific outer primer (Table 3.1), 6 µl nuclease-free water, and 10 µl of 2X SeeAmp™ ACP™ Master Mix II (Seegene). All primers

88

used in DNA walking protocol were 5 µM concentration. Veriti 96 well Thermal Cycler (Thermo

Fisher Scientific, Inc., Waltham, MA, USA) PCR reaction was set for one initial cycle of 94°C for

5 min followed by 42°C for 1 min, and then 72°C for 2 min. The initial cycle was followed by 30

cycles of the following: 94°C for 40 s, 55°C for 40 s, and 72°C for 90 s, and then a final

elongation period of 7 min at 72°C. The first PCR product was purified with the QIAquick PCR

Purification Kit (Qiagen Inc.). The QIAquick protocol was followed, with care taken to remove

ethanol from the O rings after the Buffer PE wash. DNA was eluted with 30 µl Buffer EB.

For the second PCR, 3 µl of the first PCR product, 1 µl of each primer, including the

ACPgC forward primer and the Mstn R5 nested gene-specific reverse primer (Table 3.1), and 5

µl of nuclease-free water was used. The DNA Walking protocol (Seegene) was followed, except

10 µl of GoTaq Green® Master Mix (Promega Corp., Madison, WI, USA) was used instead of

the ACP Master Mix II (Qiagen Inc.) that came with the kit. The second PCR settings were an

initial denaturation of 94°C for 3 min followed by 35 cycles of 94°C for 40 s, 60°C for 40 s and

72°C for 90 s. The 35 cycles were followed by 7 min at 72°C. The PCR product was then diluted

1/1000 to eliminate nonspecific bands.

The third PCR was the same as the second PCR, except each tube contained 30 µl total

volume, with components increased proportionately, and the nested reverse primer was Mstn

R2 (Table 3.1). The third PCR product was run on 1.5% agarose gel at 100 volts for 35 min. An

approximately 1100 base pair (bp) DNA band was extracted with the QIAquick Gel Extraction

Kit (Qiagen Inc.), following the manufacturer's protocol. DNA was eluted with 10 µl EB buffer,

and quantified (64ng/µl.) with a NanoDrop 1000 V3.8.1 (Thermo Fisher Scientific, Inc.). This

product was then used for ligation into the pCR™2.1-TOPO® vector (Thermo Fisher Scientific,

Inc.).

DNA Walking product cloning, sequencing and sequence analysis

The ~1100 base pair DNA Walking product was ligated into the pCR™2.1-TOPO® vector

using the TOPO® TA Cloning® kit (Thermo Fisher Scientific, Inc.). 2 µl (~130 µg) of the gel-

extracted 3rd PCR product was added to 0.5 μl of salt solution (1.2 M NaCl and 0.06 M MgCl$_2$)

supplied with the TOPO cloning kit and 0.5 μl of the pCR^{TM}2.1-TOPO$^®$ vector for a 3 μl total

reaction. The pCR^{TM}2.1-TOPO$^®$ vector is supplied in a linear form with topoisomerase I

covalently bound. The reaction was incubated for 25 min at 22°C, and then the entire ligation

product was added to 25 μl of One Shot$^®$ chemically competent cells received with the TOPO$^®$

TA Cloning$^®$ kit. Cells were incubated on ice 30 min, placed in a 42°C bath for 90 s, and then

immediately transferred back to ice. S.O.C medium (125 μl, supplied with the TOPO$^®$ TA

Cloning$^®$ kit) were added to the cells, which were then incubated for 1 h in a 37°C Innova 4300

incubator shaker (New Brunswick Scientific, Woburn, MA, USA) set at 200 RPM. A 150 μl

sample of culture was transferred to a 100 mm X 15 mm polystyrene Petri plate (Thermo Fisher

Scientific, Inc.) containing Luria-Bertani (LB) agar with 100 μg/ml ampicillin and incubated at

37°C in a Thelco (Precision Scientific Instruments, Buffalo, NY, USA) incubator for 18 h. Ten

colonies were selected from numerous colonies on the plate, and each was placed in 0.5 ml LB

media with 100 μg/ml ampicillin. The bacteria were incubated 6 h at 37°at 200 RPM. After

incubating 3 h, 1 μl of culture was removed to use as template for an insert check. The template

was amplified by PCR in a reaction containing 1 μl each of the M13 primers (supplied with the

TOPO kit), 2 μl nuclease-free water, and 5 μl of GoTaq Green$^®$ Master Mix (Promega Corp.,

Madison, WI, USA). PCR amplification settings were an initial denaturation for 3 min at 94°C, 26

cycles of 94°C for 30 s, 50°C for 30 s and 72°C for 90 s followed by 94°C for 7 min for final

elongation. PCR product was separated on a 1% agarose gel at 100 volts for approximately 1 h.

Insert check results showed that all colonies contained the 1 kb insert. A 100 μl sample of

culture was transferred to 3.5 ml LB broth with 100 μg/ml ampicillin and incubated overnight in

the 37°C at 200 RPM. Glycerol stock was prepared by adding 360 μl of broth containing CH3

Blue competent cells containing the pCR^{TM}2.1-TOPO$^®$ vector with the 1000 bp insert to 60 μl

sterile 70% glycerol and stored in a -80°C freezer. Plasmids were extracted from the remaining

overnight culture with the QIAprep Spin Miniprep Kit (Qiagen Inc.) following the manufacturer's

protocol and eluting with 50 µl buffer EB. Plasmids were sent to Davis Sequencing (Davis Sequencing, Davis, CA, USA). A BLASTN search with the nr/nt database of NCBI was used to compare the obtained sequence with other sequences. The MacVector software program, version 11.0 (MacVector, Inc., Apex, NC, USA), was used to identify transcription factor binding sites within the *Gl-Mstn* promoter.

Construction of vectors and cell transformation

The *Gl-Mstn* promoter was amplified from *G. lateralis* claw muscle genomic DNA template. F1/R1, then F1/R2 primers (Table 3.2) were used in semi-nested PCR reactions using a Veriti 96 well Thermal Cycler (Thermo Fisher Scientific, Inc.). Nested PCR reactions contained 4 µl template, 2 µl each primer, 2 µl nuclease-free water, and 10 µl GoTaq Green® Master Mix (Promega Corp., Madison, WI, USA) in a 20 µl reaction. Primer concentrations were 10 uM for all genomic DNA amplification. The thermal cycler settings were an initial denaturation for 3 min at 94°C, followed by 35 cycles of 30 s at 94°C, 30 s at 53°C for annealing, and 80 s at 72°C for elongation, as the PCR products were expected to be 1,091 and 934 bp for the first and second PCR reactions, respectively. The cycles were followed by 7 min at 72°C for final elongation. A third PCR reaction with F1/R2 primers was required for further amplification using the same thermal cycler settings in a 10 µl reaction, and using the second nested PCR product as template. The amplified genomic DNA was then re-amplified with primers which included a *Kpn*I restriction site in the forward primer and *Xho*I in the reverse primer (Table 3.3). The forward primer included the first five bases after the satellite DNA, as these bases had been excluded in the F1 *Gl-Mstn* forward primer. PCR reaction settings were the same as for the genomic amplification, except the annealing temperature was 56°C (Table 3.3), and elongation time was 90 s. In addition, only 1 µl template (3rd PCR product) was used in 10µl reactions. After amplification, the PCR product with the *Kpn*I and *Xho*I restriction sites was purified with the QIAquick PCR Purification Kit (Qiagen Inc.) according to manufacturer's protocol, and then PCR amplified again with the same settings as the previous first PCR with restriction site primers.

The PCR product was separated on a 1% agarose gel at 100 volts for 75 min, and a 900+ base pair (bp) DNA band was extracted with the QIAquick Gel Extraction Kit (Qiagen Inc.). The extraction product was then used as the *Gl- Mstn* promoter restriction digest template.

A *Gl-Mstn* promoter without the putative ecdysone response element (EcRE) was created with a primer which included a *Kpn*I restriction site and excluded the first 35 bp after the end of the satellite DNA, including a putative EcRE (GCTCACTCTCA) located 18 – 28 bp after the 3' end of the satellite DNA. Genomic DNA was amplified from claw muscle using F2/R1, then F1/R2 (Table 3.2) nested PCR reactions. PCR reactions were the same as described for the full-length *Gl-Mstn* promoter except annealing temperature was 54°C and elongation time was 1 min for both nested PCR reactions, with expected product sizes of 1108 bp in the first PCR, and 891 bp in the second nested PCR. Each reaction was 10 µl total, and multiple reactions were combined for agarose gel electrophoresis as described above. The second PCR product was amplified with a forward primer which contained the *Kpn*I restriction site, but deleted the EcRE (KpnI noRE) and the same reverse primer with *Xho*I as used in the full-length *Gl-Mstn* promoter (Table 3.3). The PCR product was separated by agarose gel electrophoresis and extracted as described above. This PCR product was then used as the template to repeat the PCR with restriction primers to increase DNA concentration.

Bacterial cultures containing the *Uca pugilator* ecdysone receptor (*Up-EcR*) and two isoforms of Retinoid X Receptor (*Up-RXR*) inserted into pBluescript phagemids (Agilent Technologies, Santa Clara, CA, USA) were provided by David S. Durica (University of Oklahoma). The two *Up-RXR* isoforms included a full-length *Up-RXR* (GenBank accession U31832) and *Up-RXR* coding for a 33 amino acid deletion (*Up-RXR* (-33)) (GenBank accession AF032983) (Chung et al., 1998; Durica and Hopkins, 1996; Durica et al., 2002). The *Up-EcR* clone included 2 bases of the 5'UTR, the 1557 bp open reading frame (ORF), and at least 165 bp of the 3' UTR. The *Up-RXR* and *Up-RXR* (-33) clones included only the entire 1398 bp and 1299 bp ORF, respectively.

Up-EcR, *Up-RXR*, and *Up-RXR*(-33) were amplified from the inserted genes in pBSII

phagemids. For *Up-EcR*, the forward primer included a *Bam*HI restriction site and the reverse

primer included a *Cla*I restriction site. For both *Up-RXR*, and *Up-RXR*(-33), the forward primer

included a *Hin*dIII restriction site and the reverse primer included an *Xba* restriction site (Table

3.3). Expected product sizes were 1592 bp for *Up-EcR,* 1429 bp for *Up-RXR*, and 1330 bp for

Up-RXR(-33). The reaction mix for *Up-EcR* consisted of 1 µl template, 0.5 µl 10 µM forward and

reverse primers, 3 µl nuclease-free water, and 5 µl GoTaq Green® Master Mix (Promega

Corp.). The reaction mixes for *Up-RXR* and *Up-RXR*(-33) were similar, but 1 µl of each primer

was used in *Up-RXR*, and 2 µl template and 1 µl of each primer was used in *Up-RXR*(-33). The

thermocycler settings for *Up-EcR* were 4 min at 94°C for initial denaturation, then 30 cycles of

94°C for 30 s, 60°C for 30 s, and 72°C for 2 min with a final elongation at 72°C for 7 min. The

thermocycler settings for *Up-RXR* and *Up-RXR*(-33) were 3 min at 94°C, then 3 cycles of 94°C

for 30 s, 37°C for 30 s and 72°C for 100 s to increase binding of the long primers to the

relatively short primer-binding template sequence. This was directly followed by 28 cycles of

94°C for 30 s, 56.5°C for 30 s, and 72°C for 105 s. A final elongation at 72°C for 7 min

concluded the run. The PCR product was separated on a 1% agarose gel at 100 volts for 1 h.

The DNA bands were extracted with the QIAquick Gel Extraction Kit (Qiagen Inc.), following

protocol, and the extraction products were used for restriction digests.

The full-length *Gl-Mstn* promoter and the *Gl-Mstn* promoter without the EcRE amplified

with primers containing restriction sites, and the pGL3 plasmid were double digested with Fast

Digest *Kpn*I and *Xho*I (Thermo Fisher Scientific, Inc.). The *Up-EcR* product amplified with

primers with restriction sites and the pKH3 plasmid were double digested with *Bam*HI and *Cla*I.

The *Up-RXR* and *Up-RXR*(-33) products amplified with primers containing restriction sites and

the pKH3 plasmid were double digested with H*in*dIII and *Xba*. The PCR product or plasmid DNA

protocols were followed, as appropriate, except the digestion incubations were extended to one

h. The products were separated on a 1% agarose gel followed by gel extraction, as described

above. These double-digested and gel-extracted products were then used for ligation reactions.

The *Kpn*I and *Xho*I restriction digested *Gl-Mstn* promoter and pGL3 plasmid were placed

in a ligation reaction in a 5:1 insert:vector ratio with 1 µl T4 DNA ligase (Thermo Fisher

Scientific, Inc.) and nuclease-free water to make 20 µl total reaction. For all other ligations,

including the *Gl-Mstn* promoter without the EcRE with the pGL3 plasmid, *Up-EcR*, *Up-RXR* and

Up-RXR(-33) with the pKH3 plasmid, the insert:vector ratio was 3:1. Both *Gl-Mstn* promoters

were incubated with pGL3 at 37°C for 1 h, followed by 5 min at 80°C to inactivate enzymes,

followed by a 16°C overnight incubation according to the T4 DNA ligase overnight ligation

protocol. The linearized and digested *Up-EcR*, *Up-RXR* and *Up-RXR*(-33) with pKH3 ligation

followed the same protocol, with one modification to increase ligation success; the overnight

ligation started in a room temperature water bath which was then placed in a 4°C refrigerator for

slow cooling. All ligated plasmids were then used for transformation into *Escherichia coli*

bacteria cells, except *Up-EcR* was first run on a gel, extracted, and then used for

transformation.

The full-length *Gl-Mstn* promoter and the *Gl-Mstn* promoter without the EcRE, both in

pGL3, and *Up-EcR, Up-RXR*, and *Up-RXR*(-33) all in pKH3, were transformed into chemically

competent CH3 Blue *Escherichia coli* cells (Bioline, Taunton, MA, USA. Ligation reaction (1 µl)

was added to 25 µl competent cells and incubated on ice for 30 min. Cells were then placed in a

42°C water bath for 40 s, then returned to ice for 2 min. LB broth without ampicillin (125 µl) was

added, and the cell culture was incubated one h in a 37°C Innova 4300 incubator shaker (New

Brunswick Scientific, Woburn, MA, USA) set at 200 RPM. Culture (50 µl) was transferred to a

100 mm X 15 mm polystyrene Petri plate (Thermo Fisher Scientific, Inc.) containing LB agar

with 100 µg/ml ampicillin and incubated at 37°C in a Thelco (Precision Scientific Instruments,

Buffalo, NY, USA) incubator for 18 h. Colonies were selected and placed in 0.5 ml LB media

with 100 µg/ml ampicillin. The bacteria were incubated 6 h at 37°C in the Innova incubator

shaker set at 200 RPM. After 3 h of incubation, an insert check, similar to the DNA walking insert check, but with gene-specific primers and settings confirmed cultures with DNA of interest inserts (Table 3.4). Elongation times were based on the elongation rate of ~ 1000 bases per min. The PCR product was run on a 1% agarose gel. If a PCR amplification contained bands of the appropriate size, 100 µl of that culture was transferred to 3.5 ml of LB broth with 100 µg/ml ampicillin and incubated overnight in the 37°C, 200 RPM Innova incubator shaker. Glycerol stock was prepared by adding 360 µl of broth containing transformed CH3 Blue cells to 60 µl of 70% glycerol, and stored at -80°C. After the glycerol stock was made, all transformed plasmids were extracted from the remaining overnight culture with the QIAprep Spin Miniprep Kit (Qiagen Inc.), following protocol, and eluted with buffer EB. Plasmids were prepared and sent to Davis Sequencing (Davis, CA, USA) according to Davis' protocol.

Western blot

HeLa cell extracts (20 µg) were separated on a BIO-RAD Tris-HCl 12% gel (BIO-RAD, Hercules, CA, USA) in Tris base running buffer (25 mM Tris base, 0.2 M glycine and 1% sodium dodecyl sulfate). Running time was 1 h 45 min at 100 volts. Proteins were transferred to a 0.2 µm polyvinylidene difluoride (PVDF) blotting membrane in Towbin's transfer buffer for 1 h at 100 volts. The blot was rinsed 3 times, 1 minute each, in 20 ml Towbin's transfer buffer, then blocked with 4% BSA in tris-buffered saline (TBS) (25 mM tris base, 225 mM NaCl). The membrane was then incubated overnight in a 1:1,000 dilution of affinity isolated anti-hemagglutinin antibody produced in rabbit (Sigma-Aldritch, St. Louis, MO, USA). The blot was rinsed 3 times, 5 minutes each, in TBS with 0.1% Tween (TTBS), then incubated in TTBS with a 1:10,000 dilution of goat anti-rabbit IgG conjugated to horse radish peroxidase (Southern Biotech, Birmingham, AL, USA) for 1 h. The blot was developed with Western Bright Sirius (Advansta, Menlo Park, CA, USA).

HeLa cell transfection and luciferase assay

HeLa cells were maintained and passaged in growth medium (Dulbecco's Modified Eagle Medium (DMEM) (Thermo Fisher Scientific Inc.) with 10% fetal bovine serum (FBS) (Thermo Fisher Scientific, Inc.) and 2% glutamine (Thermo Fisher Scientifi, Inc.). When cells were ~ 80% confluent, the supernatant was discarded, and cells were washed with Dulbecco's phosphate buffered saline (PBS) (Thermo Fisher Scientific, Inc.). Trypsin (Thermo Fisher Scientific, Inc.) was added to the washed cells and the flask was placed in the 37°C, 5% CO_2 incubator (NuAire, Plymouth, MN, USA) four min to dissociate cells from the flask. Growth medium was added, and cells were centrifuged in a 15 ml tube for 5 min at 400 X g. The pellet was resuspended in growth medium, and approximately 1 X 10^5 cells were transferred in 1 ml growth medium to 24-well plates. Plates with HeLa cells were placed in a 37°C, 5% CO_2 incubator overnight, and used for transfections the next day.

pGL3 Luciferase reporter vectors (Promega Corp.) and pKH3 expression vectors (Addgene, Cambridge, MA, USA) were provided by Sandra Quackenbush (Colorado State University). The luciferase plasmids included pGL3-basic with no promoter or enhancers before the *Photinus* luciferase gene, pGL3-control with SV40 promoter and enhancer sequences resulting in strong *Photinus* luciferase expression, and pRL-TK, containing an SV40 promoter and enhancers before the *Renilla* luciferase gene. The pRL-TK plasmid was used as a control to normalize *Photinus* luciferase expression. pKH3 is a reporter plasmid containing a triple hemagglutinin (HA) sequence which tags the protein of interest, with multiple restriction sites both before and after the HA tag. In addition to the pKH3 plasmid, a pKH3 plasmid containing an approximately 38 kilobase (kb) ORF (pKH3-ORF-A) was provided. This served as a positive control for protein expression. The pGL3-Mstn plasmid contained the full-length *Gl-Mstn* promoter inserted 5' to the luciferase gene. The pGL3 (-) EcRE contained the *Gl-Mstn* promoter without the EcRE 5' to the luciferase gene. pKH3-EcR had the *Up-EcR* open reading frame (ORF) inserted in-frame 3' of the hemagglutinin (HA) tag. pKH3-RXR and pKH3-RXR(-33) had

the *Up-RXR* and *Up-RXR*(-33) ORFs, respectively, inserted in-frame 5' of the HA tag (Table 3.5). pKH3 was the empty plasmid used as a negative control.

For each of the pGL3 reporter plasmids (pGL3 Basic, pGL3 Control, pGL3 Mstn, and pGL3 (-) EcRE), 0.3 µg plasmids per well were used for transfections. For pRL-TK, 0.01 µg plasmid was added to every well as a transfection control, allowing a dual luciferase assay for each sample. For the expression plasmids (pKH3, pKH3-EcR, pKH3-RXR and pKH3-RXR(-33)), 0.05 µg plasmid was used for transfections. DNA was mixed with plasmid in the appropriate amount of buffer containing 10 mM Tris and 0.1 mM EDTA (TLE buffer) for each well.

In the first ecdysteroid transfection experiment, two 24-well plates were used to compare the effect of 20-hydroxyecdysone (20E) on the activity of the full-length *Gl-Mstn* promoter with the *Gl-Mstn* promoter without a putative EcRE (*Gl-Mstn* (-) EcRE). All 48 wells were transfected with pRL-TK, pKH3-EcR and pKH3-RXR at the concentrations described above. In addition, pGL3 Basic, pGL3 Control, pGL3-Mstn, or pGL3-Mstn (-) EcRE were each added to 12 of the 48 wells.

In the second ecdysteroid transfection experiment, two 24-well plates were used to determine the effect of 1 µM, 25 µM, 50 µM, or 100 µM 20E or Pon A on the full-length *Gl-Mstn* promoter. All 48 wells were transfected with pRL-TK. pGL3-Mstn, pKH3-EcR and pKH3-RXR were used in transfections of 32 wells. pGL3 Basic, pKH3-EcR and pKH3-RXR were used in transfections of 4 wells. pGL3 Control, pKH3-EcR and pKH3-RXR were used in transfections of 4 wells. pGL3-Mstn was used in transfections of 8 wells (Table 3.6).

In the third transfection experiment, combinations of the expression plasmids pKH3-EcR, pKH3-RXR, pKH3-RXR(-33) and pKH3 were used with the reporter vectors pGL3-Mstn, pGL3-Mstn (-) EcRE, pGL3 Basic, and pGL3 Control to determine the effect of *Up-EcR* and the *Up-RXR* isoforms on the *Gl-Mstn* promoters (Table 3.7). Each of the 14 different plasmid combinations was added to four wells.

DNA plasmid in TLE buffer (1 μl each), 20 μl Opti Mem I (Thermo Fisher Scientific, Inc.), and 1 μl Lipofectamine® 2000 Transfection Reagent (Thermo Fisher Scientific, Inc.) was used for each well. In the first ecdysteroid transfection experiment, 130 μl of Opti Mem I was combined with 13 μl Lipofectamine® 2000 Transfection Reagent in each of 4 microcentrifuge tubes (1.5 ml)—one tube for each plasmid combination—and incubated at room temperature for 5 min. In another set of 4 tubes, 130 μl Opti Mem I and 13 μl of each of the 4 DNA plasmids in TLE buffer were combined. Each μl of DNA contained the appropriate concentration of plasmids, as described above. After 5 min of incubation, the contents of each tube containing DNA was combined with one of the tubes containing Lipofectamine, and incubated at room temperature for 20 min to allow lipofectamine-DNA complexes to form. A 25 μl sample from each tube was added to each of 12 wells containing HeLa cells and 1 ml of growth medium, and placed in the 37°C, 5% CO_2 incubator for 48 h.

The same protocol was followed in the second ecdysteroid transfection experiment with some exceptions. The plasmid combination of pRL-TK, pGL3-Mstn, pKH3-EcR and pKH3-RXR was used in 32 wells, the pRL-TK and pGL3-Mstn plasmid combination was used in 8 wells, the pGL3 Basic, pKH3-EcR and pKH3-RXR plasmid combination was used in 4 wells, and the pGL3 Control, pKH3-EcR and pKH3-RXR combination was used in 4 wells. For the plasmid combination needed for the 32 wells, 340 μl Opti Mem I and 34 μl lipofectamine were combined, and 34 μl of each of the four plasmids was added to 340 μl Opti Mem I. For the plasmid combination of pRL-TK and pGL3-Mstn, 100 μl Opti Mem I and 10 μl of lipofectamine were combined, and 10 μl of each plasmid was added to 100 μl Opti Mem I. For the final two plasmid combinations, each needed for 4 wells, 50 μl Opti Mem I and 5 μl lipofectamine were combined, with 5 μl of each plasmid added to 50 μl of Opti Mem I. Finally, 0.5 ml was removed from the wells containing HeLa cells before the lipofectamine-DNA complexes were added. Then 0.5 ml of ecdysteroids in growth medium was added to each well for a total of 1 ml of growth medium for each well.

For the third transfection experiment determining the effect of *Up-RXR* and *Up-RXR* on

Gl-Mstn and *Gl-Mstn* (-) EcRE promoter activity, the protocol for the four-well mixtures in the

second ecdysteroid transfection experiment was followed for preparing DNA for transfection.

DNA was added to the wells with growth medium and HeLa cells according to the first

transfection experiment. No ecdysteroids were used in this experiment.

Transfected HeLa cells were harvested with the Dual-Luciferase® Reporter Assay kit

(Promega Corp., Madison, WI, USA) using a combination of passive and active lysis of cells.

The growth medium was removed from the transfected HeLa cells and each well was rinsed

with 500 µl phosphate buffered saline (PBS). PBS consisted of 1.15 g Na_2HPO_4, 0.2 g KH_2PO_4,

8 g NaCl and 0.2 g KCl per liter. 100 µl of 1X Passive Lysis Buffer was added to each well, and

culture plates were placed on a rocking platform at room temperature for 15 min. Wells were

then scraped with the pipet tip, and the lysate was transferred to a microcentrifuge tube from

each well. Contents from each tube (20 µl) were used in the Dual-Luciferase Reporter Assay,

following the manufacturer's directions, and using a TD-20/20 luminometer (Turner BioSystems,

Inc., Sunnyvale, CA, USA). Relative light unit (RLU) readings were taken for both *Photinus*

luciferase and *Renilla* luciferase for each sample. The ratio of the relative light units (RLUs)

between the luciferase activity of *Photinus* to *Renilla* for each sample was used in all further

analyses. Tube contents were stored at -20°C to be used for *Up-EcR, Up-RXR*, and *Up-RXR*(-

33) protein expression confirmation.

Statistics

Sigma Plot 12.5 software (Systat Software, Inc., Chicago, IL, USA) was used for all

graphs and statistical analyses. The student's t-test and one-way ANOVAs were used to

compare luciferase activity between the *Gl*-Mstn full-length promoter, the *Gl*-Mstn (-) EcRE

promoter, and the pGL3 positive control promoter under various ecdysteroid concentrations and

co-transfected plasmids. If a significant difference was found in a one-way ANOVA, then the

Holm-Sidak All Pairwise Multiple Comparison Procedure was initiated. An alpha level of 0.05 was used for all tests.

Results

Cloning and characterization of the Gl-Mstn promoter

Genomic DNA walking identified a 976 base pair (bp) sequence upstream of the *Gl-Mstn* transcription start site. A BLASTN search of the *Gl-Mstn* 976 bp upstream sequence revealed that the upstream 139 bps had 94% identity with *G. lateralis* satellite DNA (Fowler et al., 1985). Satellite DNA in *G. lateralis* consists of ~ 16,000 copies (Fowler et al., 1985; Skinner et al., 1983) of a 2.1 kb repeat per genome (Fowler et al., 1985; LaMarca et al., 1981), which has no known function. We used the 837 bps immediately upstream of the *Gl-Mstn* transcription start site, but excluded the satellite DNA, for promoter analysis.

Analysis with transcription factor software (see Materials and Methods) identified a TATA box and a CAAT box as core transcription elements in the *Gl-Mstn* promoter (Fig. 3.1). The TATA box is the binding site for the RNA polymerase II preinitiation complex, allowing transcription initiation (Carninci et al., 2006). The preferred TATA starting position for the majority of promoters is located at -30 or -31 (Carninci et al., 2006; Smale and Kadonaga, 2003). The CAAT box, also involved in transcription initiation (Romier et al., 2003), can be located 50 to 164 bases upstream of the TSS in promoters containing TATA boxes, although a location between 60 to 100 bases upstream of the TSS is typical (Mantovani, 1998; Romier et al., 2003).

One enhancer box (E-box) sequence and two cAMP response element (CRE) half-sites were identified in the *Gl-Mstn* upstream sequence (Fig. 3.1). An E-box is a binding site for muscle-specific transcription factors. The cAMP response element binding protein (CREB) transcription factor binds CRE half-sites or palindromic full CRE sites, and interact with other transcription factors to regulate gene expression (Zhang et al., 2005).

Transcription factor software analysis also identified a putative EcRE in the *Gl-Mstn* promoter, located between -821 and -810 bps upstream of the TSS (Fig. 3.1). The consensus sequence for an EcRE is (A/G)G(G/T)TCANTGA(C/A)C(C/T) (Cherbas et al., 1991; Nishita, 2014). EcREs can be perfect of imperfect palindromes, separated by one nucleotide (Cherbas et al., 1991; Gauhar et al., 2009; Lehmann and Korge, 1995; Nishita, 2014), or perfect or imperfect direct repeats with no spacer (Antoniewski et al., 1996; D'Avino et al., 1995). The putative EcRE in the *Gl-Mstn* promoter is CGCTCACTCTCA, an imperfect direct repeat with no spacer nucleotide (Fig. 3.1). An alignment with the *Eriocheir sinensis* Mstn promoter showed high variability in the upstream portion of the promoter, but 90% identity between the downstream 441 nucleotides (Fig. 3.2). The TATA box and the CAAT box were perfectly aligned, but other transcription factor binding sites were present in both, but not aligned (Fig. 3.2).

Mstn promoter functional studies

Mammalian cells lack endogenous ecdysteroids. Therefore, expression of Up-*EcR* and *Up-RXR* in HeLa cells, along with the *Gl-Mstn* promoter upstream of a luciferase reporter, allowed a heterologous cell culture system in which ecdysteroid levels could be precisely controlled. A Western blot showed a specific band at the expected size of ~67 kDa, indicating that HA-tagged EcR was expressed in the HeLa cells (Fig. 3.3).

The *Gl-Mstn* upstream sequence inserted upstream of the luciferase gene in the pGL3 plasmid showed increased luciferase activity compared to the pGL3 basic plasmid, which lacked a promoter (Fig. 3.4). This result indicated that the upstream *Gl-Mstn* sequence is a functional promoter. The *Gl-Mstn* (-) EcRE sequence showed similar activity to the *Gl*-Mstn promoter, indicating that it is also a functional promoter (Fig. 3.4).

When the heterologous cell system—Up-*EcR*, *Up-RXR*, and either the *Gl-Mstn* or the *Gl-Mstn* (-) EcRE promoter transfected into HeLa cells—was incubated with up to 25 µM 20E, there was no change in luciferase activity, compared to the cell systems lacking ecdysteroids (Fig

101

3.4). Further assays with up to 100 μM Pon A or 20E had no significant effect on *Gl-Mstn* promoter activity (3.5).

Co-transfection of RXR and EcR had no significant effect on the activity of the full-length or (-) EcRE *Gl-Mstn* promoter (3.6). However, co-transfection with *Up-RXR* and *Up-EcR* significantly decreased the activity of both the full-length promoter and the (-) EcRE *Gl-Mstn* promoter compared to no co-transfection, whether incubated with 50 μM 20E or not (Fig. 3.6). Compared to co-transfection of the empty pGL3 plasmid, co-transfection of RXR(-33) and EcR had a significant positive effect on both the full-length and the (-) EcRE *Gl-Mstn* promoter (Fig. 3.7). Interestingly, RXR and EcR co-transfection had a significant positive effect on the pGL3 positive control promoter (Fig. 3.7).

Discussion

The presence of core promoter elements—the TATA box and the CAAT box—indicates that the *Gl-Mstn* upstream sequence may be a functional promoter. Vertebrate Mstn promoters that have been analyzed all have at least one copy of each element (Deng et al., 2012; Du et al., 2011; Du et al., 2005; Funkenstein et al., 2009; Galt et al., 2014; Grade et al., 2009; Kerr et al., 2005; Li et al., 2012a; Li et al., 2012b; Ma et al., 2001; Nadjar-Boger et al., 2012; Nadjar-Boger et al., 2013; Singh et al., 2014). The *Gl-Mstn* promoter TATA box is located between -30 and -24 bases upstream of the TSS, similar to the location in vertebrates (Deng et al., 2012; Du et al., 2011; Grade et al., 2009; Ma et al., 2001). The *Gl-Mstn* CAAT box is located between -130 and -126 bps upstream of the TSS—further upstream than vertebrate Mstn promoters which are located 60 to 100 bps upstream of the TSS (Du et al., 2011; Grade et al., 2009; Ma et al., 2001). This may indicate weaker transcription initiation than normal, as the CAAT box is an additional binding site for preinitiation complex proteins (Romier et al., 2003). The locations of the *Gl-Mstn* TATA box and CAAT box are identical to *Eriochier sinensis*, the only other crab Mstn promoter which has been analyzed (Kim et al., 2009a).

Only one enhancer box (E-box) sequence was identified in the *Gl-Mstn* promoter (Fig. 3.1), compared to 3 to 16 E-boxes in the Mstn promoters of vertebrates (Du et al., 2011; Du et al., 2005; Funkenstein et al., 2009; Kerr et al., 2005; Li et al., 2012a; Li et al., 2012b; Ma et al., 2001; Nadjar-Boger et al., 2012; Nadjar-Boger et al., 2013; Singh et al., 2014). The Mstn promoter of the decapod *E. sinensis* also contains one E-box sequence. The presence of a putative E-box indicates that *Gl-Mstn* may be regulated by muscle-specific transcription factors such as myogenic differentiation 1 (MyoD), myogenic factor 5 (myf5), myogenic factor 6 (myf6) (synonym: MRF4) and myogenin (Apone and Hauschka, 1995). Transcription factor binding to E-boxes upregulate promoter activity (Apone and Hauschka, 1995), while inactive E-boxes in vertebrates are often a site of methylation, causing repression of transcription (Ceccarelli et al., 1999). As invertebrates do not normally methylate promoter regions (Sarda et al., 2012), the inactive E-box in *Gl-Mstn* would not be down-regulated by methylation. The presence of only one E-box in the promoter of *Gl-Mstn*, compared to three to 16 E-boxes in vertebrates could indicate less regulation by muscle-specific transcription factors in the *Gl-Mstn* promoter, as E-boxes have shown an additive effect on promoter activity (Salerno et al., 2004). However, mutation studies indicate that deletion of only specific E-boxes in promoters with multiple E-boxes cause decreased transcriptional activity, and deletion of more than one of these specific E-boxes did not result in an additive down-regulation effect (Du et al., 2007). Functional studies will be necessary to determine if the E-box in the Mstn promoter is actively upregulated by muscle-specific transcription factors.

Two cAMP response element (CRE) half-sites were identified in the G*l-Mstn* promoter (Fig. 3.1). Likewise, one to two CRE sites have been identified in vertebrate Mstn promoters (Deng et al., 2012; Grade et al., 2009; Ma et al., 2001; Nadjar-Boger et al., 2012; Nadjar-Boger et al., 2013). The presence of CRE binding sites in the *Gl-Mstn* promoter is intriguing. In mammals, IGF-1 signaling activates CREB to initiate transcription of the Mstn promoter (Zuloaga et al., 2013). Stimulation of Mstn expression by IGF-1 allows a negative feedback

mechanism to modulate IGF-1-stimulated growth (Chien et al., 2013; Garikipati and Rodgers, 2012; Kawada and Ishii, 2009; Marcotte et al., 2014; Matsakas et al., 2006; Paoli et al., 2015; Price et al., 2011; Yang et al., 2007; Zhou et al., 2015). In IGF-1-stimulated growth promoting situations, Mstn acts as a chalone—a modulator of excessive growth (Chien et al., 2013; Garikipati and Rodgers, 2012; Kawada and Ishii, 2009; Marcotte et al., 2014; Matsakas et al., 2006; Paoli et al., 2015; Price et al., 2011; Shafer, 1916; Yang et al., 2007; Zhou et al., 2015). The presence of CRE response elements in the *Gl-Mstn* promoter indicates that IGF-1 signaling may activate the Mstn promoter to modulate muscle growth in invertebrates as well.

In vertebrates, steroids regulate gene expression. In response to stress, glucocorticoid signaling stimulates the breakdown of carbohydrates, fats and proteins, to allow synthesis of glucose to combat the stressful situation (Braun and Marks, 2015; Goldberg et al., 1980; Kuo et al., 2012; Lofberg et al., 2002; Sapolsky et al., 2000; Schakman et al., 2008; Tomas et al., 1979). Glucocorticoids also inhibit anabolic processes such as muscle protein synthesis to conserve energy (Braun and Marks, 2015; Goldberg et al., 1980; Kuo et al., 2012; Lofberg et al., 2002; Sapolsky et al., 2000; Tomas et al., 1979). Glucocorticoids signal by binding the glucocorticoid receptor, and stimulating the ligand/receptor complex to bind GREs to regulate transcription of target genes (Kuo et al., 2012; Yamamoto, 1985). GREs have been identified in vertebrate Mstn promoters (Du et al., 2005; Kerr et al., 2005; Ma et al., 2001; Nadjar-Boger et al., 2012; Nadjar-Boger et al., 2013; Singh et al., 2014). Glucocorticoid receptor binding to a Mstn GRE (Ma et al., 2001; Qin et al., 2013) stimulates Mstn expression, resulting in decreased protein synthesis (Zhang et al., 2007) and increased protein degradation (Allen and Loh, 2011; Braun and Marks, 2015; Gilson et al., 2007; Ma et al., 2003; Schakman et al., 2013), including degradation of myofilaments (Hasselgren and Fischer, 2001; Schakman et al., 2008). Thus, glucocorticoid signaling can result in rapid muscle atrophy in vertebrates, due to decreased protein synthesis and increased protein degradation (Braun and Marks, 2015; Piccirillo et al., 2014; Qin et al., 2013).

Androgens, which are growth promoting steroids, also stimulate Mstn expression. Similar to glucocorticoids, androgens bind the androgen receptor, and the androgen/androgen receptor complex binds androgen response elements (AREs) to regulate transcription of target genes. AREs have been identified in the Mstn promoters of humans (Ma et al., 2001) and three fish species (Kerr et al., 2005; Nadjar-Boger et al., 2012; Nadjar-Boger et al., 2013). Androgen stimulation upregulates Mstn transcription, thereby modulating the effect of the growth-promoting steroids (Dubois et al., 2014). Mstn acts as a chalone for androgens, similar to the role Mstn has in modulating IGF-1-stimulated muscle growth (Dubois et al., 2014; Shafer, 1916).

The transcription factor software did not identify a GRE or an ARE in the *Gl-Mstn* promoter. However, a putative EcRE of twelve nucleotides, consisting of the six-nucleotide imperfect direct repeat, CGCTCACTCTCA, was identified. Ecdysteroid signaling initiates transcriptional changes in target genes via ecdysteroid receptors bound to EcREs (Henrich et al., 2009; Hu et al., 2003; Nakagawa and Henrich, 2009; Riddiford et al., 2001). Ecdysteroid signaling occurs when ecdysteroid levels dramatically increase during premolt (Covi et al., 2010; McCarthy and Skinner, 1979). Increased premolt ecdysteroid levels are associated with decreased *Gl-Mstn* expression in the claw closer muscle of *G. lateralis* (Covi et al., 2010). As vertebrates do not undergo ecdysis, vertebrate promoters do not contain EcREs.

Functional studies

Expression of *Up-EcR* and *Up-RXR* in HeLa cells, along with the *Gl-Mstn* promoter sequence upstream of a luciferase reporter vector revealed that the *Gl-Mstn* upstream sequence is a functional promoter (Fig. 3.2A). We also attempted to determine if the putative EcRE in the *Gl-Mstn* promoter regulated *Gl-Mstn* transcription in response to ecdysteroid signaling in this heterologous cell culture system. The full-length *Gl-Mstn* promoter was compared to a *Gl-Mstn* promoter mutation in which the EcRE had been deleted. Our results indicated that there was no significant change in the activity of either promoter when incubated with up to 25 µM 20E, compared to incubation without ecdysteroids (Fig. 3.4).

In this heterologous cell system, concentrations up to 100 µM of 20E or PonA had no effect on the transcriptional activity of the full-length *Gl-Mstn* promoter. A negative result is often challenging to interpret, as there may be many possibilities for this result. The EcRE in the *Gl-Mstn* promoter may not be functional, *Up-RXR* and/or *Up-EcR* may not be functional with the *Gl-Mstn* promoter, the *Up-RXR* and/or *Up-EcR* A/B domains may be inhibitory, or 20E and Ponasterone A may not activate this cell system.

If the EcRE is not functional, deletion of the putative EcRE would have no effect on the *Gl-Mstn* promoter activity. Previously, three putative EcREs near the ecdysone-inducible polypeptide 28/29 (Eip 28/29) gene in *Drosophila* were identified (Cherbas et al., 1991). One was 440 base pairs upstream of the TSS, and two were located downstream of the poly A site. From functional studies, they determined that both downstream sites were necessary for fully functional ecdysteroid signaling to the Eip gene, but the putative EcRE in the promoter region at -440, was not a functional EcRE (Cherbas et al., 1991).

Different ecdysteroids elicit various responses in heterologous cell systems. 1 µM 20E was unable to activate a heterologous ecdysteroid system in 293 cells, whereas 1 µM Muristerone A elicited a strong transcriptional response, and 1 µM Pon A elicited a weak transcriptional response to incubation with ecdysteroids (Christopherson et al., 1992). To my knowledge, 20E has not been used successfully in a heterologous cell system. 10 µM Muristerone A has been used successfully as the ligand to stimulate a heterologous ecdysteroid system in HeLa cells (Mouillet et al., 2001). Pon A has been used to stimulate ecdysteroid heterologous systems in several cell lines, including 293 cells (Christopherson et al., 1992; Vaillancourt and Felts, 2003), CHO cells (Palli et al., 2003; Vaillancourt and Felts, 2003), A549 cells (Hoppe et al., 2000), CV-1 cells (Hoppe et al., 2000), and CRE8 cells (Hoppe et al., 2000). However, I did not find any research that used Pon A as the ligand to stimulate a heterologous ecdysteroid system in HeLa cells.

Uca pugilator EcR (*Up-EcR*) and RXR (*Up-RXR*) (Chung et al., 1998; Durica and Hopkins, 1996; Durica et al., 2002) were used in our heterologous cell system, as the entire *G. lateralis* EcR (*Gl*-EcR) has not been cloned. The entire *G. lateralis* RXR (*Gl*-RXR) (Kim et al., 2005b), and 1516 nucleotides of *Gl-EcR* (Kim et al., 2005a) have been cloned. The cloned portion of *Gl-EcR* includes approximately 64% of the C domain (the DBD) through to about eleven amino acids short of the 3' end of the ORF. A nucleotide BLAST (NCBI) of the entire *Gl-RXR* coding sequence showed 93% identity with the *Up-RXR* coding sequence, while a protein BLAST of the ORF indicated 98% conservation with *Up*-RXR. BLAST searches of the available *Gl-EcR* revealed 95% nucleotide identity, and 97% amino acid identity with *Up-EcR*. It is possible that these slight differences in protein sequence prevented ecdysteroid signaling through the EcRE in the *Gl-Mstn* promoter.

Previous work has shown that the A/B domain of EcR (Mouillet et al., 2001; No et al., 1996) and RXR (Betanska et al., 2009; Palli et al., 2003) may inhibit ecdysteroid signaling in heterologous cell systems. Many heterologous system researchers have replaced the A/B domains of EcR (Christopherson et al., 1992; No et al., 1996; Palli et al., 2003; Panguluri et al., 2006; Vaillancourt and Felts, 2003; Wu et al., 2004; Wyborski et al., 2001) and/or RXR (Betanska et al., 2009; Palli et al., 2003; Panguluri et al., 2006; Wu et al., 2004) with a mutated activation domain of herpes simplex virus, virus protein 16 (Vp16).

We also looked at the effect of RXR and EcR on the transcriptional activity of the full-length *Gl-Mstn* promoter. When RXR and EcR were co-transfected with the *Gl-Mstn* promoter, there was decreased transcriptional activity of the promoter, compared to no co-transfections (Fig. 3.4). This negative effect on *Gl-Mstn* promoter activity may have been due to inhibition by the plasmid itself, or to the co-transfection process, because co-transfection of RXR and EcR compared to co-transfection of a similar amount of empty plasmid showed no inhibitory effect of RXR and EcR (Fig. 3.5). In fact, there was a trend toward increased activity, both of the full-length *Gl-Mstn* promoter and the *Gl-Mstn* promoter without the EcRE, although there was not a

significant difference. Co-transfection with EcR and the RXR(-33) isoform, compared to co-transfection with empty plasmid, resulted in significantly increased luciferase activity in the full-length *Gl-Mstn* promoter and the *Gl-Mstn* promoter without the EcRE. Surprisingly, co-transfection of RXR and EcR significantly increased activity of the pGL3 positive control promoter compared to co-transfection with the empty promoter (Fig. 3.7). All three promoters (*Gl-Mstn, Gl-Mstn* (-) EcRE, and pGL3*)* showed between a 2-3-fold increase in luciferase expression with co-transfection of *Up-EcR* and an isoform of *Up-RXR*. Previous work has shown that some combinations of EcR isoforms and RXR isoforms in ecdysteroid heterologous mammalian cell cultures can increase basal transcriptional levels at EcRE-activated genes, even without ecdysteroid stimulation (Beatty et al., 2006). No explanation was given for this increase in basal transcription levels (Beatty et al., 2006). But does the luciferase reporter plasmid used in this study contain an EcRE? Sequence analysis revealed a possible EcRE, an imperfect six-base palindromic repeat with no spacer, sequence TGATCATGAACT. Except for the first nucleotide in the sequence and the lack of a 1 nucleotide spacer, this sequence matches the consensus sequence for an EcRE—RG(T/A)TCANTGA(C/A)C(C/A) (Nishita, 2014). Mutation analysis has shown that EcREs without a G in the first position (Antoniewski et al., 1993), or without a spacer (Wang et al., 1998) are functional, but with weaker transcriptional activation. This implies that the possible EcRE located in the promoter plasmid may be responsible for the similar response of all three promoters, including the positive control, to co-transfection of *Up-EcR* and *Up-RXR*.

In conclusion, the *Gl-Mstn* upstream sequence is a functional promoter, but further studies will be necessary to determine if ecdysteroid signaling controls *Gl-Mstn* promoter activity through the EcRE located in the *Gl-Mstn* promoter. Future research should include replacement of the A/B domains of EcR and RXR with the modified activation domain of Vp16, and possibly changing the reporter vector to test the possibility of an EcRE in the promoter itself.

Table 3.1: DNA Walking Primers for three consecutive PCR runs. The first PCR run used genomic DNA from the thoracic ganglia of *G. lateralis*, and the following PCR runs each used the PCR product of the previous PCR run as the template DNA. The forward non-specific primers have ACP in the name, the reverse gene-specific primers have Mstn in the name.

PCR #	Primer pairs	Sequence (5'- 3')	Annealing Temperature
1st	ACP11	AGGAGTTTAGGTCCAGCGTCCGTIIIIICAGTC	55
	Mstn R4	GTTGTGGTGCTGAGTTCGATGTGT	
2nd	ACPgC	GGAGTTTAGGTCCAGCGTCCGTGGGGGC	60
	Mstn R5	GCAGCTCACTGAACTCACTCTCTG	
3rd	ACPgC	GGAGTTTAGGTCCAGCGTCCGTGGGGGC	60
	Mstn R2	ACGGCATGTTACTGTTACTGGGCT	

Table 3.2. Primers for genomic DNA amplification of the full-length Mstn promoter.

Primers	Sequence (5'- 3')	Tm, °C
F1	GTCATTTCTTACGCTCACTCTCA	54.6
F2	AACTCCACGAGGAATTAGTCATTT	54.2
R1	CTGAACTCACTCTCTGCTGTTC	55.2
R2	CACTATCAGGTTCACGGTAAGAG	54.6
R3	ACGGCATGTTACTGTTACTGG	55.0

Table 3.3. Primers with restriction sites. For each primer pair, the forward primer is listed first, and the reverse primer second. Restriction sites in each primer are bold. NoRE is the primer sequence resulting in no response element in the *Gl-Mstn* promoter. Primer pair names indicate the restriction site included near the 5' end of the sequence.

DNA	Primer pairs	Sequence (5'- 3')	Annealing Temp., °C
MP compl.	*Kpn*I	TTAA**GGTACC**AATTAGTCATTTCTTACGCTC	56
	*Xho*I	ATAG**CTCGAG**AGAGCTGATGCAAGATTGAC	
MP, no EcRE	*Kpn*I NoRE	AA**GGTACC**TCGTGCCCAAAGGTGAG	56
	*Xho*I	ATAG**CTCGAG**AGAGCTGATGCAAGATTGAC	
EcR	*Bam*HI	CCAGA**GGATCC**ATGGCCAAGGTGCTG	60
	*Cla*I	CAAGA**ATCGAT**AGGTGGTTCAGGCTCA	
RXR & (-33)	*Hin*dIII	CCGCT**AAGCTT**CCCATGATTATGATT	37, 56.5
	Xba	ACGTG**TCTAGA**CTCGAGATAGCTGGTG	

Table 3.4. Insert check primers. For Mstn, The forward primer was gene-specific, and the reverse primer annealed to the pGL3 plasmid. These Mstn primers were used for both the *Gl-Mstn* and the *Gl-Mstn* (-) EcRE promoters, with the same size amplification product expected for both. The RXR primers were used for both the *Up-RXR* and the *Up-RXR*(-33) genes, with the same product size expected in both isoforms. For RXR and EcR, the forward primer annealed to the pKH3 plasmid while the reverse primers were gene-specific.

Gene	Primer pairs	Sequence (5'- 3')	Annealing Temperature	Product size
Mstn	F	AACCAATGAGAGCACGAGTT	54	199
	R	TCTTCCATGGTGGCTTTACC		
EcR	F	GTGCCAAGAGTGACGTAAGTA	51.5	577
	R	GTTAAGGTCGAGATCCCAGAAG		
RXR	F	GTGCCAAGAGTGACGTAAGTA	52	429
	R	GTGAAGGGAGGTGTGGATATG		

Table 3.5. Plasmids used in transfections, including the luciferase reporter plasmids pRL-TK and pGL3, and the gene expression plasmid pKH3. The final column is the µg of the particular plasmid added to a well.

Plasmid name	Plasmid contents	µg /well
pRL-TK	*Renilla* Luciferase gene with strong promoter	0.01
pGL3 Basic	Luciferase gene with no promoter	0.30
pGL3 Control	Luciferase gene with strong promoter	0.30
pGL3-Mstn	Luciferase gene with *Gl-Mstn* full-length promoter	0.30
pGL3-Mstn (-) EcRE	Luciferase gene with *Gl-Mstn* promoter (-) EcRE	0.30
pKH3	Empty vector	0.05
pKH3-EcR	pKH3 with *Up-EcR* 3' to HA tag	0.05
pKH3-RXR	pKH3 with *Up-RXR* 5' to HA tag	0.05

Table 3.6. Plasmid and ecdysteroid concentrations, in the second ecdysteroid transfection experiment, used in each transfection well. Four replicate wells of each combination were made. 100 µM 20E was hydrated in 100% ethanol, and 100 µM Pon A was hydrated in 95% ethanol. [C] = concentration.

Reporter plasmid	Expression plasmids	Ecdysteroid	Ecdysteroid [C]
pGL3-Mstn	pKH3-EcR, pKH3-RXR	20E	25 µM
pGL3-Mstn	pKH3-EcR, pKH3-RXR	20E	50 µM
pGL3-Mstn	pKH3-EcR, pKH3-RXR	20E	100 µM
pGL3-Mstn	pKH3-EcR, pKH3-RXR	Pon A	25 µM
pGL3-Mstn	pKH3-EcR, pKH3-RXR	Pon A	50 µM
pGL3-Mstn	pKH3-EcR, pKH3-RXR	Pon A	100 µM
pGL3-Mstn	pKH3-EcR, pKH3-RXR	None (100% EtOH)	0
pGL3-Mstn	pKH3-EcR, pKH3-RXR	None (No EtOH)	0
pGL3-Mstn	None	20E	50 µM
pGL3-Mstn	None	20E	50 µM
pGL3 Basic	pKH3-EcR, pKH3-RXR	None (100% EtOH)	0
pGL3 Control	pKH3-EcR, pKH3-RXR	None (100% EtOH)	0

Table 3.7. Reporter and expression plasmids used in the transfection comparing the effects of the expression proteins *Up-EcR*, *Up-RXR*, and *Up-RXR*(-33) on the full-length *Gl-Mstn* promoter and the *Gl-Mstn* (-) EcRE promoter. 0.01 µl of pRL-TK,.05 µl of each expression plasmid, and 0.3 µl of each reporter plasmid was used.

Reporter plasmid	Expression plasmids		
pGL3-Mstn	pKH3-EcR	pKH3-RXR	
pGL3-Mstn	pKH3-EcR		pKH3
pGL3-Mstn		pKH3-RXR	pKH3
pGL3-Mstn			pKH3, pKH3
pGL3-Mstn	pKH3-EcR	pKH3-RXR(-33)	
pGL3-Mstn (-) EcRE	pKH3-EcR	pKH3-RXR	
pGL3-Mstn (-) EcRE	pKH3-EcR		pKH3
pGL3-Mstn (-) EcRE		pKH3-RXR	pKH3
pGL3-Mstn (-) EcRE			pKH3, pKH3
pGL3-Mstn (-) EcRE	pKH3-EcR	pKH3-RXR(-33)	
pGL3 Basic	pKH3-EcR	pKH3-RXR	
pGL3 Basic			pKH3, pKH3
pGL3 Control	pKH3-EcR	pKH3-RXR	
pGL3 Control			pKH3, pKH3

```
-837 AATTAGTCATTTCTTA**CGCTCACTCT**CA TCTG CCGTCGTGCCCAAAGGTGAGCCGCCACG

-777 CCACGGCGGCCGGGTGGCCGGGGAATCGCATCCCCCCAGGGGTTCTGTGTCCCTGCCCAA

-717 GGCTAGCAGTCAGCCCAGTCCCTGATCTGGACTGGTTGGGGTGGCGACGGGCCTTGAAAG

-657 GAAGCCCACCACCCCGTAAAAGATG***CGTCA***TCTCGCTCGCGCAACGCAACAGAGCGGGAG

-597 TTACAGGCCGGCGTCGGTCGACACTCAGGTCTAGTGCCTGGCCTGAGAGTGCTCTCAGGT

-537 GGCGAGGGGAGGAGGAGGTGGAGGAGGAGGAGGGGGAGGAGGAGGAAGAGAAGGAGGGGG

-477 AGTAGGAGGAGGAGGAGGAGGAGGAGGAGGAGGAGGAGGAGGAGGAGGAGGAGGAGGAGG

-417 AGGAGGAGAATTAAGGCAAAGAATTACGTAAGAGTGACAATTTTGCGTGCAGGGTGTAGG

-357 GTTAGGTTGGGTGGCCTAGAGACAGGTAGGACGAGGCAGGAGGGACAGAGGATACCTCGT

-297 GGGAGGAGCCGGAGGAGGAGAAGGAGGGTACGGAGGAGGG***TGACG***ATAGAGAGGTAGGGG

-237 GAGCGGAGGGGCGGCAGGTAGCAAGGCGCCCGGGAAGGCAGCCACGCCCACGGGGAAGAA

-177 AGGAGGGCGGTGATTGGCCCCCTGCTTTCCTTCGGCACGGCGACCAACCAATGAGAGCAC

-117 GAGTTAACCCGCTTGAAAAGTTAATTGGTTCGAATCTGAGGCTAGACACTCCCCTTGTAC
                                                              -1 ➤
- 57 TGGTAGCATTAACTCCCAGACATAATGTATAAAAGAGCTTGTCAATCTTGCATCAGCTCT
```

Fig. 3.1. *Gl-Mstn* contiguous promote, including the transcription start site (TSS). The entire contiguous promoter of *Gl*-Mstn is 837 bps in length to the TSS. Core promoter elements, including the CAAT box and the TATA box (both underlined) are present. A putative EcRE is located near the upstream end of the promoter (Bold and underlined). Two CRE half-sites, which CREB binds, are located in the *Gl-Mstn* promoter (bold and italics). An E-box, a binding site for muscle-specific transcription factors, is boxed, and partially overlapping the EcRE. A bent arrow indicates the TSS.

```
                                          ▼         ▼
Gl : AATTAGTCATTTCTTACGCTCACTCTCATCTGCCGTCGTGCCCAAAGGTGAGCCGCCACG 60
Es : ------------------------------------------------------------  -

Gl : CCACGGCGGCCGGGTGGCCGGGGAATCGCATCCCCCCAGGGGTTCTGTGTCCCTGCCCAA 120
Es : ------------------------------------------------------------  -

Gl : GGCTAGCAGTCAGCCCAGTCCCTGATCTGGACTGGTTGGGGTGGCGACGGGCATTGAAAG 180
Es : ------------------------------------------------------------  -

                                  CRE
Gl : GAAGCCCACCACCCCGTAAAAGATGCGTCATCTCGCTCGCGCAACGCAACAGAGCGGGCG 240
Es : ------------------------------------------------------------  -

Gl : TTACAGGCCGGCGTCGGTCGACACTCAGGTCTAGTGCCTGGCCTGAGAGTGCTCTCAGGT 300
Es : -----------CCCTTTTTTACCTTCCCTTCTACTCCCCCCCCCCCTTGCCATTGTC--TC  46

Gl : GGCGCGGAGAGGGAGGGAGGGAGGGAGGGAGTGAGGGAGGGAGGGGTGGTAGGGAGGCAA 360
Es : AGCCTCAAAGAGCAGCATCTCCCCTCGGTAATGGCTTCATCCCTGCCTATAAAGAAACAA 106

Gl : GGGGGGGGGGGGGAGGAGGAGGAGGAGGAGGAGGAGGAGGAGGAGGAG-----GAGGAGG 415
Es : GTGTAATTGATTGCTGGGTTTTCTTCCGCCTGTGACTCACCCGCTCGGCCTGCGACTGAA 166

Gl : AGGAGGAGGAGGTGGGGGAAGAGGAGGAGGAGGAGGAGGAGGAGGAGGAGGAGAATTAAGGCA 475
Es : GGAAGGACGAGAAAAAGGAGGAGGAGGAGGAGGAGGAGGAAGAGGGAAAAGATAATTAAGTCA 226

Gl : AAGAATTACGTAAGAGTGACAATTTTGCGTGCAGGGTGTAGGGTTAGGTTGGGTGGCCTA 535
Es : AAGAATTACGTAAGAGTGACAATTTCGCGTGGCCGGTGCAGGGTGAGGCAGGGTGGCCTA 286

Gl : GAGACAGGTAGGACGAGGCAGGAGGGACAGAGGATACCTCGTGGGAGGAGCTGGAGGAGG 595
Es : GAGACAGGTAGTACGAGGCAGGAGGGACTGAGGATACCTCGTGGGAGGAGCCGGAGGAGG 346

                       CRE
Gl : AGAAGGAGGGTACGGAGGAGGGTGACGATAGAGAGGTAGGGGGAGCGGAGGGGCGGCAGG 655
Es : ---AGGAGGGTACGCAGGAGGGTAGGGATCGGGAGGGAGGGGGAGGGGAGGGGCGTCAGG 403
                                                          CRE
Gl : TAGCAAGGCGCCCGGGAAGGCAGCCACGCCCACGGGGAAGAGAGGAGGGCGGTGATTGGT 715
Es : TAGCAAGGCGCCCGGGAAGGCAGCCACACCCACGGGGAAGAAAGACGGGCTGCGATTGGT 463

                           CCAAT
Gl : CCCCTGCTTTCCTTCGGCACGGCGACCAACCAATGAGAGCACGAGTTAACCCGCTTGAAA 775
Es : CCCGAGCTTTCCTTCGGTACGGCGACCGACCAATGGCACCACGAGTTAACCCGCTTGAAA 523

Gl : AGTTAATTGGTTCGAATCTGAGGCTAGACACTCCCCTTGTACTGGTAGCATTAACTCCCA 835
Es : AATTAATTGGTTCGAATCTGAGGCTAGACACTCCCCTTGTACTGGTAGCATTAACTCCCA 583

            TATAAA
Gl : GACATAATGTATAAAAGAGCTTGTCAATCTTGCATCAGCTCT 877
Es : GACATAATGTATAAAAGAGCTTGTCAATCTTGCATCAGCTCT 625
```

Fig. 3.2. *Gl-Mstn* **promoter aligned with the** *E. sinensis* **Mstn promoter.** The first part of the overlap between the two sequences is very dissimilar, but starting from *Gl* nucleotide 436, the remaining 441 nucleotides between the two promoters are 90% identical. A black bar under each sequence indicates the position of a putative EcRE in each promoter, located near the beginning of each sequence. E-box start/finish is indicated with arrowheads above (*Gl*) and below (*Es*) each sequence. CRE binding half-sites (TGACG or CGTCA), two in the *Gl-Mstn* promoter, and one in the *Es* promoter, are indicated above (*Gl*) and below (*Es*) each sequence. The CAAT-Box and TATA sequences are perfectly aligned, and are indicated above the sequences.
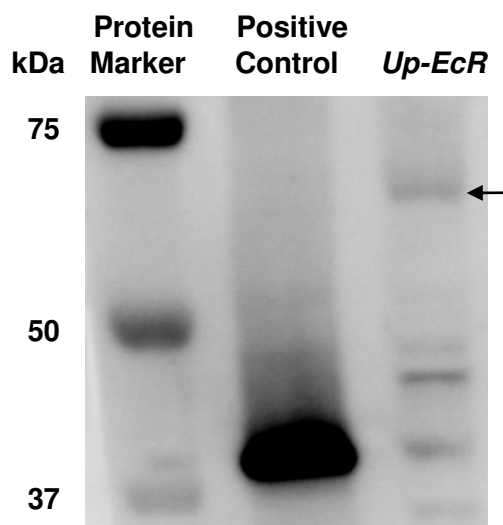
Fig. 3.3. *Up-EcR* was expressed in the heterologous HeLa cell system. Expected size of the HA-tagged *Up-EcR* band was ~67 kDa, marked by an arrow in the last lane. The positive control (second lane) was an HA-tagged ORF with an expected size of ~ 38 kDa.
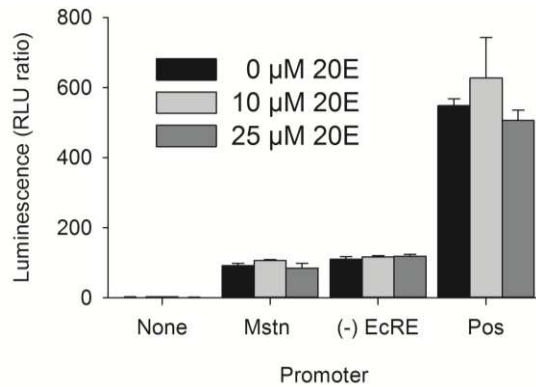
Fig. 3.4. Effect of 20E concentrations on the *Gl-Mstn* promoter and controls. The effect of 0 µM, 10 µM and 25 µM 20E on the full-length *Gl-Mstn* promoter and the *Gl-Mstn* promoter without the EcRE (*Gl-Mstn* (-) EcRE) (A). Compared to pGL3 Basic, both the full-length *Gl-Mstn* promoter and the *Gl-Mstn* (-) EcRE promoter showed increased luciferase activity, indicating they are both functional promoters. An ANOVA indicated no significant differences between 0 µM, 10 µM and 25 µM 20E on the activity of any individual promoter.

A. 20E.

Luminescence (RLU ratio)

B. Pon A.

Luminescence (RLU ratio)

0 µM
25
50
100
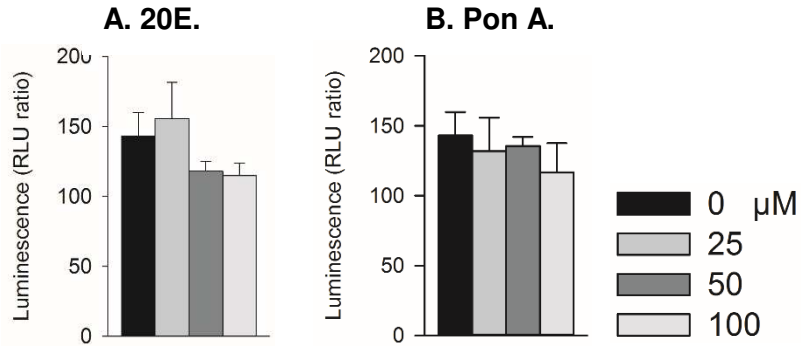
3.5. Effect of 20E concentrations on the full-length *Gl-Mstn* promoter. The effect of 0 µM, 25 µM 20E, 50 µM and 100 µM of 20E (A) or Pon A (B) on the full-length *Gl-Mstn* promoter. The addition of both ecdysteroids at 100 µM concentration appears to decrease the complete *Gl-Mstn* promoter activity, resulting in decreased luciferase activity, but it is not a significant decrease at an alpha level of 0.05.

A. No 20E.　　　　**B. 50 µM 20E.**
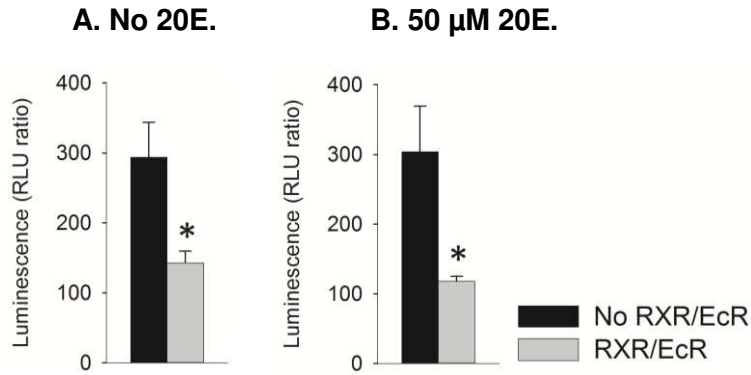
3.6. Effect of *Up-EcR* and *Up-RXR* on activity of the full-length *Gl-Mstn* promoter. Co-transfection of *Up-EcR* and *Up-RXR* significantly decreased *Gl-Mstn* promoter activity compared to no co-transfections. This occurred without 20E (A), and in the presence of 50 µM 20E (B). Statistical significance at a 0.05 alpha level is indicated by an asterisk.

A. *Gl-Mstn* complete.

B. *Gl-Mstn* (-) EcRE.

C. pGL3 Positive Control.
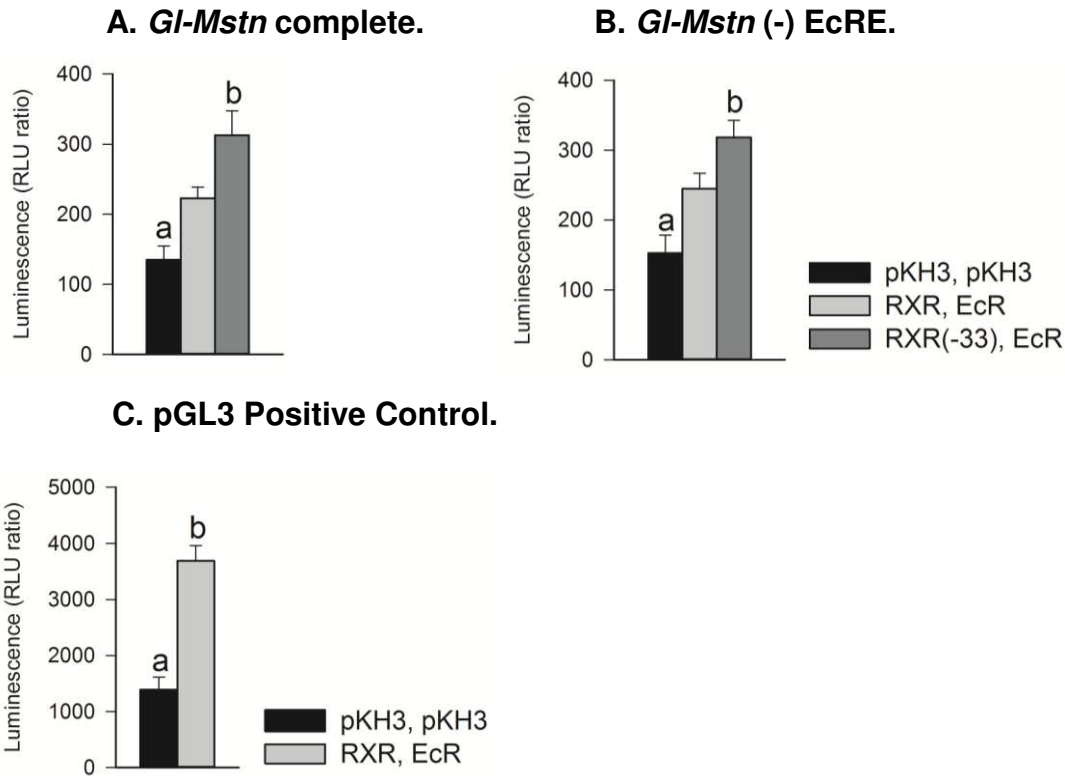
Fig. 3.7. Effect of *Up-EcR* and *Up-RXR* on promoter activity. For both the full-length *Gl-Mstn* promoter and the *Gl-Mstn* (-) EcRE promoter, activity was significantly increased when *Up-EcR* and *Up-RXR*(-33) were co-transfected, compared to co-transfection of pKH3. For the pGL3 positive control promoter, activity was significantly increased when *Up-EcR* and *Up-RXR* were co-transfected, compared to pKH3 co-transfection. Statistical significance at a 0.05 alpha level is indicated by different letters.

Chapter 4

Myostatin and mTOR pathway mRNA expression levels in *Carcinus maenas* skeletal muscles in response to molt manipulation and during natural molt.

Summary

Increasing ecdysteroid levels initiate the physiological and anatomical changes of premolt in decapods. Premolt changes include claw closer muscle atrophy to enable withdrawal of the claw at ecdysis, with concomitant increased protein synthesis in preparation for rapid growth after molting. Increased protein synthesis is transduced by the insulin/mTORC1-dependent protein synthesis pathway, while myostatin (Mstn) signaling inhibits this pathway. In *Gecarcinus lateralis*, the blackback land crab, increasing ecdysteroid levels are correlated with increasing Rheb (an activator of mTORC1) and decreasing Mstn mRNA levels. Previously, *Gl-Mstn* mRNA levels decreased 94%, and *Gl-Rheb* mRNA levels increased 3.4-fold during premolt. Here, we look at the effects of increasing ecdysteroids on insulin/mTORC1 signaling components and Mstn mRNA levels in the claw muscle of an invasive population of *Carcinus maenas*, the green crab. Our hypothesis is that increasing ecdysteroids will be correlated with decreasing Mstn mRNA levels and increasing mRNA levels of *Cm-Rheb* or other components of the insulin/mTORC1 signaling pathway in the claw closer muscle. As this population of *C. maenas* did not respond to common molt-induction techniques used in decapods, naturally molting crabs were studied. Results indicated that as ecdysteroid levels increased during premolt, *Cm-Mstn* mRNA levels also increased, but ecdysteroids and *Cm-Mstn* mRNA levels were not correlated. mRNA levels of mTOR and S6k, two components of the insulin/mTORC1 signaling pathway, increased with increasing ecdysteroids, but were not correlated with ecdysteroid levels. However, Mstn and mTOR mRNA levels were positively correlated ($R^2=0.241$) in both the claw muscle and the thoracic muscle. These results indicate that in *C. maenas*, claw closer muscle Mstn and insulin/mTORC1 signaling component mRNA levels are not directly regulated by ecdysteroids. However, *Cm-Mstn* and *Cm-mTOR* were positively

correlated, indicating that in *C. maenas*, similar to *G. lateralis* (see chapter 3), Mstn acts as a chalone, modulating the effects of the insulin/mTORC1 pathway to prevent excess protein synthesis.

Introduction

In decapod crustaceans, molting is initiated by ecdysteroids, the molting hormones, which increase nearly 30-fold during premolt (Covi et al., 2010). During premolt, the claw closer muscle atrophies to allow withdrawal of the muscle through the narrow basi-ischial joint at ecdysis (Ismail and Mykles, 1992; Mykles and Medler, 2015; Mykles and Skinner, 1990; Skinner, 1966). This claw muscle atrophy has been studied extensively in the blackback land crab, *Gecarcinus lateralis* (Chang and Mykles, 2011; Covi et al., 2010; Koenders et al., 2002; MacLea et al., 2012; Mykles, 1992; Mykles, 1997; Mykles, 1999; Mykles and Skinner, 1981; Mykles and Skinner, 1982a; Mykles and Skinner, 1982b; Mykles and Skinner, 1990; Skinner, 1966; Yamaoka and Skinner, 1975). As premolt claw muscle atrophies, there is a concomitant increase in protein synthesis, which allows extensive remodeling of the claw muscle in preparation for rapid growth immediately after molting (Covi et al., 2010; Skinner, 1965).

In mammals, up-regulation of protein synthesis is transduced by mTORC1 in skeletal muscle (Amirouche et al., 2009), while Mstn signaling inhibits this pathway (Goodman et al., 2013; Hitachi et al., 2014; Hulmi et al., 2013; Sakuma et al., 2014; Sartori et al., 2014; Schiaffino et al., 2013; Welle et al., 2009). Steroids, both glucocorticoids (Ma et al., 2001; Qin et al., 2013; Zhang et al., 2007) and androgens (Dubois et al., 2012; Dubois et al., 2014), up-regulate Mstn expression, but with different outcomes. Glucocorticoid up-regulation of Mstn (Ma et al., 2001; Qin et al., 2013; Zhang et al., 2007) results in decreased protein synthesis and muscle atrophy, as muscle protein is converted to glucose for available energy to combat the stressful situation (Braun and Marks, 2015; Goldberg et al., 1980; Kuo et al., 2012; Lofberg et al., 2002; Sapolsky et al., 2000; Schakman et al., 2008; Tomas et al., 1979). Conversely, androgens stimulate protein synthesis (Dubois et al., 2012; Ferrando et al., 1998; Urban et al., 1995), but also

125

stimulate Mstn expression which acts as a chalone, or brake, to prevent excess protein

synthesis (Dubois et al., 2012; Dubois et al., 2014).

In *G. lateralis* claw muscle, mRNA expression of *Gl-Rheb*, an activator of mTORC1, was

up-regulated during premolt (MacLea et al., 2012), while *Gl-Mstn* mRNA was down-regulated

(Covi et al., 2010). Hemolymph ecdysteroid levels were positively correlated with claw muscle

Gl-Rheb mRNA expression (MacLea et al., 2012). However, ecdysteroid levels were negatively

correlated with *Gl-Mstn* mRNA expression (Covi et al., 2010), indicating that ecdysteroids may

down-regulate *Gl-Mstn* expression, as opposed to up-regulation of Mstn by mammalian

steroids.

Carcinus maenas, the green crab, transitions between green morphs and red morphs,

as detailed in Abuhagr et al. (Abuhagr et al., 2014a). Briefly, juveniles and younger adults are

green morphs, which invest their energy into molting and growth; whereas older adults transition

into red morphs, investing their energy into reproduction (Abuhagr et al., 2014a; Reid et al.,

1997; Styrishave et al., 2004). Red morphs can still molt back into a green morph after an

extended intermolt (Abuhagr et al., 2014a).

Two methods have been used in decapod crustaceans to initiate molting—eyestalk

ablation (ESA) (Abramowitz and Abramowitz, 1940; McCarthy and Skinner, 1977b; Mykles,

2001) and multiple leg autotomy (MLA) (Holland and Skinner, 1976). Molt inhibiting hormone

(MIH) is produced in the X-organ and secreted by the sinus gland, both located in the eyestalk

(Chang and Mykles, 2011; Chung and Webster, 2005; Klein et al., 1993; Lachaise et al., 1993;

Skinner, 1985b). ESA removes the major source of molt inhibiting hormone (MIH), thus

releasing the Y-organ from inhibition, and allowing synthesis of ecdysteroids (Abuhagr et al.,

2014a; Chang and Mykles, 2011; Covi et al., 2012; Shrivastava and Princy, 2014). Autotomy is

the self-initiated release of a limb at a preformed fracture plane in response to a mechanical

stimulation (gripping) of the limb. As limbs can only be regenerated during premolt (Holland and

Skinner, 1976; Skinner, 1985b; Skinner and Graham, 1972), MLA shortens the intermolt stage by initiating a precocious premolt.

ESA has successfully stimulated molting in diverse decapods, including *G. lateralis* (Bliss, 1956; Covi et al., 2010; Kim et al., 2005a; McCarthy and Skinner, 1977b; Skinner, 1966; Skinner and Graham, 1972), *Pachygrapsis crassipes* (striped shore crab) (Chang et al., 1976), *Uca* species (fiddler crabs) (Hopkins, 1983; Skinner, 1985b; Skinner and Graham, 1972), *Callinectes sapidus* (blue crab) (Skinner and Graham, 1972), *Orconectes limosus* (Keller and Schmid, 1979) and *Procambarus clarkii* (crayfish species) (Wheatly and Hart, 1995), *Homarus Americana* (American lobster) (Chang and Bruce, 1980), and several *Penaeus* species (shrimp) (Browdy and Samocha, 1985; Chan et al., 1990). MLA has also successfully stimulated molting in diverse species, including *G. lateralis* (Bliss, 1956; Covi et al., 2010; Koenders et al., 2002; McCarthy and Skinner, 1977b; Passano, 1960; Skinner and Graham, 1970; Skinner and Graham, 1972), *Uca* species (Ismail and Mykles, 1992; Skinner and Graham, 1972), *C. sapidus* (Skinner and Graham, 1972), and *P. clarkia* (Wheatly and Hart, 1995). However, ESA did not initiate molting in *Maia squinado* (spiny spider crab) (Carlisle, 1957) and neither ESA nor MLA initiated molting in *Libinia emarginata* (portly spider crab) (Skinner and Graham, 1972). For *C. maenas,* inconsistent results have been reported. Carlisle (Carlisle, 1957) and Saidi et al. (Saidi et al., 1994) both did research on different populations of *Carcinus maenas* in the English Channel. They both reported that ESA stimulated molting in *C. maenas.* Passano, commenting on unpublished work by Carlisle, reported that MLA did not stimulate molting in *C. maenas.* In a population of *C. maenas* on the Atlantic coast of North America, Skinner and Graham found the opposite effects—ESA did not stimulate molting, but MLA did stimulate molting (Skinner and Graham, 1972).

The primary purpose of this research was to determine the effects of molting on mRNA levels of *Cm-Mstn* and the insulin/mTORC1 signaling components in skeletal muscles of a population of *C. maenas* in Bodega Bay, on the California coast. Insulin-like peptides, insulin,

127

insulin binding proteins and insulin-like growth factors are present in decapod crustaceans (Chandler et al., 2015; Chaulet et al., 2012; Chung, 2014; Davidson et al., 1971; Gallardo et al., 2003; Gutierrez et al., 2007; Hatt et al., 1997; Kucharski et al., 1999; Kucharski et al., 2002; Richardson et al., 1997; Sanders, 1983a; Sanders, 1983b), with a function similar to vertebrates (Richardson et al., 1997). Our hypotheses are 1) *Cm-Mstn* claw closer muscle mRNA levels will decrease during premolt, and will be negatively correlated with ecdysteroid levels, and 2) *cm-Rheb* or another component of the insulin/mTORC1 protein synthesis pathway will be up-regulated in *C. maenas* claw closer muscle, and will be positively correlated with *Cm-Mstn* mRNA levels.

Materials and Methods

Animals

Adult male *Carcinus maenas* (Linnaeus, 1758), the European green crab, were collected from Bodega Bay, California. For the 90-day molt-induction experiment and the natural molt experiment, crabs were maintained at the Bodega Marine Laboratory as described previously (Abuhagr et al., 2014a). They were kept in containers at 13°C with ocean water flow-through, and fed squid two times per week (Abuhagr et al., 2014a). An additional eight animals for the natural molt experiment were shipped to Colorado, placed in 20°C aerated water with 30 parts per thousand (p.p.t.) Instant Ocean (Aquarium Systems, Mentor, OH) overnight, and then harvested the next day. Crabs for the short-term (14 day) molt induction experiment and crabs used in cloning and tissue expression experiments were shipped to Colorado, kept in salt water containers as described above, on a 12 h light:12 h dark schedule, and fed chicken liver twice weekly.

Animal Harvest

Hemolymph was removed using a 1 ml slip-tip tuberculin syringe (Becton, Dickinson & Co (BD), Franklin Lakes, NJ, USA) and a 22G sterile needle (Adegoke et al., 2012). Hemolymph (100 µl) was added to 100% methanol (300 µl) and stored at -20^{0}C until shipped to

the Chang lab at the University of California Bodega Marine lab. Hemolymph ecdysteroid levels in each sample were quantified with a competitive ELISA for ecdysteroids, which preferentially binds 20-hydroxy ecdysone (20E) and ecdysone (Abuhagr et al., 2014b; Kingan, 1989; Medler et al., 2005).

After removing the hemolymph sample, animals were placed in ice for five min to anesthetize them. Tissues were dissected out immediately following the five min on ice. Tissues were wrapped in foil, frozen immediately in liquid nitrogen, and then stored at 80^0C.

RNA isolation

RNA was isolated from tissue samples with TRIzol (Invitrogen, Carlsbad, CA, USA) as described previously ((Covi et al., 2010). Approximately 100-150 mg of animal tissue was homogenized for 5 min in 1 ml of Trizol in glass homogenizers. After 5 min at room temperature, tissues were centrifuged at 12,000g and 4°C for 15 min to remove cellular debris. Chloroform was added to the supernatant, and samples were centrifuged for 15 min at 16,000g to separate the RNA into the aqueous layer. Approximately 600 µl of the aqueous layer containing the RNA was transferred into a clean microcentrifuge tube, one volume of isopropanol (approximately 600 µl) was added to the aqueous layer and the samples were placed in a 4^0C refrigerator for 30 min to precipitate the RNA. Samples were then centrifuged at 16,000g to pellet the RNA, supernatant was removed, and the pellet was washed twice in cold 75% ethanol in DEPC-treated water, centrifuging after each wash to re-pellet the RNA. The supernatant was removed and the pellet was dried on ice. Each sample was resuspended in 22 µl nuclease-free water, then treated with DNase I (Thermo Fisher Scientific) and Ribolock RNase Inhibitor (Thermo Fisher Scientific) and incubated at 37^0C for 30 min according to the manufacturer's directions. After the DNase treatment, 170 µl nuclease-free water, 100 µl acidic phenol (pH 4.3) and 100 µl 24:1 isoamyl alcohol were added to the RNA sample and centrifuged at 21,000g for 15 min to separate the layers. The aqueous phase containing the RNA was transferred to a clean tube, and the RNA was precipitated by adding 1.5 volumes isopropanol and 0.5 volume sodium

acetate (pH 5.2) to the aqueous phase, and incubating on ice for 10 min. The precipitate was then centrifuged at 16,000g for 15 min and washed twice with 70% ethanol, similar to the first RNA precipitation. After removing the supernatant, pellets were dried on ice, then RNA was quantified with a NanoDrop 1000 V3.8.1 (Fisher Scientific, Waltham, MA, USA).

cDNA synthesis

The Superscript III first strand synthesis system (Thermo Fisher Scientific) was used to make cDNA from total RNA. Total RNA (2.5 µg), 1 µl 50 µM oligo dT(20) primers (Integrated DNA Technologies, Inc., (IDT) Coralville, IA), 1 µl 10mM dNTP and enough nuclease-free water to make a 10 µl total reaction mixture. This was incubated at 65°C for 5 min, then transferred to ice. cDNA synthesis mix (10 µl) was added, according to manufacturer's protocol, and this mixture was incubated at 55°C for 60 min. Enzymes were then inactivated by incubating at 70°C for 15 min. To remove RNA, 1 µl RNase H was added, and the mixture was incubated at 37°C for 20 min.

Cloning to obtain a partial Cm-Mstn gene sequence

Gene specific primers (Table 1) were used to verify a previously amplified and sequenced 175 nucleotide *Cm-Mstn* gene segment. 3' Rapid Amplification of cDNA ends (3'RACE) using the FirstChoice RLM-RACE kit (Thermo-Fisher Scientific, Waltham, MA, USA) and following the manufacturer's protocol was used to amplify the 3' end of the *Cm-Mstn* gene using *Cm* total RNA. Nested *Cm-Mstn* gene-specific primers (Table 1), along with the inner and outer primers supplied with the 3'RACE kit were used for amplification. To obtain sequence 5' to the known *Cm-Mstn* gene fragment, forward primers based on the *Gecarcinus lateralis* and the *Eriocheir sinensis* Mstn sequences were used with reverse primers based on the known *Cm-Mstn* sequence (Table 4.1). PCR conditions were an initial denaturation at 95°C for 5 min, followed by 35 cycles of 95°C for 30 s, 56°C for 30 s, and 72°C for 1 min, and then a final extension at 72°C for 7 min.

Cm-Mstn tissue expression

The following tissues were collected from one adult male *C. maenas*: gill, heart, hepatopancreas, midgut, hindgut, claw muscle, thoracic muscle, testes, thoracic ganglia, Y-organ and eyestalk. Tissues were collected, RNA was isolated and cDNA was synthesized as described above.

qPCR amplification of *Cm-EF2* and *Cm-Mstn* cDNA of all tissues collected was followed by agarose gel separation to visualize gene expression. *Cm-EF2* was used as a constitutive sample control which was expected to have a high level of expression in all cells. For each gene, the PCR reaction contained 1 µl cDNA, 1 µl each of 10 µM forward and reverse primers (Integrated DNA Technologies (IDT), Coralville, IA, USA) (Table 4.2), 3 µl nuclease-free water, and 5 µl GoTaq Master Mix (Promega, Madison, WI, USA). The PCR setting for *Cm-EF2* amplification was an initial denaturation at 95°C followed by 35 cycles of 95°C for 30 s, 61°C for 30 s and 72°C for 1 min, and then a final elongation at 72°C for 5 min. *Cm-Mstn* PCR settings were the same, except the annealing step was 57°C. The amplified product for *Cm-EF2* was 278 based pairs, and the amplified product for *Cm-Mstn* was 205 base pairs. Product was run on a 1.5% agarose gel for 25 min at 100 volts, stained with ethidium bromide, and photographed with a ChemiDoc XRS+ with Image lab software (Bio-Rad Laboratories, Hercules, CA, USA).

qPCR

Quantitative polymerase chain reaction (qPCR) was used to quantify the mRNA levels of the following genes: elongation factor 2 *(Cm-EF2*) [GenBank GU808334 (Kim et al., 2004a)], myostatin (*Cm-Mstn*), *Cm-Akt* (also known as protein kinase B (PKB)) [GenBank JQ864249 (Abuhagr et al., 2014)], Ras homolog enriched in brain (*Cm-Rheb*) [GenBank HM989970 (MacLea et al., 2012)], mechanistic Target of Rapamycin (*Cm-mTOR*) [GenBank JQ864248 (Abuhagr, et al., 2014)], and p70 ribosomal protein S6 kinase (*Cm-S6k*) [GenBank JQ864250, Abuhagr et al., 2014)]. One µl of cDNA (from 0.12 ng total RNA), 1 µl of each 10 µM gene-

specific primer (IDT) (Table 4.2), 3 µl of nuclease-free water and 5 µl of LightCycler 480 SYBR

Green I Master mix (Roche) was used in each reaction. LightCycler 480, 384 Multiwell Plates

(Roche) were used to run the reactions in a LightCycler 480 Real-Time PCR instrument

(Roche).

PCR settings were an initial denaturation for 5 min at 95^0C, followed by 50 cycles of

denaturation at 95^0C, gene-specific annealing temperature (Table 2) for 20s and elongation at

72^0C for 20s for *Cm-EF2* and *Cm-Mstn* in the short-term (14 day) ESA molt-induction

experiment and the long-term (90 day) ESA and MLA molt-induction experiment. In the natural

molt experiment, the same settings were used, except 45 cycles were used. PCR cycles were

followed by a melt curve cycle to analyze product homogeneity. Absolute quantification was

done by the LightCycler 480 software, version 1.5 (Roche), comparing each sample to external

standard concentrations for each gene. Concentrations from the LightCycler software were

converted to copy number per µg RNA in Microsoft Excel.

Molting experiments

Three molting experiments were done with *C. maenas*—a short-term (14 day)

experiment following ESA, a long-term (90 day) experiment following ESA, MLA or both ESA

and MLA, and a natural molt experiment. Ecdysteroid levels and *Cm-EF2* (a constitutively

expressed protein synthesis elongation factor) and *Cm-Mstn* mRNA levels were quantified in all

experiments. In addition, for the natural molt experiment, *Cm-RXR* (one portion of the

ecdysteroid receptor heterodimer), and *Cm-Akt*, *Cm-Rheb*, *Cm-mTOR* and *Cm-S6k* (all

components in the mTOR protein synthesis pathway) were quantified in the natural molt

experiment.

Short-term (14 day) molt-induction by ESA experiment

ESA, as previously described (Lee et al., 2007b), was used to attempt molt induction in

red morph and green morph intermolt *C. maenas* crabs. Animals were harvested as described

above 3, 7, and 14 days after ESA, with intact green morphs serving as controls. Ecdysteroid

levels, and claw and thoracic muscle mRNA levels for *Cm-EF2* and *Cm-Mstn* were analyzed as described above. As ecdysteroid levels indicated that ESA did not induce premolt in this short-term experiment, a long-term molt induction experiment (90 day) was initiated.

Long-term (90 day) molt induction experiment by ESA, MLA or both

Intermolt red morph *C. maenas* were induced to molt by ESA, MLA, or a combination of both methods, as part of the same experiment previously described (Abuhagr et al., 2014a). Claw and thoracic muscle tissue were harvested 90 days after attempted molt induction, with intact intermolt animals serving as control. Ecdysteroid levels, and claw and thoracic muscle mRNA levels for *Cm-EF2* and *Cm-Mstn* were analyzed as described above. As ecdysteroid levels indicated that neither ESA nor MLA induced premolt and molting in this long-term experiment, a natural molt experiment was initiated.

Natural molt experiment

Green morph *Carcinus maenas* crabs in various stages of premolt or postmolt were collected at Bodega Bay in March, during the green morph annual molting season. Postmolt animals were harvested 3 to 5 days after ecdysis. Intermolt animals included both red morphs and green morphs. Claw and thoracic muscle tissue were harvested from the same animals as described in Abuhagr et al. (Abuhagr et al., 2014a).

Molt stage of individual *C. maenas* crabs was determined by observation of maxilliped endopodite setal development under 100X microscopy (Moriyasu and Mallet, 1986). Determination between postmolt and intermolt was made by observation of granular protoplasm in setae and wide setal lumen (postmolt) versus no granular protoplasm with narrow lumen (intermolt). Apolysis of epidermis from the cuticle at the base of the setae indicated the beginning of premolt, with width of retraction zone and new setal developmental stages indicating specific progress through premolt. Late premolt was indicated by completion of setal articulations and protrusion of the shaft of the new setae through the epidermis by more than one-half their length (Moriyasu and Mallet, 1986).

Alignments and phylogenetic trees

A protein BLAST (NCBI) with the *Cm-Mstn* mature peptide sequence revealed nine additional decapod Mstn sequences. ClustalX2 (Larkin et al., 2007) and GeneDoc (Nicholas and Nicholas) were used to produce and annotate multiple sequence alignments from the decapod Mstn sequences. TreeView 1.6.6 (Page, 2001) was used to generate a radial phylogenetic tree.

Graphing and statistical analyses

Sigma Plot 12.5 software (Systat Software, Inc., Chicago, IL, USA) was used for all graphs and statistical analyses. Box plots of non-transformed and transformed data (data not shown) indicated that $\log_{10}$ transformed data had a more normal distribution with equal variances. Subsequently, all gene expression data was $\log_{10}$ transformed for further statistical analyses. In the natural molt experiment, the Pearson correlation was used to assess the linear relationship between ecdysteroid levels and mRNA levels, and between *Cm-Mstn* mRNA levels and the other mRNA levels in both muscle types.

One-way ANOVAs were used to compare molt stages for ecdysteroid levels, and mRNA levels in each muscle for *Cm-EF2*, *Cm*-RXR, *Cm-Mstn, Cm-Akt*, *Cm-Rheb*, *Cm-mTOR* and *Cm-S6k*. If a significant difference was found in a one-way ANOVA, then the Holm-Sidak All Pairwise Multiple Comparison Procedure was initiated. If the Shapiro-Wilk Normality Test or the Equal Variance Test failed, then the Kruskal-Wallis one-way ANOVA on ranks was initiated. If a significant difference was found in a one-way ANOVA on ranks, then Dunn's All Pairwise Multiple Comparison Procedure was initiated. For the molt induction experiments, an alpha level of 0.05 was used. For the natural molt experiment, an alpha level of 0.01 was chosen for all gene expression tests to control for the Type I error rate due to multiple testing.

Results

Cloning and characterization of Cm-Mstn

An 870 base pair sequence of the *Cm-Mstn* mRNA was cloned from skeletal muscle tissue (Fig. 4.1). This nucleotide segment codes for 289 amino acid residues (red letters), including most of the propeptide sequence and the entire mature peptide sequence of 110 amino acid residues (bold font). Furin cleaves just after the RSRR site (underlined and italicized), covalently cleaving the propeptide from the mature peptide. Nine cysteines contribute to formation of a cysteine knot. Eight cysteines form intrachain linkages, and one cysteine forms an interchain linkage, covalently linking two mature peptides to form the Mstn mature peptide dimer.

A protein alignment showed 80% to 95% identity between the *Cm*-Mstn mature peptide and nine other sequenced decapod Mstn mature peptides (Fig. 4.2). Each sequence contained all nine cysteines for formation of a cysteine knot. Only the first few peptides after the RXXR cleavage site were somewhat variable between sequences. Seven of the first thirteen amino acid residues of the mature peptide sequence were highly variable. The remaining 97 amino acid residues were 85% to 95% identical between the decapod mature peptide seqences, with 93% to 98% similarity. A phylogenetic tree of the ten decapod Mstn mature peptide sequences shows two major clusters, one cluster of crabs (*C. maenas, Portunus trituberculatus, Eriocheir sinensis*, and *Gecarcinus lateralis)*, one cluster of shrimp (*Penaeus monodon, Litopenaeus vannamei, Pandalopsis japonica, Macrobrachium nipponense,* and *Macrobrachium rosenbergii)*, with the lobster (*Homarus Americana*) between the two clusters. As expected, the *Cm*-Mstn mature peptide was most similar to *Portunus trituberculatus*, both of which are in the same subsection (Heterotremata) of the infraorder Brachyura, and in the same family—Portunidae. *G. lateralis* and *E. sinensis* are much more distantly related to *C. maenas*, as shown in the phylogenetic tree (Fig. 4.3). Both *G. lateralis* and *E. sinensis* are in the Thoracotremata subsection of Brachyura. They are in the same superfamily (Grapsoidea), but are only distantly

135

related to each other, as indicated in the phylogenetic tree (Fig. 4.3), diverging more than 80 million years ago (Tsang et al., 2014).

Three different splice variants of the 3' *Cm-Mstn* untranslated region were cloned (Fig. 4.4). A truncated 3' UTR with no evidence of a poly-adenylation (poly-A) signal was found that was 94 nucleotides long. Two 3' UTR sequences of 281 and 287 nucleotide length were identical except for 3 nucleotide differences, and the longer sequence had a slightly longer poly-A tail.

Cm-Mstn mRNA was expressed in all tissues, including the midgut, hingut, heart muscle, claw muscle, thoracic muscle, thoracic ganglion, Y-organ, hepatopancreas, gill, and eyestalks (4.5). *Cm-EF2* mRNA expression was relatively constant in all the tissues. As EF2 is a constitutively expressed protein elongation gene, *Cm-EF2* expression allowed a qualtitative comparison of cDNA across tissues (Fig. 4.5).

Short term, 14 day, ESA experiment

Ecdysteroid levels did not increase in either red morph or green morph *C. maenas* after ESA in a short term, two-week experiment, indicating that premolt was not initiated in these animals (4.6). Red morph ecdysteroid levels actually decreased by 69% at 7 days. Green morph crabs had significantly higher ecdysteroid levels than red morphs at all days compared, but there were no significant changes in ecdysteroid levels within green morphs.

In the same two-week experiment, *Cm-EF2* mRNA levels in thoracic muscle significantly increased (3.8-fold) from day zero to day 7 in red morphs, but there was no significant difference in green morphs (Fig. 4.7A). There were no significant changes in *Cm-EF2* mRNA levels in claw muscle (Fig. 4.7B). *Cm-EF2* expression in green morph claw muscle was 3.5-fold higher than in red morphs 3 days after ESA. There were no other significant differences in *Cm-EF2* mRNA levels between color morphs in either muscle type. Compared to day zero controls, there were no significant differences in *Cm-Mstn* mRNA levels at any time point in either muscle (Fig. 4.7C). However, green morphs showed a significant decrease (43%) in *Cm-Mstn* mRNA

levels in thoracic muscle between day 7 and day 14. Differential *Cm-Mstn* mRNA levels between color morphs occurred at day 7 in thoracic muscle, and day 3 in claw muscle, with 17-fold and 189-fold higher levels in green morphs, respectively.

Long term, 90 day, ESA and MLA experiment

As the short term ESA experiment did not induce molting, a long-term, 90-day experiment was initiated, using the same animals as described in Abuhagr et al. (Abuhagr et al., 2014a). Treatments included ESA, MLA, both ESA and MLA and no treatment (intact) controls. There were no significant ecdysteroid level changes in any treatment group, compared to controls (Fig. 4.8). However, in red morphs, the ESA treatment animals had significantly higher (4.1-fold) ecdysteroid levels than the MLA treatment animals, and the animals with both ESA and MLA treatment had significantly higher (3.4-fold) ecdysteroid levels than the MLA treatment animals. The consistent low levels of ecdysteroids, less than 40 pg/µl compared to almost 300 pg/µl during premolt in naturally molting crabs, indicated that neither ESA nor MLA initiated premolt in these animals. For a detailed account of ecdysteroid levels throughout the 90 days, see Abuhagr et al. (Abuhagr et al., 2014a).

The effect of ESA or MLA on *Cm-EF2* and *Cm-Mstn* mRNA levels was observed in thoracic muscle and claw muscle, for both red morphs and green morphs at the end of the 90-day experiment (Fig. 4.9). In red morphs, the effects of both ESA and MLA on *Cm-EF2* and *Cm-Mstn* mRNA levels were observed. In red morph thoracic muscle, *Cm-EF2* mRNA levels were significantly lower in all three treatment groups—ESA, MLA and both ESA and MLA—by 52%, 57% and 60%, respectively, compared to controls (Fig. 4.9). There were no significant differences in *Cm-EF2* mRNA levels in green morphs. In red morph claw muscle, *Cm-EF2* mRNA levels were 70% lower in the ESA/MLA treatment group, compared to controls. In green morph claw muscle, *Cm-EF2* mRNA levels were 72% lower in the MLA treatment group, compared to the ESA treatment group. There were no significant differences in *Cm-Mstn* mRNA levels in claw muscle or thoracic muscle, compared to controls. The only significant difference

137

was 95% lower *Cm-Mstn* mRNA levels in the red morph thoracic muscle MLA treatment group, compared to the ESA treatment group.

Natural molt experiment, ecdysteroid levels

As neither MLA nor ESA induced molting in the 90 day experiment, a natural molt experiment was initiated. Some of the same animals as in Abuhagr et al. were used in this experiment (Abuhagr et al., 2014a). In naturally molting green morph crabs, ecdysteroid levels increased by 13-fold (to almost 300 pg/µl) during late premolt compared to intact animals (Fig. 4.10), then dropped to levels observed in intact animals during postmolt.

Natural molt experiment, mRNA levels

The mRNA levels of seven genes were determined during intermolt, early premolt, late premolt and postmolt in claw and thoracic muscle. These genes included *Cm-EF2*, a constitutively expressed protein elongation gene, and *Cm-RXR*, one part of the heterodimeric ecdysteroid receptor. ThemRNA levels of four genes in the mTORC1-dependent protein synthesis pathway (*Cm-Akt*, *Cm-Rheb*, *Cm-mTOR*, and *Cm-S6k*) and an inhibitor of this pathway (*Cm-Mstn*) was also determined.

In thoracic muscle, there were no significant changes in mRNA levels of any of the seven genes during the molt cycle (Fig. 4.11). In claw muscle, there were no significant changes in *Cm-EF2* or *Cm-RXR* mRNA levels during the molt cycle (Fig. 4.12). *Cm-Mstn* mRNA levels were 4.4-fold higher in claw muscle during premolt, compared to intermolt animals (Fig. 4.12). Of the four mTORC1-dependent protein synthesis genes, only *Cm-mTOR* and *Cm-S6k* significantly changed in claw muscle during the molt cycle. Both *Cm-mTOR* and *Cm-S6k* mRNA levels were higher in claw muscle during premolt by 35-fold and 5-fold, respectively. *Cm-mTOR* mRNA levels remained 12-fold higher in postmolt, compared to intermolt animals. Ecdysteroid levels were not significantly correlated with the mRNA levels of any gene in thoracic or claw muscle (data not shown). *Cm-Mstn* and *Cm-mTOR* mRNA levels were positively correlated,

both in the thoracic muscle (R^2=0.251) and in the claw muscle (R^2=0.241) (Fig. 4.13). *Cm-Mstn* mRNA levels were not correlated with any other gene in either muscle.

Discussion

The *Cm-Mstn* mRNA is expressed in all observed tissues in *C. maenas*. This is similar to the ubiquitous expression of Mstn in other invertebrates (Covi et al., 2008; De Santis et al., 2011; Hu et al., 2010; Kim et al., 2004b; Kim et al., 2010; MacLea et al., 2010; Nunez-Acuna and Gallardo-Escarate, 2014; Qian et al., 2013), and in lower vertebrates (Helterline et al., 2007; Radaelli et al., 2003; Zheng et al., 2015). However, in mammals, Mstn is expressed mainly in skeletal muscle tissue (McPherron et al., 1997; Sharma et al., 2015), with limited expression in adipose tissue (McPherron and Lee, 2002; McPherron et al., 1997) and heart muscle (Sharma et al., 1999; Shyu et al., 2005)

The mature peptide, consisting of 110 amino acid residues is highly conserved (80% to 95%) with nine other decapod crustaceans. As shown before with *G. lateralis*, the decapod mature peptide can be as much as 70% conserved with vertebrates, including mammals (Covi et al., 2008). All ten decapod Mstn mature peptides contained an RXXR sequence (cleavage site for furin) between the propeptide and the mature peptide, and nine cysteines (for cysteine knot formation), which are conserved with vertebrates. A phylogenetic tree of the decapod crustacean Mstn mature peptides showed groupings as expected, according to the evolutionary relatedness of the decapods themselves.

Neither ESA nor MLA was able to initiate molting in either color morph of this population of *Carcinus maenas*, as indicated by ecdysteroid levels remaining below 30 pg/µl (4.6 and Fig. 4.8). By contrast, naturally molting crabs reached peak ecdysteroid levels during premolt of nearly 300 pg/µl. The four populations of *C. maenas* that have been studied, have reacted differently to attempted molt induction. In the English Channel (two populations, one near Plymouth England and one in Brittany, France), *C. maenas* initiated molting in response to ESA (Carlisle, 1957; Saidi et al., 1994), but not MLA (only studied in Plymouth, England) (Passano,

1960). By contrast, *C. maenas* on the Atlantic coast of North America (Massachusetts) responded to MLA (Schmiege et al., 1992; Skinner and Graham, 1972), but not ESA (Skinner and Graham, 1972). In the present study, both red morph and green morph *C. maenas* from the Bodega Bay, California population, on the Pacific coast of North America, were refractory to attempted molt stimulation by MLA and/or ESA. This population of *C. maenas* on the west coast of North America are descendants of a founding population from the eastern United States coast (Tepolt et al., 2009). The founding event occurred in 1989/1990, with a maximum of 30 founding individuals with limited genetic variation (Tepolt et al., 2009). This population of crabs is bigger (male carapace width of 65 to 75 mm, compared to Eastern North American populations of 50 to 60 mm) and are more limited in habitat (use soft substrate habitats exclusively, while other populations of green crabs are also found on soft substrate habitats and on rocky shores) (Abuhagr et al., 2014a; Grosholz and Ruiz, 1996). Perhaps the genetics in this population contributes to the contrasting results to molt induction. Also, there is recent evidence that MIH is produced in nervous tissues in addition to the eyestalks in some decapods, including *C. maenas*, which may explain why the crabs were refractory to ESA (Abuhagr et al., 2014a; Stewart et al., 2013).

Contrary to our hypothesis, *Cm-Mstn* mRNA levels increased in claw muscle during premolt of naturally molting *Carcinus maenas*. Further, there was no correlation between ecdysteroid levels and claw muscle *Cm-Mstn* mRNA levels. This contrasts with the results obtained with *G. lateralis* during premolt (Covi et al., 2010). After MLA in *G. lateralis,* ecdysteroid levels in the hemolymph rose 28-fold (Covi et al., 2010). In the atrophying claw closer muscle, soluble protein synthesis increased 13-fold, while myofibrillar protein synthesis increased 11-fold (Covi et al., 2010). Concomitantly, the levels of *Gl-Mstn* mRNA in the claw muscle decreased 94% (Covi et al., 2010). Further, there was a strong negative correlation between *Gl-Mstn* and ecdysteroid levels (Covi et al., 2010). These results suggest that unlike *Gl-Mstn, Cm-Mstn* mRNA levels are not regulated by ecdysteroids. It is not completely

140

surprising that the two crab species have developed different regulatory mechanisms, as the thoracotremata (including *G. lateralis*) diverged from the heterotremata (including *Carcinus maenas*) approximately 150 million years ago, during the late Jurassic period (Tsang et al., 2014).

Our second hypothesis was that some components of the insulin/mTORC1 protein synthesis pathway would be up-regulated and positively correlated with *Cm-Mstn* in *C. maenas* claw closer muscle. The mRNA levels of *Cm-mTOR* and *Cm-S6k* of the insulin/mTORC1-dependent protein synthesis pathway were both upregulated in claw muscle, which supported our second hypothesis. Further, *Cm-mTOR* and *Cm-Mstn* mRNA levels were positively correlated. mTOR up-regulation of protein synthesis, and Mstn down-regulation of protein synthesis is evolutionarily conserved in metazoans. Up-regulation of both together, demonstrated in this study, suggests that Mstn is up-regulated to act as a chalone, providing a fine control by modulating the activity of the insulin/mTORC1 protein synthesis pathway, similar to the action of Mstn in *G. lateralis* (see chapter 2 of this dissertation).

In conclusion, *Cm-Mstn* expression is not limited to muscle and adipose tissue as in mammals, but is expressed in many tissues, similar to *Gl-Mstn*, The *Cm-Mstn* mature peptide is highly conserved with other decapods, indicating similar functions in different species. Unlike *Gl-Mstn*, *Cm-Mstn* mRNA levels do not appear to be regulated by ecdysteroids in the claw muscle. However, *Cm-Mstn* and *Cm-mTOR* mRNA levels are positively correlated in claw and thoracic muscle, similar to *G. lateralis*. It appears that Mstn acts as a chalone to modulate excessive protein synthesis in the claw muscle of both *C. maenas* and *G. lateralis*.

Table 4.1. **Oligonucleotide primer sets and forward primers used in 3' RACE for sequencing of *Cm-Mstn* cDNA.** The *Cm-Mstn* primer set was used to confirm the previously cloned 175 nucleotide *Cm-Mstn* sequence, including the mature peptide. The *Cm-Mstn* 3' RACE primers are gene-specific primers used with 3' RACE kit reverse primers.

Primer name	Primer sequence (5'-3')	Use
Cm-Mstn F1	CAACCCTGACGTGCAGGGCAT	Mstn verification
Cm-Mstn R1	GTGCTGGGCGTTGGTGTTGTTC	Mstn verification
Cm-Mstn 3' Out	CACCGCCTTCATCCAGAAAAT	3' RACE (outer)
Cm-Mstn 3' In	ACGACATGGTAGTAGACCGCTGC	3' RACE (inner)
Cm-Mstn F2	ATGCCCAGCAACGAGCCAATC	5' Mstn amplified
Cm-Mstn R1	GTGCTGGGCGTTGGTGTTGTTC	5' Mstn amplified

Table 4.2. Oligonucleotide primers used for qPCR amplification. For *Cm-Mstn*, 58°C annealing temperature was used in the molt-induced experiments, but a 62°C annealing temperature was used in the natural molt experiment.

Primer name	Primer sequence (5'-3')	Annealing Temp. (°C)	Product size
Cm-EF2 F	CCATCAAGAGCTCCGACAATGAGCG	62	260
Cm-EF2 R	CATTTCGGCACGGTACTTCTGAGCG		
Cm-Mstn F	GAACTTTGTGGAGCTGGGATGG	58/62	205
Cm-Mstn R	GTGGTCGTAGTACAACATCTT		
Cm-Akt F	GTGAAGCAATGCCAGATCCTG	55	259
Cm-Akt R	CGGGTGTATCATCATCATCG		
Cm-Rheb F	ATGGGCAAAGTCACAGTTCCTG	53	281
Cm-Rheb R	GTCAGGAAGATGGTGGCAATAAAG		
Cm-mTOR F	CATCCCTCAAACCTCATGCTG	53	319
Cm-mTOR R	CACCCACCACAGAACGCTTTC		
Cm-S6k F	GTACATGGCACCCGAGATCCT	55	258
Cm-S6k R	TCTCCGTCATCTGAGCCGCTGC		
Cm-EcR F	CAAGTGACATGAGATTCAGGCA	53	263
Cm-EcR R	TTGTGACGACTCTCCCAAACCAG		
Cm-RXR F	TACGGCGTGTACAGTTGTGAAGGATC	59	143
Cm-RXR R	TTCTGGTACCGGCAATACTGGCAAC		

```
ATGGAATCCGCGTTGCCTATGACTTACCTCGAGGAACCGCTTTATAACGAGGACGAGCCG   60
 M   E   S   A   L   P   M   T   Y   L   E   E   P   L   Y   N   E   D   E   P    20
GATGTGAAAACGGAAATGCTGTTCTTTCCCGTTCAGCCAGCGCCTTCCGATTTGAACATT  120
 D   V   K   T   E   M   L   F   F   P   V   Q   P   A   P   S   D   L   N   I    40
CCCCCTGGCACGGATGTCCTGTACTTCAACCTGAGTAGGACGCGCCTAGGCAACAGGGCA  180
 P   P   G   T   D   V   L   Y   F   N   L   S   R   T   R   L   G   N   R   A    60
AGGAGAGCCATCCTGCACGTGTGGCTCAAACCAATGAGTACGGAGATGCTGAGCCACGTG  240
 R   R   A   I   L   H   V   W   L   K   P   M   S   T   E   M   L   S   H   V    80
CCAGTTTCAATATACAAAGTGTCGAGACCGCGGAAACCTAGCGGGGAAATTGAAAGAAAG  300
 P   V   S   I   Y   K   V   S   R   P   R   K   P   S   G   E   I   E   R   K   100
GCCGTAACCACCGTCATGGTGTCGTTCAACCCTCACAAAGGCAACTGGGTCAAGATAGAA  360
 A   V   T   T   V   M   V   S   F   N   P   H   K   G   N   W   V   K   I   E   120
GTGTACCAGCTACTGCAGGAGTGGCTGACGCGGCCGGAGAAGAACCTAGGACTCATAGTA  420
 V   Y   Q   L   L   Q   E   W   L   T   R   P   E   K   N   L   G   L   I   V   140
GTGGCAATGGACTCCCAGGGGCATCAAGTGGCCGTCACAGATCCTCAGGAGTCCCCCTCG  480
 V   A   M   D   S   Q   G   H   Q   V   A   V   T   D   P   Q   E   S   P   S   160
AACGCTCCCCTTCTAGAGATCCACATGGAGGAATGGAACCGTAGT**CGTAGTCGCCGTAAC** **540**
 N   A   P   L   L   E   I   H   M   E   E   W   N   R   S   *R   S   R   R*   **N**   180
**AGTGGTAACTTTATGTGTACCAACGAGGTGGAGTCCCGCTGTTGTCGTTACCACCTCACC** **600**
 **S   G   N   F   M   C̲   T   N   E   V   E   S   R   C̲   C̲   R   Y   H   L   T**   200
**GTGAACTTTGTGGAGCTGGGATGGGACTTCATTGTGGCGCCAAAAGTATACGAGGCCAAC** **660**
 **V   N   F   V   E   L   G   W   D   F   I   V   A   P   K   V   Y   E   A   N**   **220**
**TTCTGCAACGGCGAGTGTCCCTTCCTGTACGCCCACAAGTACGCCCACACCGCCCTCATC** **720**
 **F   C̲   N   G   E   C̲   P   F   L   Y   A   H   K   Y   A   H   T   A   L   I**   **240**
**CAGAAAATGAACAACACCAACGCCCAGCACGGCCCTTGTTGCGGCGCCCGGAAGTTGTCG** **780**
 **Q   K   M   N   N   T   N   A   Q   H   G   P   C̲   C̲   G   A   R   K   L   S**   **260**
**CCCATGAAGATGTTGTACTACGACCACGACCACAAGATTCGGTTTGACATTATTAACGAC** **840**
 **P   M   K   M   L   Y   Y   D   H   D   H   K   I   R   F   D   I   I   N   D**   **280**
**ATGGTAGTAGACCGCTGCGGCTGCTCCTAA** **870**
 **M   V   V   D   R   C̲   G   C̲   S**   **289**
```

144

Figure 4.1. Partial *C. maenas*-*Mstn* (*Cm-Mstn*) cDNA open reading frame and amino acid sequence. The nucleotide sequence (870 bp) (black letters) includes code for a portion of the propeptide (PP) region and the entire mature peptide (MP) region (bold). Partial peptide sequence is 289 residues (red letters), with mature peptide sequence 110 residues (bold font). Furin cleaves just after the RSRR site (underlined and italicized), cleaving the propeptide from the mature peptide. Nine cysteines contribute to formation of a cysteine knot. Eight of these cysteines form intrachain linkages, and one cysteine forms an interchain linkage, covalently linking two mature peptides to form the mature Mstn dimer.

```
          *            20            *            40            *
Cm :  NSGN-FMCT-NEVESRCCRYHLTVNFVELGWDFIVAPKVYEANFCNGECPFLYAHKYA
Pt :  NSGN-FMCT-NENESRCCRYHLTVNFVEMGWDFIVAPKVYEANFCNGECPFLYAHKYA
Es :  NSAG-SQCV-NRNDSRCCRYALTVDFVDMGWDFIVAPKVYEANFCNGECPFLYAQKYA
Gl :  NSGN-FMCT-NKNESRCCRYHLTVDFVELGWDFIVAPKVYEANFCNGECPFLYAHKYA
Ha :  NSGNNFFCTNNKKESRCCRYQLVVNFIELGWDFIVAPKTYEANFCNGECPFLYAHKYA
Pm :  NSSR-NQCTTSQIESRCCRYPLLVNFVELGWDFIVAPKVYEANFCNGECPYLYAHKYA
Lv :  NSIR-NQCTTSQIESRCCRYPLLVNFVELGWDFIVAPKVYEANFCNGECPYLYAHKYA
Pj :  NSGN-FFCTNNDTD-RCCRYPLAVNFVEMGWDFIVAPKVYDANFCNGECPYLYAQKYA
Mn :  NSGN-VFCTNNDTD-RCCRYPLSVNFVEMGWDFIVAPKVYDANFCNGECPYLYAQKYA
Mr :  NSGM-SMCT------RCCRYPLLVNFVEMGWDFIVAPKVYDANICNGECPYLYAQKYA

      60            *            80            *            100           *
Cm :  HTALIQKMNNTNAQHGPCCGARKLSPMKMLYYDHDHKIRFDIINDMVVDRCGCS
Pt :  HTALIQKMNSTNAQHGPCCGARKLSPMKMLYYDHDHMIKFDIINDMVVDHCGCS(95%)
Es :  HTSLIQKMNSS-AQHGPCCGARKLSPMKMLYYDHDHQIKFDIIQDMVVDHCGCT(80%)
Gl :  HTALIQKLNSSSAQHGPCCGARKLSPMKMLYYDHDHKIKFDIIQDMVVDRCGCS(92%)
Ha :  HTSLVQKLNSNAHHGPCCGARKLSPMKMLYYDHDHKIKFDTIQDMVVDRCGCS(84%)
Pm :  HSALIQKMNSTNAKHGPCCGARKLSPMKMLYYDHDHKIKFDTIQDMVVDRCGCS(85%)
Lv :  HSALIQKMNSTSAKHGPCCGARKLSPMKMLYYDHDHKIKFDTIQDMVVDRCGCS(85%)
Pj :  HSALVQKMNSTNAKHGPCCGARKLSPMKMLYYDHDHKIKFDTIQDMVVDRCGCS(84%)
Mn :  HSALIQKMNSSSAKHGPCCGARKLSPMKMLYYDHDHKIKFDTIQDMVVDRCGCS(82%)
Mr :  HSALIQKMNSSSAKHGPCCGARKLSPMKMLYYDHDHKIKFDTIQDMVVDRCGCS(80%)
```

Figure 4.2. Alignment of the *Cm-Mstn* mature peptide with other decapods crustaceans. Amino acids conserved with *Carcinus maenas* are indicated with white letters on a black background. The percent identity between *Cm-Mstn* and other decapods sequences is indicated in parenthesis after each sequence. Nine cysteines, conserved in all Mstn factors, are indicated by black triangles below the sequence. Abbreviations and GenBank accession numbers for Mstn genes: Pt, *Portunus trituberculatus* (ADV78228); Es, *Eriocheir sinensis* (ACF40953); Gl, *Gecarcinus lateralis* (ACB98643); Ha, *Homarus Americana* (ADK79107); Pm, *Penaeus monodon* (ADO34177); Lv, *Litopenaeus vannamei* (AEY11334); Pj, *Pandalopsis japonica* (ADK62522); Mn, *Macrobrachium nipponense* (AHA80844); Mr, *Macrobrachium rosenbergii* (AFP74567).
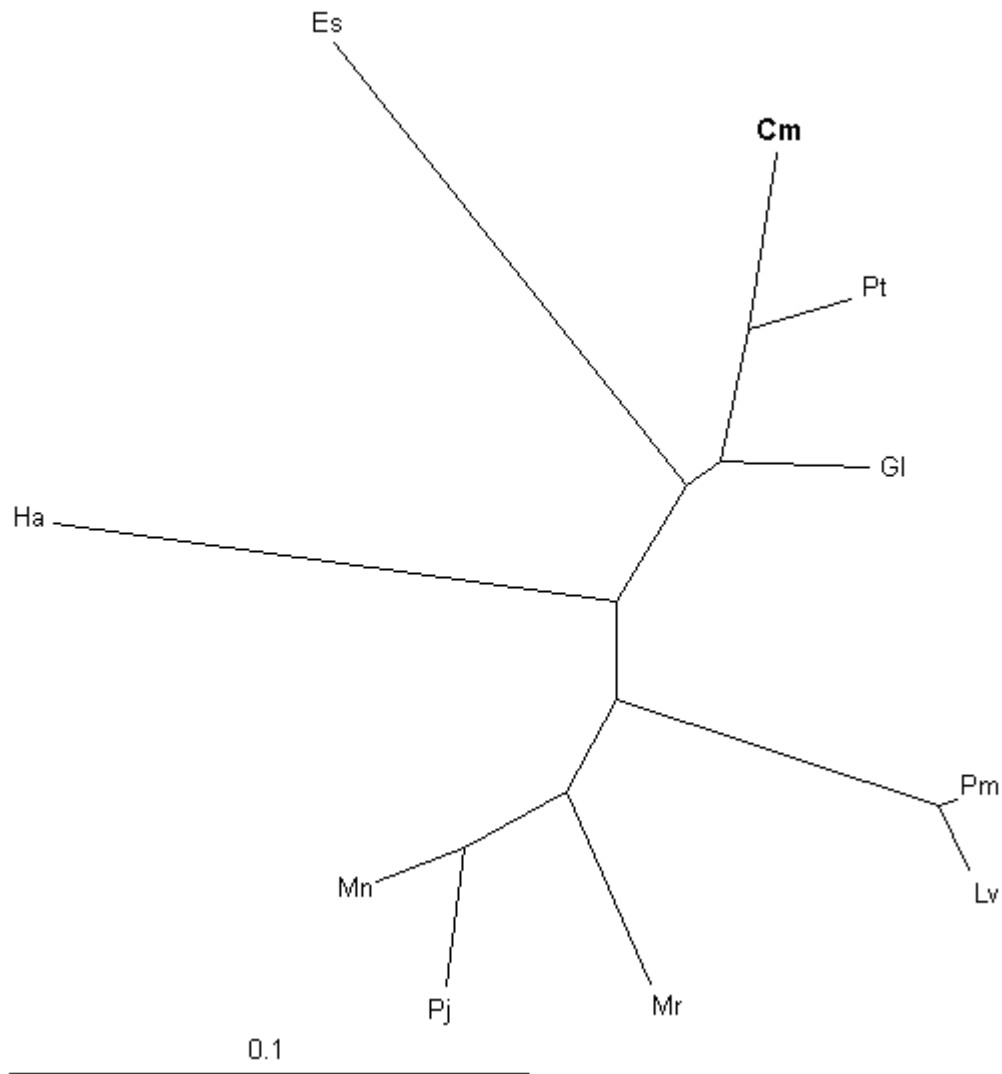
Figure 4.3. Phylogenetic relationships among decapod Mstn mature peptide sequences. The crabs (Cm, Pt, Gl and Es) form one cluster, the shrimp (Pm, Lv, Mr, Mn and Pj) form another cluster, and lobster is isolated between the other two groups. Abbreviations and GenBank accession numbers are the same as in figure 2.

1) GGCCCCACAGCCACTCACAGACAATCATGAGTGCCCGAATTGCTATCAGTTAGAGAT

GAGAAAGAAGCTCAGACTGGCACAGATAAAAAAAAAA

2) GGCCCCACCACCACCACCACCACCCCTCCCCCAACACCTCCCCCTCCTACACTCAC

CTAAACCCCCCCCACCCTC***A***CCTCACCTGGGGTGCGTCACACCTGAGGAACGTGTGTG

GGCACCACCACTCGATAATATTACGCTGCCACGCTGGGTGTGTGTGTGTGTGTGTGTGT

GTGTGTGTGTGTGTGTGTGTGTGTGTGTGTGTGTGTGTGTGTGTGTGTGTGTGTGTGTG

TGTG<u>TATAATT</u>CTAGCTTTAGCAAA<u>AAATATATATATAAT</u>CAAA***TT***AAA

3) GGCCCCACCACCACCACCACCACCCCTCCCCCAACACCTCCCCCTCCTACACTCAC

CTAAACCCCCCCCACCCTC***G***CCTCACCTGGGGTGCGTCACACCTGAGGAACGTGTGTG

GGCACCACCACTCGATAATATTACGCTGCCACGCTGGGTGTGTGTGTGTGTGTGTGTGT

GTGTGTGTGTGTGTGTGTGTGTGTGTGTGTGTGTGTGTGTGTGTGTGTGTGTGTGTGTG

TGTG<u>TATAATT</u>CTAGCTTTAGCAAA<u>AAATATATATATAAT</u>CAAA***AA***AAAAAAAAA

Figure 4.4. Three splice variants of the *Cm-Mstn* 3'UTR. Sequence #1 is 94 nucleotides long, sequence #2 is 281 nucleotides long, and sequence #3 is 287 nucleotides long. Sequences #2 and #3 are identical except for three nucleotide differences (italicized and bold), and one has a slightly longer poly-A tail. Underlined sequence include several putative poly(A) signals of the 3' UTR's.
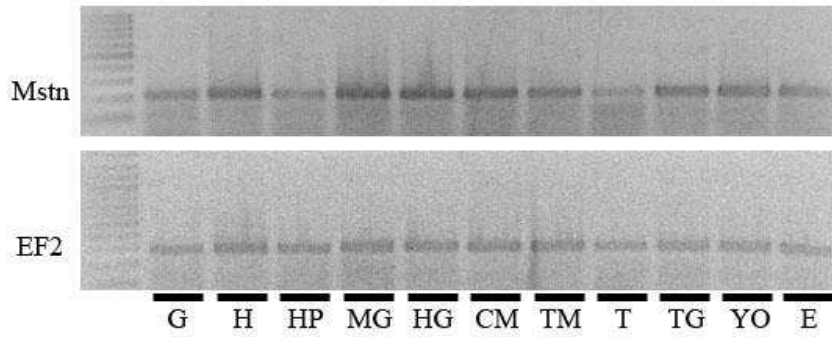
Figure 4.5. Expression of *Cm-Mstn* mRNA in *C. maenas* tissues using RT-PCR.
Expression of Mstn was highest in claw muscle (CM), thoracic muscle (Anderson et al.),
heart muscle (H) midgut muscle (MG), and hindgut muscle (HG). Thoracic ganglia (TG) and
Y-organ (YO) also showed strong expression of *Cm-Mstn*. Less *Cm-Mstn* mRNA was
detected in gill (G), hepatopancreas (Liu et al.), and eyestalk ganglia (E), with the lowest *Cm-
Mstn* mRNA level in the testes (T). Expression of EF2 was relatively consistent across all
tissues.
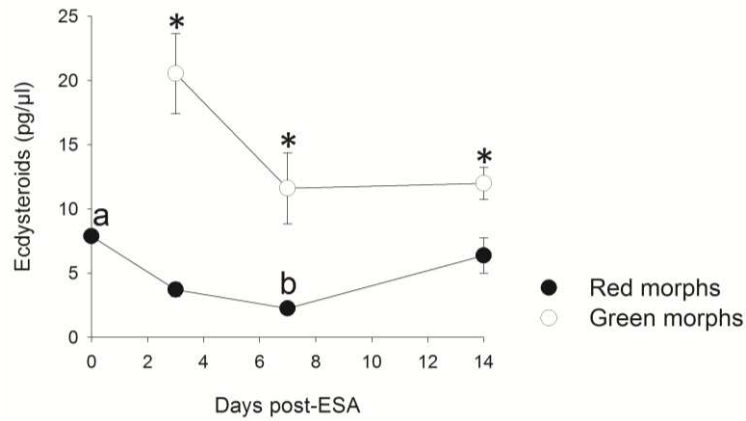
4.6. Ecdysteroid levels in the hemolymph during the short-term ESA experiment of green morph and red morph *C. maenas.* Ecdysteroids decreased by 7 days after ESA in the red morph crabs, but not in the green morph crabs. Different letters indicate significant differences among red morphs. Asterisks indicate significant differences between red morphs and green morphs. One Way ANOVA was used to test significant differences within a morph type (p < 0.05), and t-tests were used to test significant differences between morph types. (n = 6 for all groups, except n=5 for red morph day 7 and green morph day 14.)

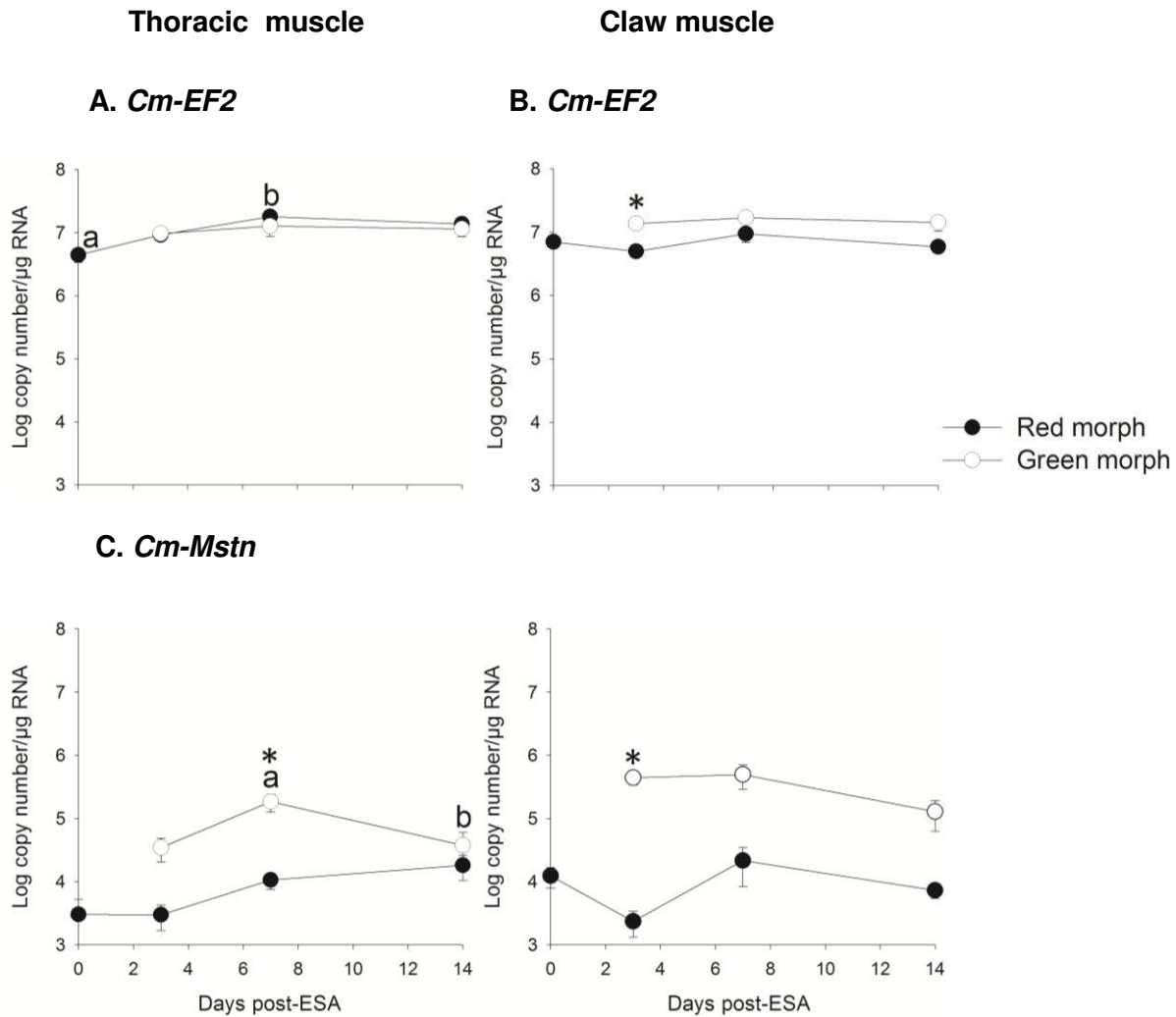**Thoracic muscle**   **Claw muscle**

A. *Cm-EF2*   **B.** *Cm-EF2*

C. *Cm-Mstn*

Fig. 4.7. After ESA, short-term *Cm-EF2* and Cm-*Mstn* mRNA expression in skeletal muscle of *C. maenas* red morphs and green morphs. The only change in mRNA expression from day zero controls was an increase in *Cm-EF2* in thoracic muscle at day 7 In red morphs. Differential expression between red morphs and green morphs occurred in thoracic muscle at day 7 with *Cm-Mstn,* and at day three with both *Cm-EF2* and *Cm-*Mstn. In each case, mRNA expression was higher in green morphs. Significant differences are indicated with different letters within a color morph, and with asterisks between color morphs. Significant differences were tested with a One Way ANOVA within morph types, and with t-tests between morph types (p < 0.05). (For *Cm-EF2*, n=5 or 6 for all groups. For *Cm-Mstn*, n=5 or 6 for all groups, except n=3 for day 0 thoracic muscle and n=4 for day 7 claw muscle).
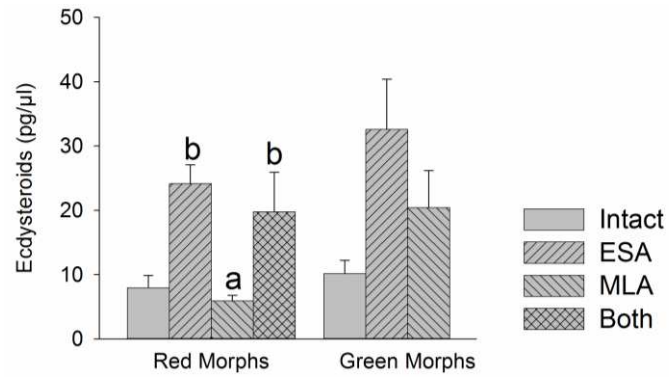
151

Fig. 4.8. Ecdysteroid levels in the hemolymph at 90 days post attempted molt induction. There were no significant ecdysteroid changes, compared to control, in any group. Different letters indicate significant differences between treatment groups. One Way ANOVA was used to test significant differences among morph type ($p < 0.05$). (For red morph animals, n=3 for intact, n=4 for ESA, n=5 for MLA, and n=4 for both MLA and ESA; for green morphs, n=6 to 17).

Thoracic muscle **Claw muscle**

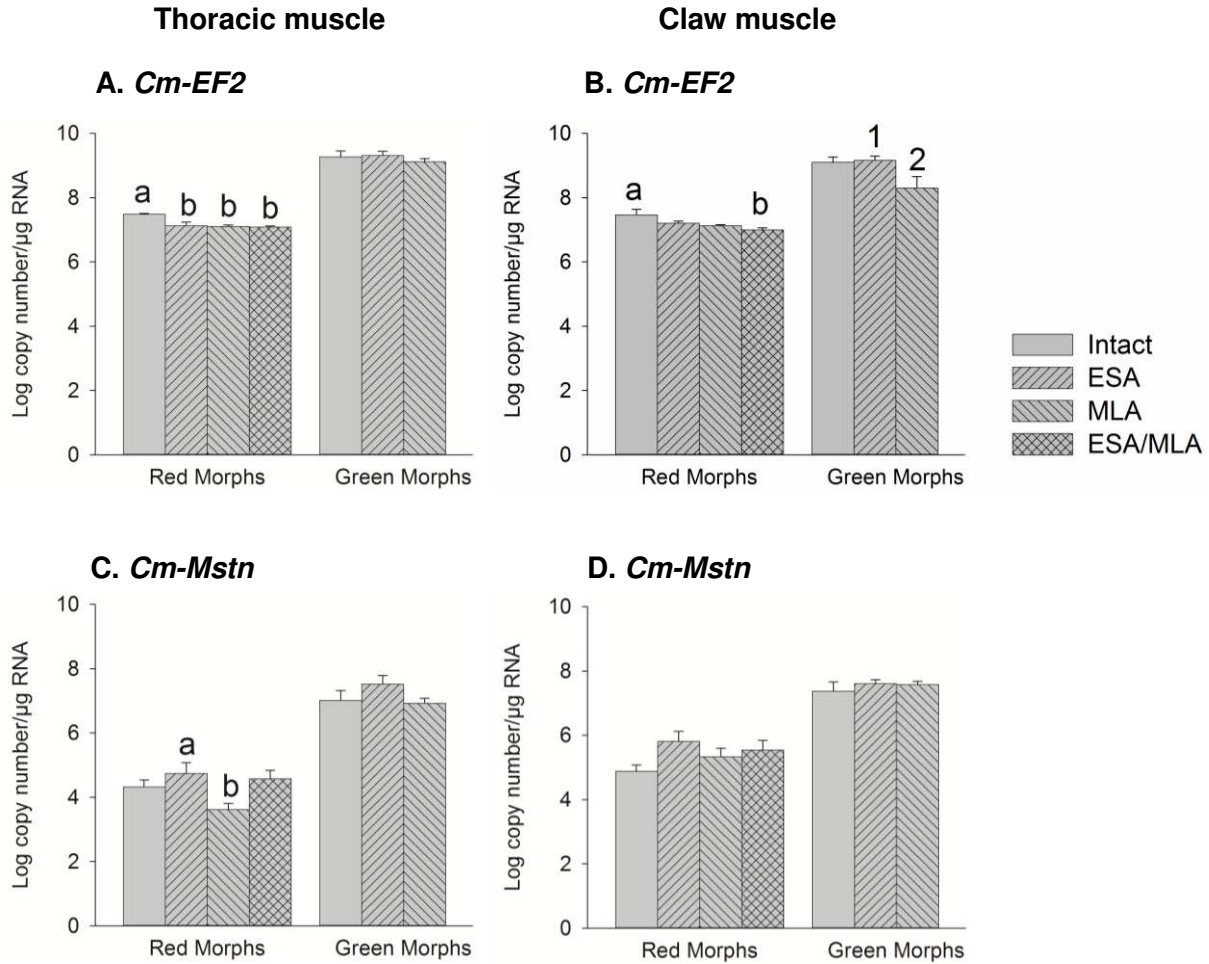**A.** *Cm-EF2* **B.** *Cm-EF2*

C. *Cm-Mstn* **D.** *Cm-Mstn*

Fig. 4.9. Long-term *Cm-EF2* and Cm-*Mstn* mRNA expression in the muscle of green morph and red morph *Carcinus maenas* 90 days after attempted molt induction. *Cm-EF2* expression in thoracic muscle was significantly decreased in all treatment groups, compared to intact animals in the green morphs, while *Cm-EF2* was only decreased in the treatment group of ESA and MLA together, compared to intact animals in green morph claw muscle. There were no significant changes, compared to intact animals, in *Cm-Mstn* gene expression. One Way ANOVA was used to test significant differences among morph type ($p < 0.05$). Different letters for red morphs and different numbers for green morphs indicate significant differences between molt stages. (For red morph animals, n=3 for intact, n=4 for ESA, n=5 for MLA, and n=4 for both MLA and ESA for both genes; for green morphs, n=6 to 17 for both genes).
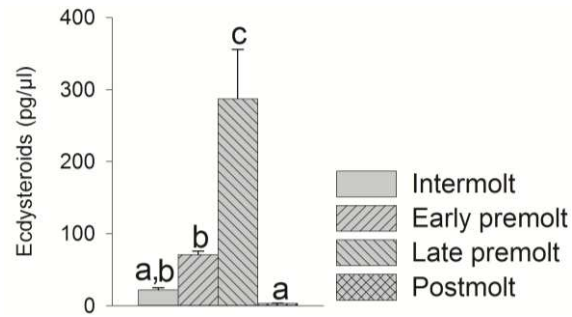
Fig. 4.10. Ecdysteroid levels in the hemolymph of naturally molting *Carcinus maenas* crabs. Ecdysteroid levels increased significantly during late premolt, then decreased significantly at postmolt. One Way ANOVA was used to test significant differences among molt stages ($p < 0.001$). Different letters indicate significant differences between molt stages. (Intermolt, n=6; early premolt, n=16; late premolt, n=8; and postmolt, n=7.)
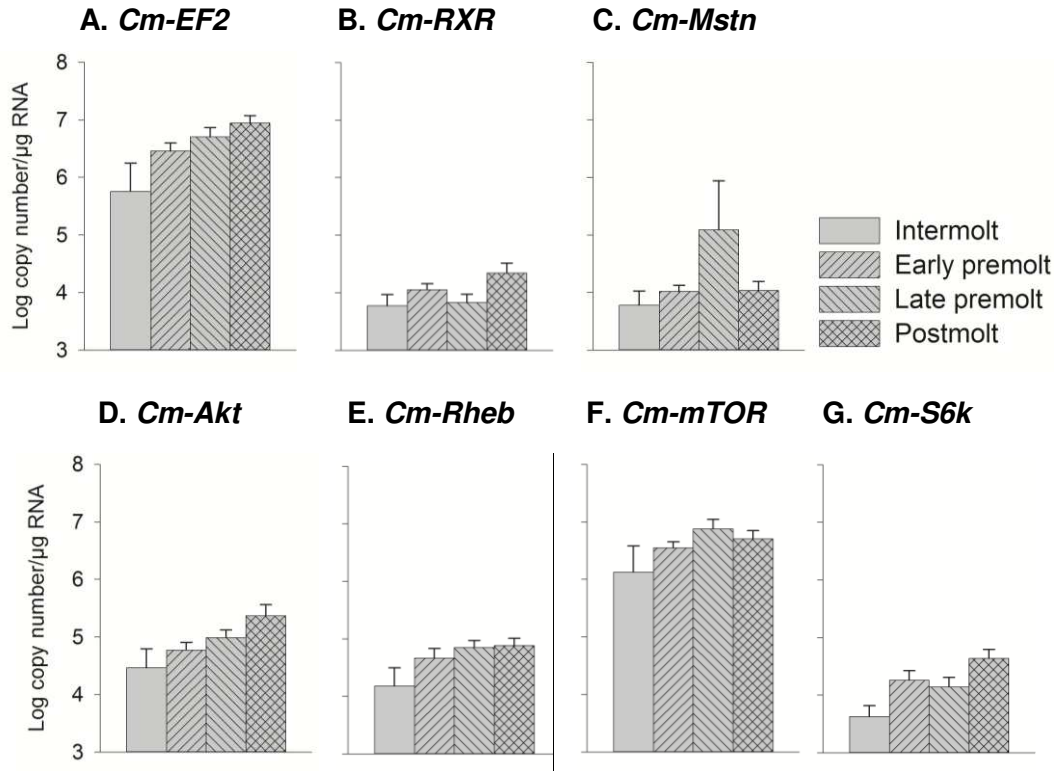
Fig. 4.11. Natural molt mRNA expression in the thoracic muscle of green morph *Carcinus maenas* **at different molt stages.** There were no significant differences in the mRNA expression of these genes. One Way ANOVA was used to test significant differences among molt stages (p=0.01). (Intermolt, n=6; Early premolt, n=15; Late premolt, n=8; and Postmolt, n=7 for all genes except early premolt for *Cm-RXR*, n=14).
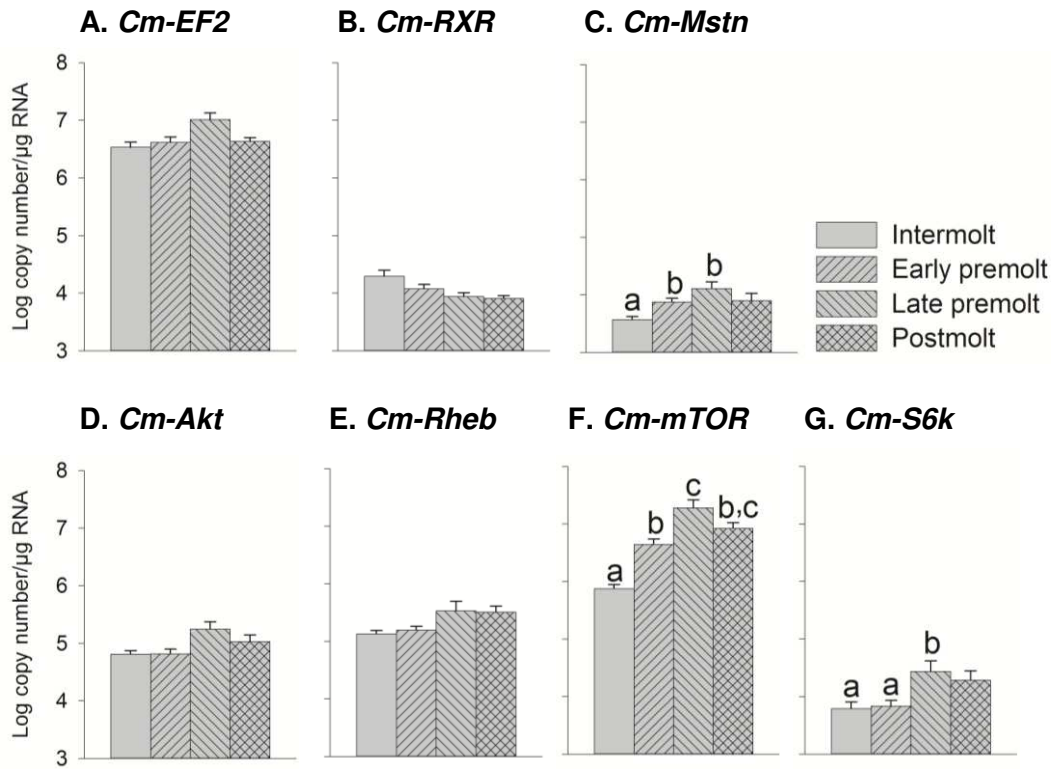
Fig. 4.12. Natural molt mRNA expression in the claw muscle of green morph *Carcinus maenas* at different molt stages. *Cm-Mstn*, *Cm-mTOR*, and *Cm-S6k* mRNA expression was all significantly increased in the claw muscle of premolt animals. By contrast, in thoracic muscle there were no significant changes in gene expression (Fig. 4.11). One Way ANOVA was used to test significant differences among molt stages (p=0.01). Different letters indicate significant differences between molt stages. (Intermolt, n=6; Early premolt, n=16; Late premolt, n=8; and Postmolt, n=7 for all genes except early premolt for *Cm-RXR*, n=15).

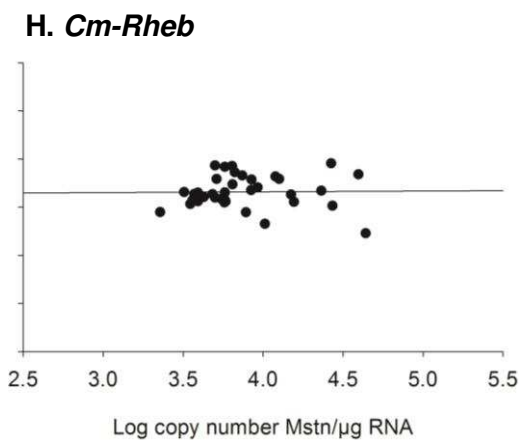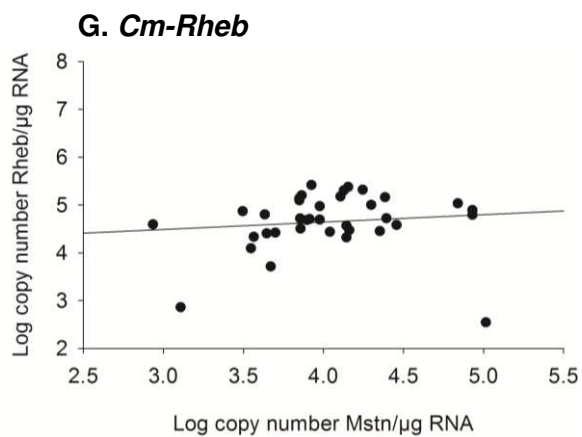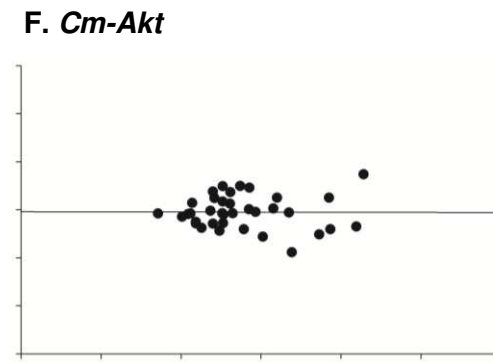**Thoracic muscle**   **Claw muscle**

A. *Cm-EF2*

B. *Cm-EF2*

C. *Cm-RXR*

D. *Cm-RXR*

E. *Cm-Akt*

F. *Cm-Akt*

G. *Cm-Rheb*

H. *Cm-Rheb*

Log copy number EF2/μg RNA

Log copy number RXR/μg RNA

Log copy number Akt/μg RNA

Log copy number Rheb/μg RNA

Log copy number Mstn/μg RNA

Thoracic muscle **Claw muscle**

I. *Cm-mTOR*

J. *Cm-mTOR*

K. *Cm-S6k*

L. *Cm-S6k*
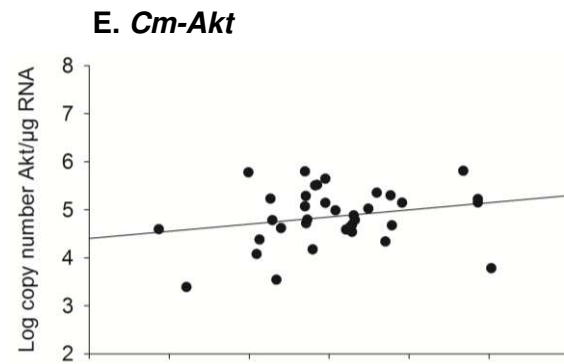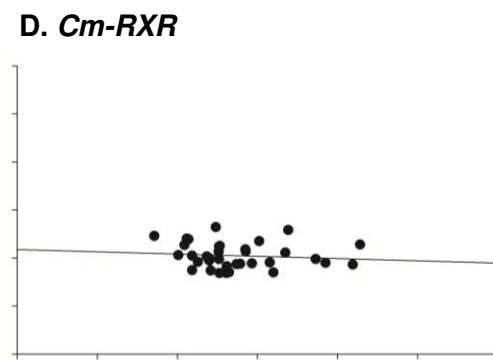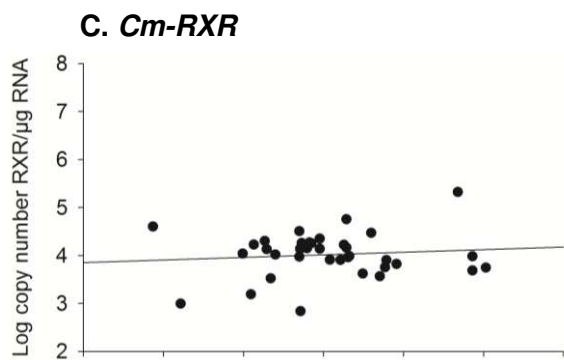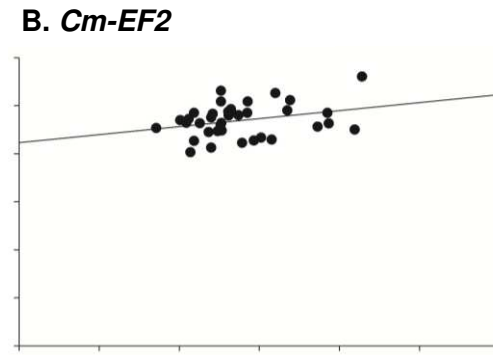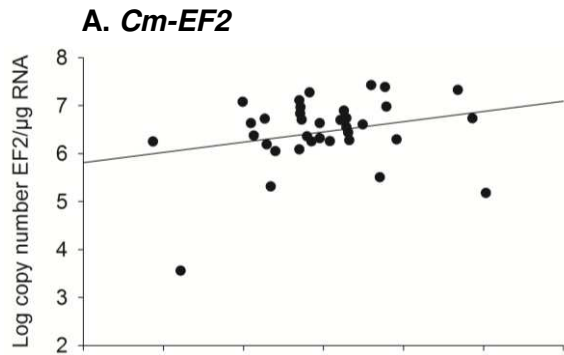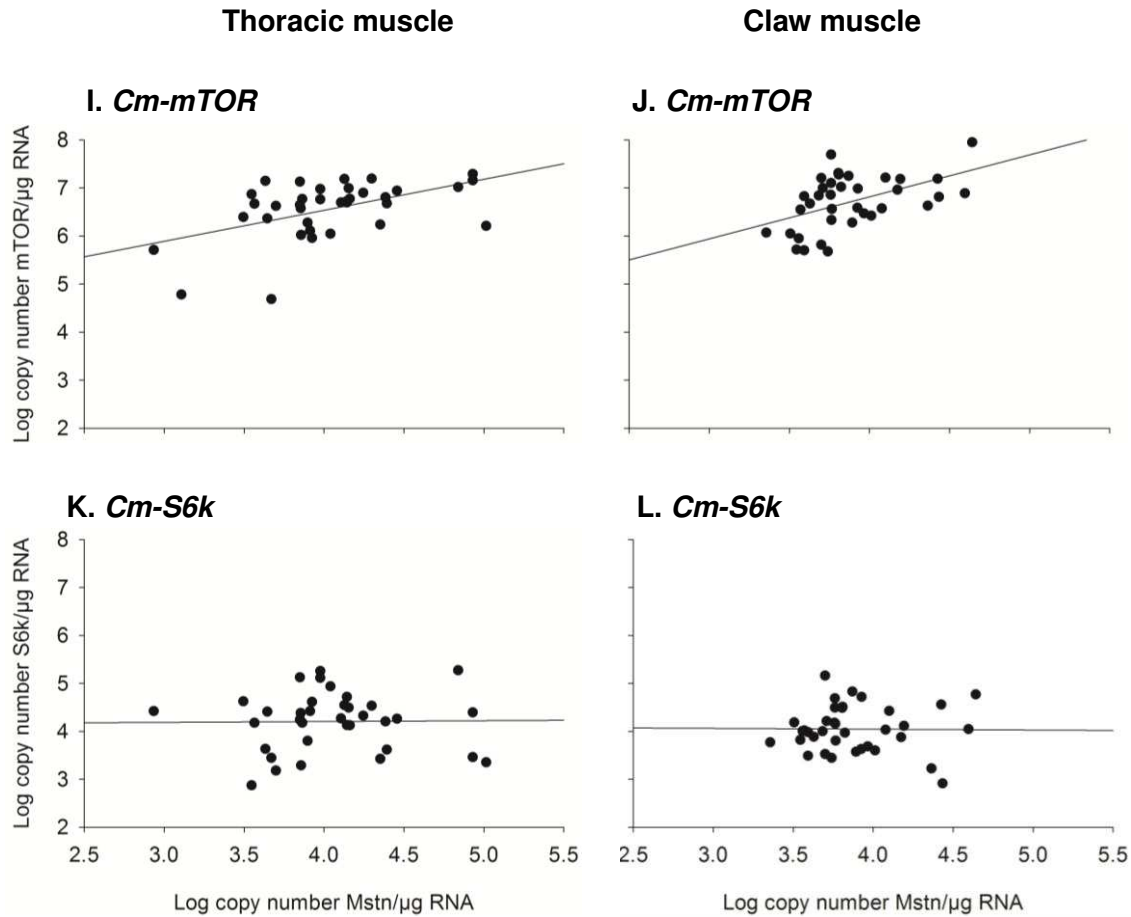
Fig. 4.13. *Cm-Mstn* mRNA expression correlated with all other genes tested in thoracic muscle and claw muscle of the naturally molting crabs. *Cm-Mstn* was positively correlated with *Cm-mTOR*, both in the thoracic muscle (p=0.002, R^2=0.251) and in the claw muscle (p=0.002, R^2=0.241). *Cm-Mstn* was not significantly correlated with any other gene tested in either muscle. p=0.01. (Thoracic muscle, n=37; claw muscle, n=36.)

158

Chapter 5

Summary and future directions

Regulation of crustacean Mstn expression by ecdysteroids appears to vary between tissues in the same species, and between species. In *G. lateralis*, there is a negative correlation between ecdysteroid levels and *Gl-Mstn* mRNA levels in the claw muscle. However, a direct regulation of Mstn through the ecdysteroid receptor and a putative EcRE in the *Gl-Mstn* promoter was not confirmed in this study. Ecdysteroids do not appear to regulate Mstn levels in either the thoracic muscle or limb bud muscle in *G. lateralis*. In *C. maenas*, ecdysteroids are not correlated with Mstn mRNA levels in either claw or thoracic muscle.

In the premolt claw closer muscle, which undergoes a dramatic increase in protein synthesis to prepare for rapid hypertrophy immediately after ecdysis, Mstn mRNA levels are positively correlated with mRNA levels of at least some components in the insulin/mTOR-dependent protein synthesis pathway in both *G. lateralis* and *C. maenas*. This indicates that in some situations of rapidly changing protein synthesis, Mstn has a role as a chalone to prevent excess protein synthesis in crustaceans, similar to the role of Mstn in vertebrates. However, in *G. lateralis* limb buds, Mstn mRNA levels remain extremely low, whether limb buds are rapidly growing or growth suspended. This indicates that Mstn is not involved in regulating protein synthesis in the limb buds.

Ecdysteroid levels were not correlated with mRNA levels of any of the components of the insulin/mTORC1-dependent protein synthesis pathway in the claw muscle of either *G. lateralis* or *C. maenas*. Mstn mRNA levels were moderately correlated with some mTOR pathway components in both species. However, multiple linear regression showed that the combination of ecdysteroid levels and Mstn mRNA levels was stronger than Mstn alone, in predicting the mRNA levels of some components of the pathway in both species. In *G. lateralis*, ecdysteroids and *Gl-Mstn* mRNA levels strongly predicted both *Gl-Rheb* and *Gl-S6k*. In *C. maenas*, ecdysteroids and *Cm-Mstn* mRNA levels moderately predicted *Cm-mTOR* mRNA

levels. This indicates that ecdysteroids, Mstn and mTOR pathway components are all involved in regulating protein synthesis in the claw muscle of both species.

We determined that the *Gl-Mstn* upstream sequence that we obtained with DNA walking is a functional promoter in a heterologous ecdysteroid cell system in mammalian cells. However, we were not able to determine if ecdysteroids directly control *Gl-Mstn* promoter activity through a putative EcRE located in the *Gl-Mstn* promoter.

Further development of the heterologous ecdysteroid cell system is recommended to determine whether ecdysteroids directly regulate *Gl-Mstn* promoter activity through the putative EcRE. First, the A/B domains of both RXR and EcR can be inhibitory in heterologous cell systems (Betanska et al., 2009; Mouillet et al., 2001; No et al., 1996; Palli et al., 2003). The A/B domains should be replaced with the activator domain of virus protein 16 in the herpes simplex virus to determine if the A/B domains inhibited ecdysteroid interactions with the Mstn promoter. Another change could be using *G. lateralis* RXR and EcR, rather than *U. pugilator* RXR and EcR, as the small differences between the two species could affect ecdysteroid interactions with the Mstn promoter. A different expression plasmid could be used to carry the RXR and EcR DNA sequence, as the pGL3 plasmid, itself, contains a sequence that could possibly be recognized by the ecdysteroid receptor. A different line of mammalian cells, or different ecdysteroids, such as murine A or a synthetic ecdysteroid could be used to attempt to develop the heterologous cell system into a functional system for ecdysteroid signaling through the *Gl-Mstn* promoter.

References

Abdollah, S., Macias-Silva, M., Tsukazaki, T., Hayashi, H., Attisano, L. and Wrana, J. L. (1997). T beta RI phosphorylation of Smad2 on Ser(465) and Ser(467) is required for Smad2-Smad4 complex formation and signaling. *J. Biol. Chem.* **272**, 27678-27685.

Abraham, R. T. (1996). Phosphatidylinositol 3-kinase related kinases. *Curr. Opin. Immunol.* **8**, 412-418.

Abramowitz, R. K. and Abramowitz, A. A. (1940). Moulting, growth, and survival after eyestalk removal in *Uca pugilator. Biol. Bull.* **78**, 179-188.

Abuhagr, A. M., Blindert, J. L., Nimitkul, S., Zander, I. A., LaBere, S. M., Chang, S. A., MacLea, K. S., Chang, E. S. and Mykles, D. L. (2014a). Molt regulation in green and red color morphs of the crab Carcinus maenas: gene expression of molt-inhibiting hormone signaling components. *J. Exp. Biol.* **217**, 796-808.

Abuhagr, A. M., Maclea, K. S., Chang, E. S. and Mykles, D. L. (2014b). Mechanistic target of rapamycin (mTOR) signaling genes in decapod crustaceans: Cloning and tissue expression of mTOR, Akt, Rheb, and p70 S6 kinase in the green crab, *Carcinus maenas*, and blackback land crab, *Gecarcinus lateralis. Comp Biochem Physiol A Mol Integr Physiol* **168**, 25-39.

Adegoke, O. A., Abdullahi, A. and Tavajohi-Fini, P. (2012). mTORC1 and the regulation of skeletal muscle anabolism and mass. *Appl. Physiol. Nutr. Metab.* **37**, 395-406.

Agrawal, R. K., Penczek, P., Grassucci, R. A., Li, Y. H., Leith, A., Nierhaus, K. H. and Frank, J. (1996). Direct visualization of A-, P-, and E-site transfer RNAs in the Escherichia coli ribosome. *Science* **271**, 1000-1002.

Aguilar, V., Alliouachene, S., Sotiropoulos, A., Sobering, A., Athea, Y., Djouadi, F., Miraux, S., Thiaudiere, E., Foretz, M., Viollet, B. et al. (2007). S6 kinase deletion suppresses muscle growth adaptations to nutrient availability by activating AMP kinase. *Cell metabolism* **5**, 476-487.

Aguirre, V., Uchida, T., Yenush, L., Davis, R. and White, M. F. (2000). The c-Jun NH2-terminal kinase promotes insulin resistance during association with insulin receptor substrate-1 and phosphorylation of Ser(307). *J. Biol. Chem.* **275**, 9047-9054.

Alayev, A. and Holz, M. K. (2013). mTOR signaling for biological control and cancer. *Journal of cellular physiology* **228**, 1658-1664.

Alessi, D. R., Andjelkovic, M., Caudwell, B., Cron, P., Morrice, N., Cohen, P. and Hemmings, B. A. (1996). Mechanism of activation of protein kinase B by insulin and IGF-1. *EMBO J.* **15**, 6541-6551.

Alessi, D. R., Kozlowski, M. T., Weng, Q. P., Morrice, N. and Avruch, J. (1998). 3 Phosphoinositide-dependent protein kinase 1 (PDK1) phosphorylates and activates the p70 S6 kinase in vivo and in vitro. *Curr. Biol.* **8**, 69-81.

Allen, D. L., Bandstra, E. R., Harrison, B. C., Thorng, S., Stodieck, L. S., Kostenuik, P. J., Morony, S., Lacey, D. L., Hammond, T. G., Leinwand, L. L. et al. (2009). Effects of spaceflight on murine skeletal muscle gene expression. *J Appl Physiol (1985)* **106**, 582-595.

Allen, D. L. and Du, M. (2008). Comparative functional analysis of the cow and mouse myostatin genes reveals novel regulatory elements in their upstream promoter regions. *Comparative Biochemistry and Physiology Part B: Biochemistry and Molecular Biology* **150**, 432-439.

Allen, D. L. and Loh, A. S. (2011). Posttranscriptional mechanisms involving microRNA-27a and b contribute to fast-specific and glucocorticoid-mediated myostatin expression in skeletal muscle. *American Journal of Physiology-Cell Physiology* **300**, C124-C137.

Amaldi, F. and Pierandrei-Amaldi, P. (1997). TOP genes: a translationally controlled class of genes including those coding for ribosomal proteins. In *Cytoplasmic fate of messenger RNA*, pp. 1-17: Springer.

Amali, A. A., Lin, C. J., Chen, Y. H., Wang, W. L., Gong, H. Y., Lee, C. Y., Ko, Y. L., Lu, J. K., Her, G. M., Chen, T. T. et al. (2004). Up-regulation of muscle-specific transcription factors during embryonic somitogenesis of zebrafish (*Danio rerio*) by knock-down of myostatin-1. *Dev. Dyn.* **229**, 847-856.

Amirouche, A., Durieux, A. C., Banzet, S., Koulmann, N., Bonnefoy, R., Mouret, C., Bigard, X., Peinnequin, A. and Freyssenet, D. (2009). Down-regulation of Akt/mammalian target of rapamycin signaling pathway in response to myostatin overexpression in skeletal muscle. *Endocrinology* **150**, 286-294.

Amthor, H., Otto, A., Vulin, A., Rochat, A., Dumonceaux, J., Garcia, L., Mouisel, E., Hourde, C., Macharia, R., Friedrichs, M. et al. (2009). Muscle hypertrophy driven by myostatin blockade does not require stem/precursor-cell activity. *Proceedings of the National Academy of Sciences of the United States of America* **106**, 7479-7484.

Anderson, S. B., Goldberg, A. L. and Whitman, M. (2008). Identification of a novel pool of extracellular pro-myostatin in skeletal muscle. *J. Biol. Chem.* **283**, 7027-7035.

Andrade, M. A. and Bork, P. (1995). HEAT repeats in the Huntingtons-disease protein. *Nat. Genet.* **11**, 115-116.

Antoniewski, C., Laval, M. and Lepesant, J. A. (1993). Structural features critical to the activity of an ecdysone receptor-binding site. *Insect Biochem. Mol. Biol.* **23**, 105-114.

Antoniewski, C., Mugat, B., Delbac, F. and Lepesant, J. A. (1996). Direct repeats bind the EcR/USP receptor and mediate ecdysteroid responses in *Drosophila melanogaster. Mol. Cell. Biol.* **16**, 2977-2986.

Apone, S. and Hauschka, S. D. (1995). Muscle gene e-box control elements: Evidence for quantitatively different transcriptional activities and the binding of distinct regulatory factors. *J. Biol. Chem.* **270**, 21420-21427.

Aramburu, J., Carmen Ortells, M., Tejedor, S., Buxade, M. and Lopez-Rodriguez, C. (2014). Transcriptional regulation of the stress response by mTOR. *Science signaling* **7**.

Argadine, H. M., Hellyer, N. J., Mantilla, C. B., Zhan, W.-Z. and Sieck, G. C. (2009). The effect of denervation on protein synthesis and degradation in adult rat diaphragm muscle. *J. Appl. Physiol.* **107**, 438-444.

Argadine, H. M., Mantilla, C. B., Zhan, W.-Z. and Sieck, G. C. (2011). Intracellular signaling pathways regulating net protein balance following diaphragm muscle denervation. *American Journal of Physiology-Cell Physiology* **300**, C318-C327.

Atherton, P. J., Babraj, J. A., Smith, K., Singh, J., Rennie, M. J. and Wackerhage, H. (2005). Selective activation of AMPK-PGC-1 alpha or PKB-TSC2-mTOR signaling can explain specific adaptive responses to endurance or resistance training-like electrical muscle stimulation. *FASEB J.* **19**, 786-+.

Aumais, J. P., Lee, H. S., DeGannes, C., Horsford, J. and White, J. H. (1996). Function of directly repeated half-sites as response elements for steroid hormone receptors. *J. Biol. Chem.* **271**, 12568-12577.

Bai, X., Ma, D., Liu, A., Shen, X., Wang, Q. J., Liu, Y. and Jiang, Y. (2007). Rheb activates mTOR by antagonizing its endogenous inhibitor, FKBP38. *Science* **318**, 977-980.

Baird, F. E., Bett, K. J., MacLean, C., Tee, A. R., Hundal, H. S. and Taylor, P. M. (2009). Tertiary active transport of amino acids reconstituted by coexpression of System A and L transporters in Xenopus oocytes. *American Journal of Physiology-Endocrinology and Metabolism* **297**, E822-E829.

Bar-Peled, L., Chantranupong, L., Cherniack, A. D., Chen, W. W., Ottina, K. A., Grabiner, B. C., Spear, E. D., Carter, S. L., Meyerson, M. and Sabatini, D. M. (2013). A Tumor

suppressor complex with GAP activity for the Rag GTPases that signal amino acid sufficiency to mTORC1. *Science* **340**, 1100-1106.

Bar-Peled, L., Schweitzer, L. D., Zoncu, R. and Sabatini, D. M. (2012). Ragulator Is a GEF for the Rag GTPases that Signal Amino Acid Levels tomTORC1. *Cell* **150**, 1196-1208.

Barbet, N. C., Schneider, U., Helliwell, S. B., Stansfield, I., Tuite, M. F. and Hall, M. N. (1996). TOR controls translation initiation and early G1 progression in yeast. *Molecular Biology of the Cell* **7**, 25-42.

Baretic, D. and Williams, R. L. (2014). The structural basis for mTOR function. *Semin. Cell Dev. Biol.* **36**, 91-101.

Barfod, N. M. and Bichel, P. (1976). Characterization of a G1 inhibitor from old JB-1 ascites tumor fluid - interaction with polyions and ion-exchangers. *Virchows Archiv B-Cell Pathology Including Molecular Pathology* **21**, 249-258.

Bargis-Surgey, P., Lavergne, J. P., Gonzalo, P., Vard, C., Filhol-Cochet, O. and Reboud, J. P. (1999). Interaction of elongation factor eEF-2 with ribosomal P proteins. *Eur. J. Biochem.* **262**, 606-611.

Bassel-Duby, R. and Olson, E. N. (2006). Signaling pathways in skeletal muscle remodeling. In *Annu. Rev. Biochem.*, vol. 75, pp. 19-37.

Beatty, J., Fauth, T., Callender, J. L., Spindler-Barth, M. and Henrich, V. C. (2006). Analysis of transcriptional activity mediated by *Drosophila melanogaster* ecdysone receptor isoforms in a heterologous cell culture system. *Insect Mol. Biol.* **15**, 785-795.

Beck, A., Moeschel, K., Deeg, M., Haring, H. U., Voelter, W., Schleicher, E. D. and Lehmann, R. (2003). Identification of an in vitro insulin receptor substrate-1 phosphorylation site by negative-ion mu LC/ES-API-CID-MS hybrid scan technique. *J. Am. Soc. Mass Spectrom.* **14**, 401-405.

Beckmann, H., Chen, J. L., Obrien, T. and Tjian, R. (1995). Coactivator and promoter-selective properties of RNA-polymerase-I TAFS. *Science* **270**, 1506-1509.

Betanska, K., Czogalla, S., Spindler-Barth, M. and Spindler, K. D. (2009). Influence of cell cycle on ecdysteroid receptor in CHO-K1 cells. *Arch. Insect Biochem. Physiol.* **72**, 142-153.

Bichel, P. (1973). Self-limitation of ascites tumor growth - possible chalone regulation. *National Cancer Institute Monographs*, 197-203.

Bliss, D. E. (1956). Neurosecretion and the control of growth in a decapod crustacean. In *Bertil Hanström; Zoological Papers in Honour of his Sixty-fifth Birthday*, (ed. K. G. Wingstrand), pp. 56-75. Lund, Sweden: Zoological Institute.

Bliss, D. E. (1979). From sea to tree - Saga of a land crab. *Am. Zool.* **19**, 385-410.

Bliss, D. E. and Boyer, J. R. (1964). Environmental regulation of growth in the decapod crustacean *Gecarcinus lateralis. Gen. Comp. Endocrinol.* **4**, 15-41.

Bodine, S. and Furlow, J. D. (2015). Glucocorticoids and Skeletal Muscle. In *Glucocorticoid Signaling*, vol. 872 eds. J.-C. Wang and C. Harris), pp. 145-176: Springer New York.

Bodine, S. C., Latres, E., Baumhueter, S., Lai, V. K. M., Nunez, L., Clarke, B. A., Poueymirou, W. T., Panaro, F. J., Na, E. Q., Dharmarajan, K. et al. (2001). Identification of ubiquitin ligases required for skeletal muscle atrophy. *Science* **294**, 1704-1708.

Boldingh, W. H. and Laurence, E. B. (1968). Extraction purification and preliminary characterisation of the epidermal chalone - a tissue specific mitotic inhibitor obtained from vertebrate skin. *Eur. J. Biochem.* **5**, 191-&.

Bolster, D. R., Crozier, S. J., Kimball, S. R. and Jefferson, L. S. (2002). AMP-activated protein kinase suppresses protein synthesis in rat skeletal muscle through down-regulated mammalian target of rapamycin (mTOR) signaling. *J. Biol. Chem.* **277**, 23977-23980.

Bosotti, R., Isacchi, A. and Sonnhammer, E. L. L. (2000). FAT: a novel domain in PIK-related kinases. *Trends Biochem. Sci.* **25**, 225-227.

Boudeau, J., Baas, A. F., Deak, M., Morrice, N. A., Kieloch, A., Schutkowski, M., Prescott, A. R., Clevers, H. C. and Alessi, D. R. (2003). MO25 alpha/beta interact with STRAD alpha/beta enhancing their ability to bind, activate and localize LKB1 in the cytoplasm. *EMBO J.* **22**, 5102-5114.

Bouzakri, K., Roques, M., Gual, P., Espinosa, S., Guebre-Egziabher, F., Riou, J. P., Laville, M., Le Marchand-Brustel, Y., Tanti, J. F. and Vidal, H. (2003). Reduced activation of phosphatidylinositol-3 kinase and increased serine 636 phosphorylation of insulin receptor substrate-1 in primary culture of skeletal muscle cells from patients with type 2 diabetes. *Diabetes* **52**, 1319-1325.

Brandt, R. and Grosse, R. (1992). Purification of a mammary-derived growth inhibitor (MDGI) related polypeptide expressed during pregnancy. *Biochem. Biophys. Res. Commun.* **189**, 406-413.

Braulke, L., Heldmaier, G., Berriel Diaz, M., Rozman, J. and Exner, C. (2010). Seasonal changes of myostatin expression and its relation to body mass acclimation in the Djungarian hamster, Phodopus sungorus. *Journal of Experimental Zoology Part A: Ecological Genetics and Physiology* **313**, 548-556.

Braun, T. P. and Marks, D. L. (2015). The regulation of muscle mass by endogenous glucocorticoids. *Frontiers in physiology* **6**.

Browdy, C. and Samocha, T. (1985). The effect of eyestalk ablation on spawning, molting and mating of Penaeus semisulcatus de Haan. *Aquaculture* **49**, 19-29.

Brown, E. J., Beal, P. A., Keith, C. T., Chen, J., Shin, T. B. and Schreiber, S. L. (1995). Control of p70 S6 kinase by kinase-activity of FRAP in-vivo. *Nature* **377**, 441-446.

Bruce, D. L. and Sapkota, G. P. (2012). Phosphatases in SMAD regulation. *FEBS Lett.* **586**, 1897-1905.

Brugal, G. and Pelmont, J. (1975). Existence of 2 chalone-like substances in intestinal extract from adult newt, inhibiting embryonic intestinal cell-proliferation. *Cell and Tissue Kinetics* **8**, 171-187.

Brunn, G. J., Fadden, P., Haystead, T. A. J. and Lawrence, J. C. (1997a). The mammalian target of rapamycin phosphorylates sites having a (Ser/Thr)-Pro motif and is activated by antibodies to a region near its COOH terminus. *J. Biol. Chem.* **272**, 32547-32550.

Brunn, G. J., Hudson, C. C., Sekulic, A., Williams, J. M., Hosoi, H., Houghton, P. J., Lawrence, J. C. and Abraham, R. T. (1997b). Phosphorylation of the translational repressor PHAS-I by the mammalian target of rapamycin. *Science* **277**, 99-101.

Buday, L. and Downward, J. (1993). Epidermal growth factor regulates p21 ras through the formation of a complex of receptor, Grb2 adapter protein, and Sos nucleotide exchange factor. *Cell* **73**, 611-620.

Bullough, W., Hewett, C. and Laurence, E. B. (1964). The epidermal chalone: a preliminary attempt at isolation. *Exp. Cell Res.* **36**, 192-200.

Bullough, W. and Laurence, E. B. (1964). Mitotic control by internal secretion: the role of the chalone-adrenalin complex. *Exp. Cell Res.* **33**, 176-194.

Bullough, W. S. (1962). Control of mitotic activity in adult mammalian tissues. *Biol. Rev. Camb. Philos. Soc.* **37**, 307-342.

Bullough, W. S. (1965). Mitotic and functional homeostasis - a speculative review. *Cancer Res.* **25**, 1683-1727.

Burnett, P. E., Barrow, R. K., Cohen, N. A., Snyder, S. H. and Sabatini, D. M. (1998). RAFT1 phosphorylation of the translational regulators p70 S6 kinase and 4E-BP1. *Proceedings of the National Academy of Sciences of the United States of America* **95**, 1432-1437.

Byfield, M. P., Murray, J. T. and Backer, J. M. (2005). hVps34 is a nutrient-regulated lipid kinase required for activation of p70 S6 kinase. *J. Biol. Chem.* **280**, 33076-33082.

Cai, J. C., Fang, L. S., Huang, Y. B., Li, R., Yuan, J., Yang, Y., Zhu, X., Chen, B. X., Wu, J. H. and Li, M. F. (2013). miR-205 Targets PTEN and PHLPP2 to Augment AKT Signaling and Drive Malignant Phenotypes in Non-Small Cell Lung Cancer. *Cancer Res.* **73**, 5402-5415.

Cai, S. L., Tee, A. R., Short, J. D., Bergeron, J. M., Kim, J., Shen, J. J., Guo, R. F., Johnson, C. L., Kiguchi, K. and Walker, C. L. (2006). Activity of TSC2 is inhibited by AKT-mediated phosphorylation and membrane partitioning. *J. Cell Biol.* **173**, 279-289.

Cantley, L. C. (2002). The phosphoinositide 3-kinase pathway. *Science* **296**, 1655-1657.

Carbone, J. W., McClung, J. P. and Pasiakos, S. M. (2012). Skeletal muscle responses to negative energy balance: effects of dietary protein. *Advances in Nutrition: An International Review Journal* **3**, 119-126.

Carling, D., Clarke, P. R., Zammit, V. A. and Hardie, D. G. (1989). Purification and characterization of the AMP-activated protein-kinase: copurification of acetyl-coA carboxylase kinase and 3-hydroxy-3-methylglutaryl-coA reductase kinase-activities. *Eur. J. Biochem.* **186**, 129-136.

Carlisle, D. (1957). On the hormonal inhibition of moulting in Decapod Crustacea II. The terminal anecdysis in crabs. *J. Mar. Biol. Assoc. U.K.* **36**, 291-307.

Carlson, C. J., White, M. F. and Rondinone, C. M. (2004). Mammalian target of rapamycin regulates IRS-1 serine 307 phosphorylation. *Biochem. Biophys. Res. Commun.* **316**, 533-539.

Carninci, P., Sandelin, A., Lenhard, B., Katayama, S., Shimokawa, K., Ponjavic, J., Semple, C. A., Taylor, M. S., Engström, P. G. and Frith, M. C. (2006). Genome-wide analysis of mammalian promoter architecture and evolution. *Nat. Genet.* **38**, 626-635.

Caron, E., Ghosh, S., Matsuoka, Y., Ashton-Beaucage, D., Therrien, M., Lemieux, S., Perreault, C., Roux, P. P. and Kitano, H. (2010). A comprehensive map of the mTOR signaling network. *Mol. Syst. Biol.* **6**.

Carpenter, G., King, L. and Cohen, S. (1979). Rapid enhancement of protein phosphorylation in A-431 cell membrane preparations by epidermal growth factor. *J. Biol. Chem.* **254**, 4884-4891.

Carpentier, J. L. (1993). The journey of the insulin-receptor into the cell - from cellular biology to pathophysiology. *Histochemistry* **100**, 169-184.

Carpentier, J. L. (1994). Insulin-receptor internalization - molecular mechanisms and physiopathological implications. *Diabetologia* **37**, S117-S124.

Carriere, A., Romeo, Y., Acosta-Jaquez, H. A., Moreau, J., Bonneil, E., Thibault, P., Fingar, D. C. and Roux, P. P. (2011). ERK1/2 Phosphorylate Raptor to Promote Ras-dependent Activation of mTOR Complex 1 (mTORC1). *J. Biol. Chem.* **286**, 567-577.

Ceccarelli, E., McGrew, M. J., Nguyen, T., Grieshammer, U., Horgan, D., Hughes, S. H. and Rosenthal, N. (1999). An E box comprises a positional sensor for regional differences in skeletal muscle gene expression and methylation. *Dev. Biol.* **213**, 217-229.

Chan, S.-M., Rankin, S. M. and Keeley, L. L. (1990). Effects of 20-hydroxyecdysone injection and eyestalk ablation on the moulting cycle of the shrimp, Penaeus vannamei. *Comparative Biochemistry and Physiology Part A: Physiology* **96**, 205-209.

Chan, T. O., Rittenhouse, S. E. and Tsichlis, P. N. (1999). AKT/PKB and other D3 phosphoinositide-regulated kinases: Kinase activation by phosphoinositide-dependent phosphorylation. *Annu. Rev. Biochem.* **68**, 965-1014.

Chandler, J. C., Aizen, J., Elizur, A., Hollander-Cohen, L., Battaglene, S. C. and Ventura, T. (2015). Discovery of a novel insulin-like peptide and insulin binding proteins in the Eastern rock lobster Sagmariasus verreauxi. *Gen. Comp. Endocrinol.* **215**, 76-87.

Chang, E. S. and Bruce, M. J. (1980). Ecdysteroid titers of juvenile lobsters following molt induction. *J. Exp. Zool.* **214**, 157-160.

Chang, E. S. and Mykles, D. L. (2011). Regulation of crustacean molting: A review and our perspectives. *Gen. Comp. Endocrinol.* **172**, 323-330.

Chang, E. S., Sage, B. A. and Oconnor, J. D. (1976). Qualitative and quantitative determinations of ecdysones in tissues of crab, *Pachygrapsus crassipes*, following molt induction. *Gen. Comp. Endocrinol.* **30**, 21-33.

Chantranupong, L., Wolfson, R. L. and Sabatini, D. M. (2015). Nutrient-Sensing Mechanisms across Evolution. *Cell* **161**, 67-83.

Chaudhuri, J., Chowdhury, D. and Maitra, U. (1999). Distinct functions of eukaryotic translation initiation factors eIF1A and eIF3 in the formation of the 40 S ribosomal preinitiation complex. *J. Biol. Chem.* **274**, 17975-17980.

Chaulet, A., Medesani, D. A., Freitas, J., Cervino, A., Cervino, N. and Rodriguez, E. M. (2012). Induction of somatic growth in juvenile crayfish Cherax quadricarinatus (Decapoda, Parastacidae), by ecdysone and insulin growth factor. *Aquaculture* **370**, 1-6.

Chauvin, C., Koka, V., Nouschi, A., Mieulet, V., Hoareau-Aveilla, C., Dreazen, A., Cagnard, N., Carpentier, W., Kiss, T., Meyuhas, O. et al. (2014). Ribosomal protein S6 kinase activity controls the ribosome biogenesis transcriptional program. *Oncogene* **33**, 474-483.

Chen, J., Zheng, X. F., Brown, E. J. and Schreiber, S. L. (1995). Identification of an 11-kDa FKBP12-rapamycin-binding domain within the 289-kDa FKBP12-rapamycin-associated protein and characterization of a critical serine residue. *Proceedings of the National Academy of Sciences of the United States of America* **92**, 4947-4951.

Chen, X., Huang, Z., Chen, D., Yang, T. and Liu, G. (2013). MicroRNA-27a Is Induced by Leucine and Contributes to Leucine-Induced Proliferation Promotion in C2C12 Cells. *International Journal of Molecular Sciences* **14**, 14076-14084.

Cheng, S. W., Fryer, L. G., Carling, D. and Shepherd, P. R. (2004). Thr2446 is a novel mammalian target of rapamycin (mTOR) phosphorylation site regulated by nutrient status. *J. Biol. Chem.* **279**, 15719-15722.

Cherbas, L., Lee, K. and Cherbas, P. (1991). Identification of ecdysone response elements by analysis of the *Drosophila* EIP28/29 gene. *Genes Dev.* **5**, 120-131.

Cheung, P. C. F., Salt, I. P., Davies, S. P., Hardie, D. G. and Carling, D. (2000). Characterization of AMP-activated protein kinase gamma-subunit isoforms and their role in AMP binding. *Biochem. J.* **346**, 659-669.

Chien, Y.-H., Han, D.-S., Hwu, W.-L., Thurberg, B. L. and Yang, W.-S. (2013). Myostatin and insulin-like growth factor I: potential therapeutic biomarkers for pompe disease. *PloS one* **8**, e71900.

Chiu, M. I., Katz, H. and Berlin, V. (1994). RAPT1, A MAMMALIAN HOMOLOG OF YEAST TOR, INTERACTS WITH THE FKBP12 RAPAMYCIN COMPLEX. *Proceedings of the National Academy of Sciences of the United States of America* **91**, 12574-12578.

Choo, A. Y., Kim, S. G., Heiden, M. G. V., Mahoney, S. J., Vu, H., Yoon, S. O., Cantley, L. C. and Blenis, J. (2010). Glucose Addiction of TSC Null Cells Is Caused by Failed

mTORC1-Dependent Balancing of Metabolic Demand with Supply. *Mol. Cell* **38**, 487-499.

Chopra, D. P. and Simnett, J. D. (1969). Demonstration of an organ-specific mitotic inhibitor in amphibian kidney . Effects of adult X*enopus* tissue extracts on mitotic rate of embryonic tissue (in-vitro). *Exp. Cell Res.* **58**, 319-&.

Christopherson, K. S., Mark, M. R., Bajaj, V. and Godowski, P. J. (1992). Ecdysteroid-dependent regulation of genes in mammalian-cells by a D*rosophila* ecdysone receptor and chimeric transactivators. *Proceedings of the National Academy of Sciences of the United States of America* **89**, 6314-6318.

Chung, A. C. K., Durica, D. S., Clifton, S. W., Roe, B. A. and Hopkins, P. M. (1998). Cloning of crustacean ecdysteroid receptor and retinoid-X receptor gene homologs and elevation of retinoid-X receptor mRNA by retinoic acid. *Mol. Cell. Endocrinol.* **139**, 209-227.

Chung, J. S. (2014). An insulin-like growth factor found in hepatopancreas implicates carbohydrate metabolism of the blue crab *Callinectes sapidus*. *Gen. Comp. Endocrinol.* **199**, 56-64.

Chung, J. S. and Webster, S. G. (2005). Dynamics of in vivo release of molt-inhibiting hormone and crustacean hyperglycemic hormone in the shore crab, Carcinus maenas. *Endocrinology* **146**, 5545-5551.

Ciarmela, P., Bloise, E., Gray, P. C., Carrarelli, P., Islam, M. S., De Pascalis, F., Severi, F. M., Vale, W., Castellucci, M. and Petraglia, F. (2010). Activin-A and myostatin response and steroid regulation in human myometrium: disruption of their signalling in uterine fibroid. *The Journal of Clinical Endocrinology & Metabolism* **96**, 755-765.

Ciciliot, S., Rossi, A. C., Dyar, K. A., Blaauw, B. and Schiaffino, S. (2013). Muscle type and fiber type specificity in muscle wasting. *The international journal of biochemistry & cell biology* **45**, 2191-2199.

Cigan, A. M., Feng, L. and Donahue, T. F. (1988). Transfer RNA(iMet) functions in directing the scanning ribosome to the start site of translation. *Science* **242**, 93-97.

Clayton, G. M., Peak-Chew, S. Y., Evans, R. M. and Schwabe, J. W. R. (2001). The structure of the ultraspiracle ligand-binding domain reveals a nuclear receptor locked in an inactive conformation. *Proceedings of the National Academy of Sciences of the United States of America* **98**, 1549-1554.

Clermont, Y. and Mauger, A. (1974). Existence of a spermatogonial chalone in rat testis. *Cell and Tissue Kinetics* **7**, 165-172.

Cohen, S., Brault, J. J., Gygi, S. P., Glass, D. J., Valenzuela, D. M., Gartner, C., Latres, E. and Goldberg, A. L. (2009). During muscle atrophy, thick, but not thin, filament components are degraded by MuRF1-dependent ubiquitylation. *The Journal of cell biology* **185**, 1083-1095.

Cohen, S., Nathan, J. A. and Goldberg, A. L. (2015). Muscle wasting in disease: molecular mechanisms and promising therapies. *Nature Reviews Drug Discovery* **14**, 58-74.

Cohen, S., Ushiro, H., Stoscheck, C. and Chinkers, M. (1982). A native 170,000 epidermal growth factor receptor-kinase complex from shed plasma membrane vesicles. *J. Biol. Chem.* **257**, 1523-1531.

Coleman, M. E., Demayo, F., Yin, K. C., Lee, H. M., Geske, R., Montgomery, C. and Schwartz, R. J. (1995). Myogenic vector expression of insulin-like growth-factor-I stimulates muscle-cell differentiation and myofiber hypertrophy in transgenic mice. *J. Biol. Chem.* **270**, 12109-12116.

Conery, A. R., Cao, Y. N., Thompson, E. A., Townsend, C. M., Ko, T. C. and Luo, K. X. (2004). Akt interacts directly with Smad3 to regulate the sensitivity to TGF-beta-induced apoptosis. *Nat. Cell Biol.* **6**, 366-372.

Corton, J. M., Gillespie, J. G. and Hardie, D. G. (1994). Role of the AMP-activated protein-kinase in the cellular stress-response. *Curr. Biol.* **4**, 315-324.

Covi, J. A., Bader, B. D., Chang, E. S. and Mykles, D. L. (2010). Molt cycle regulation of protein synthesis in skeletal muscle of the blackback land crab, *Gecarcinus lateralis*, and the differential expression of a myostatin-like factor during atrophy induced by molting or unweighting. *J. Exp. Biol.* **213**, 172-183.

Covi, J. A., Chang, E. S. and Mykles, D. L. (2009). Conserved role of cyclic nucleotides in the regulation of ecdysteroidogenesis by the crustacean molting gland. *Comp Biochem Physiol A Mol Integr Physiol* **152**, 470-477.

Covi, J. A., Chang, E. S. and Mykles, D. L. (2012). Neuropeptide signaling mechanisms in crustacean and insect molting glands. *Invertebr. Reprod. Dev.* **56**, 33-49.

Covi, J. A., Kim, H. W. and Mykles, D. L. (2008). Expression of alternatively spliced transcripts for a myostatin-like protein in the blackback land crab, *Gecarcinus lateralis*. *Comp Biochem Physiol A Mol Integr Physiol* **150**, 423-430.

Cronauer, M., Braun, S., Tremmel, C., Kröncke, K. D. and Spindler-Barth, M. (2007). Nuclear localization and DNA binding of ecdysone receptor and ultraspiracle. *Arch. Insect Biochem. Physiol.* **65**, 125-133.

D'Avino, P. P., Crispi, S., Cherbas, L., Cherbas, P. and Furia, M. (1995). The moulting hormone ecdysone is able to recognize target elements composed of direct repeats. *Mol. Cell. Endocrinol.* **113**, 1-9.

Dai, F. Y., Shen, T., Li, Z. Y., Lin, X. and Feng, X. H. (2011). PPM1A dephosphorylates RanBP3 to enable efficient nuclear export of Smad2 and Smad3. *EMBO reports* **12**, 1175-1181.

Danielson, L. S., Park, D. S., Rotllan, N., Chamorro-Jorganes, A., Guijarro, M. V., Fernandez-Hernando, C., Fishman, G. I., Phoon, C. K. L. and Hernando, E. (2013). Cardiovascular dysregulation of miR-17-92 causes a lethal hypertrophic cardiomyopathy and arrhythmogenesis. *FASEB J.* **27**, 1460-1467.

Das, S. (2014). *Gecarcinus lateralis* proteome analysis *Unpublished raw data.*

Das, S. and Durica, D. S. (2013). Ecdysteroid receptor signaling disruption obstructs blastemal cell proliferation during limb regeneration in the fiddler crab, Uca pugilator. *Mol. Cell. Endocrinol.* **365**, 249-259.

Daughaday, W. H., Salmon, W. D. and Alexander, F. (1959). Sulfation factor activity of sera from patients with pituitary disorders. *Journal of Clinical Endocrinology & Metabolism* **19**, 743-758.

Davidson, J. K., Falkmer, S., Mehrotra, B. K. and Wilson, S. (1971). Insulin assays and light microscopical studies of digestive organs in protostomian and deuterostomian species and in coelenterates. *Gen. Comp. Endocrinol.* **17**, 388-&.

Davies, S. P., Hawley, S. A., Woods, A., Carling, D., Haystead, T. A. J. and Hardie, D. G. (1994). Purification of the AMP-activated protein-kinase on ATP-gamma-sepharose and analysis of its subunit structure. *Eur. J. Biochem.* **223**, 351-357.

Davies, S. P., Helps, N. R., Cohen, P. T. W. and Hardie, D. G. (1995). 5'-AMP inhibits dephosphorylation, as well as promoting phosphorylation, of the AMP-activated protein kinase. Studies using bacterially expressed human protein phosphatase-2C alpha and native bovine protein phosphatase-2A(c). *FEBS Lett.* **377**, 421-425.

De Meyts, P., Palsgaard, J., Sajid, W., Theede, A.-M. and Aladdin, H. (2004). Structural biology of insulin and IGF-1 receptors. *Biology of IGF-1: Its Interaction with Insulin in Health and Malignant States*, 160.

De Santis, C., Wade, N. M., Jerry, D. R., Preston, N. P., Glencross, B. D. and Sellars, M. J. (2011). Growing backwards: An inverted role for the shrimp ortholog of vertebrate myostatin and GDF11. *J. Exp. Biol.* **214**, 2671-2677.

Delany, A. M., Durant, D. and Canalis, E. (2001). Glucocorticoid suppression of IGF I transcription in osteoblasts. *Mol. Endocrinol.* **15**, 1781-1789.

Deng, B., Wen, J., Ding, Y., Gao, Q., Huang, H., Ran, Z., Qian, Y., Peng, J. and Jiang, S. (2012). Functional analysis of pig myostatin gene promoter with some adipogenesis-and myogenesis-related factors. *Mol. Cell. Biochem.* **363**, 291-299.

Dennis, P. B., Pullen, N., Kozma, S. C. and Thomas, G. (1996). The principal rapamycin-sensitive p70(s6k) phosphorylation sites, T-229 and T-389, are differentially regulated by rapamycin-insensitive kinase kinases. *Mol. Cell. Biol.* **16**, 6242-6251.

Dewey, D. L. (1973). Melanocyte chalone. *National Cancer Institute Monographs*, 213-216.

Dey, N., Ghosh-Choudhury, N., Kasinath, B. S. and Choudhury, G. G. (2012). TGF beta-Stimulated MicroRNA-21 Utilizes PTEN to Orchestrate AKT/mTORC1 Signaling for Mesangial Cell Hypertrophy and Matrix Expansion. *PloS one* **7**.

DeYoung, M. P., Horak, P., Sofer, A., Sgroi, D. and Ellisen, L. W. (2008). Hypoxia regulates TSC1/2-mTOR signaling and tumor suppression through REDD1-mediated 14-3-3 shuttling. *Genes Dev.* **22**, 239-251.

Diallinas, G., Gorfinkiel, L., Arst, H. N., Cecchetto, G. and Scazzocchio, C. (1994). Genetic and molecular characterization of purine permease genes of aspergillus-nidulans reveals a novel family of transporters conserved in prokaryotes and eukaryotes. *Folia Microbiol.* **39**, 513-514.

Dodd, K. M. and Tee, A. R. (2012). Leucine and mTORC1: A complex relationship. *American journal of physiology. Endocrinology and metabolism* **302**, E1329-1342.

Dorrello, N. V., Peschiaroli, A., Guardavaccaro, D., Colburn, N. H., Sherman, N. E. and Pagano, M. (2006). S6K1- and beta TRCP-mediated degradation of PDCD4 promotes protein translation and cell growth. *Science* **314**, 467-471.

Downward, J., Parker, P. and Waterfield, M. D. (1984). Autophosphorylation sites on the epidermal growth-factor receptor. *Nature* **311**, 483-485.

Drach, P. (1939). Mue et cycle d'intermue chez les crustacés décapodes. Paris: Masson.

Dreyer, H. C., Fujita, S., Cadenas, J. G., Chinkes, D. L., Volpi, E. and Rasmussen, B. B. (2006). Resistance exercise increases AMPK activity and reduces 4E-BP1 phosphorylation and protein synthesis in human skeletal muscle. *The Journal of physiology* **576**, 613-624.

Druet, T., Ahariz, N., Cambisano, N., Tamma, N., Michaux, C., Coppieters, W., Charlier, C. and Georges, M. (2014). Selection in action: dissecting the molecular underpinnings of the increasing muscle mass of Belgian Blue Cattle. *BMC Genomics* **15**, 796.

Drummond, M. J., Dreyer, H. C., Fry, C. S., Glynn, E. L. and Rasmussen, B. B. (2009a). Nutritional and contractile regulation of human skeletal muscle protein synthesis and mTORC1 signaling. *J Appl Physiol (1985)* **106**, 1374-1384.

Drummond, M. J., Glynn, E. L., Fry, C. S., Dhanani, S., Volpi, E. and Rasmussen, B. B. (2009b). Essential Amino Acids Increase MicroRNA-499,-208b, and-23a and Downregulate Myostatin and Myocyte Enhancer Factor 2C mRNA Expression in Human Skeletal Muscle. *J. Nutr.* **139**, 2279-2284.

Du, R., An, X.-R., Chen, Y.-F. and Qin, J. (2007). Some motifs were important for myostatin transcriptional regulation in sheep (Ovis aries). *BMB Reports* **40**, 547-553.

Du, R., Du, J., Qin, J., Cui, L. C., Hou, J., Guan, H. and An, X. R. (2011). Molecular cloning and sequence analysis of the cat myostatin gene 5 ' regulatory region. *Afr. J. Biotechnol.* **10**, 10366-10372.

Du, R., Du, R., Chen, Y.-F., An, X.-R., Yang, X.-Y., Ma, Y., Zhang, L., Yuan, X.-L., Chen, L.-M. and Qin, J. (2005). Cloning and sequence analysis of myostatin promoter in sheep: Full Length Research Paper. *DNA Sequence* **16**, 412-417.

Duan, S., Skaar, J. R., Kuchay, S., Toschi, A., Kanarek, N., Ben-Neriah, Y. and Pagano, M. (2011). mTOR generates an auto-amplification loop by triggering the betaTrCP- and CK1alpha-dependent degradation of DEPTOR. *Mol. Cell* **44**, 317-324.

Duan, Y. H., Li, F. N., Tan, K. R., Liu, H. N., Li, Y. H., Liu, Y. Y., Kong, X. F., Tang, Y. L., Wu, G. Y. and Yin, Y. L. (2015). Key mediators of intracellular amino acids signaling to mTORC1 activation. *Amino Acids* **47**, 857-867.

Dubois, V., Laurent, M., Boonen, S., Vanderschueren, D. and Claessens, F. (2012). Androgens and skeletal muscle: cellular and molecular action mechanisms underlying the anabolic actions. *Cell. Mol. Life Sci.* **69**, 1651-1667.

Dubois, V., Laurent, M. R., Sinnesael, M., Cielen, N., Helsen, C., Clinckemalie, L., Spans, L., Gayan-Ramirez, G., Deldicque, L., Hespel, P. et al. (2014). A satellite cell-specific knockout of the androgen receptor reveals myostatin as a direct androgen target in skeletal muscle. *FASEB J.* **28**, 2979-2994.

Duncan, R. and McConkey, E. H. (1982). Rapid alterations in initiation rate and recruitment of inactive RNA are temporally correlated with S6 phosphorylation. *Eur. J. Biochem.* **123**, 539-544.

Duran, R. V., Oppliger, W., Robitaille, A. M., Heiserich, L., Skendaj, R., Gottlieb, E. and Hall, M. N. (2012). Glutaminolysis Activates Rag-mTORC1 Signaling. *Mol. Cell* **47**, 349-358.

Durica, D. S. and Hopkins, P. M. (1996). Expression of the genes encoding the ecdysteroid and retinoid receptors in regenerating limb tissues from the fiddler crab, *Uca pugilator*. *Gene* **171**, 237-241.

Durica, D. S., Wu, X., Anilkumar, G., Hopkins, P. M. and Chung, A. C.-K. (2002). Characterization of crab EcR and RXR homologs and expression during limb regeneration and oocyte maturation. *Mol. Cell. Endocrinol.* **189**, 59-76.

Ebisawa, T., Fukuchi, M., Murakami, G., Chiba, T., Tanaka, K., Imamura, T. and Miyazono, K. (2001). Smurf1 interacts with transforming growth factor-beta type I receptor through Smad7 and induces receptor degradation. *J. Biol. Chem.* **276**, 12477-12480.

Efeyan, A. and Sabatini, D. M. (2013). Nutrients and growth factors in mTORC1 activation. *Biochem. Soc. Trans.* **41**, 902-905.

Egerman, M. A. and Glass, D. J. (2014). Signaling pathways controlling skeletal muscle mass. *Crit. Rev. Biochem. Mol. Biol.* **49**, 59-68.

Elgjo, K. and Reichelt, K. L. (1984). Purification of an endogeneous mitotic inhibitor (chalone) in mouse epidermis. *Cell and Tissue Kinetics* **17**, 275-275.

Elgjo, K. and Reichelt, K. L. (1994). Beta-receptor blockade by propranolol modifies the effect of the inhibitory, endogenous epidermal pentapeptide on epidermal-cell flux at the G(2)-m transition but not at the G(1)-s transition. *Epithelial Cell Biology* **3**, 32-37.

Elgjo, K. and Reichelt, K. L. (2004). Chalones–from aqueous extracts to oligopeptides. *Cell Cycle* **3**, 1206-1209.

Ellman, R., Spatz, J., Cloutier, A., Palme, R., Christiansen, B. A. and Bouxsein, M. L. (2013). Partial reductions in mechanical loading yield proportional changes in bone density, bone architecture, and muscle mass. *J. Bone Miner. Res.* **28**, 875-885.

Emerling, B. M., Weinberg, F., Snyder, C., Burgess, Z., Mutlu, G. M., Viollet, B., Budinger, G. R. S. and Chandel, N. S. (2009). Hypoxic activation of AMPK is dependent on mitochondrial ROS but independent of an increase in AMP/ATP ratio. *Free Radical Biol. Med.* **46**, 1386-1391.

Emery, P. W., Edwards, R. H. T., Rennie, M. J., Souhami, R. L. and Halliday, D. (1984). Protein-synthesis in muscle measured invivo in cachectic patients with cancer. *Br. Med. J.* **289**, 584-586.

Emmel, V. E. (1910). A study of the differentiation of tissues tn the regenerating crustacean limb. *American Journal of Anatomy* **10**, 109-+.

Evans, K., Nasim, Z., Brown, J., Butler, H., Kauser, S., Varoqui, H., Erickson, J. D., Herbert, T. P. and Bevington, A. (2007). Acidosis-sensing glutamine pump SNAT2 determines amino acid levels and mammalian target of rapamycin signalling to protein synthesis in L6 muscle cells. *Journal of the American Society of Nephrology* **18**, 1426-1436.

Fadden, P., Haystead, T. A. J. and Lawrence, J. C. (1997). Identification of phosphorylation sites in the translational regulator, PHAS-I, that are controlled by insulin and rapamycin in rat adipocytes. *J. Biol. Chem.* **272**, 10240-10247.

Fan, J. Y., Carpentier, J. L., Vanobberghen, E., Blackett, N. M., Grunfeld, C., Gorden, P. and Orci, L. (1983). The interaction of I-125-insulin with cultured 3T3-L1 adipocytes - quantitative-analysis by the hypothetical grain method. *Journal of Histochemistry & Cytochemistry* **31**, 859-870.

Fang, Y., Vilella-Bach, M., Bachmann, R., Flanigan, A. and Chen, J. (2001). Phosphatidic acid-mediated mitogenic activation of mTOR signaling. *Science* **294**, 1942-1945.

Fang, Y. M., Park, I. H., Wu, A. L., Du, G. W., Huang, P., Frohman, M. A., Walker, S. J., Brown, H. A. and Chen, J. (2003). PLD1 regulates mTOR signaling and mediates Cdc42 activation of S6K1. *Curr. Biol.* **13**, 2037-2044.

Fang, Y. X., Xue, J. L., Shen, Q., Chen, J. Z. and Tian, L. (2012). MicroRNA-7 inhibits tumor growth and metastasis by targeting the phosphoinositide 3-kinase/Akt pathway in hepatocellular carcinoma. *Hepatology* **55**, 1852-1862.

Ferrando, A. A., Tipton, K. D., Doyle, D., Phillips, S. M., Cortiella, J. and Wolfe, R. R. (1998). Testosterone injection stimulates net protein synthesis but not tissue amino acid transport. *American Journal of Physiology-Endocrinology And Metabolism* **275**, E864-E871.

Ferrer, A., Caelles, C., Massot, N. and Hegardt, F. G. (1985). Activation of rat-liver cytosolic 3-hydroxy-3-methylglutaryl coenzyme a reductase kinase by adenosine 5'-monophosphate. *Biochem. Biophys. Res. Commun.* **132**, 497-504.

Festuccia, W. T., Laplante, M., Brule, S., Houde, V. P., Achouba, A., Lachance, D., Pedrosa, M. L., Silva, M. E., Guerra-Sa, R., Couet, J. et al. (2009). Rosiglitazone-induced heart remodelling is associated with enhanced turnover of myofibrillar protein and mTOR activation. *Journal of molecular and cellular cardiology* **47**, 85-95.

Finsterer, J. (2014). Locomotor Principles: Anatomy and Physiology of Skeletal Muscles. In *Comparative Medicine*, pp. 45-60: Springer.

Fitts, R. H., Riley, D. R. and Widrick, J. J. (2000). Microgravity and skeletal muscle. *J. Appl. Physiol.* **89**, 823-839.

Florenti, R. A., Nam, S. C., Janakide.K, Lee, K. T., Reiner, J. M. and Thomas, W. A. (1973). Population dynamics of arterial smooth-muscle cells .2. In-vivo inhibition of entry into mitosis of swine arterial smooth-muscle cells by aortic tissue extracts. *Archives of Pathology* **95**, 317-320.

Fogarty, S. and Hardie, D. G. (2010). Development of protein kinase activators: AMPK as a target in metabolic disorders and cancer. *Biochimica Et Biophysica Acta-Proteins and Proteomics* **1804**, 581-591.

Fornari, F., Milazzo, M., Chieco, P., Negrini, M., Calin, G. A., Grazi, G. L., Pollutri, D., Croce, C. M., Bolondi, L. and Gramantieri, L. (2010). MiR-199a-3p regulates mTOR and c-Met to influence the doxorubicin sensitivity of human hepatocarcinoma cells. *Cancer Res.* **70**, 5184-5193.

Fornari, F., Milazzo, M., Chieco, P., Negrini, M., Marasco, E., Capranico, G., Mantovani, V., Marinello, J., Sabbioni, S., Callegari, E. et al. (2012). In hepatocellular carcinoma miR-519d is up-regulated by p53 and DNA hypomethylation and targets CDKN1A/p21, PTEN, AKT3 and TIMP2. *J. Pathol.* **227**, 275-285.

Foster, K. G., Acosta-Jaquez, H. A., Romeo, Y., Ekim, B., Soliman, G. A., Carriere, A., Roux, P. P., Ballif, B. A. and Fingar, D. C. (2010). Regulation of mTOR Complex 1 (mTORC1) by Raptor Ser(863) and Multisite Phosphorylation. *J. Biol. Chem.* **285**, 80-94.

Foti, M., Ahmed Moukil, M., Dudognon, P. and Carpentier, J. L. (2004). Insulin and IGF-1 receptor trafficking and signalling. In *Biology of IGF-1: Its Interaction with Insulin in Health and Malignant States*, eds. G. Bock and J. Goode), pp. 125-147. Hoboken, NJ: Wiley Online Library.

Fowler, R. F., Bonnewell, V., Spann, M. S. and Skinner, D. M. (1985). Sequences of 3 closely related variants of a complex satellite DNA diverge at specific domains. *J. Biol. Chem.* **260**, 8964-8972.

Froese, G. (1971). Regulation of growth in chinese hamster cells by a local inhibitor. *Exp. Cell Res.* **65**, 297-&.

Fu, X., Tian, J., Zhang, L., Chen, Y. and Hao, Q. (2012). Involvement of microRNA-93, a new regulator of PTEN/Akt signaling pathway, in regulation of chemotherapeutic drug cisplatin chemosensitivity in ovarian cancer cells. *FEBS Lett.* **586**, 1279-1286.

Funkenstein, B., Balas, V., Rebhan, Y. and Pliatner, A. (2009). Characterization and functional analysis of the 5' flanking region of *Sparus aurata* myostatin-1 gene. *Comp Biochem Physiol A Mol Integr Physiol* **153**, 55-62.

Gale, N. W., Kaplan, S., Lowenstein, E. J., Schlessinger, J. and Bar-Sagi, D. (1993). Grb2 mediates the EGF-dependent activation of guanine nucleotide exchange on Ras.

Gallardo, N., Carrillo, O., Molto, E., Deas, M., Gonzalez Suarez, R., Carrascosa, J., Ros, M. and Andrés, A. (2003). Isolation and biological characterization of a 6-kDa protein from hepatopancreas of lobster *Panulirus argus* with insulin-like effects. *Gen. Comp. Endocrinol.* **131**, 284-290.

Galt, N. J., Froehlich, J. M., Remily, E. A., Romero, S. R. and Biga, P. R. (2014). The effects of exogenous cortisol on myostatin transcription in rainbow trout, Oncorhynchus mykiss. *Comparative Biochemistry and Physiology a-Molecular & Integrative Physiology* **175**, 57-63.

Gao, S., Duan, C., Gao, G., Wang, X. and Yang, H. (2015). Alpha-synuclein overexpression negatively regulates insulin receptor substrate 1 by activating mTORC1/S6K1 signaling. *The international journal of biochemistry & cell biology* **64**, 25-33.

Garikipati, D. K. and Rodgers, B. D. (2012). Myostatin regulation of myosatellite cells in a novel model system: Ii. Differentiation and gene subfunctionalization. *American Journal of Physiology-Regulatory, Integrative and Comparative Physiology*.

Gauhar, Z., Sun, L. V., Hua, S., Mason, C. E., Fuchs, F., Li, T.-R., Boutros, M. and White, K. P. (2009). Genomic mapping of binding regions for the Ecdysone receptor protein complex. *Genome Res.* **19**, 1006-1013.

Gembitsky, D. S., Reichelt, K. L., Haakonsen, P., Paulsen, J. E. and Elgjo, K. (1998). Identification of a melanocyte growth-inhibiting tripeptide and determination of its structure. *Journal of Peptide Research* **51**, 80-84.

Georges, M. (2010). When less means more: impact of myostatin in animal breeding. *Immunology, Endocrine & Metabolic Agents in Medicinal Chemistry (Formerly Current Medicinal Chemistry-Immunology, Endocrine and Metabolic Agents)* **10**, 240-248.

Gianfranceschi, G. L., Czerwinski, A., Angiolillo, A., Marsili, V., Castigli, E., Mancinelli, L., Miano, A., Bramucci, M. and Amici, D. (1994). Molecular-models of small phosphorylated chromatin peptides - structure-function relationship and regulatory activity on in-vitro transcription and on cell-growth and differentiation. *Peptides* **15**, 7-13.

Gilson, H., Schakman, O., Combaret, L., Lause, P., Grobet, L., Attaix, D., Ketelslegers, J. M. and Thissen, J. P. (2007). Myostatin gene deletion prevents glucocorticoid-induced muscle atrophy. *Endocrinology* **148**, 452-460.

Gingras, A. C., Raught, B. and Sonenberg, N. (1999). eIF4 initiation factors: Effectors of mRNA recruitment to ribosomes and regulators of translation. *Annu. Rev. Biochem.* **68**, 913-963.

Giraud, J., Leshan, R., Lee, Y. H. and White, M. F. (2004). Nutrient-dependent and insulin-stimulated phosphorylation of insulin receptor substrate-1 on serine 302 correlates with increased insulin signaling. *J. Biol. Chem.* **279**, 3447-3454.

Gokoffski, K. K., Wu, H.-H., Beites, C. L., Kim, J., Kim, E. J., Matzuk, M. M., Johnson, J. E., Lander, A. D. and Calof, A. L. (2011). Activin and GDF11 collaborate in feedback control of neuroepithelial stem cell proliferation and fate. *Development* **138**, 4131-4142.

Goldberg, A. L., Tischler, M., Demartino, G. and Griffin, G. (1980). Hormonal-regulation of protein-degradation and synthesis in skeletal-muscle. *Federation Proceedings* **39**, 31-36.

Goldspink, D. F. (1976). Effects of denervation on protein turnover of rat skeletal-muscle. *Biochem. J.* **156**, 71-80.

Goldspink, G. (2012). Age-related loss of muscle mass and strength. *Journal of aging research* **2012**.

Goodman, C. A., Mayhew, D. L. and Hornberger, T. A. (2011). Recent progress toward understanding the molecular mechanisms that regulate skeletal muscle mass. *Cell. Signal.* **23**, 1896-1906.

Goodman, C. A., McNally, R. M., Hoffmann, F. M. and Hornberger, T. A. (2013). Smad3 Induces Atrogin-1, Inhibits mTOR and Protein Synthesis, and Promotes Muscle Atrophy In Vivo. *Mol. Endocrinol.* **27**, 1946-1957.

Govind, C. K., Atwood, H. L. and Lang, F. (1973). Synaptic differentiation in a regenerating crab-limb muscle. *Proceedings of the National Academy of Sciences of the United States of America* **70**, 822-826.

Grade, C. V. C., Salerno, M. S., Schubert, F. R., Dietrich, S. and Alvares, L. E. (2009). An evolutionarily conserved Myostatin proximal promoter/enhancer confers basal levels of transcription and spatial specificity in vivo. *Dev. Genes Evol.* **219**, 497-508.

Grebe, M., Przibilla, S., Henrich, V. C. and Spindler-Barth, M. (2004). Characterization of the ligand-binding domain of the ecdysteroid receptor from Drosophila melanogaster. *Biol. Chem.* **384**, 105-116.

Greene, M. W., Sakaue, H., Wang, L. H., Alessi, D. R. and Roth, R. A. (2003). Modulation of insulin-stimulated degradation of human insulin receptor substrate-1 by serine 312 phosphorylation. *J. Biol. Chem.* **278**, 8199-8211.

Greenfield, C., Hiles, I., Waterfield, M. D., Federwisch, M., Wollmer, A., Blundell, T. L. and McDonald, N. (1989). Epidermal growth-factor binding induces a conformational change in the external domain of its receptor. *EMBO J.* **8**, 4115-4123.

Grey, A., Chen, Q., Xu, X., Callon, K. and Cornish, J. (2003). Parallel phosphatidylinositol-3 kinase and p42/44 mitogen-activated protein kinase signaling pathways subserve the mitogenic and antiapoptotic actions of insulin-like growth factor I in osteoblastic cells. *Endocrinology* **144**, 4886-4893.

Groenewoud, M. J. and Zwartkruis, F. J. T. (2013). Rheb and Rags come together at the lysosome to activate mTORC1. *Biochem. Soc. Trans.* **41**, 951-955.

Grosholz, E. D. and Ruiz, G. M. (1996). Predicting the impact of introduced marine species: Lessons from the multiple invasions of the European green crab Carcinus maenas. *Biol. Conserv.* **78**, 59-66.

Grundmann, S., Hans, F. P., Kinniry, S., Heinke, J., Helbing, T., Bluhm, F., Sluijter, J. P., Hoefer, I., Pasterkamp, G. and Bode, C. (2011). MicroRNA-100 regulates neovascularization by suppression of mammalian target of rapamycin in endothelial and vascular smooth muscle cells. *Circulation* **123**, 999-1009.

Gu, Z., Zhang, Y., Shi, P., Zhang, Y. P., Zhu, D. and Li, H. (2004). Comparison of avian myostatin genes. *Anim. Genet.* **35**, 470-472.

Gual, P., Gremeaux, T., Gonzalez, T., Le Marchand-Brustel, Y. and Tanti, J. F. (2003). MAP kinases and mTOR mediate insulin-induced phosphorylation of Insulin Receptor Substrate-1 on serine residues 307, 612 and 632. *Diabetologia* **46**, 1532-1542.

Gual, P., Le Marchand-Brustel, Y. and Tanti, J.-F. (2005). Positive and negative regulation of insulin signaling through IRS-1 phosphorylation. *Biochimie* **87**, 99-109.

Guertin, D. A., Stevens, D. M., Thoreen, C. C., Burds, A. A., Kalaany, N. Y., Moffat, J., Brown, M., Fitzgerald, K. J. and Sabatini, D. M. (2006). Ablation in mice of the mTORC components raptor, rictor, or mLST8 reveals that mTORC2 is required for signaling to Akt-FOXO and PKC alpha but not S6K1. *Dev. Cell* **11**, 859-871.

Gulati, P., Gaspers, L. D., Dann, S. G., Joaquin, M., Nobukuni, T., Natt, F., Kozma, S. C., Thomas, A. P. and Thomas, G. (2008). Amino acids activate mTOR Complex 1 via Ca2+/CaM signaling to hVps34. *Cell metabolism* **7**, 456-465.

Guo, L., Li, L., Zhang, S. and Zhang, G. (2012). Molecular cloning and characterization of the myostatin gene in a cultivated variety of bay scallop, *Argopecten irradians. Aquaculture* **350-353**, 192-199.

Gutierrez, A., Nieto, J., Pozo, F., Stern, S. and Schoofs, L. (2007). Effect of insulin/IGF-I like peptides on glucose metabolism in the white shrimp Penaeus vannamei. *Gen. Comp. Endocrinol.* **153**, 170-175.

Gwinn, D. M., Shackelford, D. B., Egan, D. F., Mihaylova, M. M., Mery, A., Vasquez, D. S., Turk, B. E. and Shaw, R. J. (2008). AMPK phosphorylation of raptor mediates a metabolic checkpoint. *Mol. Cell* **30**, 214-226.

Haghighat, A., Mader, S., Pause, A. and Sonenberg, N. (1995). Repression of cap-dependent translation by 4E-binding protein-1 - competition with P220 for binding to eukaryotic initiation factor-4E. *EMBO J.* **14**, 5701-5709.

Hahn, K., Miranda, M., Francis, V. A., Vendrell, J., Zorzano, A. and Teleman, A. A. (2010). PP2A Regulatory Subunit PP2A-B ' Counteracts S6K Phosphorylation. *Cell metabolism* **11**, 438-444.

Haissaguerre, M., Saucisse, N. and Cota, D. (2014). Influence of mTOR in energy and metabolic homeostasis. *Mol. Cell. Endocrinol.* **397**, 67-77.

Han, D. S., Huang, H. P., Wang, T. G., Hung, M. Y., Ke, J. Y., Chang, K. T., Chang, H. Y., Ho, Y. P., Hsieh, W. Y. and Yang, W. S. (2010). Transcription activation of myostatin by trichostatin A in differentiated C2C12 myocytes via ASK1-MKK3/4/6-JNK and p38 mitogen-activated protein kinase pathways. *J. Cell. Biochem.* **111**, 564-573.

Han, J. M., Jeong, S. J., Park, M. C., Kim, G., Kwon, N. H., Kim, H. K., Ha, S. H., Ryu, S. H. and Kim, S. (2012). Leucyl-tRNA synthetase is an intracellular leucine sensor for the mTORC1-signaling pathway. *Cell* **149**, 410-424.

Hannan, K. M., Brandenburger, Y., Jenkins, A., Sharkey, K., Cavanaugh, A., Rothblum, L., Moss, T., Poortinga, G., McArthur, G. A., Pearson, R. B. et al. (2003). mTOR-Dependent regulation of ribosomal gene transcription requires S6K1 and is mediated by phosphorylation of the carboxy-terminal activation domain of the nucleolar transcription factor UBF. *Mol. Cell. Biol.* **23**, 8862-8877.

Hara, K., Maruki, Y., Long, X. M., Yoshino, K., Oshiro, N., Hidayat, S., Tokunaga, C., Avruch, J. and Yonezawa, K. (2002). Raptor, a binding partner of target of rapamycin (TOR), mediates TOR action. *Cell* **110**, 177-189.

Hara, K., Yonezawa, K., Weng, Q. P., Kozlowski, M. T., Belham, C. and Avruch, J. (1998). Amino acid sufficiency and mTOR regulate p70 S6 kinase and eIF-4E BP1 through a common effector mechanism. *J. Biol. Chem.* **273**, 14484-14494.

Hardie, D. G. (2004). The AMP-activated protein kinase pathway - new players upstream and downstream. *J. Cell Sci.* **117**, 5479-5487.

Hardie, D. G., Carling, D. and Carlson, M. (1998). The AMP-activated/SNF1 protein kinase subfamily: Metabolic sensors of the eukaryotic cell? *Annu. Rev. Biochem.* **67**, 821-855.

Harris, R. R. and Andrews, M. B. (1982). Extracellular fluid volume changes in *Carcinus maenas* during acclimation to low and high environmental salinities. *J. Exp. Biol.* **99**, 161-173.

Harrison, C. A., Al-Musawi, S. L. and Walton, K. L. (2011). Prodomains regulate the synthesis, extracellular localisation and activity of TGF-beta superfamily ligands. *Growth Factors* **29**, 174-186.

Hartley, D. and Cooper, G. M. (2002). Role of mTOR in the degradation of IRS-1: Regulation of PP2A activity. *J. Cell. Biochem.* **85**, 304-314.

Hartnoll, R. G. (1988). Growth and molting. In *Biology of the Land Crabs*, eds. W. W. Burggren and B. R. McMahon), pp. 186-210. New York: Cambridge University Press.

Hasselgren, P. O. and Fischer, J. E. (2001). Muscle cachexia: Current concepts of intracellular mechanisms and molecular regulation. *Annals of Surgery* **233**, 9-17.

Hatakeyama, N., Kojima, T., Iba, K., Murata, M., Thi, M., Spray, D., Osanai, M., Chiba, H., Ishiai, S., Yamashita, T. et al. (2008). IGF-I regulates tight-junction protein claudin-1 during differentiation of osteoblast-like MC3T3-E1 cells via a MAP-kinase pathway. *Cell Tissue Res.* **334**, 243-254.

Hatt, P. J., Liebon, C., Moriniere, M., Oberlander, H. and Porcheron, P. (1997). Activity of insulin growth factors and shrimp neurosecretory organ extracts on a lepdopteran cell line. *Arch. Insect Biochem. Physiol.* **34**, 313-328.

Hawley, S. A., Boudeau, J., Reid, J. L., Mustard, K. J., Udd, L., Mäkelä, T. P., Alessi, D. R. and Hardie, D. G. (2003). Complexes between the LKB1 tumor suppressor, STRADα/β and MO25α/β are upstream kinases in the AMP-activated protein kinase cascade. *J. Biol.* **2**, 28.

Hawley, S. A., Davison, M., Woods, A., Davies, S. P., Beri, R. K., Carling, D. and Hardie, D. G. (1996). Characterization of the AMP-activated protein kinase kinase from rat liver and

identification of threonine 172 as the major site at which it phosphorylates AMP-activated protein kinase. *J. Biol. Chem.* **271**, 27879-27887.

Hawley, S. A., Selbert, M. A., Goldstein, E. G., Edelman, A. M., Carling, D. and Hardie, D. G. (1995). 5'-AMP activates the amp-activated protein-kinase cascade and Ca2+/calmodulin activates the calmodulin-dependent protein-kinase-i cascade, via 3 independent mechanisms. *J. Biol. Chem.* **270**, 27186-27191.

Hayashita, Y., Osada, H., Tatematsu, Y., Yamada, H., Yanagisawa, K., Tomida, S., Yatabe, Y., Kawahara, K., Sekido, Y. and Takahashi, T. (2005). A polycistronic microRNA cluster, miR-17-92, is overexpressed in human lung cancers and enhances cell proliferation. *Cancer Res.* **65**, 9628-9632.

Heard, J. J., Fong, V., Bathaie, S. Z. and Tamanoi, F. (2014). Recent progress in the study of the Rheb family GTPases. *Cell. Signal.* **26**, 1950-1957.

Helterline, D. L. I., Garikipati, D., Stenkamp, D. and Rodgers, B. (2007). Embryonic and tissue-specific regulation of myostatin-1 and -2 gene expression in zebrafish. *Gen. Comp. Endocrinol.* **151**, 90-97.

Hempel, W. M., Cavanaugh, A. H., Hannan, R. D., Taylor, L. and Rothblum, L. I. (1996). The species-specific RNA polymerase I transcription factor SL-1 binds to upstream binding factor. *Mol. Cell. Biol.* **16**, 557-563.

Henrich, V. (2009). The ecdysteroid receptor. In *Insect Development: Morphogenesis, Molting and Metamorphosis*, (ed. L. E. Gilbert), pp. 261-303. London: Academic.

Henrich, V., Beatty, J., Ruff, H., Callender, J., Grebe, M. and Spindler-Barth, M. (2009). The Multidimensional Partnership of EcR and USP. In *Ecdysone: Structures and Functions*, (ed. G. Smagghe), pp. 361-375: Springer Netherlands.

Henrich, V. C., Burns, E., Yelverton, D. P., Christensen, E. and Weinberger, C. (2003). Juvenile hormone potentiates ecdysone receptor-dependent transcription in a mammalian cell culture system. *Insect Biochem. Mol. Biol.* **33**, 1239-1247.

Herpin, A., Lelong, C. and Favrel, P. (2004). Transforming growth factor-beta-related proteins: An ancestral and widespread superfamily of cytokines in metazoans. *Dev. Comp. Immunol.* **28**, 461-485.

Hill, C. S. (2009). Nucleocytoplasmic shuttling of Smad proteins. *Cell Res.* **19**, 36-46.

Hill, J. J., Davies, M. V., Pearson, A. A., Wang, J. H., Hewick, R. M., Wolfman, N. M. and Qiu, Y. (2002). The myostatin propeptide and the follistatin-related gene are inhibitory binding proteins of myostatin in normal serum. *J. Biol. Chem.* **277**, 40735-40741.

Hill, J. J., Qiu, Y. C., Hewick, R. M. and Wolfman, N. M. (2003). Regulation of myostatin in vivo by growth and differentiation factor-associated serum protein-1: A novel protein with protease inhibitor and follistatin domains. *Mol. Endocrinol.* **17**, 1144-1154.

Hill, R. J., Graham, L. D., Turner, K. A., Howell, L., Tohidi-Esfahani, D., Fernley, R., Grusovin, J., Ren, B., Pilling, P., Lu, L. et al. (2012). Chapter Four - Structure and Function of Ecdysone Receptors—Interactions with Ecdysteroids and Synthetic Agonists. In *Adv. Insect Physiol.*, vol. Volume 43 (ed. S. D. Tarlochan), pp. 299-351: Academic Press.

Hinderer, H., Volm, M. and Wayss, K. (1970). Specific inhibition of DNA synthesis in hela cells by endometrium extracts. *Exp. Cell Res.* **59**, 464-&.

Hinnebusch, A. G. (2005). Translational regulation of GCN4 and the general amino acid control of yeast. In *Annu. Rev. Microbiol.*, vol. 59, pp. 407-450.

Hirosumi, J., Tuncman, G., Chang, L. F., Gorgun, C. Z., Uysal, K. T., Maeda, K., Karin, M. and Hotamisligil, G. S. (2002). A central role for JNK in obesity and insulin resistance. *Nature* **420**, 333-336.

Hitachi, K., Nakatani, M. and Tsuchida, K. (2014). Myostatin signaling regulates Akt activity via the regulation of miR-486 expression. *International Journal of Biochemistry & Cell Biology* **47**, 93-103.

Holland, C. A. and Skinner, D. M. (1976). Interactions between molting and regeneration in the land crab. *Biol. Bull.* **150**, 222-240.

Holly, J. (2004). Physiology of the IGF system. In *Biology of IGF-1: its interaction with insulin in health and malignant states*, eds. G. Bock and J. Goode). Chichester, UK ;: John Wiley & Sons.

Holz, M. K., Ballif, B. A., Gygi, S. P. and Blenis, J. (2005). mTOR and S6K1 mediate assembly of the translation preinitiation complex through dynamic protein interchange and ordered phosphorylation events. *Cell* **123**, 569-580.

Hopkins, P. M. (1983). Patterns of serum ecdysteroids during induced and uninduced proecdysis in the fiddler crab, Uca pugilator. *Gen. Comp. Endocrinol.* **52**, 350-356.

Hopkins, P. M. (1993). Regeneration of walking legs in the fiddler-crab *Uca-pugilator*. *Am. Zool.* **33**, 348-356.

Hopkins, P. M. (2009). Crustacean ecdysteroids and their receptors. In *Ecdysone: Structures and Functions*, (ed. G. Smagghe), pp. 73-97. Dordrecht: Springer eBook collection. Retreived from http://link.springer.com.ezproxy2.library.colostate.edu.

Hoppe, U. C., Marbán, E. and Johns, D. C. (2000). Adenovirus-mediated inducible gene expression in vivo by a hybrid ecdysone receptor. *Mol. Ther.* **1**, 159-164.

Horman, S., Browne, G. J., Krause, U., Patel, J. V., Vertommen, D., Bertrand, L., Lavoinne, A., Hue, L., Proud, C. G. and Rider, M. H. (2002). Activation of AMP-activated protein kinase leads to the phosphorylation of elongation factor 2 and an inhibition of protein synthesis. *Curr. Biol.* **12**, 1419-1423.

Houck, J. C., Irausqui.H and Leikin, S. (1971). Lymphocyte DNA synthesis inhibition. *Science* **173**, 1139-&.

Hu, X., Cherbas, L. and Cherbas, P. (2003). Transcription activation by the ecdysone receptor (EcR/USP): Identification of activation functions. *Mol. Endocrinol.* **17**, 716-731.

Hu, X. L., Guo, H. H., He, Y., Wang, S. A., Zhang, L. L., Wang, S., Huang, X. T., Roy, S. W., Lu, W., Hu, J. J. et al. (2010). Molecular Characterization of Myostatin Gene from Zhikong scallop *Chlamys farreri* (Jones et Preston 1904). *Genes Genet. Syst.* **85**, 207-218.

Hu, Z. Y., Wang, H. L., Lee, I. H., Du, J. and Mitch, W. E. (2009). Endogenous glucocorticoids and impaired insulin signaling are both required to stimulate muscle wasting under pathophysiological conditions in mice. *J. Clin. Invest.* **119**, 3059-3069.

Huang, K. Z. and Fingar, D. C. (2014). Growing knowledge of the mTOR signaling network. *Semin. Cell Dev. Biol.* **36**, 79-90.

Hulmi, J. J., Oliveira, B. M., Silvennoinen, M., Hoogaars, W. M. H., Ma, H. Q., Pierre, P., Pasternack, A., Kainulainen, H. and Ritvos, O. (2013). Muscle protein synthesis, mTORC1/MAPK/Hippo signaling, and capillary density are altered by blocking of myostatin and activins. *American Journal of Physiology-Endocrinology and Metabolism* **304**, E41-E50.

Iadevaia, V., Liu, R. and Proud, C. G. (2014). mTORC1 signaling controls multiple steps in ribosome biogenesis. *Semin. Cell Dev. Biol.* **36**, 113-120.

Ikushima, H. and Miyazono, K. (2011). Biology of transforming growth factor-beta signaling. *Curr. Pharm. Biotechnol.* **12**, 2099-2107.

Imataka, H., Gradi, A. and Sonenberg, N. (1998). A newly identified N-terminal amino acid sequence of human eIF4G binds poly (A)-binding protein and functions in poly (A)-dependent translation. *The EMBO Journal* **17**, 7480-7489.

Inman, G. J., Nicolas, F. J. and Hill, C. S. (2002). Nucleocytoplasmic shuttling of Smads 2, 3, and 4 permits sensing of TGF-beta receptor activity. *Mol. Cell* **10**, 283-294.

Inoki, K., Zhu, T. Q. and Guan, K. L. (2003). TSC2 mediates cellular energy response to control cell growth and survival. *Cell* **115**, 577-590.

Ismail, S. Z. M. and Mykles, D. L. (1992). Differential molt-induced atrophy in the dimorphic claws of male fiddler-crabs, *Uca pugnax. J. Exp. Zool.* **263**, 18-31.

Ito, N., Ruegg, U. T., Kudo, A., Miyagoe-Suzuki, Y. and Takeda, S. (2013). Activation of calcium signaling through Trpv1 by nNOS and peroxynitrite as a key trigger of skeletal muscle hypertrophy. *Nat. Med.* **19**, 101-106.

Iwaya, T., Yokobori, T., Nishida, N., Kogo, R., Sudo, T., Tanaka, F., Shibata, K., Sawada, G., Takahashi, Y. and Ishibashi, M. (2012). Downregulation of miR-144 is associated with colorectal cancer progression via activation of mTOR signaling pathway. *Carcinogenesis*, bgs288.

Jefferies, H. B. J., Fumagalli, S., Dennis, P. B., Reinhard, C., Pearson, R. B. and Thomas, G. (1997). Rapamycin suppresses 5'TOP mRNA translation through inhibition of p70(S6k). *EMBO J.* **16**, 3693-3704.

Jewell, J. L., Kim, Y. C., Russell, R. C., Yu, F. X., Park, H. W., Plouffe, S. W., Tagliabracci, V. S. and Guan, K. L. (2015). Differential regulation of mTORC1 by leucine and glutamine. *Science* **347**, 194-198.

Jewell, J. L., Russell, R. C. and Guan, K. L. (2013). Amino acid signalling upstream of mTOR. *Nature Reviews Molecular Cell Biology* **14**, 133-139.

Jia, C. Y., Li, H. H., Zhu, X. C., Dong, Y. W., Fu, D., Zhao, Q. L., Wu, W. and Wu, X. Z. (2011). MiR-223 Suppresses Cell Proliferation by Targeting IGF-1R. *PloS one* **6**.

Jin, Y., Tymen, S. D., Chen, D., Fang, Z. J., Zhao, Y., Dragas, D., Dai, Y., Marucha, P. T. and Zhou, X. F. (2013). MicroRNA-99 Family Targets AKT/mTOR Signaling Pathway in Dermal Wound Healing. *PloS one* **8**.

Kahvejian, A., Svitkin, Y. V., Sukarieh, R., M'Boutchou, M.-N. and Sonenberg, N. (2005). Mammalian poly (A)-binding protein is a eukaryotic translation initiation factor, which acts via multiple mechanisms. *Genes Dev.* **19**, 104-113.

Kalinowski, F. C., Giles, K. M., Candy, P. A., Ali, A., Ganda, C., Epis, M. R., Webster, R. J. and Leedman, P. J. (2012). Regulation of Epidermal Growth Factor Receptor Signaling and Erlotinib Sensitivity in Head and Neck Cancer Cells by miR-7. *PloS one* **7**.

Kantidakis, T., Ramsbottom, B. A., Birch, J. L., Dowding, S. N. and White, R. J. (2010). mTOR associates with TFIIIC, is found at tRNA and 5S rRNA genes, and targets their

repressor Maf1. *Proceedings of the National Academy of Sciences of the United States of America* **107**, 11823-11828.

Kassavetis, G. A., Braun, B. R., Nguyen, L. H. and Geiduschek, E. P. (1990). S. cerevisiae TFIIIB is the transcription initiation factor proper of RNA polymerase III, while TFIIIA and TFIIIC are assembly factors. *Cell* **60**, 235-245.

Kavsak, P., Rasmussen, R. K., Causing, C. G., Bonni, S., Zhu, H. T., Thomsen, G. H. and Wrana, J. L. (2000). Smad7 binds to Smurf2 to form an E3 ubiquitin ligase that targets the TGF beta receptor for degradation. *Mol. Cell* **6**, 1365-1375.

Kawada, S. and Ishii, N. (2009). Peripheral venous occlusion causing cardiac hypertrophy and changes in biological parameters in rats. *Eur. J. Appl. Physiol.* **105**, 909-917.

Keith, C. T. and Schreiber, S. L. (1995). PIK-RELATED KINASES - DNA-REPAIR, RECOMBINATION, AND CELL-CYCLE CHECKPOINTS. *Science* **270**, 50-51.

Keller, R. and Schmid, E. (1979). In vitro secretion of ecdysteroids by Y-organs and lack of secretion by mandibular organs of the crayfish following molt induction. *Journal of comparative physiology* **130**, 347-353.

Kerr, T., Roalson, E. H. and Rodgers, B. D. (2005). Phylogenetic analysis of the myostatin gene sub-family and the differential expression of a novel member in zebrafish. *Evolution & development* **7**, 390-400.

Khan, S. and Wang, C. H. (2014). ER stress in adipocytes and insulin resistance: Mechanisms and significance. *Molecular Medicine Reports* **10**, 2234-2240.

Kim, D. H., Sarbassov, D. D., Ali, S. M., King, J. E., Latek, R. R., Erdjument-Bromage, H., Tempst, P. and Sabatini, D. M. (2002). MTOR interacts with Raptor to form a nutrient-sensitive complex that signals to the cell growth machinery. *Cell* **110**, 163-175.

Kim, E., Goraksha-Hicks, P., Li, L., Neufeld, T. P. and Guan, K. L. (2008). Regulation of TORC1 by Rag GTPases in nutrient response. *Nat. Cell Biol.* **10**, 935-945.

Kim, H. W., Batista, L. A., Hoppes, J. L., Lee, K. J. and Mykles, D. L. (2004a). A crustacean nitric oxide synthase expressed in nerve ganglia, Y-organ, gill and gonad of the tropical land crab, *Gecarcinus lateralis*. *J. Exp. Biol.* **207**, 2845-2857.

Kim, H. W., Chang, E. S. and Mykles, D. L. (2005a). Three calpains and ecdysone receptor in the land crab *Gecarcinus lateralis*: Sequences, expression and effects of elevated ecdysteroid induced by eyestalk ablation. *J. Exp. Biol.* **208**, 3177-3197.

Kim, H. W., Lee, S. G. and Mykles, D. L. (2005b). Ecdysteroid-responsive genes, RXR and E75, in the tropical land crab, *Gecarcinus lateralis*: Differential tissue expression of multiple RXR isoforms generated at three alternative splicing sites in the hinge and ligand-binding domains. *Mol. Cell. Endocrinol.* **242**, 80-95.

Kim, H. W., Mykles, D. L., Goetz, F. W. and Roberts, S. B. (2004b). Characterization of a myostatin-like gene from the bay scallop, *Argopecten irradians*. *Biochim. Biophys. Acta* **1679**, 174-179.

Kim, J. and Guan, K. L. (2011). Amino Acid Signaling in TOR Activation. In *Annual Review of Biochemistry, Vol 80*, vol. 80 eds. R. D. Kornberg C. R. H. Raetz J. E. Rothman and J. W. Thorner), pp. 1001-1032.

Kim, K.-S., Jeon, J.-M. and Kim, H.-W. (2009a). A Myostain-like Gene Expressed Highly in the Muscle Tissue of Chinese mitten crab, Eriocheir sinensis. *Fisheries and aquatic sciences* **12**, 185-193.

Kim, K.-y., Baek, A., Hwang, J.-E., Choi, Y. A., Jeong, J., Lee, M.-S., Cho, D. H., Lim, J.-S., Kim, K. I. and Yang, Y. (2009b). Adiponectin-activated AMPK stimulates dephosphorylation of AKT through protein phosphatase 2A activation. *Cancer Res.* **69**, 4018-4026.

Kim, K. S., Kim, Y. J., Jeon, J. M., Kang, Y. S., Kang, Y. S., Oh, C. W. and Kim, H. W. (2010). Molecular characterization of myostatin-like genes expressed highly in the muscle tissue from Morotoge shrimp, Pandalopsis japonica. *Aquacult. Res.* **41**, e862-e871.

Kim, S. G., Buel, G. R. and Blenis, J. (2013). Nutrient regulation of the mTOR Complex 1 signaling pathway. *Molecules and Cells* **35**, 463-473.

Kimura, N., Tokunaga, C., Dalal, S., Richardson, C., Yoshino, K. i., Hara, K., Kemp, B. E., Witters, L. A., Mimura, O. and Yonezawa, K. (2003). A possible linkage between AMP-activated protein kinase (AMPK) and mammalian target of rapamycin (mTOR) signalling pathway. *Genes Cells* **8**, 65-79.

King-Jones, K. and Thummel, C. S. (2005). Nuclear receptors--A perspective from Drosophila. *Nat. Rev. Genet.* **6**, 311-323.

Kingan, T. G. (1989). A competitive enzyme-linked immunosorbent-assay - Applications in the assay of peptides, steroids, and cyclic-nucleotides. *Anal. Biochem.* **183**, 283-289.

Kivilaak.E and Rytomaa, T. (1971). Erythrocytic chalone, a tissue-specific inhibitor of cell proliferation in erythron. *Cell and Tissue Kinetics* **4**, 1-&.

Klein, J. M., Dekleijn, D. P. V., Hunemeyer, G., Keller, R. and Weidemann, W. (1993). Demonstration of the cellular expression of genes encoding molt-inhibiting hormone and crustacean hyperglycemic hormone in the eyestalk of the shore crab *Carcinus-maenas*. *Cell Tissue Res.* **274**, 515-519.

Koelle, M. R., Talbot, W. S., Segraves, W. A., Bender, M. T., Cherbas, P. and Hogness, D. S. (1991). The Drosophila EcR gene encodes an ecdysone receptor, a new member of the steroid receptor superfamily. *Cell* **67**, 59-77.

Koenders, A., Yu, X., Chang, E. S. and Mykles, D. L. (2002). Ubiquitin and actin expression in claw muscles of land crab, *Gecarcinus lateralis*, and American lobster, *Homarus americanus*: Differential expression of ubiquitin in two slow muscle fiber types during molt-induced atrophy. *The Journal of experimental zoology* **292**, 618-632.

Koh, A., Lee, M. N., Yang, Y. R., Jeong, H., Ghim, J., Noh, J., Kim, J., Ryu, D., Park, S., Song, P. et al. (2013). C1-Ten Is a Protein Tyrosine Phosphatase of Insulin Receptor Substrate 1 (IRS-1), Regulating IRS-1 Stability and Muscle Atrophy. *Mol. Cell. Biol.* **33**, 1608-1620.

Koinuma, D., Tsutsumi, S., Kamimura, N., Taniguchi, H., Miyazawa, K., Sunamura, M., Imamura, T., Miyazono, K. and Aburatani, H. (2009). Chromatin Immunoprecipitation on Microarray Analysis of Smad2/3 Binding Sites Reveals Roles of ETS1 and TFAP2A in Transforming Growth Factor beta Signaling. *Mol. Cell. Biol.* **29**, 172-186.

Komamura, K., Shirotani-Ikejima, H., Tatsumi, R., Tsujita-Kuroda, Y., Kitakaze, M., Miyatake, K., Sunagawa, K. and Miyata, T. (2003). Differential gene expression in the rat skeletal and heart muscle in glucocorticoid-induced myopathy: Analysis by microarray. *Cardiovascular Drugs and Therapy* **17**, 303-310.

Kovacina, K. S., Park, G. Y., Bae, S. S., Guzzetta, A. W., Schaefer, E., Birnbaum, M. J. and Roth, R. A. (2003). Identification of a proline-rich Akt substrate as a 14-3-3 binding partner. *J. Biol. Chem.* **278**, 10189-10194.

Krieg, J., Hofsteenge, J. and Thomas, G. (1988). Identification of the 40-S-ribosomal protein S6 phosphorylation sites induced by cycloheximide. *J. Biol. Chem.* **263**, 11473-11477.

Kucharski, L. C., Capp, E., Chitto, A. L. F., Trapp, M., Da Silva, R. S. M. and Marques, M. (1999). Insulin signaling: Tyrosine kinase activity in the crab *Chasmagnathus granulata* gills. *J. Exp. Zool.* **283**, 91-94.

Kucharski, L. C., Schein, V., Capp, E. and da Silva, R. S. (2002). In vitro insulin stimulatory effect on glucose uptake and glycogen synthesis in the gills of the estuarine crab *Chasmagnathus granulata*. *Gen. Comp. Endocrinol.* **125**, 256-263.

Kume, K., Iizumi, Y., Shimada, M., Ito, Y., Kishi, T., Yamaguchi, Y. and Handa, H. (2010). Role of N-end rule ubiquitin ligases UBR1 and UBR2 in regulating the leucine-mTOR signaling pathway. *Genes Cells* **15**, 339-349.

Kuo, T., Harris, C. A. and Wang, J. C. (2013). Metabolic functions of glucocorticoid receptor in skeletal muscle. *Mol. Cell. Endocrinol.* **380**, 79-88.

Kuo, T. Y., Lew, M. J., Mayba, O., Harris, C. A., Speed, T. P. and Wang, J. C. (2012). Genome-wide analysis of glucocorticoid receptor-binding sites in myotubes identifies gene networks modulating insulin signaling. *Proceedings of the National Academy of Sciences of the United States of America* **109**, 11160-11165.

Lachaise, F., Leroux, A., Hubert, M. and Lafont, R. (1993). The molting gland of crustaceans - Localization, activity, and endocrine control (a review). *J. Crustac. Biol.* **13**, 198-234.

Laerum, O. D., Frostad, S., Ton, H. I. and Kamp, D. (1990). The sequence of the hemoregulatory peptide is present in G-1-alpha proteins. *FEBS Lett.* **269**, 11-14.

LaMarca, M., Allison, D. and Skinner, D. (1981). Irreversible denaturation mapping of a pyrimidine-rich domain of a complex satellite DNA. *J. Biol. Chem.* **256**, 6475-6479.

Lander, A. D. (2011). Pattern, growth, and control. *Cell* **144**, 955-969.

Laplante, M. and Sabatini, D. M. (2012). mTOR signaling in growth control and disease. *Cell* **149**, 274-293.

Laplante, M. and Sabatini, D. M. (2013). Regulation of mTORC1 and its impact on gene expression at a glance. *J. Cell Sci.* **126**, 1713-1719.

Larkin, M. A., Blackshields, G., Brown, N., Chenna, R., McGettigan, P. A., McWilliam, H., Valentin, F., Wallace, I. M., Wilm, A. and Lopez, R. (2007). Clustal W and Clustal X version 2.0. *Bioinformatics* **23**, 2947-2948.

Lau, G. W., Hassett, D. J., Ran, H. M. and Kong, F. S. (2004). The role of pyocyanin in Pseudomonas aeruginosa infection. *Trends Mol. Med.* **10**, 599-606.

Lau, N. C., Lim, L. P., Weinstein, E. G. and Bartel, D. P. (2001). An abundant class of tiny RNAs with probable regulatory roles in Caenorhabditis elegans. *Science* **294**, 858-862.

Lee, A. V., Gooch, J. L., Oesterreich, S., Guler, R. L. and Yee, D. (2000). Insulin-like growth factor I-induced degradation of insulin receptor substrate 1 is mediated by the 26S proteasome and blocked by phosphatidylinositol 3 '-kinase inhibition. *Mol. Cell. Biol.* **20**, 1489-1496.

Lee, S. G., Bader, B. D., Chang, E. S. and Mykles, D. L. (2007a). Effects of elevated ecdysteroid on tissue expression of three guanylyl cyclases in the tropical land crab Gecarcinus lateralis: possible roles of neuropeptide signaling in the molting gland. *J. Exp. Biol.* **210**, 3245-3254.

Lee, S. G., Kim, H. W., Bader, B. D., Chang, E. S. and Mykles, D. L. (2007b). Effects of elevated ecdysteroid on expression of three guanylyl cyclases in tropical land crab, Gecarcinus lateralis. *Integr. Comp. Biol.* **45**, 1158-1158.

Lee, S. J. (2004). Regulation of muscle mass by myostatin. *Annu. Rev. Cell. Dev. Biol.* **20**, 61-86.

Lee, S. J., Huynh, T. V., Lee, Y. S., Sebald, S. M., Wilcox-Adelman, S. A., Iwamori, N., Lepper, C., Matzuk, M. M. and Fan, C. M. (2012). Role of satellite cells versus myofibers in muscle hypertrophy induced by inhibition of the myostatin/activin signaling pathway. *Proceedings of the National Academy of Sciences of the United States of America* **109**, E2353-E2360.

Lee, S. J. and McPherron, A. C. (1999). Myostatin and the control of skeletal muscle mass. *Curr. Opin. Genet. Dev.* **9**, 604-607.

Lee, S. J. and McPherron, A. C. (2001). Regulation of myostatin activity and muscle growth. *Proceedings of the National Academy of Sciences of the United States of America* **98**, 9306-9311.

Lehmann, M. and Korge, G. (1995). Ecdysone regulation of the *Drosophila* SGS-4 gene is mediated by the synergistic action of ecdysone receptor and SEBP-3. *EMBO J.* **14**, 716-726.

Lehmann, W., Widmaier, R. and Langen, P. (1989). Response of different mammary epithelial-cell lines to a mammary derived growth inhibitor (MDGI). *Biomedica Biochimica Acta* **48**, 143-151.

Lenfant, M., Wdzieczakbakala, J., Guittet, E., Prome, J. C., Sotty, D. and Frindel, E. (1989). Inhibitor of hematopoietic pluripotent stem-cell proliferation - purification and determination of its structure. *Proceedings of the National Academy of Sciences of the United States of America* **86**, 779-782.

Lequieu, J., Chakrabarti, A., Nayak, S. and Varner, J. D. (2011). Computational Modeling and Analysis of Insulin Induced Eukaryotic Translation Initiation. *PLoS Comp. Biol.* **7**.

Li, H., Fan, J., Liu, S., Yang, Q., Mu, G. and He, C. (2012a). Characterization of a myostatin gene (MSTN1) from spotted halibut (*Verasper variegatus*) and association between its

promoter polymorphism and individual growth performance. *Comp Biochem Physiol B Biochem Mol Biol* **161**, 315-322.

Li, J., Deng, J., Yu, S., Zhang, J., Cheng, D. and Wang, H. (2012b). The virtual element in proximal promoter of porcine myostatin is regulated by myocyte enhancer factor 2C. *Biochem. Biophys. Res. Commun.* **419**, 175-181.

Li, J., You, T. and Jing, J. (2014). MiR-125b inhibits cell biological progression of Ewing's sarcoma by suppressing the PI3K/Akt signalling pathway. *Cell Proliferation* **47**, 152-160.

Li, J. B. and Goldberg, A. L. (1976). Effects of food-deprivation on protein-synthesis and degradation in rat skeletal-muscles. *American Journal of Physiology* **231**, 441-448.

Li, X. J., Luo, X. Q., Han, B. W., Duan, F. T., Wei, P. P. and Chen, Y. Q. (2013a). MicroRNA-100/99a, deregulated in acute lymphoblastic leukaemia, suppress proliferation and promote apoptosis by regulating the FKBP51 and IGF1R/mTOR signalling pathways. *Br. J. Cancer* **109**, 2189-2198.

Li, Y., Wang, X., Yue, P., Tao, H., Ramalingam, S. S., Owonikoko, T. K., Deng, X., Wang, Y., Fu, H., Khuri, F. R. et al. (2013b). Protein Phosphatase 2A and DNA-dependent Protein Kinase Are Involved in Mediating Rapamycin-induced Akt Phosphorylation. *J. Biol. Chem.* **288**, 13215-13224.

Liang, Z., Li, Y., Huang, K., Wagar, N. and Shim, H. (2011). Regulation of miR-19 to breast cancer chemoresistance through targeting PTEN. *Pharmaceutical research* **28**, 3091-3100.

Lin, X., Duan, X. Y., Liang, Y. Y., Su, Y., Wrighton, K. H., Long, J. Y., Hu, M., Davis, C. M., Wang, J. R., Brunicardi, F. C. et al. (2006). PPM1A functions as a Smad phosphatase to terminate TGF beta signaling. *Cell* **125**, 915-928.

Lindenskov, P. H. H., Paulsen, J. E., Reichelt, K. L. and Elgjo, K. (2002). Endogenous tetrapeptide from neuroblastoma and new-born pig brain inhibits neuroblastoma cell growth in vitro. *Anticancer Res.* **22**, 2847-2851.

Liu, H., Jiravanichpaisal, P., Soderhall, I., Cerenius, L. and Soderhall, K. (2006). Antilipopolysaccharide factor interferes with white spot syndrome virus replication in vitro and in vivo in the crayfish *Pacifastacus leniusculus*. *J. Virol.* **80**, 10365-10371.

Liu, H., Zhu, L., Liu, B., Yang, L., Meng, X., Zhang, W., Ma, Y. and Xiao, H. (2012). Genome-wide microRNA profiles identify miR-378 as a serum biomarker for early detection of gastric cancer. *Cancer Lett.* **316**, 196-203.

Liu, P. and Wilson, M. J. (2012). miR-520c and miR-373 upregulate MMP9 expression by targeting mTOR and SIRT1, and activate the Ras/Raf/MEK/Erk signaling pathway and NF-kappa B factor in human fibrosarcoma cells. *Journal of Cellular Physiology* **227**, 867-876.

Liu, Y., Elgjo, K., Wright, M. and Reichelt, K. L. (2000). Novel lymphocyte growth-inhibiting tripeptide: N-acetyl-glu-ser-GlyNH(2). *Biochem. Biophys. Res. Commun.* **277**, 562-567.

Liu, Y., Reichelt, W. H., Luna, L., Elgjo, K. and Reichelt, K. L. (2003). The effects of a growth-inhibiting tripeptide, AcetylGlu-Ser-GlyNH(2) (Ac-ESG), on gene expression and cell cycle progression of two lymphoma cell lines. *Anticancer Res.* **23**, 3159-3165.

Liu, Y. F., Paz, K., Herschkovitz, A., Alt, A., Tennenbaum, T., Sampson, S. R., Ohba, M., Kuroki, T., LeRoith, D. and Zick, Y. (2001). Insulin stimulates PKC zeta-mediated phosphorylation of insulin receptor substrate-1 (IRS-1) - A self-attenuated mechanism to negatively regulate the function of IRS proteins. *J. Biol. Chem.* **276**, 14459-14465.

Loewith, R., Jacinto, E., Wullschleger, S., Lorberg, A., Crespo, J. L., Bonenfant, D., Oppliger, W., Jenoe, P. and Hall, M. N. (2002). Two TOR complexes, only one of which is rapamycin sensitive, have distinct roles in cell growth control. *Mol. Cell* **10**, 457-468.

Lofberg, E., Gutierrez, A., Wernerman, J., Anderstam, B., Mitch, W. E., Price, S. R., Bergstrom, J. and Alvestrand, A. (2002). Effects of high doses of glucocorticoids on free amino acids, ribosomes and protein turnover in human muscle. *European journal of clinical investigation* **32**, 345-353.

Lokireddy, S., Mouly, V., Butler-Browne, G., Gluckman, P. D., Sharma, M., Kambadur, R. and McFarlane, C. (2011). Myostatin promotes the wasting of human myoblast cultures through promoting ubiquitin-proteasome pathway-mediated loss of sarcomeric proteins. *Am. J. Physiol. Cell Physiol.* **301**, C1316-1324.

Long, D. B., Zhang, K. Y., Chen, D. W., Ding, X. M. and Yu, B. (2009). Effects of active immunization against myostatin on carcass quality and expression of the myostatin gene in pigs. *Animal Science Journal* **80**, 585-590.

Lundholm, K., Bennegard, K., Eden, E., Svaninger, G., Emery, P. W. and Rennie, M. J. (1982). Efflux of 3-methylhistidine from the leg in cancer-patients who experience weight-loss. *Cancer Res.* **42**, 4807-4811.

Ma, K., Mallidis, C., Artaza, J., Taylor, W., Gonzalez-Cadavid, N. and Bhasin, S. (2001). Characterization of 5 '-regulatory region of human myostatin gene: Regulation by dexamethasone in vitro. *American Journal of Physiology-Endocrinology and Metabolism* **281**, E1128-E1136.

Ma, K., Mallidis, C., Bhasin, S., Mahabadi, V., Artaza, J., Gonzalez-Cadavid, N., Arias, J. and Salehian, B. (2003). Glucocorticoid-induced skeletal muscle atrophy is associated with upregulation of myostatin gene expression. *American journal of physiology. Endocrinology and metabolism* **285**, E363-371.

Ma, L., Chen, Z. B., Erdjument-Bromage, H., Tempst, P. and Pandolfi, P. P. (2005). Phosphorylation and functional inactivation of TSC2 by Erk: Implications for tuberous sclerosis and cancer pathogenesis. *Cell* **121**, 179-193.

MacDonald, E. M., Andres-Mateos, E., Mejias, R., Simmers, J. L., Mi, R. F., Park, J. S., Ying, S., Hoke, A., Lee, S. J. and Cohn, R. D. (2014). Denervation atrophy is independent from Akt and mTOR activation and is not rescued by myostatin inhibition. *Disease Models & Mechanisms* **7**, 471-481.

Macias, M. J., Martin-Malpartida, P. and Massague, J. (2015). Structural determinants of Smad function in TGF-beta signaling. *Trends Biochem. Sci.* **40**, 296-308.

MacLea, K. S., Abuhagr, A. M., Pitts, N. L., Covi, J. A., Bader, B. D., Chang, E. S. and Mykles, D. L. (2012). Rheb, an activator of target of rapamycin, in the blackback land crab, *Gecarcinus lateralis*: Cloning and effects of molting and unweighting on expression in skeletal muscle. *J. Exp. Biol.* **215**, 590-604.

MacLea, K. S., Covi, J. A., Kim, H. W., Chao, E., Medler, S., Chang, E. S. and Mykles, D. L. (2010). Myostatin from the American lobster, *Homarus americanus*: Cloning and effects of molting on expression in skeletal muscles. *Comp Biochem Physiol A Mol Integr Physiol* **157**, 328-337.

Maehama, T. and Dixon, J. E. (1999). PTEN: a tumour suppressor that functions as a phospholipid phosphatase. *Trends Cell Biol.* **9**, 125-128.

Maehama, T., Tanaka, M., Nishina, H., Murakami, M., Kanaho, Y. and Hanada, K. (2008). RalA Functions as an Indispensable Signal Mediator for the Nutrient-sensing System. *J. Biol. Chem.* **283**, 35053-35059.

Mahajan, P. B. (1994). Modulation of transcription of ribosomal-RNA genes by rapamycin. *Int. J. Immunopharmacol.* **16**, 711-721.

Mak, R. H. and Cheung, W. W. (2009). Transforming growth factors and insulin-like growth factors in chronic kidney disease. *Journal of Organ Dysfunction* **5**, 59-64.

Malik, A. R., Urbanska, M., Macias, M., Skalecka, A. and Jaworski, J. (2013). Beyond control of protein translation: What we have learned about the non-canonical regulation and function of mammalian target of rapamycin (mTOR). *Biochim. Biophys. Acta* **1834**, 1434-1448.

Mantovani, R. (1998). A survey of 178 NF-Y binding CCAAT boxes. *Nucleic Acids Res.* **26**, 1135-1143.

Marcotte, G. R., West, D. W. and Baar, K. (2014). The Molecular Basis for Load-Induced Skeletal Muscle Hypertrophy. *Calcif. Tissue Int.*, 1-15.

Martin, K. S., Blemker, S. S. and Peirce, S. M. (2015). Agent-based computational model investigates muscle-specific responses to disuse-induced atrophy. *J. Appl. Physiol.* **118**, 1299-1309.

Massague, J. (2012). TGF beta signalling in context. *Nature Reviews Molecular Cell Biology* **13**, 616-630.

Massague, J., Seoane, J. and Wotton, D. (2005). Smad transcription factors. *Genes Dev.* **19**, 2783-2810.

Matsakas, A., Bozzo, C., Cacciani, N., Caliaro, F., Reggiani, C., Mascarello, F. and Patruno, M. (2006). Effect of swimming on myostatin expression in white and red gastrocnemius muscle and in cardiac muscle of rats. *Experimental Physiology* **91**, 983-994.

Matsakas, A. and Patel, K. (2009). Intracellular signalling pathways regulating the adaptation of skeletal muscle to exercise and nutritional changes. *Histology and Histopathology* **24**, 209-222.

Mayer, C., Zhao, J., Yuan, X. J. and Grummt, I. (2004). mTOR-dependent activation of the transcription factor TIMA links rRNA synthesis to nutrient availability. *Genes Dev.* **18**, 423-434.

McBride, A., Ghilagaber, S., Nikolaev, A. and Hardie, D. G. (2009). The Glycogen-Binding Domain on the AMPK beta Subunit Allows the Kinase to Act as a Glycogen Sensor. *Cell metabolism* **9**, 23-34.

McCarthy, J. F. (1982). Ecdysone metabolism in pre-molt land crabs (*Gecarcinus lateralis*). *Gen. Comp. Endocrinol.* **47**, 323-332.

McCarthy, J. F. and Skinner, D. M. (1977a). Interactions between molting and regeneration in the land crab *Gecarcinus lateralis*. 3. Interruption of proecdysis by autotomy of partially regenerated limbs in the land crab, *Gecarcinus lateralis*. *Dev. Biol.* **61**, 299-310.

McCarthy, J. F. and Skinner, D. M. (1977b). Interactions between molting and regeneration. 2. Pro-ecdysial changes in serum ecdysone titers, gastrolith formation, and limb regeneration following molt induction by limb autotomy and-or eyestalk removal in land crab, G*ecarcinus lateralis*. *Gen. Comp. Endocrinol.* **33**, 278-292.

McCarthy, J. F. and Skinner, D. M. (1979). Metabolism of alpha-ecdysone in intermolt land crabs (*Gecarcinus lateralis*). *Gen. Comp. Endocrinol.* **37**, 250-263.

McFarlane, C., Langley, B., Thomas, M., Hennebry, A., Plummer, E., Nicholas, G., McMahon, C., Sharma, M. and Kambadur, R. (2005). Proteolytic processing of myostatin is auto-regulated during myogenesis. *Dev. Biol.* **283**, 58-69.

McFarlane, C., Plummer, E., Thomas, M., Hennebry, A., Ashby, M., Ling, N., Smith, H., Sharma, M. and Kambadur, R. (2006). Myostatin induces cachexia by activating the ubiquitin proteolytic system through an NF-kappa B-independent, FoxO1-dependent mechanism. *Journal of Cellular Physiology* **209**, 501-514.

McFarlane, C., Vajjala, A., Arigela, H., Lokireddy, S., Ge, X., Bonala, S., Manickam, R., Kambadur, R. and Sharma, M. (2014). Negative Auto-Regulation of Myostatin Expression is Mediated by Smad3 and MicroRNA-27. *PloS one* **9**.

McKnight, S. L. (1997). Gatekeepers of organ growth. *Proceedings of the National Academy of Sciences of the United States of America* **94**, 12249-12250.

McPherron, A. and Lee, S.-J. (2002). Suppression of body fat accumulation in myostatin-deficient mice. *J. Clin. Invest.* **109**, 595-601.

McPherron, A. C., Lawler, A. M. and Lee, S. J. (1997). Regulation of skeletal muscle mass in mice by a new TGF-beta superfamily member. *Nature* **387**, 83-90.

McPherron, A. C. and Lee, S. J. (1997). Double muscling in cattle due to mutations in the myostatin gene. *Proceedings of the National Academy of Sciences of the United States of America* **94**, 12457-12461.

Medler, S., Brown, K. J., Chang, E. S. and Mykles, D. L. (2005). Eyestalk ablation has little effect on actin and myosin heavy chain gene expression in adult lobster skeletal muscles. *Biol. Bull.* **208**, 127-137.

Mehra, A. and Wrana, J. L. (2002). TGF-β and the Smad signal transduction pathway. *Biochem. Cell Biol.* **80**, 605-622.

Mendez, R., Myers, M., White, M. F. and Rhoads, R. E. (1996). Stimulation of protein synthesis, eukaryotic translation initiation factor 4E phosphorylation, and PHAS-I phosphorylation by insulin requires insulin receptor substrate 1 and phosphatidylinositol 3-kinase. *Mol. Cell. Biol.* **16**, 2857-2864.

Meng, F. Y., Henson, R., Lang, M., Wehbe, H., Maheshwari, S., Mendell, J. T., Jiang, J. M., Schmittgen, T. D. and Patel, T. (2006). Involvement of human micro-RNA in growth

and response to chemotherapy in human cholangiocarcinoma cell lines. *Gastroenterology* **130**, 2113-2129.

Menon, S., Dibble, C. C., Talbott, G., Hoxhaj, G., Valvezan, A. J., Takahashi, H., Cantley, L. C. and Manning, B. D. (2014). Spatial Control of the TSC Complex Integrates Insulin and Nutrient Regulation of mTORC1 at the Lysosome. *Cell* **156**, 771-785.

Méthot, N., Song, M. S. and Sonenberg, N. (1996). A region rich in aspartic acid, arginine, tyrosine, and glycine (DRYG) mediates eukaryotic initiation factor 4B (eIF4B) self-association and interaction with eIF3. *Mol. Cell. Biol.* **16**, 5328-5334.

Michels, A. A., Robitaille, A. M., Buczynski-Ruchonnet, D., Hodroj, W., Reina, J. H., Hall, M. N. and Hernandez, N. (2010). mTORC1 Directly Phosphorylates and Regulates Human MAF1. *Mol. Cell. Biol.* **30**, 3749-3757.

Mieulet, V., Roceri, M., Espeillac, C., Sotiropoulos, A., Ohanna, M., Oorschot, V., Klumperman, J., Sandri, M. and Pende, M. (2007). S6 kinase inactivation impairs growth and translational target phosphorylation in muscle cells maintaining proper regulation of protein turnover. *American Journal of Physiology-Cell Physiology* **293**, C712-C722.

Miron, M., Lasko, P. and Sonenberg, N. (2003). Signaling from Akt to FRAP/TOR targets both 4E-BP and S6K in *Drosophila melanogaster*. *Mol. Cell. Biol.* **23**, 9117-9126.

Mirth, C. K. and Shingleton, A. W. (2012). Integrating body and organ size in *Drosophila*: Recent advances and outstanding problems. *Frontiers in endocrinology* **3**, 49.

Mitch, W. E. and Goldberg, A. L. (1996). Mechanisms of disease - Mechanisms of muscle wasting - The role of the ubiquitin-proteasome pathway. *New Engl. J. Med.* **335**, 1897-1905.

Miura, S., Takeshita, T., Asao, H., Kimura, Y., Murata, K., Sasaki, Y., Hanai, J., Beppu, H., Tsukazaki, T., Wrana, J. L. et al. (2000). Hgs (Hrs), a FYVE domain protein, is involved in Smad signaling through cooperation with SARA. *Mol. Cell. Biol.* **20**, 9346-9355.

Miyazaki, M. and Esser, K. A. (2009). Cellular mechanisms regulating protein synthesis and skeletal muscle hypertrophy in animals. *J Appl Physiol (1985)* **106**, 1367-1373.

Moir, R. D. and Willis, I. M. (2013). Regulation of pol III transcription by nutrient and stress signaling pathways. *Biochimica Et Biophysica Acta-Gene Regulatory Mechanisms* **1829**, 361-375.

Moon, H., Weissbac.H and Redfield, B. (1972). Interaction of eukaryote elongation factor EF 1 with guanosine nucleotides and aminoacyl transfer RNA. *Proceedings of the National Academy of Sciences of the United States of America* **69**, 1249-&.

Moorhead, J. F., Paraskov.E, Pirrie, A. J. and Hayes, C. (1969). Lymphoid inhibitor of human lymphocyte DNA synthesis and mitosis in vitro. *Nature* **224**, 1207-&.

Moras, D. and Gronemeyer, H. (1998). The nuclear receptor ligand-binding domain: structure and function. *Curr. Opin. Cell Biol.* **10**, 384-391.

Morgan, S. A., Sherlock, M., Gathercole, L. L., Lavery, G. G., Lenaghan, C., Bujalska, I. J., Laber, D., Yu, A., Convey, G., Mayers, R. et al. (2009). 11 beta-Hydroxysteroid Dehydrogenase Type 1 Regulates Glucocorticoid-Induced Insulin Resistance in Skeletal Muscle. *Diabetes* **58**, 2506-2515.

Moriyasu, M. and Mallet, P. (1986). Molt stages of the snow crab *Chionoecetes opilio* by observation of morphogenesis of setae on the maxilla. *J. Crustac. Biol.* **6**, 709-718.

Morrison, B. M., Lachey, J. L., Warsing, L. C., Ting, B. L., Pullen, A. E., Underwood, K. W., Kumar, R., Sako, D., Grinberg, A., Wong, V. et al. (2009). A soluble activin type IIB receptor improves function in a mouse model of amyotrophic lateral sclerosis. *Exp. Neurol.* **217**, 258-268.

Mott, J. L., Kobayashi, S., Bronk, S. F. and Gores, G. J. (2007). mir-29 regulates Mcl-1 protein expression and apoptosis. *Oncogene* **26**, 6133-6140.

Mouillet, J. F., Henrich, V. C., Lezzi, M. and Vögtli, M. (2001). Differential control of gene activity by isoforms A, B1 and B2 of the Drosophila ecdysone receptor. *Eur. J. Biochem.* **268**, 1811-1819.

Mykles, D. L. (1988). Histochemical and biochemical characterization of two slow fiber types in decapod crustacean muscles. *J. Exp. Zool.* **245**, 232-243.

Mykles, D. L. (1992). Getting out of a tight squeeze—enzymatic regulation of claw muscle atrophy in molting. *Am. Zool.* **32**, 485-494.

Mykles, D. L. (1997). Crustacean muscle plasticity: Molecular mechanisms determining mass and contractile properties. *Comparative Biochemistry and Physiology B-Biochemistry & Molecular Biology* **117**, 367-378.

Mykles, D. L. (1999). Proteolytic processes underlying molt-induced claw muscle atrophy in decapod crustaceans. *Am. Zool.* **39**, 541-551.

Mykles, D. L. (2001). Interactions between limb regeneration and molting in decapod crustaceans. *Am. Zool.* **41**, 399-406.

Mykles, D. L. (2011). Ecdysteroid metabolism in crustaceans. *J. Steroid Biochem. Mol. Biol.* **127**, 196-203.

Mykles, D. L. and Medler, S. (2015). Skeletal muscle differentiation, growth, and plasticity. In *Natural History of Crustacea*, vol. 4 Physiology eds. E. S. Chang and M. Thiel), pp. 134-167. Oxford University Press: Oxford.

Mykles, D. L. and Skinner, D. M. (1981). Preferential loss of thin-filaments during molt-induced atrophy in crab claw muscle. *Journal of Ultrastructure Research* **75**, 314-325.

Mykles, D. L. and Skinner, D. M. (1982a). Crustacean muscles - Atrophy and regeneration during molting. *J. Gen. Physiol.* **78**, A6-A7.

Mykles, D. L. and Skinner, D. M. (1982b). Molt cycle-associated changes in calcium-dependent proteinase activity that degrades actin and myosin in crustacean muscle. *Dev. Biol.* **92**, 386-397.

Mykles, D. L. and Skinner, D. M. (1990). Atrophy of crustacean somatic muscle and the proteinases that do the job - A review. *J. Crustac. Biol.* **10**, 577-594.

Nadjar-Boger, E., Hinits, Y. and Funkenstein, B. (2012). Structural and functional analysis of myostatin-2 promoter alleles from the marine fish *Sparus aurata*: Evidence for strong muscle-specific promoter activity and post-transcriptional regulation. *Mol. Cell. Endocrinol.* **361**, 51-68.

Nadjar-Boger, E., Maccatrozzo, L., Radaelli, G. and Funkenstein, B. (2013). Genomic cloning and promoter functional analysis of myostatin-2 in shi drum, *Umbrina cirrosa*: Conservation of muscle-specific promoter activity. *Comp Biochem Physiol B Biochem Mol Biol* **164**, 99-110.

Nagaraja, A. K., Creighton, C. J., Yu, Z., Zhu, H., Gunaratne, P. H., Reid, J. G., Olokpa, E., Itamochi, H., Ueno, N. T. and Hawkins, S. M. (2010). A link between mir-100 and FRAP1/mTOR in clear cell ovarian cancer. *Mol. Endocrinol.* **24**, 447-463.

Nakagawa, Y. and Henrich, V. C. (2009). Arthropod nuclear receptors and their role in molting. *FEBS J.* **276**, 6128-6157.

Narasimhan, J., Staschke, K. A. and Wek, R. C. (2004). Dimerization is required for activation of eIF2 kinase Gcn2 in response to diverse environmental stress conditions. *J. Biol. Chem.* **279**, 22820-22832.

Nho, R. S. and Peterson, M. (2011). Eukaryotic Translation Initiation Factor 4E Binding Protein 1 (4EBP-1) Function Is Suppressed by Src and Protein Phosphatase 2A (PP2A) on Extracellular Matrix. *J. Biol. Chem.* **286**, 31953-31965.

Ni, Y. G., Wang, N., Sachan, N., Morris, D. J., Gerard, R. D., Kuro-o, M., Rothemel, B. A. and Hill, J. A. (2007). Foxo transcription factors activate Akt and attenuate insulin signaling through inhibition of protein phosphatases. *Circul. Res.* **101**, E74-E74.

Nicholas, K. and Nicholas, H. J. GeneDoc: a tool for editing and annotating multiple sequence alignments. 1997. *Distributed by the author*.

Nieva, C., Gwozdz, T., Dutko-Gwozdz, J., Wiedenmann, J., Spindler-Barth, M., Wieczorek, E., Dobrucki, J., Dus, D., Henrich, V., Ozyhar, A. et al. (2005). Ultraspiracle promotes the nuclear localization of ecdysteroid receptor in mammalian cells. *Biol. Chem.* **386**, 463-470.

Nilwik, R., Snijders, T., Leenders, M., Groen, B. B., van Kranenburg, J., Verdijk, L. B. and van Loon, L. J. (2013). The decline in skeletal muscle mass with aging is mainly attributed to a reduction in type II muscle fiber size. *Experimental gerontology* **48**, 492-498.

Nishita, Y. (2014). Ecdysone response elements in the distal promoter of the Bombyx Broad-Complex gene, BmBR-C. *Insect Mol. Biol.* **23**, 341-356.

No, D., Yao, T. P. and Evans, R. M. (1996). Ecdysone-inducible gene expression in mammalian cells and transgenic mice. *Proceedings of the National Academy of Sciences of the United States of America* **93**, 3346-3351.

Nojima, H., Tokunaga, C., Eguchi, S., Oshiro, N., Hidayat, S., Yoshino, K., Hara, K., Tanaka, N., Avruch, J. and Yonezawa, K. (2003). The mammalian target of rapamycin (mTOR) partner, raptor, binds the mTOR substrates p70 S6 kinase and 4E-BP1 through their TOR signaling (TOS) motif. *J. Biol. Chem.* **278**, 15461-15464.

Nunez-Acuna, G. and Gallardo-Escarate, C. (2014). The myostatin gene of *Mytilus chilensis* evidences a high level of polymorphism and ubiquitous transcript expression. *Gene* **536**, 207-212.

O'Malley, Y. Q., Abdalla, M. Y., McCormick, M. L., Reszka, K. J., Denning, G. M. and Britigan, B. E. (2003). Subcellular localization of Pseudomonas pyocyanin cytotoxicity in human lung epithelial cells. *American Journal of Physiology-Lung Cellular and Molecular Physiology* **284**, L420-L430.

Oakhill, J. S., Chen, Z. P., Scott, J. W., Steel, R., Castelli, L. A., Ling, N. M., Macaulay, S. L. and Kemp, B. E. (2010). beta-Subunit myristoylation is the gatekeeper for initiating

metabolic stress sensing by AMP-activated protein kinase (AMPK). *Proceedings of the National Academy of Sciences of the United States of America* **107**, 19237-19241.

Obrien, J. J., Mykles, D. L. and Skinner, D. M. (1986). Cold-induced apolysis in anecdysial Brachyurans. *Biol. Bull.* **171**, 450-460.

Oh, H.-K., Tan, A. L.-K., Das, K., Ooi, C.-H., Deng, N.-T., Tan, I. B., Beillard, E., Lee, J., Ramnarayanan, K. and Rha, S.-Y. (2011). Genomic loss of miR-486 regulates tumor progression and the OLFM4 antiapoptotic factor in gastric cancer. *Clin. Cancer. Res.* **17**, 2657-2667.

Oldham, S., Montagne, J., Radimerski, T., Thomas, G. and Hafen, E. (2000). Genetic and biochemical characterization of dTOR, the Drosophila homolog of the target of rapamycin. *Genes Dev.* **14**, 2689-2694.

Olive, V., Bennett, M. J., Walker, J. C., Ma, C., Jiang, I., Cordon-Cardo, C., Li, Q. J., Lowe, S. W., Hannon, G. J. and He, L. (2009). miR-19 is a key oncogenic component of mir-17-92. *Genes Dev.* **23**, 2839-2849.

Ozes, O. N., Akca, H., Mayo, L. D., Gustin, J. A., Maehama, T., Dixon, J. E. and Donner, D. B. (2001). A phosphatidylinositol 3-kinase/Akt/mTOR pathway mediates and PTEN antagonizes tumor necrosis factor inhibition of insulin signaling through insulin receptor substrate-1. *Proceedings of the National Academy of Sciences of the United States of America* **98**, 4640-4645.

Ozyhar, A. and Pongs, O. (1993). Mutational analysis of the interaction between ecdysteroid receptor and its response element. *J. Steroid Biochem. Mol. Biol.* **46**, 135-145.

Page, R. D. (2001). TreeView. *Glasgow University, Glasgow, UK*.

Palli, S. R., Kapitskaya, M. Z., Kumar, M. B. and Cress, D. E. (2003). Improved ecdysone receptor-based inducible gene regulation system. *Eur. J. Biochem.* **270**, 1308-1315.

Palli, S. R., Kapitskaya, M. Z. and Potter, D. W. (2005). The influence of heterodimer partner ultraspiracle/retinoid X receptor on the function of ecdysone receptor. *FEBS J.* **272**, 5979-5990.

Panguluri, S. K., Kumar, P. and Palli, S. R. (2006). Functional characterization of ecdysone receptor gene switches in mammalian cells. *FEBS J.* **273**, 5550-5563.

Paoli, A., Pacelli, Q. F., Neri, M., Toniolo, L., Cancellara, P., Canato, M., Moro, T., Quadrelli, M., Morra, A. and Faggian, D. (2015). Protein Supplementation Increases Postexercise Plasma Myostatin Concentration After 8 Weeks of Resistance Training in Young Physically Active Subjects. *J. Med. Food* **18**, 137-143.

Park, S., Zhao, D. W., Hatanpaa, K. J., Mickey, B. E., Saha, D., Boothman, D. A., Story, M. D., Wong, E. T., Burma, S., Georgescu, M. M. et al. (2009). RIP1 Activates PI3K-Akt via a Dual Mechanism Involving NF-kappa B-Mediated Inhibition of the mTOR-S6K-IRS1 Negative Feedback Loop and Down-regulation of PTEN. *Cancer Res.* **69**, 4107-4111.

Passano, L. M. (1960). Molting and its control. In *The physiology of crustacea*, vol. 1 (ed. T. H. Waterman), pp. 473-536. New York: Academic Press.

Passmore, L. A., Schmeing, T. M., Maag, D., Applefield, D. J., Acker, M. G., Algire, M. A., Lorsch, J. R. and Ramakrishnan, V. (2007). The eukaryotic translation initiation factors eIF1 and eIF1A induce an open conformation of the 40S ribosome. *Mol. Cell* **26**, 41-50.

Paukovits, W. R. and Laerum, O. D. (1982). Isolation and synthesis of a hemoregulatory peptide. *Zeitschrift Fur Naturforschung C-a Journal of Biosciences* **37**, 1297-1300.

Paulsen, J. E., Reichelt, K. L. and Petersen, A. K. (1987). Purification and characterization of a growth inhibitory hepatic peptide - a preliminary note. *Virchows Archiv B-Cell Pathology Including Molecular Pathology* **54**, 152-154.

Paz, K., Hemi, R., LeRoith, D., Karasik, A., Elhanany, E., Kanety, H. and Zick, Y. (1997). Elevated serine/threonine phosphorylation of IRS-1 and IRS-2 inhibits their binding to the juxtamembrane region of the insulin receptor and impairs their ability to undergo insulin-induced tyrosine phosphorylation. *J. Biol. Chem.* **272**, 29911-29918.

Paz, K., Liu, Y. F., Shorer, H., Hemi, R., LeRoith, D., Quan, M., Kanety, H., Seger, R. and Zick, Y. (1999). Phosphorylation of insulin receptor substrate-1 (IRS-1) by protein kinase B positively regulates IRS-1 function. *J. Biol. Chem.* **274**, 28816-28822.

Pende, M., Um, S. H., Mieulet, V., Sticker, M., Goss, V. L., Mestan, J., Mueller, M., Fumagalli, S., Kozma, S. C. and Thomas, G. (2004). S6K1(-/-)/S6K2(-/-) mice exhibit perinatal lethality and rapamycin-sensitive 5 '-terminal oligopyrimidine mRNA translation and reveal a mitogen-activated protein kinase-dependent S6 kinase pathway. *Mol. Cell. Biol.* **24**, 3112-3124.

Peterson, T. R., Laplante, M., Thoreen, C. C., Sancak, Y., Kang, S. A., Kuehl, W. M., Gray, N. S. and Sabatini, D. M. (2009). DEPTOR Is an mTOR Inhibitor Frequently Overexpressed in Multiple Myeloma Cells and Required for Their Survival. *Cell* **137**, 873-886.

Phillips, B. E., Hill, D. S. and Atherton, P. J. (2012). Regulation of muscle protein synthesis in humans. *Current Opinion in Clinical Nutrition and Metabolic Care* **15**, 58-63.

Phillips, S. M., Glover, E. I. and Rennie, M. J. (2009). Alterations of protein turnover underlying disuse atrophy in human skeletal muscle. *J Appl Physiol (1985)* **107**, 645-654.

Philpott, G. W. (1971). Tissue-specific inhibition of cell proliferation in embryonic stomach epithelium in-vitro. *Gastroenterology* **61**, 25-&.

Piccirillo, R., Demontis, F., Perrimon, N. and Goldberg, A. L. (2014). Mechanisms of muscle growth and atrophy in mammals and *Drosophila. Dev. Dyn.* **243**, 201-215.

Piccirillo, R. and Goldberg, A. L. (2012). The p97/VCP ATPase is critical in muscle atrophy and the accelerated degradation of muscle proteins. *EMBO J.* **31**, 3334-3350.

Populo, H., Lopes, J. M. and Soares, P. (2012). The mTOR Signalling Pathway in Human Cancer. *International Journal of Molecular Sciences* **13**, 1886-1918.

Potter, C. J., Pedraza, L. G. and Xu, T. (2002). Akt regulates growth by directly phosphorylating Tsc2. *Nat. Cell Biol.* **4**, 658-665.

Powers, T. and Walter, P. (1999). Regulation of ribosome biogenesis by the rapamycin-sensitive TOR-signaling pathway in Saccharomyces cerevisiae. *Molecular Biology of the Cell* **10**, 987-1000.

Price, E. R., Bauchinger, U., Zajac, D. M., Cerasale, D. J., McFarlan, J. T., Gerson, A. R., McWilliams, S. R. and Guglielmo, C. G. (2011). Migration- and exercise-induced changes to flight muscle size in migratory birds and association with IGF1 and myostatin mRNA expression. *J. Exp. Biol.* **214**, 2823-2831.

Proud, C. G. (2009). mTORC1 signalling and mRNA translation. *Biochem. Soc. Trans.* **37**, 227-231.

Qian, Z. Y., Mi, X., Wang, X. Z., He, S. L., Liu, Y. J., Hou, F. J., Liu, Q. and Liu, X. L. (2013). cDNA cloning and expression analysis of myostatin/GDF11 in shrimp, *Litopenaeus vannamei. Comparative Biochemistry and Physiology a-Molecular & Integrative Physiology* **165**, 30-39.

Qin, J., Du, R., Yang, Y. Q., Zhang, H. Q., Li, Q., Liu, L., Guan, H., Hou, J. and An, X. R. (2013). Dexamethasone-induced skeletal muscle atrophy was associated with upregulation of myostatin promoter activity. *Res. Vet. Sci.* **94**, 84-89.

Quy, P. N., Kuma, A., Pierre, P. and Mizushima, N. (2013). Proteasome-dependent activation of mammalian target of rapamycin complex 1 (mTORC1) is essential for autophagy suppression and muscle remodeling following denervation. *J. Biol. Chem.* **288**, 1125-1134.

Radaelli, G., Rowlerson, A., Mascarello, F., Patruno, M. and Funkenstein, B. (2003). Myostatin precursor is present in several tissues in teleost fish: a comparative immunolocalization study. *Cell Tissue Res.* **311**, 239-250.

Raught, B., Peiretti, F., Gingras, A. C., Livingstone, M., Shahbazian, D., Mayeur, G. L., Polakiewicz, R. D., Sonenberg, N. and Hershey, J. W. B. (2004). Phosphorylation of eucaryotic translation initiation factor 4B Ser422 is modulated by S6 kinases. *EMBO J.* **23**, 1761-1769.

Ravichandran, L. V., Esposito, D. L., Chen, J. and Quon, M. J. (2001). Protein kinase C-zeta phosphorylates insulin receptor substrate-1 and impairs its ability to activate phosphatidylinositol 3-kinase in response to insulin. *J. Biol. Chem.* **276**, 3543-3549.

Reid, D., Abello, P., Kaiser, M. and Warman, C. (1997). Carapace colour, inter-mould duration and the behavioural and physiological ecology of the shore crab Carcinus maenas. *Oceanographic Literature Review* **7**, 731.

Remy, I., Montmarquette, A. and Michnick, S. W. (2004). PKB/Akt modulates TGF-beta signalling through a direct interaction with Smad3. *Nat. Cell Biol.* **6**, 358-365.

Rhoads, R. E. (1988). Cap recognition and the entry of messenger-RNA into the protein-synthesis initiation cycle. *Trends Biochem. Sci.* **13**, 52-56.

Richardson, N. A., Anderson, A. J. and Sara, V. R. (1997). The effects of insulin/IGF-I on glucose and leucine metabolism in the redclaw crayfish (*Cherax quadricarinatus*). *Gen. Comp. Endocrinol.* **105**, 287-293.

Riddiford, L. M., Cherbas, P. and Truman, J. W. (2001). Ecdysone receptors and their biological actions. *Vitamins and Hormones - Advances in Research and Applications* **60**, 1-73.

Riddihough, G. and Pelham, H. R. B. (1987). An ecdysone response element in the *Drosophila* HSP27 promoter. *EMBO J.* **6**, 3729-3734.

Rinderknecht, E. and Humbel, R. E. (1978). Amino-acid sequence of human insulin-like growth factor-I and its structural homology with proinsulin. *J. Biol. Chem.* **253**, 2769-2776.

Rivas, D. A., Yaspelkis, B. B., Hawley, J. A. and Lessard, S. J. (2009). Lipid-induced mTOR activation in rat skeletal muscle reversed by exercise and 5 '-aminoimidazole-4-carboxamide-1-beta-D-ribofuranoside. *J. Endocrinol.* **202**, 441-451.

Robinson-Rechavi, M., Garcia, H. E. and Laudet, V. (2003). The nuclear receptor superfamily. *J. Cell Sci.* **116**, 585-586.

Rodriguez, J., Vernus, B., Chelh, I., Cassar-Malek, I., Gabillard, J. C., Sassi, A. H., Seiliez, I., Picard, B. and Bonnieu, A. (2014). Myostatin and the skeletal muscle atrophy and hypertrophy signaling pathways. *Cell. Mol. Life Sci.* **71**, 4361-4371.

Romier, C., Cocchiarella, F., Mantovani, R. and Moras, D. (2003). The NF-YB/NF-YC structure gives insight into DNA binding and transcription regulation by CCAAT factor NF-Y. *J. Biol. Chem.* **278**, 1336-1345.

Rommel, C., Bodine, S. C., Clarke, B. A., Rossman, R., Nunez, L., Stitt, T. N., Yancopoulos, G. D. and Glass, D. J. (2001). Mediation of IGF-1-induced skeletal myotube hypertrophy by PI (3) K/Akt/mTOR and PI (3) K/Akt/GSK3 pathways. *Nat. Cell Biol.* **3**, 1009-1013.

Ross, S. and Hill, C. S. (2008). How the Smads regulate transcription. *The international journal of biochemistry & cell biology* **40**, 383-408.

Roux, P. P., Ballif, B. A., Anjum, R., Gygi, S. P. and Blenis, J. (2004). Tumor-promoting phorbol esters and activated Ras inactivate the tuberous sclerosis tumor suppressor complex via p90 ribosomal S6 kinase. *Proceedings of the National Academy of Sciences of the United States of America* **101**, 13489-13494.

Ruvinsky, I. and Meyuhas, O. (2006). Ribosomal protein S6 phosphorylation: from protein synthesis to cell size. *Trends Biochem. Sci.* **31**, 342-348.

Rytomaa, T. and Kiviniem.K. (1968). Control of cell production in rat chloroleukaemia by means of granulocytic chalone. *Nature* **220**, 136-&.

Saetren, H. (1956). A principle of auto-regulation of growth - production of organ specific mitose-inhibitors in kidney and liver. *Exp. Cell Res.* **11**, 229-232.

Saidi, B., Debesse, N., Sedlmeier, D., Lachaise, F., Saïdi, B., de Bessé, N. and Webster, S. G. (1994). Involvement of cAMP and cGMP in the mode of action of molt-inhibiting hormone (MIH) a neuropeptide which inhibits steroidogenesis in a crab. *Mol. Cell. Endocrinol.* **102**, 53-61.

Sakuma, K., Aoi, W. and Yamaguchi, A. (2014). The intriguing regulators of muscle mass in sarcopenia and muscular dystrophy. *Frontiers in Aging Neuroscience* **6**.

Sakuma, K. and Yamaguchi, A. (2012). Sarcopenia and cachexia: the adaptations of negative regulators of skeletal muscle mass. *Journal of cachexia, sarcopenia and muscle* **3**, 77-94.

Salerno, M. S., Thomas, M., Forbes, D., Watson, T., Kambadur, R. and Sharma, M. (2004). Molecular analysis of fiber type-specific expression of murine myostatin promoter. *American Journal of Physiology-Cell Physiology* **287**, C1031-C1040.

Saltiel, A. R. (1994). The paradoxical regulation of protein-phosphorylation in insulin action. *FASEB J.* **8**, 1034-1040.

Sancak, Y., Bar-Peled, L., Zoncu, R., Markhard, A. L., Nada, S. and Sabatini, D. M. (2010). Ragulator-Rag Complex Targets mTORC1 to the Lysosomal Surface and Is Necessary for Its Activation by Amino Acids. *Cell* **141**, 290-303.

Sancak, Y., Peterson, T. R., Shaul, Y. D., Lindquist, R. A., Thoreen, C. C., Bar-Peled, L. and Sabatini, D. M. (2008). The Rag GTPases bind raptor and mediate amino acid signaling to mTORC1. *Science* **320**, 1496-1501.

Sanders, B. (1983a). Insulin-like peptides in the lobster *Homarus americanus*.1. Insulin immunoreactivity. *Gen. Comp. Endocrinol.* **50**, 366-373.

Sanders, B. (1983b). Insulin-like peptides in the lobster *Homarus americanus*. 2. Insulin-like biological-activity. *Gen. Comp. Endocrinol.* **50**, 374-377.

Sandri, M. (2008). Signaling in muscle atrophy and hypertrophy. *Physiology (Bethesda)* **23**, 160-170.

Sandri, M., Barberi, L., Bijlsma, A. Y., Blaauw, B., Dyar, K. A., Milan, G., Mammucari, C., Meskers, C. G., Pallafacchina, G., Paoli, A. et al. (2013). Signalling pathways regulating muscle mass in ageing skeletal muscle: The role of the IGF1-Akt-mTOR-FoxO pathway. *Biogerontology* **14**, 303-323.

Sanij, E. and Hannan, R. D. (2009). The role of UBF in regulating the structure and dynamics of transcriptionally active rDNA chromatin. *Epigenetics* **4**, 274-281.

Sapolsky, R. M., Romero, L. M. and Munck, A. U. (2000). How do glucocorticoids influence stress responses? Integrating permissive, suppressive, stimulatory, and preparative actions. *Endocr. Rev.* **21**, 55-89.

Sarda, S., Zeng, J., Hunt, B. G. and Soojin, V. Y. (2012). The evolution of invertebrate gene body methylation. *Mol. Biol. Evol.* **29**, 1907-1916.

Sartori, R., Gregorevic, P. and Sandri, M. (2014). TGF beta and BMP signaling in skeletal muscle: potential significance for muscle-related disease. *Trends Endocrinol. Metab.* **25**, 464-471.

Sartori, R., Milan, G., Patron, M., Mammucari, C., Blaauw, B., Abraham, R. and Sandri, M. (2009). Smad2 and 3 transcription factors control muscle mass in adulthood. *Am. J. Physiol. Cell Physiol.* **296**, C1248-1257.

Schakman, O., Gilson, H. and Thissen, J. P. (2008). Mechanisms of glucocorticoid-induced myopathy. *J. Endocrinol.* **197**, 1-10.

Schakman, O., Kalista, S., Barbe, C., Loumaye, A. and Thissen, J. P. (2013). Glucocorticoid-induced skeletal muscle atrophy. *International Journal of Biochemistry & Cell Biology* **45**, 2163-2172.

Schalm, S. S., Fingar, D. C., Sabatini, D. M. and Blenis, J. (2003). TOS motif-mediated raptor binding regulates 4E-BP1 multisite phosphorylation and function. *Curr. Biol.* **13**, 797-806.

Schauer, S., Azoitei, A., Braun, S. and Spindler-Barth, M. (2011). Influence of hormone response elements (HREs) on ecdysteroid receptor concentration. *Insect Mol. Biol.* **20**, 701-711.

Schiaffino, S., Dyar, K. A., Ciciliot, S., Blaauw, B. and Sandri, M. (2013). Mechanisms regulating skeletal muscle growth and atrophy. *FEBS J.* **280**, 4294-4314.

Schmiege, D. L., Ridgway, R. L. and Moffett, S. B. (1992). Ultrastructure of autotomy-induced atrophy of muscles in the crab *Carcinus maenas*. *Canadian Journal of Zoology-Revue Canadienne De Zoologie* **70**, 841-851.

Scott, J. W., Hawley, S. A., Green, K. A., Anis, M., Stewart, G., Scullion, G. A., Norman, D. G. and Hardie, D. G. (2004). CBS domains form energy-sensing modules whose binding of adenosine ligands is disrupted by disease mutations. *J. Clin. Invest.* **113**, 274-284.

Seiliez, I., Taty Taty, G. C., Bugeon, J., Dias, K., Sabin, N. and Gabillard, J. C. (2013). Myostatin induces atrophy of trout myotubes through inhibiting the TORC1 signaling and promoting Ubiquitin-Proteasome and Autophagy-Lysosome degradative pathways. *Gen. Comp. Endocrinol.* **186**, 9-15.

Sengupta, S., Peterson, T. R. and Sabatini, D. M. (2010). Regulation of the mTOR Complex 1 Pathway by Nutrients, Growth Factors, and Stress. *Mol. Cell* **40**, 310-322.

Shafer, E. A. (1916). The endocrine organs: An introduction to the study of internal secretions. London: Longmans, Green, and Co.

Sharma, M., Kambadur, R., Matthews, B. G., Somers, W. G., Devlin, G. P., Conaglen, J. V., Fowke, P. J. and Bass, J. J. (1999). Myostatin, a transforming growth factor-beta

superfamily member, is expressed in heart muscle and is upregulated in cardiomyocytes after infarct. *Journal of Cellular Physiology* **180**, 1-9.

Sharma, M., McFarlane, C., Kambadur, R., Kukreti, H., Bonala, S. and Srinivasan, S. (2015). Myostatin: Expanding horizons. *IUBMB life* **67**, 589-600.

Shaw, R. J., Kosmatka, M., Bardeesy, N., Hurley, R. L., Witters, L. A., DePinho, R. A. and Cantley, L. C. (2004). The tumor suppressor LKB1 kinase directly activates AMP-activated kinase and regulates apoptosis in response to energy stress. *Proceedings of the National Academy of Sciences of the United States of America* **101**, 3329-3335.

Sheffield-Moore, M. (2000). Androgens and the control of skeletal muscle protein synthesis. *Ann. Med.* **32**, 181-186.

Shi, J., Luo, L. Q., Eash, J., Ibebunjo, C. and Glass, D. J. (2011). The SCF-Fbxo40 Complex Induces IRS1 Ubiquitination in Skeletal Muscle, Limiting IGF1 Signaling. *Dev. Cell* **21**, 835-847.

Shi, W. B., Sun, C. X., He, B., Xiong, W. C., Shi, X. M., Yao, D. C. and Cao, X. (2004). GADD34-PP1c recruited by Smad7 dephosphorylates TGF beta type 1 receptor. *J. Cell Biol.* **164**, 291-300.

Shi, Y. G. and Massague, J. (2003). Mechanisms of TGF-beta signaling from cell membrane to the nucleus. *Cell* **113**, 685-700.

Shor, B., Wu, J., Shakey, Q., Toral-Barza, L., Shi, C., Follettie, M. and Yu, K. (2010). Requirement of the mTOR Kinase for the Regulation of Maf1 Phosphorylation and Control of RNA Polymerase III-dependent Transcription in Cancer Cells. *J. Biol. Chem.* **285**, 15380-15392.

Shrivastava, S. and Princy, S. A. (2014). Crustacean hyperglycemic hormone family Neurohormones: A prevailing tool to decipher the physiology of crustaceans. *Indian Journal of Geo-Marine Sciences* **43**, 434-440.

Shyu, K. G., Ko, W. H., Yang, W. S., Wang, B. W. and Kuan, P. (2005). Insulin-like growth factor-1 mediates stretch-induced upregulation of myostatin expression in neonatal rat cardiomyocytes. *Cardiovascular Research* **68**, 405-414.

Simms, H. S. and Stillman, N. P. (1937). A growth inhibitor in adult tissue. *J. Gen. Physiol.* **20**, 621-629.

Simnett, J. D., Fisher, J. M. and Hepplest.Ag. (1969). Tissue-specific inhibition of lung alveolar cell mitosis in organ culture. *Nature* **223**, 944-&.

Singh, S. P., Kumar, R., Kumari, P., Kumar, S. and Mitra, A. (2014). Characterization of 5′ Upstream Region and Investigation of TTTTA Deletion in 5′ UTR of Myostatin (MSTN) Gene in Indian Goat Breeds. *Anim. Biotechnol.* **25**, 55-68.

Skinner, D., Bonnewell, V. and Fowler, R. (1983). Sites of divergence in the sequence of a complex satellite DNA and several cloned variants. In *Cold Spring Harbor Symp. Quant. Biol.*, vol. 47, pp. 1151-1157: Cold Spring Harbor Laboratory Press.

Skinner, D. M. (1962). Structure and metabolism of a crustacean integumentary tissue during a molt cycle. *Biol. Bull.* **123**, 635-647.

Skinner, D. M. (1965). Amino acid incorporation into protein during the molt cycle of the land crab *Gecarcinus lateralis*. *J. Exp. Zool.* **160**, 225-233.

Skinner, D. M. (1966). Breakdown and reformation of somatic muscle during the molt cycle of the land crab, *Gecarcinus lateralis*. *J. Exp. Zool.* **163**, 115-&.

Skinner, D. M. (1985a). Interacting factors in the control of the crustacean molt cycle. *Am. Zool.* **25**, 275-284.

Skinner, D. M. (1985b). Molting and regeneration. In *The Biology of Crustacea*, vol. 9 eds. D. E. Bliss and L. H. Mantel), pp. 43-146. New York: Academic Press.

Skinner, D. M. and Graham, D. E. (1970). Molting in land crabs: Stimulation by leg removal. *Science* **169**, 383-&.

Skinner, D. M. and Graham, D. E. (1972). Loss of limbs as a stimulus to ecdysis in Brachyura (true crabs). *Biol. Bull.* **143**, 222-233.

Skraastad, Ø., Fossli, T., Edminson, P. and Reichelt, K. (1987). Purification and characterisation of a mitosis inhibitory tripeptide from mouse intestinal extracts. *Epithelia* **1**, 107-119.

Smadja-Lamere, N., Shum, M., Deleris, P., Roux, P. P., Abe, J. and Marette, A. (2013). Insulin Activates RSK (p90 Ribosomal S6 Kinase) to Trigger a New Negative Feedback Loop That Regulates Insulin Signaling for Glucose Metabolism. *J. Biol. Chem.* **288**, 31165-31176.

Smale, S. T. and Kadonaga, J. T. (2003). The RNA polymerase II core promoter. *Annu. Rev. Biochem.* **72**, 449-479.

Small, E. M., O'Rourke, J. R., Moresi, V., Sutherland, L. B., McAnally, J., Gerard, R. D., Richardson, J. A. and Olson, E. N. (2010). Regulation of PI3-kinase/Akt signaling by

muscle-enriched microRNA-486. *Proceedings of the National Academy of Sciences of the United States of America* **107**, 4218-4223.

Sofer, A., Lei, K., Johannessen, C. M. and Ellisen, L. W. (2005). Regulation of mTOR and cell growth in response to energy stress by REDD1. *Mol. Cell. Biol.* **25**, 5834-5845.

Song, K. Y., Wang, H., Krebs, T. L. and Danielpour, D. (2006). Novel roles of Akt and mTOR in suppressing TGF-beta/ALK5-mediated Smad3 activation. *EMBO J.* **25**, 58-69.

Spahn, C. M. T., Gomez-Lorenzo, M. G., Grassucci, R. A., Jorgenson, R., Andersen, G. R., Beckmann, R., Penczek, P. A., Ballesta, J. P. G. and Frank, J. (2004). Domain movements of elongation factor eEF2 and the eukaryotic 80S ribosome facilitate tRNA translocation. *EMBO J.* **23**, 1008-1019.

Spiller, M. P., Kambadur, R., Jeanplong, F., Thomas, M., Martyn, J. K., Bass, J. J. and Sharma, M. (2002). The myostatin gene is a downstream target gene of basic helix-loop-helix transcription factor MyoD. *Mol. Cell. Biol.* **22**, 7066-7082.

Spindler, K.-D., Betanńska, K., Nieva, C., Gwóźoanna, T., Dutko-Gwóźdź, J., Ożyhar, A. and Spindler-Barth, M. (2009). Intracellular Localization of the Ecdysteroid Receptor. In *Ecdysone: Structures and Functions*, (ed. G. Smagghe), pp. 389-409: Springer Netherlands.

Steinberg, G. R. and Kemp, B. E. (2009). AMPK in Health and Disease. *Physiol. Rev.* **89**, 1025-1078.

Stetten, D. (1953). Metabolic effects of insulin. *Bulletin of the New York Academy of Medicine* **29**, 466.

Stewart, M. J., Stewart, P., Sroyraya, M., Soonklang, N., Cummins, S. F., Hanna, P. J., Duan, W. and Sobhon, P. (2013). Cloning of the crustacean hyperglycemic hormone and evidence for molt-inhibiting hormone within the central nervous system of the blue crab *Portunus pelagicus*. *Comp Biochem Physiol A Mol Integr Physiol* **164**, 276-290.

Styrishave, B., Rewitz, K. and Andersen, O. (2004). Frequency of moulting by shore crabs Carcinus maenas (L.) changes their colour and their success in mating and physiological performance. *J. Exp. Mar. Biol. Ecol.* **313**, 317-336.

Sun, J., Chen, Z., Tan, X., Zhou, F., Tan, F., Gao, Y., Sun, N., Xu, X., Shao, K. and He, J. (2013). MicroRNA-99a/100 promotes apoptosis by targeting mTOR in human esophageal squamous cell carcinoma. *Medical oncology* **30**, 1-9.

Sun, X. J., Crimmins, D. L., Myers, M. G., Miralpeix, M. and White, M. F. (1993). Pleiotropic insulin signals are engaged by multisite phosphorylation of IRS-1. *Mol. Cell. Biol.* **13**, 7418-7428.

Sun, X. J. and Liu, F. (2009). Phosphorylation of irs proteins: Yin-yang regulation of insulin signaling. In *Vitamins and Hormones Insulin and Igfs*, vol. 80 (ed. G. Litwack), pp. 351-+.

Sun, Y., Fang, Y., Yoon, M. S., Zhang, C., Roccio, M., Zwartkruis, F. J., Armstrong, M., Brown, H. A. and Chen, J. (2008). Phospholipase D1 is an effector of Rheb in the mTOR pathway. *Proceedings of the National Academy of Sciences of the United States of America* **105**, 8286-8291.

Szent-Gyérgyi, A. (2010). Cellular growth control and cancer. *A Cybernetic View of Biological Growth: The Maia Hypothesis*, 292.

Takahara, T. and Maeda, T. (2013). Evolutionarily conserved regulation of TOR signalling. *Journal of biochemistry* **154**, 1-10.

Takano, T., Usui, I., Haruta, T., Kawahara, J., Uno, T., Iwata, M. and Kobayashi, M. (2001). Mammalian target of rapamycin pathway regulates insulin signaling via subcellular redistribution of insulin receptor substrate 1 and integrates nutritional signals and metabolic signals of insulin. *Mol. Cell. Biol.* **21**, 5050-5062.

Taylor, D. J., Nilsson, J., Merrill, A. R., Andersen, G. R., Nissen, P. and Frank, J. (2007). Structures of modified eEF2· 80S ribosome complexes reveal the role of GTP hydrolysis in translocation. *The EMBO journal* **26**, 2421-2431.

Tepolt, C. K., Darling, J. A., Bagley, M. J., Geller, J. B., Blum, M. J. and Grosholz, E. D. (2009). European green crabs (Carcinus maenas) in the northeastern Pacific: genetic evidence for high population connectivity and current-mediated expansion from a single introduced source population. *Diversity & distributions* **15**, 997-1009.

Thomas, G. and Hall, M. N. (1997). TOR signalling and control of cell growth. *Curr. Opin. Cell Biol.* **9**, 782-787.

Thomas, G., Martinperez, J., Siegmann, M. and Otto, A. M. (1982). The effect of serum, EGF, PGF 2-alpha and insulin on S6-phosphorylation and the initiation of protein and DNA-synthesis. *Cell* **30**, 235-242.

Tomas, F. M., Munro, H. N. and Young, V. R. (1979). Effect of glucocorticoid administration on the rate of muscle protein breakdown invivo in rats, as measured by urinary-excretion of N-tau-methylhistidine. *Biochem. J.* **178**, 139-146.

Tran, H. T., Askari, H. B., Shaaban, S., Price, L., Palli, S. R., Dhadialla, T. S., Carlson, G. R. and Butt, T. R. (2001). Reconstruction of ligand-dependent transactivation of Choristoneura fumiferana ecdysone receptor in yeast. *Mol. Endocrinol.* **15**, 1140-1153.

Tremblay, F., Brule, S., Um, S. H., Li, Y., Masuda, K., Roden, M., Sun, X. J., Krebs, M., Polakiewicz, R. D., Thomas, G. et al. (2007). Identification of IRS-1 Ser-1101 as a target of S6K1 in nutrient- and obesity-induced insulin resistance. *Proceedings of the National Academy of Sciences of the United States of America* **104**, 14056-14061.

Trendelenburg, A. U., Meyer, A., Rohner, D., Boyle, J., Hatakeyama, S. and Glass, D. J. (2009). Myostatin reduces Akt/TORC1/p70S6K signaling, inhibiting myoblast differentiation and myotube size. *Am. J. Physiol. Cell Physiol.* **296**, C1258-1270.

Trevillyan, J. M., Perisic, O., Traugh, J. A. and Byus, C. V. (1985). Insulin-stimulated and phorbol ester-stimulated phosphorylation of ribosomal-protein S6. *J. Biol. Chem.* **260**, 3041-3044.

Tsang, C. K., Liu, H. and Zheng, X. F. S. (2010). mTOR binds to the promoters of RNA polymerase I- and III-transcribed genes. *Cell Cycle* **9**, 953-957.

Tsang, L. M., Schubart, C. D., Ahyong, S. T., Lai, J. C., Au, E. Y., Chan, T.-Y., Ng, P. K. and Chu, K. H. (2014). Evolutionary history of true crabs (Crustacea: Decapoda: Brachyura) and the origin of freshwater crabs. *Mol. Biol. Evol.* **31**, 1173-1187.

Tsuchida, K., Sunada, Y., Noji, S., Murakami, T., Uezumi, A. and Nakatani, M. (2006). Inhibitors of the TGF-beta superfamily and their clinical applications. *Mini-Rev. Med. Chem.* **6**, 1255-1261.

Tsuchiya, A., Kanno, T. and Nishizaki, T. (2014). Dipalmitoleoylphosphoethanolamine as a PP2A Enhancer Obstructs Insulin Signaling by Promoting Ser/Thr Dephosphorylation of Akt. *Cellular Physiology and Biochemistry* **34**, 617-627.

Tsukazaki, T., Chiang, T. A., Davison, A. F., Attisano, L. and Wrana, J. L. (1998). SARA, a FYVE domain protein that recruits Smad2 to the TGF beta receptor. *Cell* **95**, 779-791.

Tumaneng, K., Schlegelmilch, K., Russell, R. C., Yimlamai, D., Basnet, H., Mahadevan, N., Fitamant, J., Bardeesy, N., Camargo, F. D. and Guan, K. L. (2012). YAP mediates crosstalk between the Hippo and PI(3)K-TOR pathways by suppressing PTEN via miR-29. *Nat. Cell Biol.* **14**, 1322-+.

Tzatsos, A. and Kandror, K. V. (2006). Nutrients suppress phosphatidylinositol 3-kinase/Akt signaling via raptor-dependent mTOR-mediated insulin receptor substrate 1 phosphorylation. *Mol. Cell. Biol.* **26**, 63-76.

Ullrich, A., Gray, A., Tam, A. W., Yang-Feng, T., Tsubokawa, M., Collins, C., Henzel, W., Le Bon, T., Kathuria, S. and Chen, E. (1986). Insulin-like growth factor I receptor primary structure: comparison with insulin receptor suggests structural determinants that define functional specificity. *The EMBO Journal* **5**, 2503.

Um, S. H., Frigerio, F., Watanabe, M., Picard, F., Joaquin, M., Sticker, M., Fumagalli, S., Allegrini, P. R., Kozma, S. C., Auwerx, J. et al. (2004). Absence of S6K1 protects against age- and diet-induced obesity while enhancing insulin sensitivity. *Nature* **431**, 200-205.

Unbehaun, A., Borukhov, S. I., Hellen, C. U. T. and Pestova, T. V. (2004). Release of initiation factors from 48S complexes during ribosomal subunit joining and the link between establishment of codon-anticodon base-pairing and hydrolysis of eIF2-bound GTP. *Genes Dev.* **18**, 3078-3093.

Urano, F., Wang, X. Z., Bertolotti, A., Zhang, Y. H., Chung, P., Harding, H. P. and Ron, D. (2000). Coupling of stress in the ER to activation of JNK protein kinases by transmembrane protein kinase IRE1. *Science* **287**, 664-666.

Urban, R. J., Bodenburg, Y. H., Gilkison, C., Foxworth, J., Coggan, A. R., Wolfe, R. R. and Ferrando, A. (1995). Testosterone administration to elderly men increases skeletal muscle strength and protein synthesis. *American Journal of Physiology-Endocrinology And Metabolism* **269**, E820-E826.

Vaillancourt, P. and Felts, K. A. (2003). Retroviral Delivery of the Ecdysone-Regulatable Gene Expression System. *Biotechnol. Prog.* **19**, 1750-1755.

Valášek, L., Nielsen, K. H., Zhang, F., Fekete, C. A. and Hinnebusch, A. G. (2004). Interactions of eukaryotic translation initiation factor 3 (eIF3) subunit NIP1/c with eIF1 and eIF5 promote preinitiation complex assembly and regulate start codon selection. *Mol. Cell. Biol.* **24**, 9437-9455.

Valdes, J. A., Flores, S., Fuentes, E. N., Osorio-Fuentealba, C., Jaimovich, E. and Molina, A. (2013). IGF-1 induces IP3 -dependent calcium signal involved in the regulation of myostatin gene expression mediated by NFAT during myoblast differentiation. *Journal of cellular physiology* **228**, 1452-1463.

Vander Haar, E., Lee, S.-i., Bandhakavi, S., Griffin, T. J. and Kim, D.-H. (2007). Insulin signalling to mTOR mediated by the Akt/PKB substrate PRAS40. *Nat. Cell Biol.* **9**, 316-323.

Verly, W. G. (1973). Hepatic chalone. *National Cancer Institute Monographs*, 175-184.

Voaden, M. J. (1968). A chalone in rabbit lens. *Experimental eye research* **7**, 326-&.

Vögtli, M., Elke, C., Imhof, M. O. and Lezzi, M. (1998). High level transactivation by the ecdysone receptor complex at the core recognition motif. *Nucleic Acids Res.* **26**, 2407-2414.

Wang, B. Y., Wang, H. and Yang, Z. A. (2012). MiR-122 Inhibits Cell Proliferation and Tumorigenesis of Breast Cancer by Targeting IGF1R. *PloS one* **7**.

Wang, H. M., Kubica, N., Ellisen, L. W., Jefferson, L. S. and Kimball, S. R. (2006). Dexamethasone represses signaling through the mammalian target of rapamycin in muscle cells by enhancing expression of REDD1. *J. Biol. Chem.* **281**, 39128-39134.

Wang, L., Chang, L., Li, Z., Gao, Q., Cai, D., Tian, Y., Zeng, L. and Li, M. (2014a). miR-99a and-99b inhibit cervical cancer cell proliferation and invasion by targeting mTOR signaling pathway. *Medical Oncology* **31**, 1-8.

Wang, L., Lawrence, J. C., Sturgill, T. W. and Harris, T. E. (2009). Mammalian Target of Rapamycin Complex 1 (mTORC1) Activity Is Associated with Phosphorylation of Raptor by mTOR. *J. Biol. Chem.* **284**, 14693-14697.

Wang, L. F., Harris, T. E., Roth, R. A. and Lawrence, J. C. (2007). PRAS40 regulates mTORC1 kinase activity by functioning as a direct inhibitor of substrate binding. *J. Biol. Chem.* **282**, 20036-20044.

Wang, S.-F., Miura, K., Miksicek, R. J., Segraves, W. A. and Raikhel, A. S. (1998). DNA binding and transactivation characteristics of the mosquito ecdysone receptor-Ultraspiracle complex. *J. Biol. Chem.* **273**, 27531-27540.

Wang, S. F., Li, C., Zhu, J. S., Miura, K., Miksicek, R. J. and Raikhel, A. S. (2000). Differential expression and regulation by 20-hydroxyecdysone of mosquito ultraspiracle isoforms. *Dev. Biol.* **218**, 99-113.

Wang, X. M., Beugnet, A., Murakami, M., Yamanaka, S. and Proud, C. G. (2005). Distinct signaling events downstream of mTOR cooperate to mediate the effects of amino acids and insulin on initiation factor 4E-binding proteins. *Mol. Cell. Biol.* **25**, 2558-2572.

Wang, X. M., Li, W., Williams, M., Terada, N., Alessi, D. R. and Proud, C. G. (2001). Regulation of elongation factor 2 kinase by p90(RSK1) and p70 S6 kinase. *EMBO J.* **20**, 4370-4379.

Wang, X. M. and Proud, C. G. (2006). The mTOR pathway in the control of protein synthesis. *Physiology* **21**, 362-369.

Wang, Y., Wang, X. L., Meng, X. Y., Wang, H. D., Jiang, Z. Q. and Qiu, X. M. (2014b). Identification of two SNPs in myostatin (MSTN) gene of Takifugu rubripes and their association with growth traits. *Mol. Cell. Probes* **28**, 200-203.

Watson, J. D. (1964). Synthesis of proteins upon ribosomes. *Bulletin De La Societe De Chimie Biologique* **46**, 1399-+.

Weigert, C., Hennige, A. M., Brischmann, T., Beck, A., Moeschel, K., Schauble, M., Brodbeck, K., Haring, H. U., Schleicher, E. D. and Lehmann, R. (2005). The phosphorylation of Ser(318) of insulin receptor substrate 1 is not per se inhibitory in skeletal muscle cells but is necessary to trigger the attenuation of the insulin-stimulated signal. *J. Biol. Chem.* **280**, 37393-37399.

Weinmann, R. and Roeder, R. G. (1974). Role of DNA-dependent RNA polymerase III in the transcription of the tRNA and 5S RNA genes. *Proceedings of the National Academy of Sciences* **71**, 1790-1794.

Weissbach, H., Redfield, B. and Moon, H. M. (1973). Further studies on interactions of elongation factor-1 from animal tissues. *Archives of Biochemistry and Biophysics* **156**, 267-275.

Welle, S., Burgess, K. and Mehta, S. (2009). Stimulation of skeletal muscle myofibrillar protein synthesis, p70 S6 kinase phosphorylation, and ribosomal protein S6 phosphorylation by inhibition of myostatin in mature mice. *American journal of physiology. Endocrinology and metabolism* **296**, E567-572.

Wells, S. E., Hillner, P. E., Vale, R. D. and Sachs, A. B. (1998). Circularization of mRNA by eukaryotic translation initiation factors. *Mol. Cell* **2**, 135-140.

Wheatly, M. G. and Hart, M. K. (1995). Hemolymph ecdysone and electrolytes during the molting cycle of crayfish: a comparison of natural molts with those induced by eyestalk removal or multiple limb autotomy. *Physiol. Zool.*, 583-607.

White, M. F., Maron, R. and Kahn, C. R. (1985). Insulin rapidly stimulates tyrosine phosphorylation of a MR-185,000 protein in intact-cells. *Nature* **318**, 183-186.

White, M. F., Shoelson, S., Keutmann, H. and Kahn, C. (1988). A cascade of tyrosine autophosphorylation in the beta-subunit activates the phosphotransferase of the insulin receptor. *J. Biol. Chem.* **263**, 2969-2980.

Wiza, C., Nascimento, E. B. M. and Ouwens, D. M. (2012). Role of PRAS40 in Akt and mTOR signaling in health and disease. *American Journal of Physiology-Endocrinology and Metabolism* **302**, E1453-E1460.

Wolfman, N. M., McPherron, A. C., Pappano, W. N., Davies, M. V., Song, K., Tomkinson, K. N., Wright, J. F., Zhao, L., Sebald, S. M., Greenspan, D. S. et al. (2003). Activation of latent myostatin by the BMP-1/tolloid family of metalloproteinases. *Proceedings of the National Academy of Sciences of the United States of America* **100**, 15842-15846.

Wu, T. Q., Wieland, A., Araki, K., Davis, C. W., Ye, L. L., Hale, J. S. and Ahmed, R. (2012). Temporal expression of microRNA cluster miR-17-92 regulates effector and memory CD8(+) T-cell differentiation. *Proceedings of the National Academy of Sciences of the United States of America* **109**, 9965-9970.

Wu, X., Hopkins, P. M., Palli, S. R. and Durica, D. S. (2004). Crustacean retinoid-X receptor isoforms: Distinctive DNA binding and receptor-receptor interaction with a cognate ecdysteroid receptor. *Mol. Cell. Endocrinol.* **218**, 21-38.

Wu, X. L., Bhayani, M. K., Dodge, C. T., Nicoloso, M. S., Chen, Y. Y., Yan, X. F., Adachi, M., Thomas, L., Galer, C. E., Jiffar, T. et al. (2013). Coordinated Targeting of the EGFR Signaling Axis by MicroRNA-27a*. *Oncotarget* **4**, 1388-1398.

Wurtz, J. M., Bourguet, W., Renaud, J. P., Vivat, V., Chambon, P., Moras, D. and Gronemeyer, H. (1996). A canonical structure for the ligand-binding domain of nuclear receptors. *Nat. Struct. Biol.* **3**, 87-94.

Wyborski, D. L., Bauer, J. C. and Vaillancourt, P. (2001). Bicistronic expression of ecdysone-inducible receptors in mammalian cells. *BioTechniques* **31**, 618-625.

Xu, Q., Jiang, Y., Yin, Y., Li, Q., He, J., Jing, Y., Qi, Y. T., Xu, Q., Li, W., Lu, B. et al. (2013). A regulatory circuit of miR-148a/152 and DNMT1 in modulating cell transformation and tumor angiogenesis through IGF-IR and IRS1. *Journal of Molecular Cell Biology* **5**, 3-13.

Xu, X. S., Sarikas, A., Dias-Santagata, D. C., Dolios, G., Lafontant, P. J., Tsai, S. C., Zhu, W. Q., Nakajima, H., Nakajima, H. O., Field, L. J. et al. (2008). The CUL7 E3 ubiquitin ligase targets insulin receptor substrate 1 for ubiquitin-dependent degradation. *Mol. Cell* **30**, 403-414.

Xue, M., Yao, S. H., Hu, M. M., Li, W., Hao, T. T., Zhou, F., Zhu, X. F., Lu, H. M., Qin, D., Yan, Q. et al. (2014). HIV-1 Nef and KSHV oncogene K1 synergistically promote angiogenesis by inducing cellular miR-718 to regulate the PTEN/AKT/mTOR signaling pathway. *Nucleic Acids Res.* **42**, 9862-9879.

Xue, Q., Sun, K., Deng, H. J., Lei, S. T., Dong, J. Q. and Li, G. X. (2013). Anti-miRNA-221 sensitizes human colorectal carcinoma cells to radiation by upregulating PTEN. *World Journal of Gastroenterology* **19**, 9307-9317.

Yamamoto, K. R. (1985). Steroid-receptor regulated transcription of specific genes and gene networks. *Annu. Rev. Genet.* **19**, 209-252.

Yamaoka, L. H. and Skinner, D. M. (1975). Cytolytic enzymes in relation to the breakdown of the chelae muscle of the land crab, *Gecarcinus lateralis*. *Comparative Biochemistry and Physiology B-Biochemistry & Molecular Biology* **52**, 499-502.

Yan, L., Mieulet, V., Burgess, D., Findlay, G. M., Sully, K., Procter, J., Goris, J., Janssens, V., Morrice, N. A. and Lamb, R. F. (2010). PP2A(T61 epsilon) Is an Inhibitor of MAP4K3 in Nutrient Signaling to mTOR. *Mol. Cell* **37**, 633-642.

Yang, W., Zhang, Y., Li, Y. F., Wu, Z. G. and Zhu, D. H. (2007). Myostatin induces cyclin D1 degradation to cause cell cycle arrest through a phosphatidylinositol 3-kinase/AKT/GSK-3 beta pathway and is antagonized by insulin-like growth factor 1. *J. Biol. Chem.* **282**, 3799-3808.

Yao, T. P., Forman, B. M., Jiang, Z. Y., Cherbas, L., Chen, J. D., McKeown, M., Cherbas, P. and Evans, R. M. (1993). Functional ecdysone receptor is the product of EcR and ultraspiracle genes. *Nature* **366**, 476-479.

Yoon, M. S., Du, G. W., Backer, J. M., Frohman, M. A. and Chen, J. (2011). Class III PI-3-kinase activates phospholipase D in an amino acid-sensing mTORC1 pathway. *J. Cell Biol.* **195**, 435-447.

Yoon, M. S., Rosenberger, C. L., Wu, C., Truong, N., Sweedler, J. V. and Chen, J. (2015). Rapid Mitogenic Regulation of the mTORC1 Inhibitor, DEPTOR, by Phosphatidic Acid. *Mol. Cell* **58**, 549-556.

Youngren, J. F. (2007). Regulation of insulin receptor function. *Cell. Mol. Life Sci.* **64**, 873-891.

Yu, T., Li, J., Yan, M., Liu, L., Lin, H., Zhao, F., Sun, L., Zhang, Y., Cui, Y., Zhang, F. et al. (2015). MicroRNA-193a-3p and -5p suppress the metastasis of human non-small-cell lung cancer by downregulating the ERBB4/PIK3R3/mTOR/S6K2 signaling pathway. *Oncogene* **34**, 413-423.

Yu, Y., Yoon, S. O., Poulogiannis, G., Yang, Q., Ma, X. M., Villen, J., Kubica, N., Hoffman, G. R., Cantley, L. C., Gygi, S. P. et al. (2011). Phosphoproteomic analysis identifies Grb10 as an mTORC1 substrate that negatively regulates insulin signaling. *Science* **332**, 1322-1326.

Zhande, R., Mitchell, J. J., Wu, J. and Sun, X. J. (2002). Molecular mechanism of insulin-induced degradation of insulin receptor substrate 1. *Mol. Cell. Biol.* **22**, 1016-1026.

Zhang, H. B., Stallock, J. P., Ng, J. C., Reinhard, C. and Neufeld, T. P. (2000). Regulation of cellular growth by the Drosophila target of rapamycin dTOR. *Genes Dev.* **14**, 2712-2724.

Zhang, P., Chen, X. and Fan, M. (2007). Signaling mechanisms involved in disuse muscle atrophy. *Medical hypotheses* **69**, 310-321.

Zhang, X., Odom, D. T., Koo, S.-H., Conkright, M. D., Canettieri, G., Best, J., Chen, H., Jenner, R., Herbolsheimer, E. and Jacobsen, E. (2005). Genome-wide analysis of cAMP-response element binding protein occupancy, phosphorylation, and target gene activation in human tissues. *Proceedings of the National Academy of Sciences of the United States of America* **102**, 4459-4464.

Zhang, Y. (2008). Modulators of Bone Morphogenetic Protein-1/Tolloid-like Metalloproteinases and Their Potential Applications in the Treatment of Fibrotic Diseases: ProQuest.

Zhang, Y., Nicholatos, J., Dreier, J. R., Ricoult, S. J., Widenmaier, S. B., Hotamisligil, G. S., Kwiatkowski, D. J. and Manning, B. D. (2014). Coordinated regulation of protein synthesis and degradation by mTORC1. *Nature* **513**, 440-443.

Zheng, G. D., Sun, C. F., Pu, J. W., Chen, J., Jiang, X. Y. and Zou, S. M. (2015). Two myostatin genes exhibit divergent and conserved functions in grass carp (Ctenopharyngodon idellus). *Gen. Comp. Endocrinol.* **214**, 68-76.

Zhou, F., Sun, R., Chen, H., Fei, J. and Lu, D. (2015). Myostatin Gene Mutated Mice Induced with TALE Nucleases. *Anim. Biotechnol.* **26**, 169-179.

Zhou, Y., Xiong, M. X., Fang, L., Jiang, L., Wen, P., Dai, C. S., Zhang, C. Y. and Yang, J. W. (2013). miR-21-Containing Microvesicles from Injured Tubular Epithelial Cells Promote Tubular Phenotype Transition by Targeting PTEN Protein. *American Journal of Pathology* **183**, 1183-1196.

Zhu, H., Wu, H., Liu, X., Evans, B. R., Medina, D. J., Liu, C.-G. and Yang, J.-M. (2008). Role of MicroRNA miR-27a and miR-451 in the regulation of MDR1/P-glycoprotein expression in human cancer cells. *Biochem. Pharmacol.* **76**, 582-588.

Zick, Y. (2004). Molecular basis of insulin action. In *Biology of IGF-1: its interaction with insulin in health and malignant states*, eds. G. Bock and J. Goode). Chichester, UK ;: John Wiley & Sons.

Zimmers, T. A., Davies, M. V., Koniaris, L. G., Haynes, P., Esquela, A. F., Tomkinson, K. N., McPherron, A. C., Wolfman, N. M. and Lee, S. J. (2002). Induction of cachexia in mice by systemically administered myostatin. *Science* **296**, 1486-1488.

Zoncu, R., Bar-Peled, L., Efeyan, A., Wang, S. Y., Sancak, Y. and Sabatini, D. M. (2011a). mTORC1 Senses Lysosomal Amino Acids Through an Inside-Out Mechanism That Requires the Vacuolar H+-ATPase. *Science* **334**, 678-683.

Zoncu, R., Efeyan, A. and Sabatini, D. M. (2011b). mTOR: From growth signal integration to cancer, diabetes and ageing. *Nature Reviews Molecular Cell Biology* **12**, 21-35.

Zuloaga, R., Fuentes, E., Molina, A. and Valdés, J. (2013). The cAMP response element binding protein (CREB) is activated by insulin-like growth factor-1 (IGF-1) and regulates myostatin gene expression in skeletal myoblast. *Biochem. Biophys. Res. Commun.* **440**, 258-264.

Appendix

RNAi experiment

Materials and Methods

Animals

Male *Gecarcinus lateralis* (Fréminville 1835), blackback land crabs, were collected from the Dominican Republic and kept in plastic containers at 27ºC and 75-90% relative humidity on a 12 h light: 12 h dark schedule. Containers held eight to twelve crabs in aspen bedding dampened with 5 parts per thousand (p.p.t.) Instant Ocean (Aquarium Systems, Mentor, OH). Crabs were fed lettuce, carrots and raisins twice per week.

Preparation of dsRNA

Genomic DNA, purified from claw muscle, was used as template in 40 µl semi-nested PCR reactions. Each PCR reaction consisted of 4 µl template, 2 µl each primer (10 µM) (gene-specific outer and inner forward primers and gene-specific outer/inner reverse primers), 12 µl nuclease-free water and 20 µl GoTaq Green® Master Mix (Promega Corp., Madison, WI, USA) (Table I.A). PCR settings were an initial 94°C for 4 min followed by 35 cycles of 94°C for 30 s, 57°C for 30 s and elongation at 72°C for gene product-specific time based on 60 s for 1000 bp (Table I.A). Mstn outer product was 920 bp, inner product was 449 bp, EcR outer product was 673 bp, inner product was 390 bp, and RXR outer product was 410 bp, inner product 334 bp (Table I.A). Second PCR product was separated on a 1% agarose gel at 120 V for 45 minutes. The DNA bands were extracted with the QIAquick Gel Extraction Kit (Qiagen Inc., Frederick, MD, USA), following the manufacturer's protocol. PCR products were ligated into pGEM-T Easy vectors with T4 DNA ligase using a 1:1 (Mstn), or 3:1 (EcR and RXR) insert to vector ratios following manufacturer's protocol.

pGEM-T Easy vectors with inserted gene segments were transformed into chemically competent CH3 Blue *Escherichia coli* cells (Bioline, Taunton, MA, USA). One µl ligation reaction was added to 25 µl competent cells and incubated on ice 30 min. Cells were heat-shocked at

42°C for 30 s, placed on ice for 2 min, then 125 µl SOC medium was added and the cells were incubated one h in a 37°C incubator shaker set at 200 RPM. Fifty µl culture was transferred to a 100 mm X 15 mm polystyrene Petri plate (Thermo Fisher Scientific, Inc.) containing LB agar with 100 µg/ml ampicillin and incubated at 37°C for 18 h. Selected colonies were placed in 0.5 ml LB media with 100 µg/ml ampicillin and incubated 6 h at 37°C incubator shaker set at 200 RPM. An insert check PCR with a gene-specific forward or reverse primer with the T7 primer was followed by product separation on a 1% agarose gel for 40 min at 120 V (Table I.B). Cultures that contained plasmids with inserted genes were identified, and the forward or reverse orientation of the gene in the plasmid was revealed. One hundred µl of transformed cultures for each orientation of each gene was added to 3.5 ml LB broth containing 100 µg/ml ampicillin and incubated overnight at 37°C in an incubator shaker set at 200 RPM. Glycerol stock of each gene, forward and reverse orientations, was made by adding 360 µl of culture to 60 µl of 70% glycerol. Glycerol stock was stored at -80°C. Cultures with gene inserts were sequenced at Davis Sequencing (Davis, CA, USA).

Plasmids were extracted with maxi-preps (Qiagen, Inc.) following manufacturer's protocol. Plasmids were linearized with NdeI (Mstn and EcR) or NotI (RXR), followed by PCR purification with QIAQuick (Qiagen, Inc.) following manufacturer's protocol. Linearized pGEM-T Easy plasmids were used to make double-stranded RNA (dsRNA) with the T7 RiboMAX™ Express RNAi system (Promega Corp., Madison, WI, USA). Manufacturer's protocol was followed for synthesizing single-stranded RNA (ssRNA), except incubation time was extended to 3 h to maximize yield. After forward and reverse ssRNA strands were annealed, dsRNA was purified and resuspended in 80 µl nuclease-free water. A diluted sample was separated on a 1% agarose gel to verify linearization and size of dsRNA.

RNAi Experiment

Animals with approximately equal-sized claws were selected. One claw and one merus were harvested before injections. A 50 µl Hamilton syringe (Hamilton Co., Reno, NV, USA) was

used to slowly inject dsRNA through the arthrodial membrane at the base of the left third leg.

Ethanol, dsECR, or dsRXR was injected into six crabs each, half on day 0, and half on day 1,

for a total of approximately 20 nM in the hemolymph of the crab, based on the assumption that

hemolymph volume is approximately 33% of the weight of the crab (Harris and Andrews, 1982).

Merae were harvested by limb autotomy at days 1, 2, 3, and 4 after dsRNA injection. The

second claw was also harvested on day 4.

Harvesting and qPCR

Hemolymph and claw muscle tissue were harvested as described in chapter 2. After

autotomy of a limb, the merus was immediately placed in liquid nitrogen. The frozen

exoskeleton of the merus was removed with a razor blade, and the merus tissue was placed in

a 1.5 ml microcentrifuge tube and stored at -80°C. RNA isolation was performed as described in

chapter 2. cDNA was made using Transcriptor Reverse Transcriptase (Roche, Indianapolis, IN,

USA) and 1.5 to 10 µg RNA per sample, following manufacturer's protocol. mRNA levels of *G.*

lateralis (*Gl*) *Gl-EF2*, *Gl-EcR* and *Gl-RXR* were analyzed with qPCR. qPCR reactions consisted

of 1 µl sample, 0.5 µl each forward and reverse gene-specific primers (1µM each in reaction

tube) (Integrated DNA Technologies, Inc., Coralville, IA, USA), 3 µl nuclease-free water and 5 µl

LightCycler 480 SYBR Green I Master mix (Roche) for a 10 µl total reaction. qPCR reaction

settings were an initial activation for 5 min at 95°C, followed by 45 cycles of 95°C for 10 s to

denature, 62°C (*Gl-EF2* and *Gl-RXR*) or 57°C (*Gl-EcR*) for 20 s to anneal, and 72°C for 20 s for

elongation (Table I.C). A melt curve cycle allowed analysis of product homogeneity. LightCycler

480 software, version 1.5 (Roche) was used for absolute quantification to external standards for

each gene. Concentrations were converted to copy number per µg RNA in Microsoft Excel. EF2

was used as a positive control to determine quality of the product after RNA isolation and cDNA

synthesis. Samples with EF2 values 1000-fold less than similar samples were not used.

Table I.A. Oligonucleotide primers used in RNAi synthesis of *Gecarcinus lateralis* Mstn, EcR and RXR dsRNA. Semi-nested primers were used with each gene. Product size is the product of the given forward primer with the gene-specific inner/outer reverse primer. Gene abbreviations: Mstn, myostatin; EcR, ecdysone receptor; RXR, Retinoid X Receptor; Additional abbreviations: forward primer (F), reverse primer (R), bp, base pairs, inner and outer primers (in/out).

Primer pairs	Sequence (5'- 3')	Product Size (bp)	Annealing Temperature
Mstn outer F	AATGCGAAAGAACTTGAGGCTGGC	920	57
Mstn inner F	AGAAAGGAAGGCAGTAACCACCGT	449	57
Mstn in/out R	TGGAGCTGTTCAGCTTCTGGATGA		
EcR outer F	TCACGAAGAATGCCGTGTACCAGT	673	57
EcR inner F	TATCAAGCCACTCACACGGGAACA	390	57
EcR in/out R	ATCTCTGCTGAATCTCCCAAGCCA		
RXR outer F	TTCACCATTGGCTCAAGCAACACC	410	57
RXR inner F	TCTAAGCACCTGTGCTCCATCTGT	334	57
RXR in/out R	TTATGCTGGCAATCGGCATGTCTG		

Table I.B. Oligonucleotide primers used for insertion checks of *Gecarcinus lateralis* Mstn, EcR and RXR. Gene-specific forward and reverse primers were used with T7 promoter primer (in pGEM-T Easy Vector). Product size is for the gene-specific primer and the T7 primer. Gene abbreviations: Mstn, myostatin; EcR, ecdysone receptor; RXR, Retinoid X Receptor; Additional abbreviations: forward primer (F), reverse primer (R), bp, base pairs.

Primer pairs	Sequence (5'- 3')	Product Size (bp)	Annealing Temperature
Mstn F	TCCCAAGGTGTACGAGGCAAACTT	164	55
Mstn R	GCGATTCGTTCTTGTTGGTGCACA	352	
EcR F	AGTTTGAGCAGCCAACTGAAGCAG	373	55
EcR R	TCTGCTTCAGTTGGCTGCTCAAAC	133	
RXR F	AAAGACCTGACATATGCCTGCCGT	278	55
RXR R	AGCTGTACACGCCATAGTGCTT	109	
T7	TAATACGACTCACTATAGGG		

Table I.C. Oligonucleotide primers used for qPCR for *Gecarcinus lateralis* Mstn, EcR and RXR. Gene abbreviations: Mstn, myostatin; EcR, ecdysone receptor; RXR, Retinoid X Receptor; Additional abbreviations: forward primer (F), reverse primer (R), bp, base pairs.

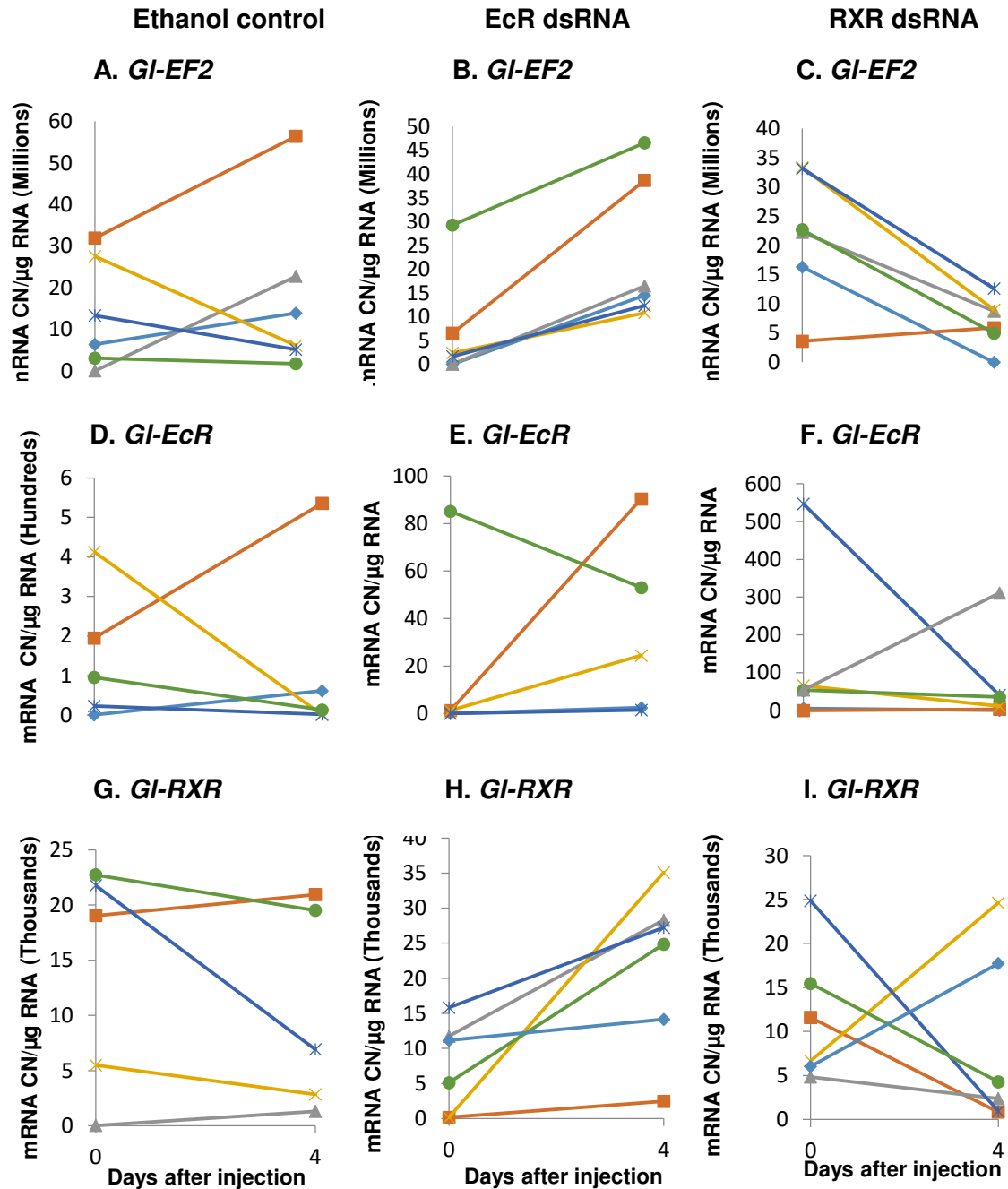| Primer pairs	Sequence (5'- 3')	Product Size (bp)	Annealing Temperature
EF2 F	TTCTATGCCTTTGGCCGTGTC	227	62
EF2 R	ATGGTGCCCGTCTTAACCA		
EcR F	AAGAATGCCGTGTACCAGTGTAAATATG	566	56
EcR R	GCTGCTCGAAGCATCATGACCTC		
RXR F	CTCAGGCAAGCACTATGGCGT	164	62
RXR R	TCAAGCACTTCTGGTAGCGGCAG		

Fig. I.A. Claw muscle. Each line connects the two time points for one crab. Column headings indicate injection contents. The first column shows *Gl-EF2*, *Gl-EcR* and *Gl-RXR* mRNA levels in animals with 10% ethanol injections before (day 0) injections, and 4 days after injections. The second and third columns show *Gl-EF2*, *Gl-EcR* and *Gl-RXR* mRNA levels in animals before (day 0) and 4 days after EcR and RXR dsRNA injections, respectively. If knockdown had been successful, Fig. I.A.E and fig. I.A.I would have shown decreased mRNA levels of EcR and RXR, respectively. As there was no consistent decrease from day 0 to day 4, EcR and RXR knockdown was not achieved in the claw muscle. Abbreviation: CN, copy number.
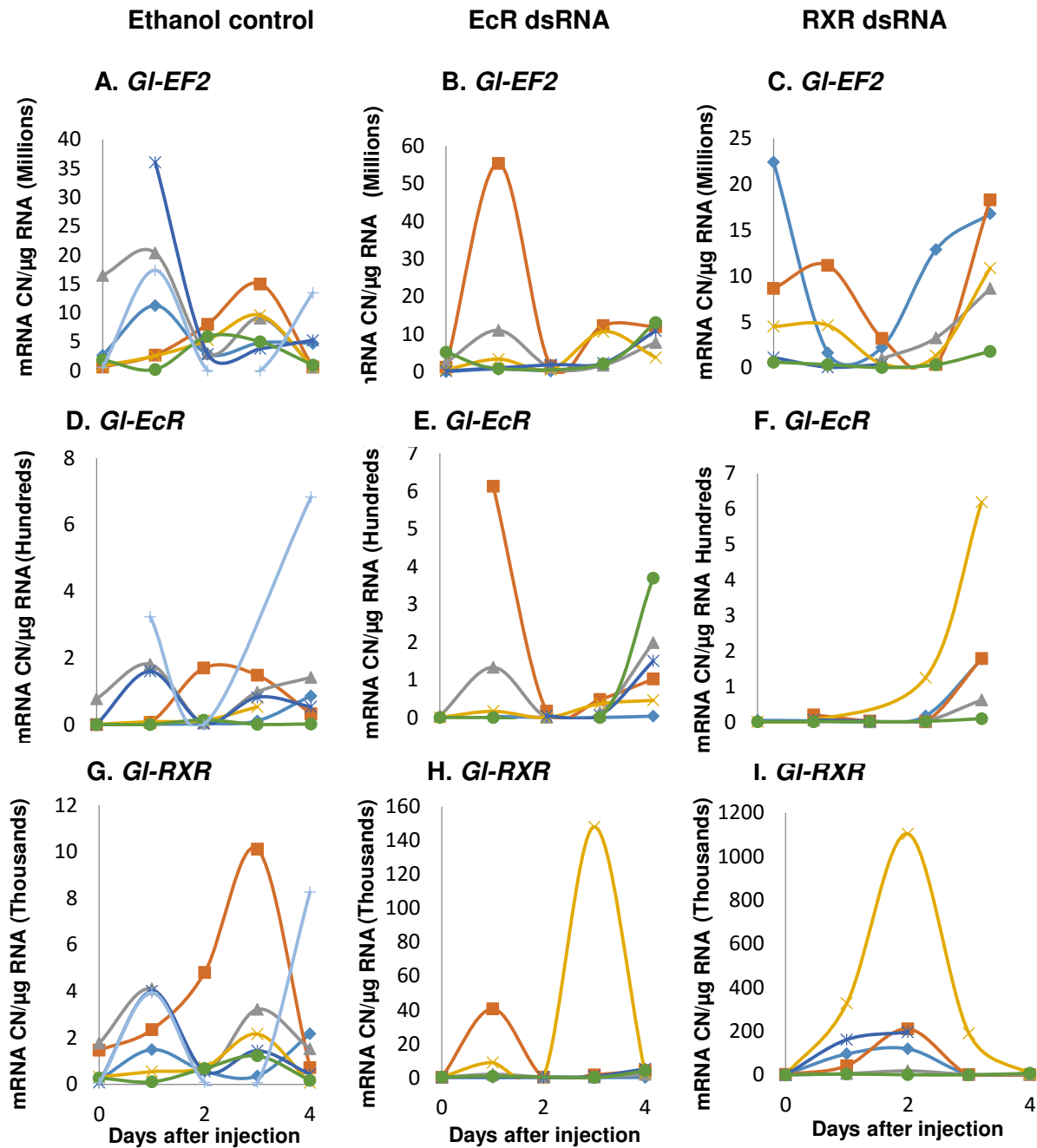
Fig. I.B. Merae. Each line connects merae from one crab. Column headings indicate injection contents. The first column shows *Gl-EF2*, *Gl-EcR* and *Gl-RXR* mRNA levels in animals with 10% ethanol injections before (day 0) injections, and 1, 2, 3, and 4 days after injections. The second and third columns show *Gl-EF2*, *Gl-EcR* and *Gl-RXR* mRNA levels in animals before (day 0) 1, 2, 3 and 4 days after EcR and RXR dsRNA injections, respectively. If knockdown had been successful, Fig. I.B.E and fig. I.B.I would have shown decreased mRNA levels of EcR and RXR, respectively. As there was no consistent decrease from day 0 to day 4, EcR and RXR knockdown was not achieved in the limb merae. Abbreviation: CN, copy number.